Amino acids as chiral building blocks. Synthesis of *anti*-β-amino alcohols and dipeptides with antiproliferative activity.

MEMORIA

Presentada para optar al grado

de Doctor en Ciencias Biomédicas por

Rodolfo Gastón Silveira Dorta

La Laguna, setiembre de 2015

Dr. José Manuel Padrón Carrillo

Universidad de La Laguna

D. JOSÉ MANUEL PADRON CARRILLO, PROFESOR CONTRATADO DOCTOR DE LA UNIVERSIDAD DE LA LAGUNA

CERTIFICA: Como director de la Tesis titulada **Amino acids as chiral building blocks. Synthesis of *anti*-β-amino alcohols and dipeptides with antiproliferative activity**, que ha sido realizada en las dependencias del Instituto Universitario de Bio-Orgánica "Antonio González", durante el periodo 2012-2015, constituyendo la memoria que presenta Don. Rodolfo Gastón Silveira Dorta para optar al grado de Doctor en Ciencias Biomédicas.

AUTORIZA: La lectura de esta Memoria, ya que reúne los requisitos de calidad necesarios para la presentación de la misma.

La Laguna a 3 de julio de 2015.

Fdo.: José M. Padrón

Los trabajos que constituyen la presente memoria han sido realizados en el Instituto Universitario de Bio-Orgánica “Antonio González”, bajo la dirección del Dr. José M. Padrón a quien quiero expresar mi más sincero agradecimiento por el apoyo recibido en todo momento, así por el apreciado trato humano recibido desde el día de mi incorporación a su grupo de investigación.

Agradecimientos

Primero me gustaría agradecer a la Agencia Canaria de Investigación, Innovación y Sociedad de la Información (ACIISI) del Gobierno de Canarias por haberme concedido la beca, la cual hizo posible la realización de la presente tesis y de este sueño convertido hoy en realidad.

A José M. Padrón por darme la oportunidad de ser parte de este proyecto. Por su constante apoyo, por la libertad y confianza desde el primer día que llegué al laboratorio. Asimismo debo agradecer tu gran trato personal y tus consejos que han facilitado el desarrollo de este trabajo.

A mis compañeros de laboratorio, Julito, Sergio, Sixto, Martín, Diego, Marcelle, Fernando P. Por el apoyo recibido tanto dentro como fuera del laboratorio y ser parcialmente mi familia.

También a los chicos que han pasado de manera transitoria por el laboratorio, como Samuel, David, Isabel y Varkha, por su ayuda recibida y por haber compartido sus inquietudes y motivarme a seguir aprendiendo para disipar sus dudas.

A Juan Ignacio, Tomas y David por los buenos momentos y por aclárame las dudas.

Quiero agradecer de manera especial al Dr. Víctor S. Martín por sus sabios consejos.

A Fernando Tellado por ser el primero en abrirme las puertas de su laboratorio y permiterme conocer lo bueno que es vivir en Canarias.

A todos los chicos del IPNA-CSIC, Gabriela, Mary, Fabio, Leandro, Sara, Juanmi, Dani, por su ayuda y por su buena compañía.

A todos los chicos del Instituto, por su buen trato y hacer de mi estancia durante estos años inolvidable.

Asimismo, quiero agradecer a todo el personal técnico del Instituto, por su calidez y muy apreciada ayuda durante estos años.

Al Dr. David Díez (Universidad de Salamanca) por recibirme en su laboratorio y hacerme sentir como uno más de su grupo. A todos los chicos del laboratorio de Salamanca, sobre todo a Javi, y Marife por todo el tiempo, paciencia y amistad que me han brindado.

A Inês Sousa y al Dr. Miguel X. Fernandes por su colaboración en el desarrollo de esta investigación.

A mis padres por su cariño y comprensión a lo largo de mi vida. Gracias a mis hermanos por el apoyo de siempre.

Un agradecimiento especial al Dr. Romen Carrillo por sus consejos, por ser el modelo de perseverancia, ingenio y ser humano en el cual me reflejo.

A CUCHITA, POR ENSEÑARME QUE ES EL AMOR Y QUERER COMPARTIR SU VIDA A MI LADO. POR EL APOYO Y LA AYUDA DURANTE LA REDACCION DE ESTE MANUSCRITO. POR BANCARME!

A todos, MIL GRACIAS.

TABLE OF CONTENTS

RESUMEN

En el siguiente trabajo se llevó a cabo la síntesis de *anti*-*β*-aminoalcoholes a partir de α-*N*,*N*-dibencilamino bencil ésteres, utilizando *α*-aminoácidos como material de partida. La reacción se realizó de manera secuencial a través de la formación del aldehído con DIBAL-H a -78ºC y la adición *in situ* de reactivos de Grignard. Con esta metodología se obtuvieron tanto *anti*-*β*-amino alcoholes así como también *anti*-2-amino-1,3-dioles y *anti*-3-amino-1,4-dioles, con buenos rendimientos (60-95%) y excelente estereoselectividad (*de* > 95%). Esta técnica fue también compatible con α-*N*,*N*-dibencilamino ésteres que presentan un grupo hidroxilo libre en su estructura.

Para demostrar la versatilidad del método, se sintetizó una pequeña biblioteca de análogos de espisulosina y esfinganina. Luego, se determinó su actividad antiproliferativa frente a un panel de 5 líneas tumorales celulares de origen humano dando valores de GI_{50} en el rango 1-20 μM. El cribado reverso realizado con métodos computacionales frente a 58 proteínas involucradas en cáncer determinó que las quinasas podrían ser la posible diana. Por otro lado, la determinación de la capacidad de inhibición de manera experimental en un panel de 456 quinasas mostró que los compuestos obtenidos presentaban la característica de ser inhibidores selectivos de CK1ε. Con estos resultados encontramos el primer inhibidor de CK1ε que a su vez presenta una importante actividad antiproliferativa en líneas celulares de cáncer.

Además, en este trabajo investigamos la bencilación regioselectiva del ácido L-glutámico con cantidades subestequiométricas del agente alquilante. Nuestros resultados, demuestran de manera inequívoca que no se puede obtener el monoéster bencílico en γ del ácido *N*,*N*-dibencilglutámico por bencilación directa del ácido L-glutámico, como fue descrito erróneamente por otros autores. Sin embargo, sí pudo ser obtenido bajo las mismas condiciones el monoéster bencílico en α del ácido *N*,*N*-dibencilglutámico.

Finalmente, empleando los monoésteres bencílicos en α- y γ- del ácido *N*,*N*-dibencilglutámico se sintetizó una librería de 22 dipéptidos modificados. El estudio de la actividad antiproliferativa frente a líneas tumorales celulares de origen humano mostró que los compuestos más activos fueron el derivado de γ-glutamil metionina (GI_{50} = 6.0-41 μM) y el derivado de α-glutamil prolina (GI_{50} = 7.5-18 μM). En particular los dipéptidos derivados de glutamil serina y glutamil prolina fueron más activos que el cisplatino y el etopósido en la línea celular resistente WiDr. También observamos que el dipéptido derivado de triptófano no afecta el crecimiento celular de HBL-100 mientras que si afecta a T-47D, siendo selectiva para esta línea celular.

ABSTRACT

In this work, we showed that enantiomerically pure *anti-β*-amino alcohols were synthesized from optically pure α-*N*,*N*-dibenzylamino benzyl esters, derived from α-amino acids. The synthesis was carried out by the sequential reduction to aldehyde with DIBAL-H at –78 ºC and subsequent *in situ* addition of Grignard reagents. With this methodology we were able to obtain *anti-β*-amino alcohols, *anti*-2-amino-1,3-diols and *anti*-3-amino-1,4-diols in good yields (60-95%) and excellent stereoselectivity (*de* > 95%). This technique was also compatible with free hydroxyl groups present in the substrate.

To demonstrate the versatility of the method, a small and structure-biased library of enantiopure *anti*-β-amino alcohols (sphinganine and spisulosine analogues) was prepared in a straightforward manner. Their antiproliferative activity was tested against a panel of five human solid tumor cell lines gave GI_{50} values in the range 1-20 μM. The reverse screening by computational methods against 58 proteins involved in cancer pointed out kinases as possible therapeutic target candidates. The experimental determination of the interaction with 456 kinases indicated that the compounds behave as selective CK1ε inhibitors. These findings have demonstrated that the lead compound represents the first selective CK1ε inhibitor with proven antiproliferative activity in cancer cell lines.

Furthermore, in the present work we explored the regioselective benzylation of L-glutamic acid under substoichiometric amounts of the alkylating agent. Our results demonstrated unambiguously that *N*,*N*-dibenzylglutamic acid γ-benzyl ester was not obtained by direct benzylation of $_{L}$-glutamic acid as reported by other authors. Instead, under such reaction conditions *N*,*N*-dibenzylglutamic acid α-benzyl ester was obtained.

Then, a small and focused library of 22 dipeptides derived from *N*,*N*-dibenzylglutamic acid α- and γ-benzyl esters was prepared in a straightforward manner. Their antiproliferative evaluation in the human solid tumor cell lines provided γ-glutamyl methionine (GI_{50} = 6.0-41 μM) and α-glutamyl proline (GI_{50} = 7.5-18 μM) as lead compounds. In particular, glutamyl serine and glutamyl proline dipeptides were more active in the resistant cancer cell line WiDr than the conventional anticancer drugs cisplatin and etoposide. Glutamyl tryptophan dipeptides did not affect cell growth of HBL-100, whilst in T-47D cells proliferation was inhibited.

CHAPTER 1

GENERAL INTRODUCTION

1. Introduction

1.1. Cancer

Nowadays, cancer is one of the key problems in health care services around the world. It leaves a negative impact in the societies, above all in the more economically disadvantaged. The five most frequent type of cancer in the world that affect both women and men, are stomach, colon/rectum, breast, cervix and liver. In Spain, cancer incidence scheduled for the 2015 is about 200.000 people,[1] with Canary Islands on the top of statistics.

Cancer is a multifactorial disease, it is mainly associated with mutagenic process, where cancer cells show common particular fixtures call hallmarks.[2-4] There are uncontrolled cellular proliferation and inability to recognize signaling pathway related to the cellular growth and cell survival, like apoptosis or inhibition of cellular proliferation. In addition, tumor cells have the potential to recruit cells from the near stroma, attracting new blood vessels to acquire nutrients and oxygen. Moreover, they also have the ability to evade the immune system. All these processes take part in the progress and develop of cancer pathology which finally triggers metastases to other tissue and organs. Besides the complexity occurring in cancer pathology, tumor cells present interconnected signaling pathways for growth and survival. Therefore, the success in a good cancer therapy treatment depends on recognizing these critical pathways in the oncogenic network.

Cancer detection has been pointed out as an important problem in its treatment. At this moment, there are a lot of strategies for cancer treatment. In one hand, surgery and radiation are the most important. However, these are effective if cancer is detected in an initial stage of its development. It means that, once the disease progress to a more advanced stage, or even metastases, these therapies are less efficient. On the other hand, the combination of cytotoxic or antiproliferative drugs with radiation and surgery has been exceptionally effective in the treatment of tumors in a more advanced stage. It is particular relevant in epithelial tumors (e.g. lung, colorectal, breast, prostate and pancreas). Unfortunately, as it was aforementioned, cancer is a multifactorial disease. Therefore it is very difficult to find a clinical effective drug to treat primary and disseminated forms of cancer. In this sense, there remains the need to develop new cytotoxic agents, which must have certain requisites, to improve and to increase the antitumor efficiency, to reduce the toxicity in normal cells and to prevent the drug resistance which is caused by the genomic instability of tumor cells.

1.2. Drug discovery strategies

Nowadays it does not exist a unique established method to develop new drugs. In an indicative way it is considered that there are two fundamentally different strategies for drug discovery. One is focused on the target, whereas the other focused on the complete system. In the first one named Target Drug Discovery (TDD), a molecule is tested to interact with a single biological target, which is thought being crucial in the disease process. Phenotypic Drug Discovery (PDD) is the second approach and uses more complex systems in order to obtain more data relevant to the real in vivo situation.

1.2.1. Target Drug Discovery (TDD)

TDD has also been known as a reductionist approach. TDD refers to the fact that the responsible entity for a pathological process or disease is thought to be a single gene product (or small group of defined gene products) and is based on the premise that isolation of that gene product in a system is the most efficient and least ambiguous method of determining an attractive molecule for a target.[5] The TDD approach detects molecules of interest by their effects on specific cellular targets. They primarily target precise and measurable functions of a protein or complex of proteins, either particular enzymatic activities or specific functional interaction between defined proteins. Examples of molecules discovered by this approach include imatinib mesylate (Gleveec) (Figure 1.1).

1.2.2. Phenotypic Drug Discovery (PDD)

PDD instead of TDD approach uses cell-based assays to find the target on the basis of phenotypic changes induced by candidate drugs. Compounds can target any protein, regardless of any measurable activity, and must display some specificity to cause a precise phenotype. It starts with a phenotype that a compound of interest cause in cells or in organisms and its goal is to go from the global phenotype in a stepwise fashion to eventually arrive to the (protein) target. PDD tests molecules in complex biological systems and monitors physiological responses with minimal assumptions concerning the participation of a specific molecular target and/or signaling pathway.[7] In contrast to TDD, one of the main advantages of whole-cell system is that gives information of the ability of the molecule to penetrate the cell membrane, as well as an acute cytotoxicity profile. Nonetheless, the data obtained from cell-based assays cannot be considered definitive indicators of lead compounds absorption or toxicity; they could serve to provide an

alert for encumbered chemical series early in the lead generation process. Some successful examples of PDD approach are taxol[8] and monastrol (Figure 1.1).[9]

In chapter 4 we show that using an alternative PDD approach, we were able to find a new selective Casein Kinase Iε inhibitor implicated in cancer.

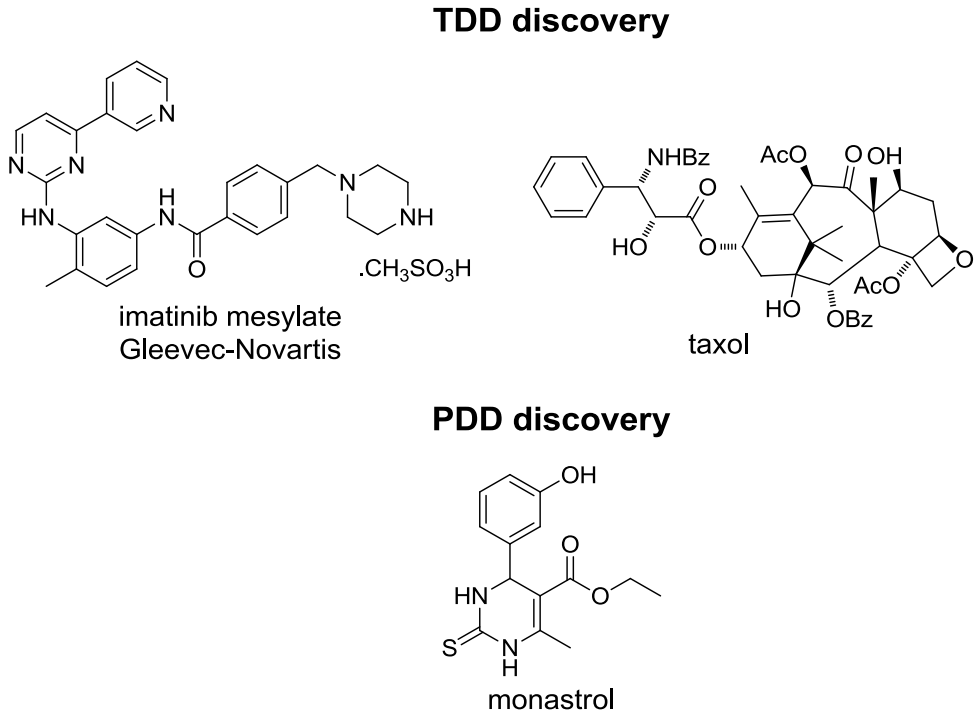

Figure 1.1. Drugs discovery under TDD and PD approach.

1.3. Privileged structures

Small organic molecules can be powerful tools with important functions in biology and medicine, as therapeutics and as probes to shed light on the macromolecules regulating biological processes.[10] It was thought that the discovery of new lead drugs in cancer treatment could have been increased with the advances of new techniques like high-throughput synthetic (HTPS) process to generate efficiently thousands of compounds with certain structural similarity. Nevertheless, the ability to make critical discoveries related to diseases remains a slow and, arguably, serendipitous process. It was demonstrated that the HTPS strategies were not entirely successful. In great extent, this state of affairs reflects the fact that we simply do not understand all the factors necessary to create compound collections that have potent and specific biochemical activity. One of the main problems in HTPS strategies is that it focused on the

quantity and not in the quality, which it is determinate by the diversity, and structural similarity with bioactive products.

The term “privileged structures” or “privileged scaffolds” (PSs) was proposed by Evans and co-workers at the end of 1980.[11] The work recognized the potential of certain molecular framework as template for derivatization to discover novel ligands for more than one type of receptor. These PSs are frequently observed in natural products or bioactive small molecules (Figure 1.2). The use of PSs in drug candidates discovery is very important due to the fact that it is efficient with high potential to unexploited bioactive regions in chemical space through a small molecule library.[12] What is clear is that certain PSs are capable of providing useful ligands for more than one receptor and that judicious modification of such structures could be a viable alternative in the search for new receptor agonists or antagonists.

Over the years, it has been demonstrated that the major challenge in the drug research field is the limited number of PSs. There are mainly two forms to identify privileged scaffolds. On one side molecules created de novo, which are now drugs, largely from the pharmaceutical industry. On the other side, compounds provided by nature in the form of natural products that either are, or have served as inspiration for, pharmaceuticals. With no doubt, this approach facilitates the discovery of new biologically useful structures and may allow for the identification of new privileged scaffolds as data on particular skeletons are collected. A second possibility is to evaluate structural motifs that have traditionally proven difficult to access, but which are present in dozens of natural products. Such examples are certainly rarer.

In this context, in chapter 4 and chapter 6 we introduce two new structural privileged motifs to maximize the unbiased coverage of chemical space with high biological relevance in cancer research through chemical libraries with some selective modification.

1.4. Natural products from marine source used in cancer therapy

Approximately one third of the compounds with therapeutic activity have been derived from natural products, or have been developed through modifications of PSs found in nature.[13] If we think about natural-product-based architectures it seems to have phylogenetically diverse origins. This diversity might suggest an evolutionary driving force to generate a particular arrangement of atoms. This outcome may not be so surprising in the sense that nature often repeats itself once it has found a suitable solution to a particular biochemical problem, and, of course, the macromolecular structures in living systems have a high level of non-random patterning.

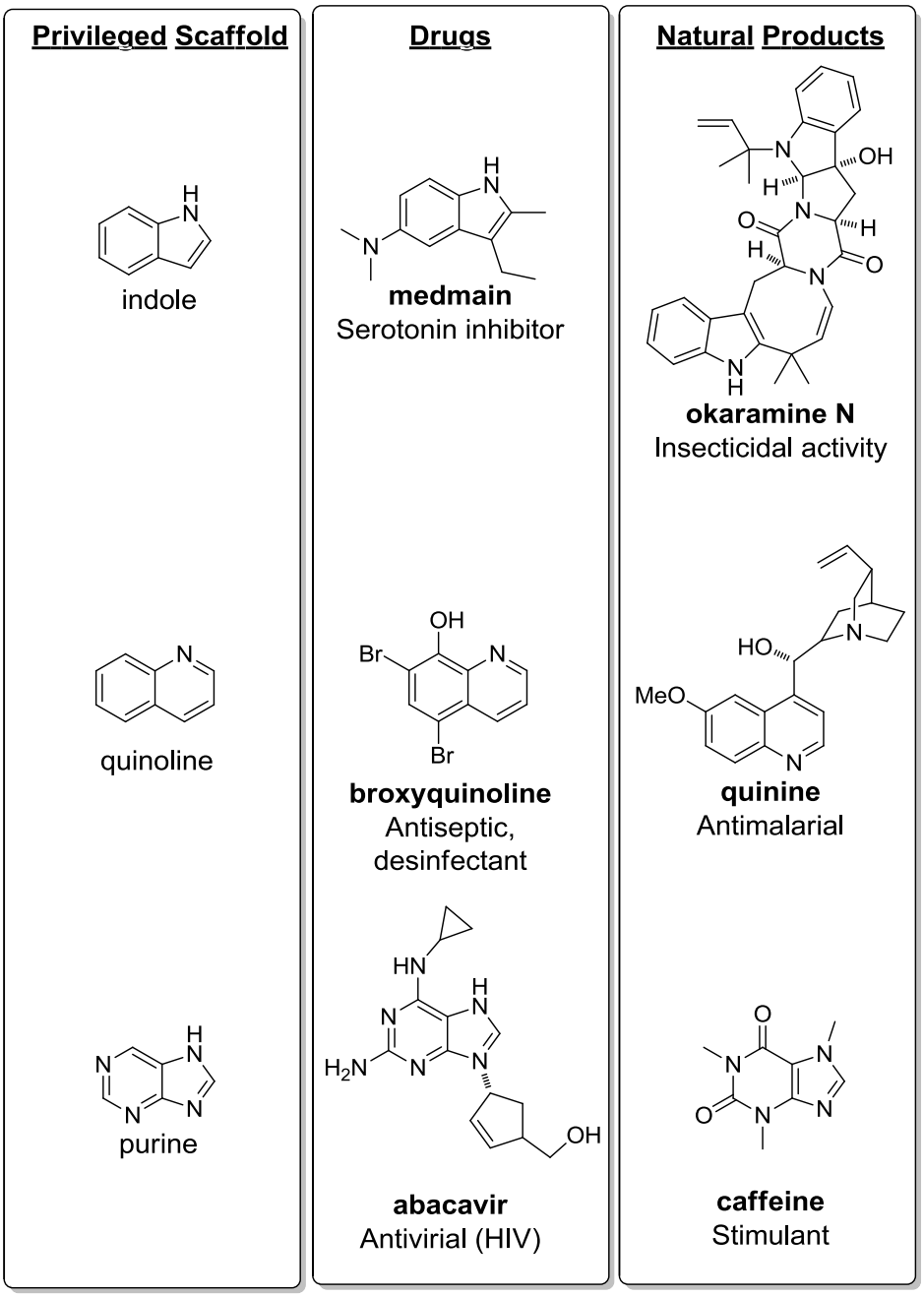

Figure 1.2. Examples of privileged scaffolds in drugs and natural products.

In the last 40 years, the pharmaceuticals companies have focused their interest in the development and discovery of natural products from marine source with relevant biological activity. Such develop have gone hand in hand with the progress of new chromatographic techniques like high-performance liquid chromatography (HPLC), or structural elucidation such as nuclear magnetic resonance (NMR), or high-resolution mass spectrometry (H-RMS) as well.

Being cancer chemotherapy the most relevant biological activity searched by pharmaceutical companies.

In this context, it was found a huge number of compounds in the area of cancer chemotherapy. [14,15] The first product from marine origin used in cancer therapy was found by Bergmann and col. in 1950 at the Caribbean sea in the organism called *Cryptotehya cripta* and it was called spongosin (Figure 1.3).[16,17] Since then, it was used as lead structure for drug research against cancer. Nowadays, it is used for cancer chemotherapy a derivative of spongosin named araC or cytrabine, sold with the name Cytosar-U (Figure 1.3).

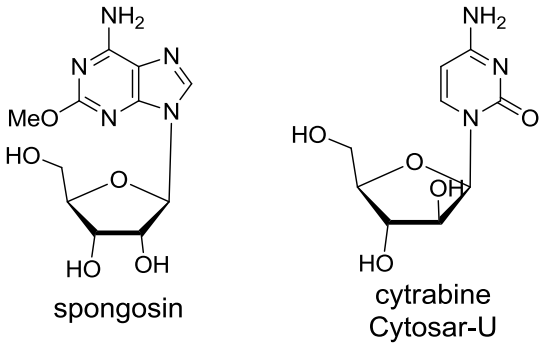

Figure 1.3. Structure of spongosine and its derivative cytrabine used in cancer therapy.

It is important to mention that almost all the marine products found come from invertebrates.[18] These molecules, which could be implicated in biological activity are called secondary metabolites (SMs). SMs play important roles in the survival of these organisms, because they present certain characteristic fixtures, e.g. soft body, slow movements and in most cases they have lacked morphologically structural defenses like shells or spines.

From the big number of invertebrates presented in marine sources the ***tunicates*** have received the major attention. ***Tunicates,*** spend practically all the time of their lives joined to rocks and bogged boats, so its recollection is very easy. In this context, very important and well documented classes of tunicates are the ascidians. Their SMs have focused the attention of the scientific community because they have produced compound with diverse interesting biological properties. For instance the amino alcohols, which are not presented in mammals, are one of the most important metabolites due to their structural simplicity and high potential in cancer research.

1.5. Long chain 1,2-amino alcohols in cancer therapy

Sphingolipids (SLs) represent a group of natural products, which by definition present a long alkyl chain 2-amino-1,3-diol scaffold or sphingoid base.[19] The mammal SLs are mainly represented by sphinganine, which show a (2*S*,3*R*)-2-aminooctadecano-1,3-diol structure and a long alkyl chain composed by 18 carbon atoms (Figure 1.4). Structurally, this central scaffold can be attached at different functionalities which give the different families of SLs found in nature (Figure 1.4). They are very important for the normal function of the mammal cells, since they play important structural roles and regulate physical properties of cell membranes. Besides, they also participate in cell signaling pathways controlling a big number of cellular functions.[20]

Another important group of long-chain amino alcohols are the 1-deoxy SLs, mainly from marine origin. These compounds have lost the C1 hydroxyl group of the SLs motif. It was found two main classes of 1-deoxy SLs. One group comprises those compounds that have an *anti*-2*R*,3*S* amino alcohol motif e.g. clavaminols A-C, G-J and M-N.[21,22] The other group is represented by spisulosine[23,24] that present the same *anti*-2*S*,3*R* amino alcohol configuration as SLs (Figure 1.5). Spisulosine was isolated from a clam tunicate *Episula polynyma* and it was initially a promising antiproliferative agent against diverse tumor cell lines.[25] However, clinical studies were discontinued in phase I because they have showed neurotoxicity, nausea, vomits, anemia, lymphopenia and skin rashes in the injection zone. In addition a low antitumor activity was observed increasing the relation risk/benefit of the patient.[26,27] After the discovery of spisulosine, a big number of antiproliferative *anti*-2*S*,3*R* amino alcohols form tunicates (*Clavelina phlegraea*) have been isolated in the Mediterrean sea. For example xestoaminol C, halamainol, amaminol (Figure 1.5) and the number is still growing.[28]

All these results make us think that there could be close structural relationships between long-chain aminoalcohols and cytotoxicity properties, which make them an attractive scaffold for anticancer drug discovery.

Due to their importance in drug research a big number of analogues have been synthetized.[29,30]

1.6. Synthetic strategies for the synthesis of 1,2-amino alcohols

In the literature, it is reported several ways to synthetize different diastereomers of 1,2-amino alcohols. However, the most widely used method is the Manfred T. Reetz strategy, due to their simplicity, big scope tolerance and high diastereoselectivity.

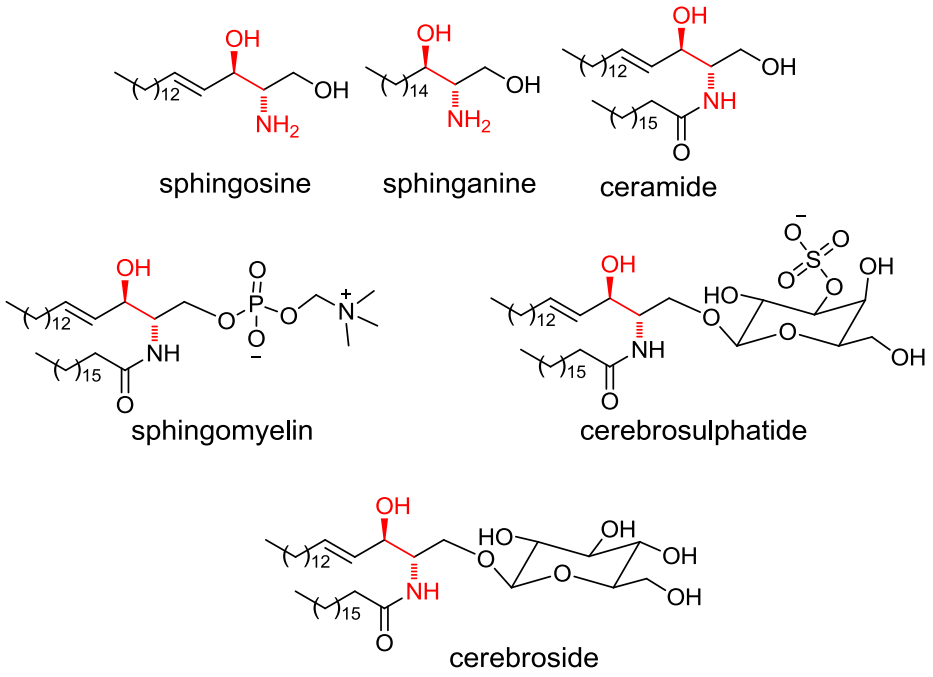

Figure 1.4. Structures of sphingosine and related sphingoid bases.

1.6.1. Manfred T. Reetz strategy

One of the most important diastereoselective methodology employed in the synthesis of *anti*-1,2-amino alcohols was developed by Manfred T. Reetz.[31] It is based on the addition of organometallic reagents to α-*N*,*N*-dibenzylamino aldehydes **4** (Scheme 1.1). These aldehydes are derived from diverse amino acids and are used as chiral building blocks. There have been reported two different strategies to obtain the aldehydes **4** (Scheme 1.1) and they only vary in the reaction sequence.

The reaction steps involved in the sequence are reduction, benzylation, and oxidation,[32] meanwhile the other sequence is benzylation, reduction and oxidation.[33-36] Both methods use amino acids as starting material. It is important to note that the aldehyde should be used in crude form avoiding chromatographic purification. Storing the aldehydes for long periods of time (months) should be avoided due to the ability of the α-amino aldehyde to suffer partial racemization and to undergo side reactions.[37-39] In this context, there have been reported two one-pot alternatives to avoid the aldehyde purification, thus reducing the time of aldehyde manipulation. Both strategies are based in the same Reetz protocol (Scheme 1.2). In the first one, benzostabase (BSB) is employed as *N*-protecting group, and the desire amino alcohol **5** is obtained by ester reduction to aldehyde, which is then submitted to the sequential addition of

the organometallic reagent.[40] The second method starts with the oxidation of the *N*,*N*-dibenzyl-aminoalcohol **2** to the aldehyde **4** and continues with the sequential addition of the corresponding organometallic reagent (Scheme 1.3).[41]

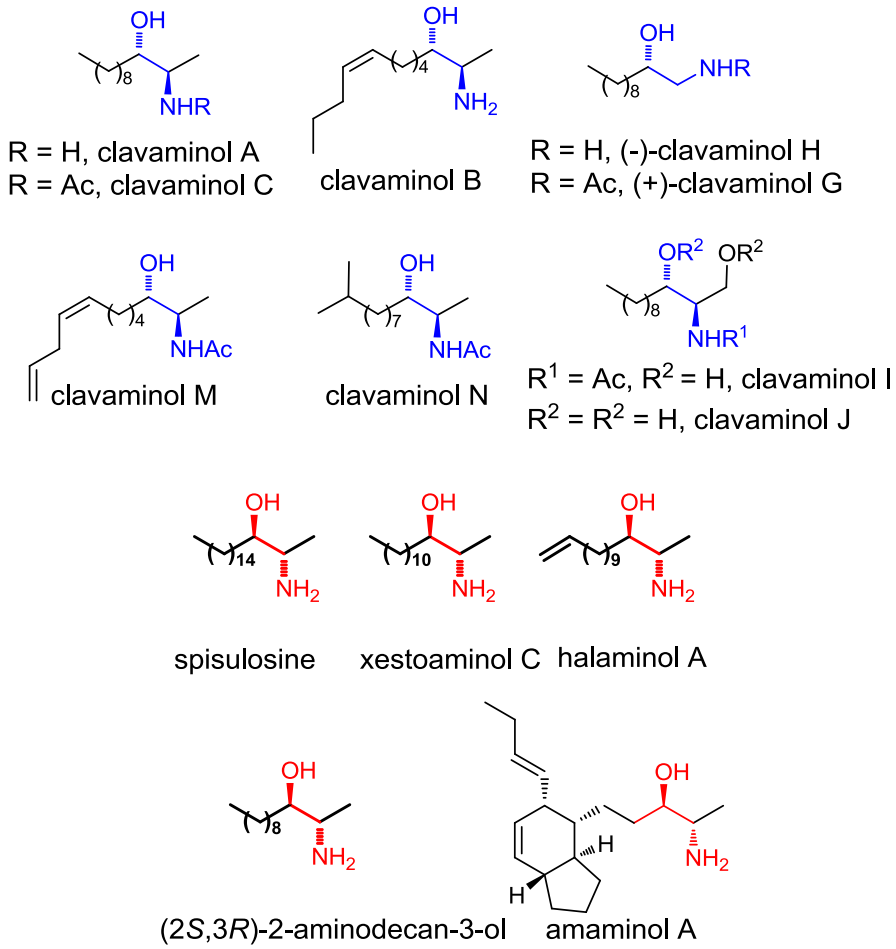

Figure 1.5. Examples of 1-deoxy-sphingolipids bases.

Once the aldehyde **4** is obtained, the next step is the diasteroselective nucleophilic addition of different organometallic reagents to form the new C-C bond (Scheme 1.1). The diastereoselectivity of the β-amino-alcohol obtained depends on the type of organometallic reagent used. In this sense there are two mechanism implicated in the addition of the organometallic reagents, named non-chelating controlled addition (NCA) to give the *anti*-**5** adduct as major product and chelation controlled addition (CCA) to obtain mainly the *syn*-**5** adduct.

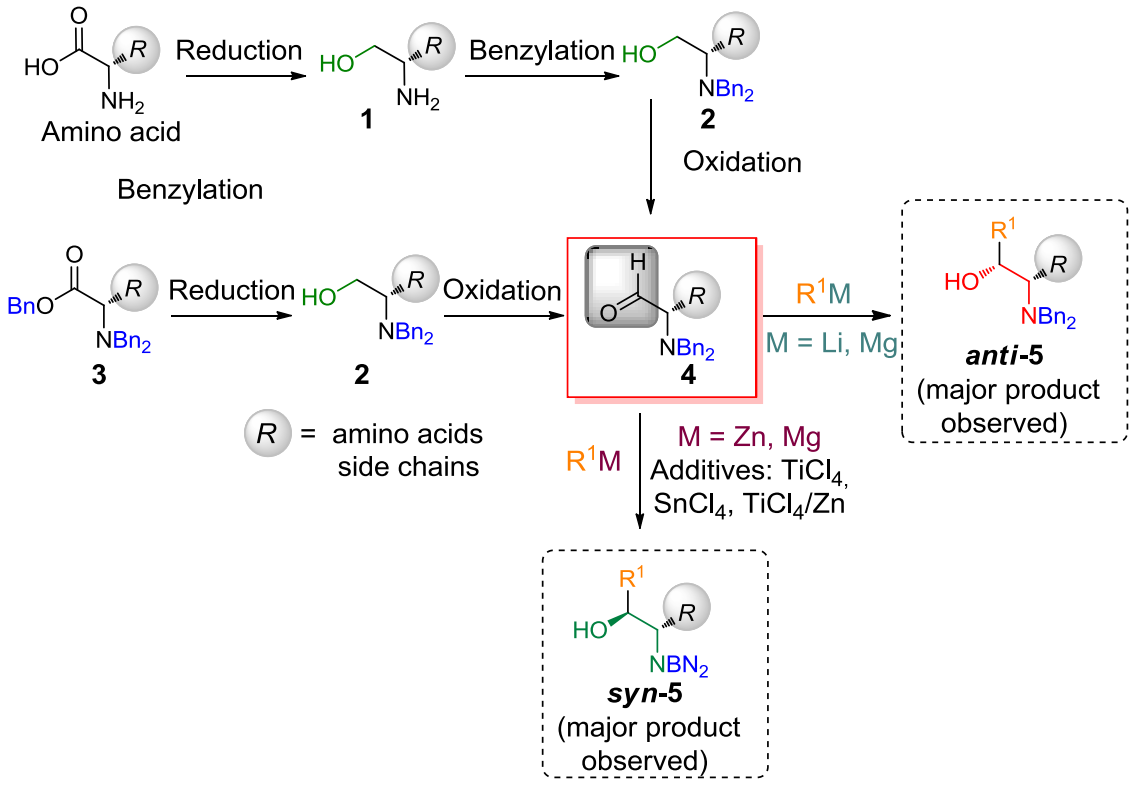

Scheme 1.1. **Synthetic strategy for the synthesis of β-aminoalcohols.**

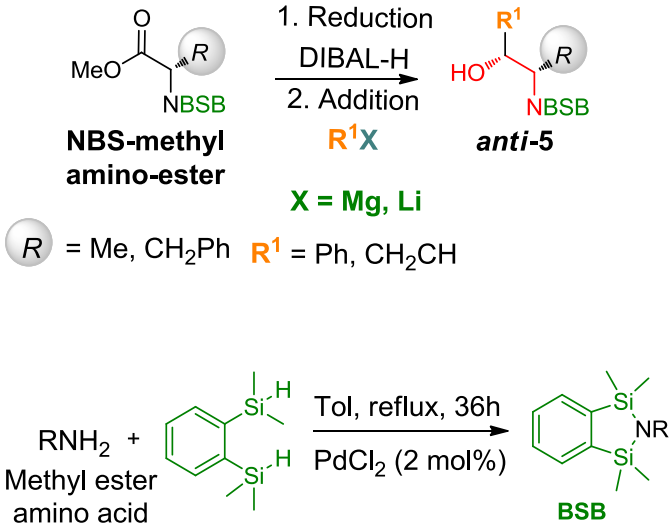

Scheme 1.2. **One-pot strategy reduction to aldehyde and organometallic addition.**

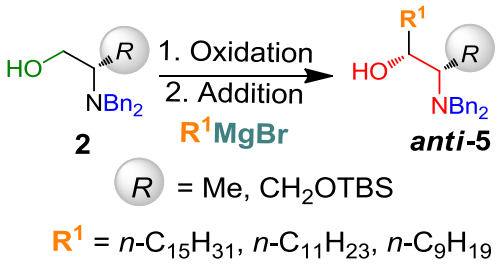

Scheme 1.3. One-pot strategy oxidation to aldehyde and organometallic addition.

1.6.2. Non-chelating controlled addition (NCA)

The reaction which goes through a NCA is observed when Grignard reagents are employed. Although it was thought that a tertiary amine group could be a better donor ligand for Mg (II), giving a pronounced chelation control, this speculation turned out to be false. Experimentally, it was observed that the amino alcohol with an *anti*-configuration was the main obtained.[32] It means that a *re*-face attack at the aldehyde was occurring. Over the time, it was found that there are a diverse family of organometallic reagents which react to form NCA with high levels of diastereoselectivity.[32] For instance, MeLi, MeTi(*Oi*-Pr)$_3$, MeCeCl$_2$ and MeMnX. In general, conventionally used reagents like RLi or RMgX give in almost all cases an enantiomeric purity > 98%.

The stereochemical course of the reaction is consistent with a nucleophilic attack of the Grignard reagent on the carbonyl and follows a non-chelating Felkin-Anh model.[42] According to the Felkin-Anh model, the eclipsed interactions are avoided, and the largest substituent should be perpendicular to the plane of the carbonyl (Figure 1.6). So, the most reactive aldehyde conformer is the one which C-NBn$_2$ σ-bond is aligned with the π-system of the carbonyl moiety in such a way that π^*-$\sigma^*_{\text{C-NBn2}}$ conjugation is maximized, causing the highest degree of LUMO lowering. Such conformers have the highest reactivity, attack of the nucleophile reagent which is then attacked in a Bürgi-Dunitz trajectory from the least hindered face.

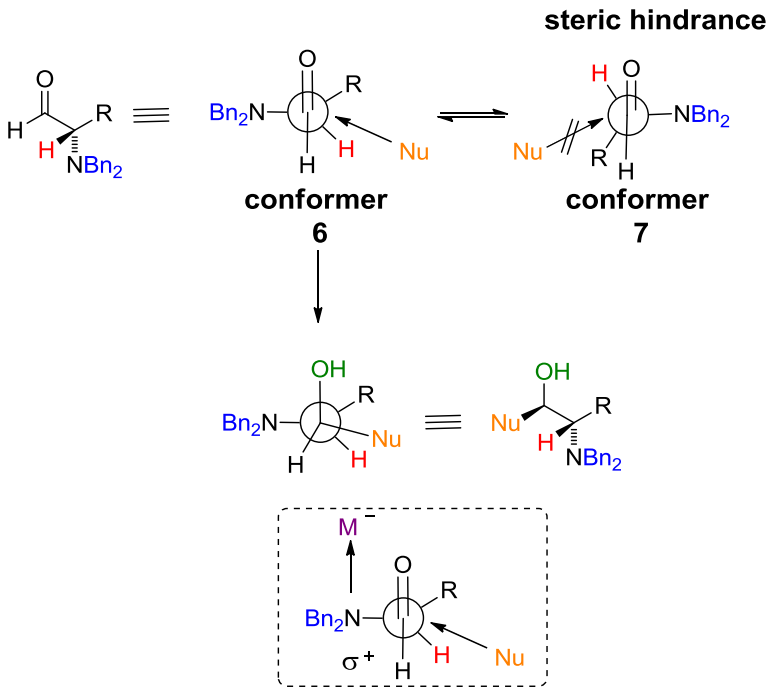

Figure 1.6. **Conformational structure more stable by Felkin Anh model.**

Accordingly, two electronically similar conformers are considered (conformer **6** and conformer **7**, Figure 1.6). However, one reacts faster, due to the steric interaction between the incoming nucleophile and the **R** α-substituent group. Nevertheless, studies in silico have shown that both conformations do not have indicative LUMO lowering, one respect to the other.[43] Consequently, it was thought that the metal may coordinate to the amino function without undergoing chelation to the carbonyl group adduct **8** (Figure 1.6), which was then confirmed in silico, showing a considerable LUMO lowering associate with the carbonyl function, caused by the drastic lowering of the $\sigma^*_{C\text{-}N}$ orbital.[44]

Another important consideration to be taken into account in the inhibition of the chelation model is the steric effect produced by the *N*,*N*-protecting groups. It was demonstrated that the bulkiness of the *N*-protecting group plays an important role in the diastereoselectivity. Thus, it was observed that the *N*,*N*-dimethyl aldehyde (**9**) react with organometallic reagents[45] with almost complete chelation control. It was also found that α-amino aldehydes protected in the form of 2-isoindoliyl derivatives (**10**), less sterically hindered than the *N*,*N*-dibenzyl analogues, react with low diastereolselectivity or even in a chelation controlled adducts.[46] Moreover, when the bulkiness increases, the diastereoselectivity goes in the same direction as it

was observed for the *N*,*N*-diallyl analogue of **11** reacting with MeLi to form the NCA preferentially with a diastereoselectivity >80%.

In contrast, when the steric bulkiness of the protecting group is increased, a high diastereoselectivity takes place, e.g. when *N*,*N*-di(o-methyl)benzylamino aldehyde (**12**) react with RMgX to form a NCA with a diastereoselectivity >99%.[45,46] The same trend is also observed in the reaction of sulfur ylides with sterically more hindered aldehydes (d.r. >90%).[46] In addition, other *N*,*N*-disubstituted amino aldehydes such as *N*-benzyl-*N*-*t*-butoxycarbonyl (**13**), *N*-benzyl-*N*-benzyloxy carbonyl (**14**), or *N*-benzyl- *N*-tosyl (**15**) derivatives also react under NCA (Figure 1.7).[47-50] However, these protecting groups require additional steps of protection and deprotection and the diastereoselectivity is reduced in some cases.

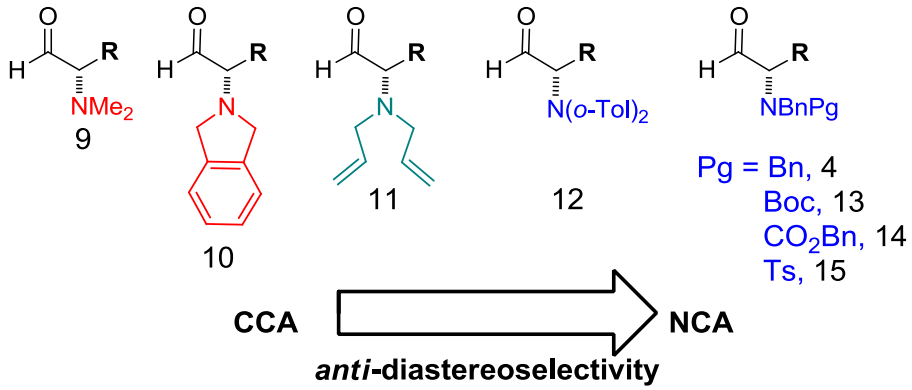

Figure 1.7. Dependence of the steric bulkiness in the *N*-protecting group on the diastereoselectivity.

1.6.3. Chelation controlled addition (CCA)

The organometallic addition in which the chelation is controlled, is obtained in non-ethereal solvents by treating the aldehyde with a Lewis acid capable of bis ligation (e.g., $TiCl_4$, $SnCl_4$, MgX_2) and reacting the intermediate chelates with nucleophiles which present organic-Zn, allylsilanes, enolsilanes, or Me_3SiCN.[51,52] It is worth mentioning that these kind of reactions are very difficult to be carried out because of the steric factor present in the aldehyde **4** (as aforementioned). To achieve this CCA, a Lewis acid MX*n* is needed to generate the intermediate **16 (**Figure 1.8**)**. However, in most cases low diastereoselectivity is observed. The steric hindrance of the *N*,*N*-dibenzyl substituent produce the hypothetical chelate **17** (Figure 1.8) but it is not the only species observed.

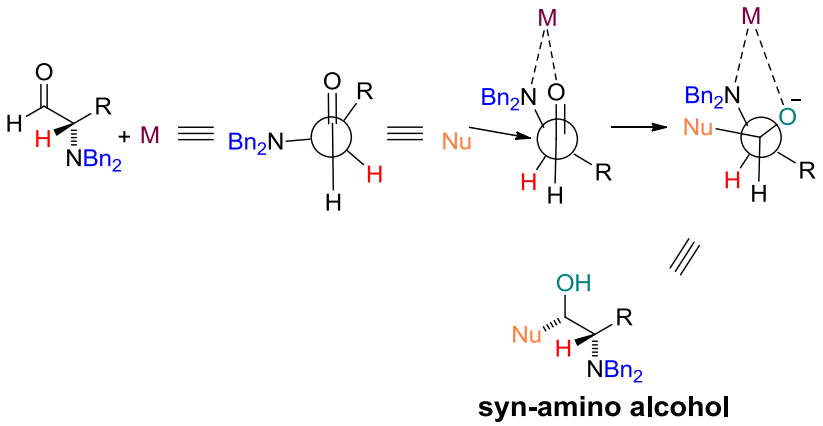

Figure 1.8. **Conformational structure in a chelating controlled addition.**

In fact, it was demonstrated that there may be two or three (Figure 1.9) different species in solution even at low temperatures, similar in energy, when aldehyde **4** is treated with $TiCl_4$. The two main species present in the reaction are shown in Figure 1.9. The chelated intermediate **17** is the main species that gives the *syn* amino alcohol and coexists with the acyclic adduct **18** in a proportion 2:1.[53]

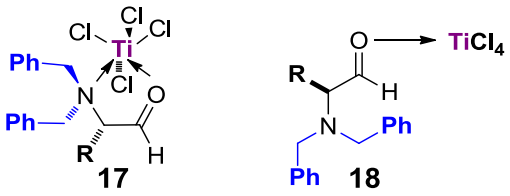

Figure 1.9. **Species observed in the chelating controlled addition.**

It was observed that the highly Lewis acidic methyl reagent $MeTiCl_3$ also leads to chelation control.[32] However, diastereseoelctivity decreases with the increase of the bulkiness of the R-group at the stereogenic center. Although some studies seem to indicate that chelated aldehydes such as bidentate complexes **17** and related species are more reactive than mono-complexed analogues **18**, it cannot be generalized.[51,54-56] It was also observed that the stereochemistry depends on the nature of the reagent added in the second stage of the one pot process when the system is comprised of **4**/$TiCl_4$.

There are some exceptional cases were the reaction occur following a CCA model. It is the case of diethylzinc (Et_2-Zn) and aldehyde **4**. The reaction of this organometallic reagent with **4** at 0ºC to afford the CCA preferentially, resulted in a diastereosoelectivity ranging 88-99%.[57] Normal aldehydes do not react with dialkylzinc reagents unless promoters such as $TiCl_4$[58] or catalysts such as α-amino alcohols[59] are present. It is proposed that the amino alcohol formed could act in autocatalytic fashion.[60]

In chapter 3 and 4 we show the development of a one pot methodology based on M. T Reetz approach. The method is based on the reduction of α-*N*,*N*-dibenzylamino benzyl esters to the aldehyde and the sequential addition of the corresponding Grignard reagent, without isolation of the aldehyde. This methodology has shown a wide scope range, even using amino acids without *O*-protecting groups.

1.7. Peptides in cancer therapy

Peptides are largely employed in a considerable number of biologically activities. Their small size and compatibility with biological systems and their synthetic accessibility, including those with a structurally complex architecture make them very important in biological structure research programs. As a consequence, structure-activity relationship (SAR) studies are relatively easy to perform. This big success is in part because they present a sequential architecture and can be synthetized step by step from monomeric building blocks in solution or in solid phase. Therefore, peptides can be efficiently modified in the backbone and in the substituent pattern of the side chain of the monomers.[61-63]

Particularly, peptides play a very important role in cancer research. They seem to solve the main problems of conventional chemotherapy, the inability to deliver the correct amount of drug directly to cancer cells without affecting normal cells,[64] drug resistance, altered biodistribution, biotransformation and drug clearance.[64] Peptides have the ability to allow the selective and effective localization of drugs at predefined targets (e.g., overexpressed protein/peptide receptors in cancer), reducing their access to normal cells thus maximizing therapeutic index and reducing toxicity.[65,66]

Clinical treating cancer peptides are used in different ways, directly as drugs (e.g., as angiogenesis inhibitors), tumor targeting agents that carry cytotoxic drugs and radionuclides (targeted chemotherapy and radiation therapy), hormones and vaccines, among others (Figure 1.10).

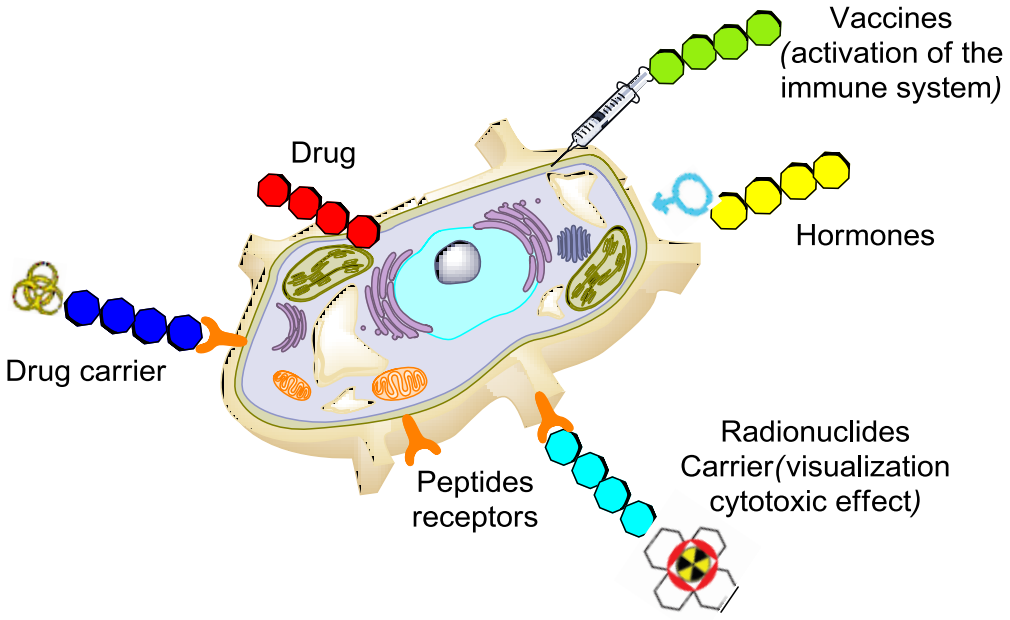

Figure 1.10. **Different clinical strategies of cancer using peptides.**

Nowadays there are a big number of peptides used as chemotherapeutic agents in cancer treatment. Examples of them are leuprolide (used in prostate cancer treatment), carfilzomib (used in the treatment of multiple myeloma, hematological cancer) and goserelin (used in breast cancer) (Figure 1.11).

Although the importance of the peptides in cancer treatment, in the literature we found that small peptides (< 5 amino acids) have not been explored exhaustively as potential anticancer agents.[67] Tyrosine- and cysteine-based dipeptides have been reported to exhibit antiproliferative activity in human solid tumor lines (Figure 1.12).[68, 69]

1.8. L-Glutamic acid as building block for the construction of biologically relevant molecules

1.8.1. *N*,*N*-Dibenzylglutamyl derivatives as chiral building blocks

L-Glutamic acid is a potentially valuable building block provided that the two carboxyl groups could be differentiated. In the literature, it has been explored extensively the use of diverse *N*-protecting groups, from which the benzyl group remains as highly useful in synthetic organic chemistry. Likewise *N*,*N*-perbenzylated glutamic acid has demonstrated being a

valuable intermediate for the preparations of important bioactive molecules. It has showed been a valuable intermediate for the preparation of biologically significant compounds (Figure 1.13).[70-73]

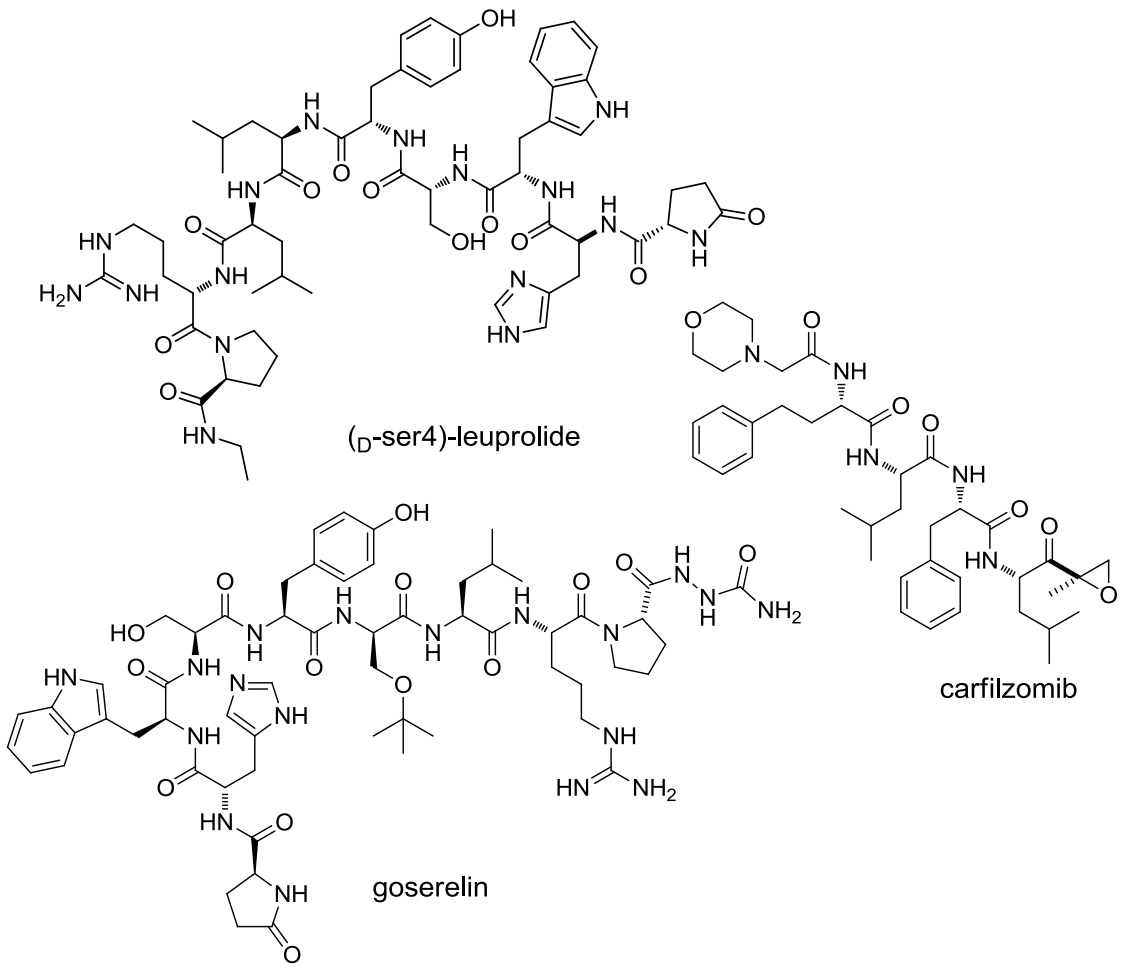

Figure 1.11. **Peptides used in clinical treatment of cancer.**

1.8.2. L-Glutamic acid in cancer therapy

There seems to be a close relation between L-glutamic acid and cytotoxicity properties. It is a common motif which is present in a number of molecules with antitumor activity. For instance, thalidomide,[74-76] aminopterin[77-80] and their analogues phtalomide[81-82] and methotrexate[83] respectively. Moreover, recent studies have pointed out L-theanine as a potential compound in cancer tetraement (Figure 1.14).[84]

tyrosine-based non natural peptides

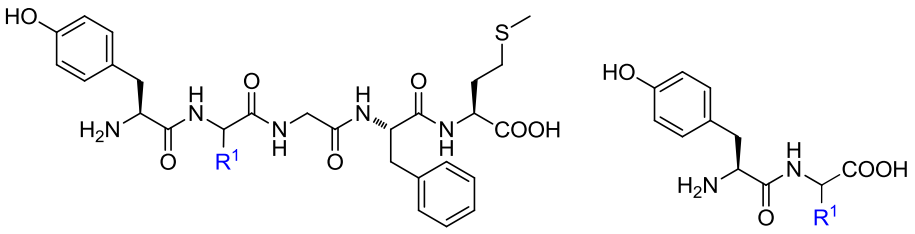

R^1 = adamantane-derived unnatural amino acids

cysteine-based dipeptides

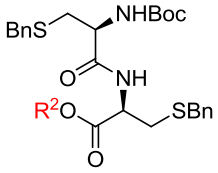

R^2 = Me, H

Figure 1.12. Peptide with < 5 amino acids residues presented in the literature.

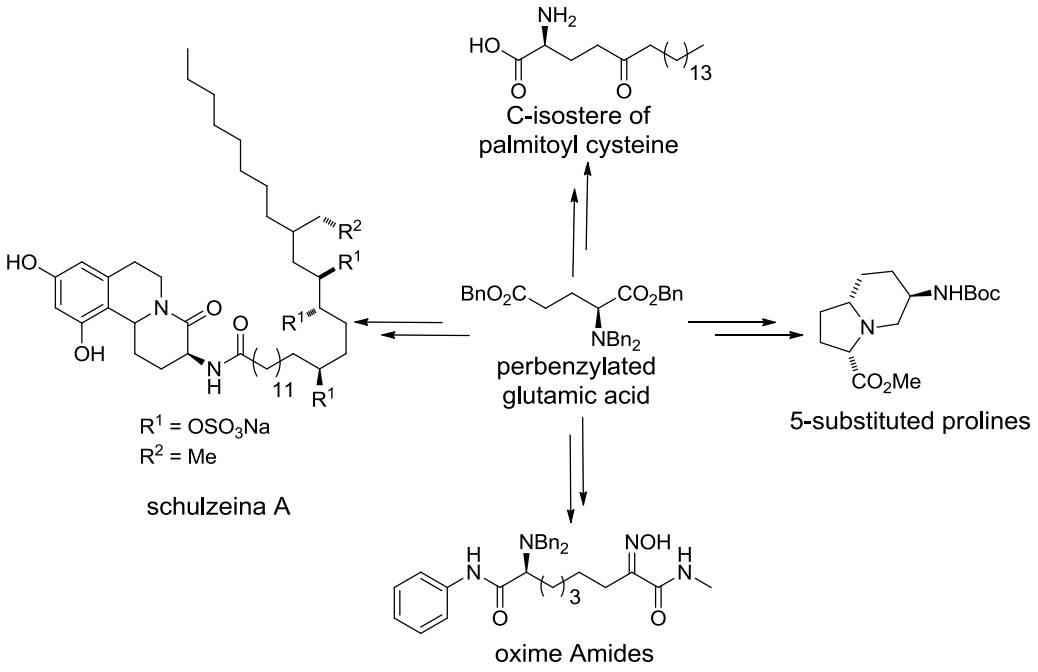

Figure1.13. Products with biological relevance obtained from $_L$-glutamic acid.

Additionally, the natural amino acid $_{L}$-glutamine (Figure 1.14) (biosynthesized from $_{L}$-glutamic acid in human cells by $_{L}$-glutamine synthetase) has been studied for such antiproliferative activity. It is essential for cell growth and proliferation and cannot be synthetized in neoplastic cells due to the lower reactivity of $_{L}$-glutamine synthetase. Thus, antagonists of this enzyme can interfere with the metabolic process of $_{L}$-glutamine and could act as anticancer agents.[85] In addition to glucose; cancer cells utilize glutamine as a carbon source for ATP production and biosynthesis. Glutamine can be internalized through cell surface transporters. One of them is a primary sodium-dependent transporter of glutamine, called ASCT2 (gene symbol *SLC1A5*), and it has been employed as a promising target for anticancer therapy. In cancer cells, *SLC1A5* expression is associated with oncogenic MYC and KRAS. Accordingly, *N*γ-glutamylanilde analogues (Figure 1.14) have been reported as novel ASCT2 probes.[86,87] *N*-(benzenesulfonyl)-$_{L}$-glutamic acid derivatives (Figure 1.14) have also been designed as $_{L}$-glutamine analogues.[88,89] Glutamic acid is also used to form conjugates as polyglutamic (Poly-Glu) acid and can be used as a drug carrier because it increases the efficacy of anticancer drug and decreases its toxicity toward normal cells.[90,91]

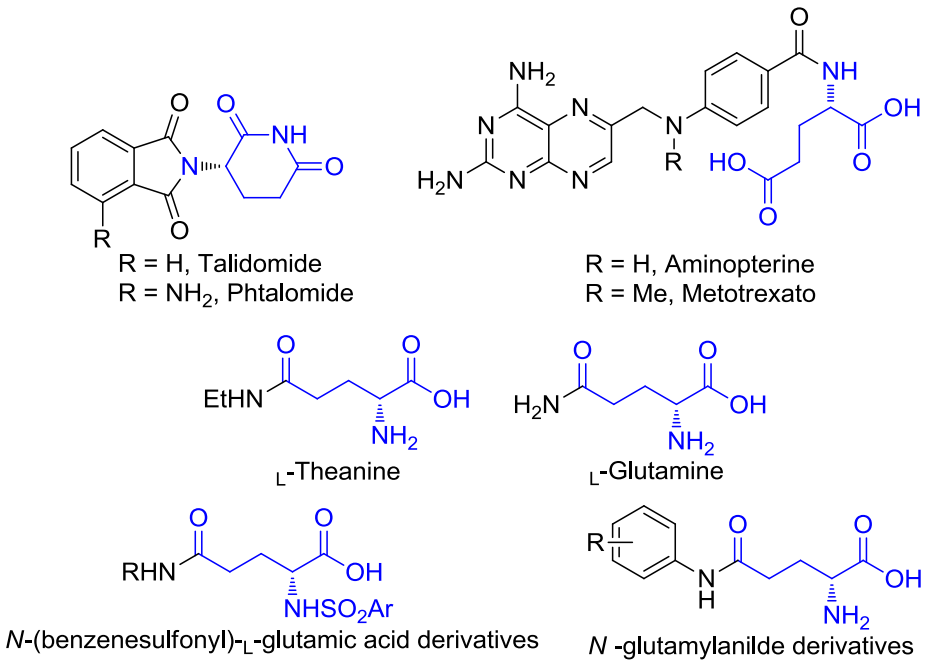

Figure 1.14. $_{L}$-Glutamic acid derivatives with antiproliferative activity and $_{L}$-glutamine.

1.9. References

1. Sociedad Española de Oncología Medica (SEOM), www.seom.org.
2. Hanhn, W. C.; Weinberg, R. A. *Nat. Rev. Cancer*. **2002**, *2*, 331.
3. Hanahan, D.; Weinberg, R.A. *Cell* **2000**, 57, 70.
4. Luo, J.; Solimini, N.; L.; Elledge, Stephen, J. *Cell* **2009**, *5*, 823.
5. Kenakin, T. *A pharmacology primer* **2009**, 215.
6. Castoreno, B. A.; Eggert, U. S. *ACS Chemical Biology* **2011**, *6*, 86.
7. Lee, J. A.; Uhlik, M. T.; Moxham, C. M.; Tomandl, D.; Sall, D. J. *J. Med. Chem*. **2012**, *55*, 4527.
8. Schiff, P. B.; Fant, J.; Horwitz, S. B. *Nature* **1979**, *277*, 665.
9. Mayer, T. U.; Kapoor, T. M.; Haggarty, S. J.; King, R. W.; Schreiber, S. L.; Mitchison, T. J. *Science* **1999**, *286*, 971.
10. Welsch, M. E.; Snyder, S. A.; Stockwell, B. R. *Curr. Opin. Chem. Biol*. **2010**, *14*, 347.
11. Evans, B. E.; Rittle, K. E.; Bock, M. G.; DiPardo, R. M.; Freidinger, R. M.; Whitter, W. L.; Lundell, G. F.; Veber, D. F.; Anderson, P. S. *J. Med. Chem.* **1988**, *31*, 2235.
12. Kim, J.; Kim, H.; Park, S. B. *J. Am. Chem. Soc*. **2014**, *136*, 14629.
13. Menna, M. *Phytochem, Rev*. **2009**, *8*, 461.
14. Amador, M. L.; Jimeneo, J.; Paz-Ares, L.; Cortes-Funes, H.; Hidalgo, M. *Ann. Oncol*. **2003**, *14*, 1607.
15. Newman, D. J.; Gragg, G. M. *J. Nat. Prod*. **2004**, *54*, 1216.
16. Bergmann, W.; Feeney, R. J. *J. Am. Chem. Soc*. **1950**, *72*, 2809.
17. Huang, R. M.; Chen, Y. N.; Zeng, Z.; Gao, C. H.; Su, X.; Peng. Y. *Mar. Drugs* **2014**, *12*, 5817.
18. Blunt, J. W.; et. al. *Nat. Prod. Rep*. **2008**, *25*, 35.
19. Chester, M. A. *Eur. J. Biochem*. **1997**. *257*: 293.
20. Gangoiti, P.; Camacho, L.; Arana, L.; Ouro, A.; Granado, M. H.; Brizuela, L.; Casas, J.; Fabrias, G.; Abad, J. L.; Delgado, A.; Gómez-Muñoz, A. *Prog. Lipid Res*. **2010**, *49*, 316.
21. Aiello, A.; Fattorusso, E.; Giordano, A.; Menna, M.; Navarrete, C.; Muñoz, E. *Bioorg. Med. Chem.* **2007**, *15*, 2920.
22. Aiello, A.; Fattorusso, E.; Giordano, A.; Menna, M.; Navarrete, C.; Muñoz, E. *Tetrahedron* **2009**, *65*, 4384.
23. Jimeneo, J.; García-Gravalos, D.; Ávila, J.; Smith, B.; Grant, W.; Faicloth G. T. *AACR-NCI-EORTC international conference on molecular targets and cancer therapeutics*. Washington DC, 16-19 Nov **1999**, Abstract no. 314.

24. Reiehart, K. L.; Fregau, N. L.; Warwick, R. A.; Garcia Gravalos, D.; Avila, J.; Faircloth, G. T. PCT WO9952521 A1 19991021, 1999.
25. Sanchez, A. M.; Malagarie-Cazenave, S.; Olea, N.; Vara, D.; Cuevas, C.; Diaz-Laviada, I. *Eur. J. Pharmacol*. **2008**, *584*, 237.
26. Vilar, E, et. al. *Invest. New Drugs* **2010**, *30*, 299.
27. Williams, R. *Expert Opin. Investig. Drugs*. **2009**, *18*, 1581.
28. Nicholas, G. M.; Hong, T. W., Molinski, T. F.; Lerch, M. L.; Cancilla, M. T.; Lebrilla, C. B. *J. Nat. Prod*. **1999**, *62*, 1678.
29. Fox, T. E.; Finnegan, C. M.; Blumenthal, R.; Kester, M. *Cell. Mol. Life Sci*. **2006**, *63*, 1017.
30. Zeidan, Y. H.; Hannun, Y. A. *Trends Mol. Med*. **2007**, *13*, 327.
31. Reetz, M. T. *Chem. Rev*. **1999**, *99*, 1121.
32. Reetz, M. T.; Drewes, M. W.; Schmitz, A. *Angew. Chem., Int. Ed. Engl.* **1987**, *26*, 1141.
33. Gage, J. R.; Evans, D. A. *Org. Synth*. **1990**, *68*, 77.
34. Abiko, A.; Masamune, S. *Tetrahedron Lett*. **1992**, *33*, 5517.
35. Beaulieu, P. L.; Wernic, D. *J. Org. Chem*. **1996**, *61*, 3635.
36. Cook, J. W. B.; Davies, S. G.; Naylor, A. *Tetrahedron* **1993**, *49*, 7955.
37. Bergmeier, S. C. *Tetrahedron* **2000**, *37*, 2561 .
38. Adia, M.; Heraff, N.; Whiting, A. *Tetrahedron Lett*. **1997**, *38*, 3101.
39. Huang, P.-Q.; Guo, Z.-Q.; Ruan, Y.-P.; *Org. Lett*. **2006**, *8*, 1435.
40. Bonar-Law, R. P.; Davis, A. P.; Dorgan, B. J.; Reetz, M. T.; Wehrsig, A. *Tetrahedron Lett.* **1990**, *31*, 6725.
41. Chen, B. S.; Yang, L. H.; Ye, J. L.; Huang, T.; Ruan, Y. P.; Fu, J.; Huang, P. Q. *Eur. J. Med. Chem*. **2011**, *46*, 5480.
42. Cherest, M.; Felkin, H.; Prudent, N. *Tetrahedron Lett*. **1968**, *18*, 2199.
43. Reetz, M. T. In Stereocontrolled Organic Synthesis; Trost, B. M., Ed.; Blackwell: Oxford, **1994**; pp 67.
44. Paquette, L. A.; Mitzel, T. M.; Isaac, M. B.; Crasto, C. F.; Schomer, W. W. *J. Org. Chem.* **1997**, *62*, 4293.
45. Reetz, M. T. *Angew. Chem., Int. Ed. Engl*. **1991**, *30*, 1531.
46. Reetz, M. T.; Binder, J. *Tetrahedron Lett*. **1989**, *30*, 5425.
47. Jurczak, J.; Golebiowski, A. *Chem. Rev.* **1989**, *89*, 149.
48. Gryko, D.; Jurczak, J. *Tetrahedron Lett*. **1997**, *38*, 8275.
49. Dondoni, A.; Perrone, D.; Merino, P. *J. Org. Chem*. **1995**, *60*, 8074.

50. Sasai, H.; Kim, W.-S.; Suzuki, T.; Shibasaki, M.; Mitsuda, M.; Hasegawa, J.; Ohashi, T. *Tetrahedron Lett*. **1994**, *35*, 6123.
51. Reetz, M. T. *Acc. Chem. Res*. **1993**, *26*, 462.
52. Reetz,M. T. *Angew. Chem., Int. Ed. Engl.* **1984**, *23*, 556.
53. Reetz, M. T.; Drewes, M. W.; Harms, K.; Reif, W. *Tetrahedron Lett*. **1988**, *29*, 3295.
54. Mikami, K.; Kaneko, M.; Loh, T.-P.; Terada, M.; Nakai, T. *Tetrahedron Lett*. **1990**, *31*, 3909.
55. Reetz, M. T.; Maus, S. *Tetrahedron* **1987**, *43*, 101.
56. Chen, X.; Hortelano, E. R.; Eliel, E. L.; Frye, S. V. *J. Am. Chem.Soc*. **1992**, *114*, 1778.
57. Andrés, J. M.; Barrio, R.; Martínez, M. A.; Pedrosa, R.; Pérez-Encabo, A. *J. Org. Chem.* **1996**, *61*, 4210.
58. Reetz, M. T.; Steinbach, R.; Wenderoth, B. *Synth. Commun.***1981**, *11*, 261.
59. Noyori, R.; Kitamura, M. *Angew. Chem., Int. Ed. Engl.* **1991**, *30*, 49.
60. Soai, K.; Shibata, T.; Morioka, H.; Choji, K. *Nature* **1995**, *378*, 767-768.
61. Tan, N.-H.; Zhou, J. *Chem. Rev.* **2006**, *106*, 840.
62. Hamada, Y.; Shioiri, T. *Chem. Rev*. **2005**, *105*, 4441.
63. Sewald, N.; Jakubke, H.-D. *Peptides: Chemistry and Biology*; Wiley-VCH: Weinheim 2002.
64. Kakde, D.; Jain, D.; Shrivastava, V.; Kakde, R.; Patil, A. T. *J. Appl. Pharm. Sci*, **2011**, *1*, 1.
65. Thundimadathil, J. *J. Amino Acids*, **2012**, ID 967347.
66. Kaspar, A. A.; Reichert, J. M. *Drug Discovery Today* **2013**, *18*, 807.
67. The CancerPPD (http://www.crdd.osdd.net/raghava/cancerppd/).
68. Horvat, S.; Mlinarić-Majerski, K.; Glavas-Obrovac, L.; Jakas, A.; Veljković, J.; Marczi, S.; Kragol, G.; Roscić, M.; Matković, M.; Milostić-Srb. *J. Med Chem*. **2006**, *49*, 3136.
69. Banerji, B.; Pramanik, S. K.; Pal, U.; Maiti, N. C. *Chem Cent J*. **2013**, *7*, 91.
70. Cini, E.; Giorgi, G.; Rodriquez, M.; Taddei, M. *Synlett*, **2008**, 1562.
71. Cini, E.; Lampariello, L. R.; Rodriquez, M.; Taddei, M. *Tetrahedron*, **2009**, *65*, 844.
72. Botta, C. B.; Cabri, W.; Cini, E.; De Cesare, L.; Fattorusso, C.; Giannini, G.; Persico M.; Petrella, A; Rondinelli, F.; Rodriquez, M.; Russo, A.; Taddei, M. *J. Med. Chem.* **2011**, *14*, 2165.
73. Kuntiyong, P.; Akkarasamiyo, S.; Piboonsrinakara, N.; Hemmara, C.; Songthammawat, P. *Tetrahedron* **2011**, *67*, 8034.
74. Verheul, H. M. W; Panigrahy, D.; Yuan, J.; D´Ámato R. J. *British J. Cancer*, **1999**, *79*, 114.

75. D´Ámato R. J.; Loughnan, M. S.; Flynn, E.; Folkman, *J. Proc. Natl. Acad. Sci.USA*. **1994**, *91*, 4082.
76. Singhal, S.; et. al. *N. Engl.J. Med*, **1999**, *341*, 1565.
77. Farber, S.; Diamond, L. K.; Mercer, R. D.; Sylvester, R. F.; Wolff, J. A. *N. Engl.J. Med*, **1948**, *238*, 787.
78. Greenspan, E. M.; Goldin, A.; Schoenbach, E. B. *Act. Chemotherapeutic agent in Cancer*. **1950**, 856.
79. Glode, L. M.; Pitman, S. W.; Ensminger, W. D.; Rosowsky, A.; Papathanasopoulos, N.; Frei, E. III. *Cancer Res*. **1979**, *39*, 3707.
80. Oaks, B. M.; Dodd, K. W.; Meinhold, C. L.; Jiao, L.; Church, T. R.; Stolzenberg-Solomon, R. Z. *Am. J. Clin. Nutr*. **2010,** *91*, 449.
81. Lentzsch, S.; Rogers, M. S.; LeBlanc, R.; Birsner, A. E.; Shah, J. H.; Treston, A. M.; Anderson, K. C.; D`Amato, R. *J. Cancer Res*. **2002**, *62*, 2300.
82. Barlett, J. B.; Dredge, K.; Daldleish, A. G. *Nature. Rev*. **2004**, *4*, 314.
83. Skeel, R. T. *Hand Book of Cancer Chemotherapy*, 7th Ed. Lippincott, Williams & Wilkins, New York, **2008**.
84. McPhee, S. J.; Papadakis, M. A.; Rabow, M. W. *Current Medical Diagnosis and Treatment*, 50 Ed. Lange Medical Books/ McGraw-Hill, New York, **2011.**
85. Luzzio, F. A.; Mayorov, A. V.; Figg, W. D. *Tetrahedron Lett*. **2000**, *41*, 2275.
86. Esslinger, C. S.; Cybulski, K. A.; Rhoderick, J. F. *Bioorg. Med. Chem*. **2005**, *13*, 1111.
87. Schulte, M. L.; Dawson, E. S.; Saleh, S. A.; Cuthbertson, M. L.; Manning, H. C. *Bioorg. Med. Chem. Lett*. **2015**, *25*, 113.
88. Xu, H.; Jiang, M.; Li, H.; Lu, D.; Ouyang, P. *Process Biochem*. **2005**, *40*, 519.
89. Srikanth, K.; Kumar, C. A.; Ghosh, B.; Jha, T. *Bioorg. Med. Chem*. **2002**, *10*, 2119.
90. Shih, I. L.; Van, Y. T.; Shen, M. H. *Mini Rev. Med. Chem*. **2004**, *4*, 179.
91. Li, C. *Adv. Drug. Delivery. Rev*. **2002**,*54*,695.

CHAPTER 2

HYPOTHESIS AND OBJECTIVES

2. Hypothesis and Objectives

2.1. Hypothesis

Our working hypothesis results from using commercial amino acids as a powerful source for the construction of compounds with antiproliferative and/or cytotoxic activity.

2.2. Objectives

2.2.1. General Objectives

The main objective of this study is to synthetize new molecular entities using natural amino acids as starting materials, and study their antiproliferative activity.

2.2.2. Specific Objectives

1. **To** develop a one pot methodology for the synthesis of *anti-β*-amino alcohols, using *N*,*N*-dibenzylamino-benzyl esters derived from amino acids as chiral building blocks.

2. To design and to synthesize a small and structure-biased library of enantiopure *anti-β*-amino alcohols (sphinganine and spisulosine analogues) and a small and focused library of dipeptides derived from *N*,*N*-dibenzylglutamic acid α- and γ-benzyl esters.

3. To determine the antiproliferative activity of the synthesized compounds against a panel of representative human solid tumor cell lines,.

4. To establish structure activity relationships (SAR) to determine the essential structural requirements necessary for the antiproliferative activity.

5. To perform computational studies (in silico) to explain the results obtained by in vitro assays.

CHAPTER 3

DIRECT STEREOSELECTIVE SYNTHESIS OF ENANTIO-MERICALLY PURE *ANTI*-β-AMINO ALCOHOLS

3. Direct stereoselective synthesis of enantiomerically pure *anti*-β-amino alcohols

3.1. Introduction

β-Amino alcohols have received much attention in the scientific community due to their versatility. They can be used as chiral ligands in asymmetric synthesis,[1,2] as chiral synthons in the synthesis of natural products,[3,4] as well as in the synthesis of products with diverse biological activities.[5-7] In addition, long chain amino alcohols exhibit promising activity as antitumor agents.[8] An important class of amino alcohols are the sphingolipids (SLs)[9] represented by dihydrosphingosine (**1a**) and sphinganine (**1b**), which show a 2-amino-1,3-diol fragment with an *anti*-2*S*,3*R* configuration (Figure 3.1).[5] Another relevant group of long-chain amino alcohols are the 1-deoxysphingolipids from marine origin, such as the clavaminols A (**2a**), C (**2b**) and H.[10,11] (Figure 3.1) These compounds have an *anti*-2*R*,3*S* amino alcohol motif, opposite to SLs, and have shown cytotoxic and pro-apoptotic properties.[6] Furthermore, spisulosine[12] (**2c**) having the same *anti*-2*S*,3*R* configuration as SLs, was initially a promising antiproliferative agent against diverse human tumor cell lines.[13] However, clinical studies were discontinued in Phase I.[14] In the literature, there are many SLs reported with antiproliferative activity[15-17] and the number is still growing.

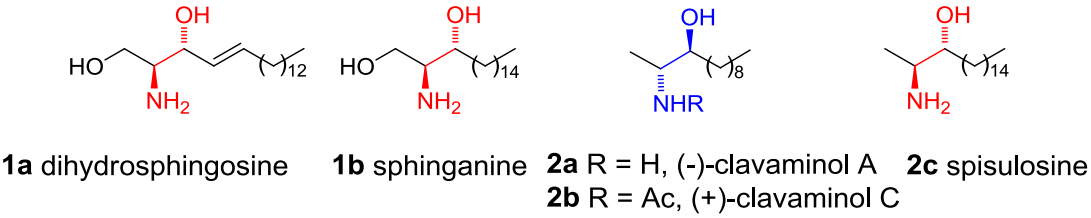

Figure 3.1. Dihydrosphingosine, sphinganine and related 1-deoxysphingolipids.

There is a close structural relationship between long-chain amino alcohols, including SLs, and cytotoxic properties, which make this type of compounds an attractive scaffold for anticancer drug discovery programs.

To shed light on the above compounds and their associated bioactive properties, and as part of our interest in synthesis of nitrogen-containing bioactive molecules,[18-23] we were engaged in the development of a more versatile and efficient methodology to synthesize *anti*-β-amino alcohols, in order to obtain new SLs analogues and test their antiproliferative activity.

We pondered a general one-pot methodology for the synthesis of functionalized *anti-β*-amino alcohols based on the *in situ* DIBAL-H reduction of α-(*N,N*-dibenzylamino)benzyl esters (**4**, **6**, **10** and **11**, Table 3.1-3.4) to their corresponding aldehyde, followed by the sequential addition of commercially available Grignard reagents. This methodology is an extension of the well-known Reetz protocol, but avoiding the three step sequence, namely reduction of the ester to alcohol, later oxidation to aldehyde and addition of the organometallic reagent.[24-26] A related one-pot process has been explored in the literature, using *N*-Boc protected amino esters, but obtaining *syn-β*-amino alcohols.[27-29] We found also a precedent in the synthesis of *anti-β*-amino alcohols using benzostabase (BSB) as *N*-protecting group.[30] However, this methodology has never been further used, maybe due to the difficulty in preparing *N*-BSB-protected amino esters. In this chapter, we describe how our one-pot approach is a very attractive form to generate *anti-β*-amino alcohols (**1**), *anti*-2-amino-1,3-diols (**2**) and *anti*-3-amino-1,4-diols (**3**) (Figure 3.2), reducing the number of chemical steps when compared to the methods reported in the literature for the synthesis of similar compounds (Figure 3.2).[31-38]

We also demonstrate that our method can be applied to serine and threonine derivatives without the need to use protecting groups for the hydroxyl moiety. This reaction proceeds in good yields and high enantioselectivity (*de* >95%). Therefore, we report the first one-pot diastereoselective addition of Grignard reagents using serine and threonine derivatives without *O*-protecting groups.

In addition, to test the applicability of this new methodology, we describe the synthesis of the naturally occurring compounds spisulosine and sphinganine.

3.2. Results and Discussion

3.2.1. Synthesis of *anti-β*-amino alcohols

The key step of this one-pot reaction is the DIBAL-H reduction of a *N,N*-dibenzyl-α-amino ester (synthesized by perbenzylation of the corresponding α-amino acid)[39,40] to its corresponding aldehyde, at −78 ºC, followed by the in situ sequential addition of the suitable Grignard reagent. First, we studied the influence of the reaction conditions taking into account the effect of solvents on the nucleophilicity, basicity of organomagnesium, and reducing ability of DIBAL-H.[28-30] We also evaluated the amount of DIBAL-H equivalents, as well as reduction time, using 3 equivalents of EtMgBr. The ratio of Grignard reagent used was chosen based on literature precedents[41] and it is consistent with our observations. The results obtained using the benzyl ester of *N,N*-dibenzyl-L-alanine (**4a**) as starting material are summarized in Table 3.1.

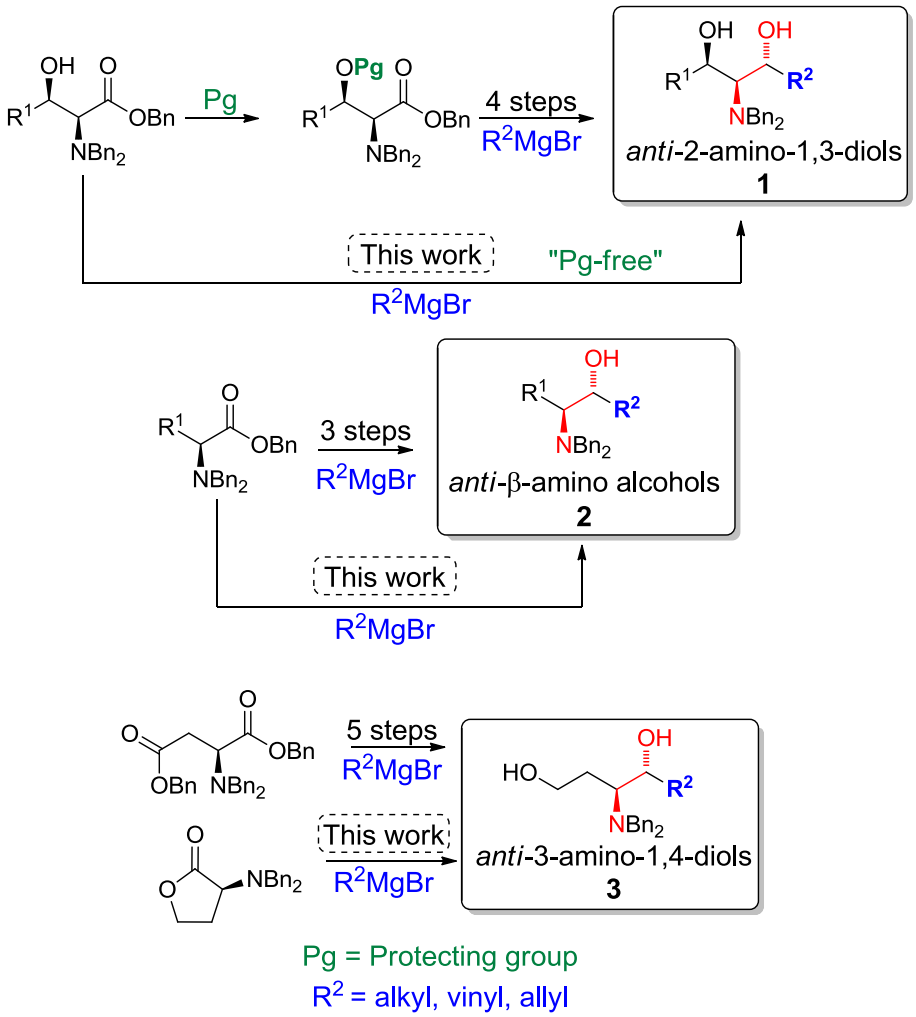

Figure 3.2. One-pot synthesis of *anti-β*-amino alcohols.

We observed that Et_2O was the best solvent, and we also determined that DIBAL-H amount and reduction time were a contributing factor in the yield of the reaction. When 3.6 equivalents of DIBAL-H during 1 h were used, a complete over-reduction to the alcohol was observed (entries 2 and 9, Table 3.1). After the amount of DIBAL-H was decreased to 1.4 equiv and the time reduction was increased to 2 h, a better yield (70%) was obtained (entry 4). The *anti*/*syn* ratio was determined by ^{1}H-NMR (400 MHz) of the crude reaction. The *anti*-diastereoisomer was always formed as the major stereoisomer and the ratio was not affected either by the reaction solvent, the amount of DIBAL-H or the reduction times.

Table 3.1. Reaction parameters for the synthesis of 5a.

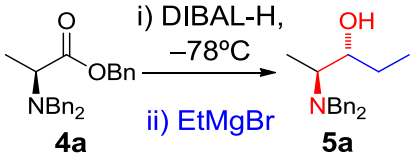

Entry	Reduction time (h)[a]	EtMgBr (equiv)	Solvent	DIBAL-H (equiv)	*anti*/*syn*[b]	Yield(%)
1	1	3	Et_2O	2.5	>95/1	35
2	1	3	Et_2O	3.6	-	-
3	2	3	Et_2O	2.5	>95/1	55
4	2	3	Et_2O	1.4	>95/1	70
5	2	1	Et_2O	1.4	>95/1	26
6	2	2	Et_2O	1.4	>95/1	33
7	2	4	Et_2O	1.4	>95/1	68
8	2	3	Et_2O	1.1	>95/1	48
9	1	3	DCM	3.6	-	-
10	2	3	DCM	2.5	>95/1	28
11	2	3	DCM	1.4	>95/1	13
12	2	3	THF	1.4	>95/1	38
13	2	3	Toluene	1.4	>95/1	63

[a] Delay time between the addition of DIBAL-H and the Grignard reagent. [b] Diastereoisomeric ratio as determined by ^{1}H NMR analysis of the crude product **5a**.

The stereochemical course of the process is consistent with the generation of a free aldehyde, while the nucleophilic attack of the Grignard reagent on the carbonyl follows a non-chelating Felkin-Anh model.[42] A S_N2-like mechanism involving elimination of a metalalkoxy group could explain the intermediate aldehyde.[41] In agreement with this proposal, the identity of the alkoxy group of the aluminoxy acetal should not affect the stereoselectivity of the alkylation

reaction. To test this hypothesis, a series of alanine esters (synthesized using different procedures)[43,44] were analyzed by ^{1}H-NMR to determine the effect of increasing the steric bulk of the alkoxy group of the ester on the stereoselectivity of the DIBAL-H reduction in Et_2O and subsequent EtMgBr addition (Table 3.2). From the results, we inferred that there is no correlation between the bulkiness of the ester group and the stereoselectivity of the reaction. We also concluded that the ester did not affect the yield of the reaction. The benzyl ester was the best choice because it is synthesized in one step by the direct perbenzylation of the free α-amino acid.

Table 3.2. Influence of the alkoxy group bulkiness in esters of *N,N*-dibenzyl-$_L$-alanine.

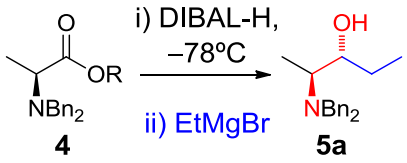

Entry	Compound	R	*anti*/*syn*[a]	Yield (%)
1	**4a**	Bn	>95/1	70
2	**4b**	*t*-Bu	92/8	68
3	**4c**	Et	94/6	65
4	**4d**	Me	>95/1	66

[a] Diastereoisomeric ratio determined by ^{1}H NMR analysis of the crude products.

Once we had adjusted the conditions, we studied the scope. Thus, **4** and **6** (synthesized by perbenzylation of the α-amino acids $_L$-alanine and $_L$-phenylalanine, respectively) were submitted, at –78 ºC, to our one-pot sequence using commercially available ethyl-, vinyl- and ethynylmagnesium bromide solutions affording the corresponding amino alcohols **5a-c** and **7a-c** (Table 3.3).

Table 3.3. Synthesis of *anti*-β-amino alcohols 5 and 7.

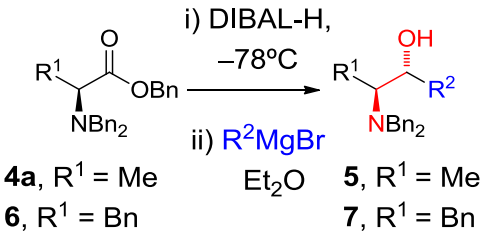

Entry	Compound	R^1	R^2	*anti*/*syn*[a]	Yield (%)
1	**5a**	Me	Et	>95/1	70
2	**5b**	Me	Vinyl	>95/1	60
3	**5c**	Me	Ethynyl	87/13	65
4	**7a**	Bn	Et	>95/1	72
5	**7b**	Bn	Vinyl	>95/1	63
6	**7c**	Bn	Ethynyl	90/10	70

[a] Diastereoisomeric ratio determined by ^{1}H NMR analysis of the crude products.

The *anti* diastereoselectivity (>95/1) of the reaction was determined by ^{1}H-NMR spectroscopy (400 MHz). We observed that the diastereoselectivity was not affected by the size of the substituent R^1 (Table 3.3), while the Grignard reagent produced a small influence. In this particular context, we observed a lower diastereomeric ratio using ethynylmagnesium bromide (entries 3 and 6). Fortunately, pure diastereoisomers of compounds **5** and **7** were obtained in good yields by flash column chromatography. The pure compounds showed good physical and spectroscopic data compliance, within the limits of experimental error, with those reported previously for **5a**,[31-33] **5c**,[35] **7a**[31,32] and **7c**.[35] To the best of our knowledge, products **5b** and **7b** are described for the first time in this work. To corroborate their structures, we synthesized the amino alcohols **8** and **9** by *N*-deprotection and double bond reduction of **5b** and **7b** respectively, with Pearlman's catalyst under hydrogen pressure (Scheme 3.1). The physical and spectral data of these compounds agree with those reported for **8** and **9** (Scheme 3.1).[31]

It has been described in the literature that during the DIBAL-H treatment, it is possible that some racemization of the enantiomerically pure aldehydes occurs. Therefore, we submitted both commercially available $_{DL}$-phenylalanine and $_{L}$-phenylalanine to our one-pot procedure

using as Grignard reagent ethylmagnesium bromide. The resulting compounds *rac*-**7a** and **7a** were analyzed by chiral HPLC to check their enantiomeric purity. The results showed that no loss of enantiomeric purity was observed.

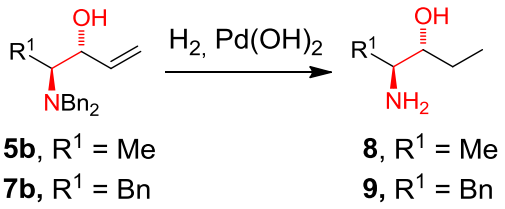

Scheme 3.1. Synthesis of amino alcohols 8 and 9.

3.2.2 Preparation of *anti*-2-amino-1,3-diols.

We wondered if our technique could be extended to the synthesis of more substituted *β*-amino alcohols and, more importantly, if it is compatible with free hydroxyl groups present in the substrate. To test this idea we selected *N*,*N*-dibenzylamino esters **10** and **11**, which were prepared by conventional methods using $_{L}$-serine and $_{L}$-threonine, respectively.[45] Gratifyingly, the synthesis of amino alcohols **12a-c** and **13a-c** were carried out using the same one-pot approach described above with good yields and excellent stereoselectivity (Table 3.4).

In this particular case, we needed to fine-tune the reaction conditions to improve the yield of **12** and **13**. We found that by using the general conditions described above, namely 1.4 equiv of DIBAL-H in ether (–78 ºC, 2 h) and 3 equivalents of Grignard reagent, we could obtain **12** and **13** although in low yields (≈ 40 %). The contaminating products were the carbinols resulting of the undesired addition of Grignard reagents to the ester groups. We suspected that because the presence of the free hydroxy group, an additional amount of DIBAL-H should be used. Fortunately, when we added, after 1 h, an extra amount of 0.7 equivalents of DIBAL-H allowing the reduction time to reach 2 h, the Grignard reagent addition produced the *anti*-diols **12** and **13** in good yields as shown in Table 3.4. It should be pointed out that necessarily the DIBAL-H addition must be done in two portions. When 2.1 equiv of the reducing agent was added in one portion and maintained during 2 h, a substantial amount of the primary alcohol was produced. In all cases, the reaction took place with a good yield and excellent stereoselectivity (*anti/syn* >95/1). Once again, the stereochemical course of the reaction could be explained by a Felkin-Anh model where the presence of a free hydroxy group did not affect

the stereoselectivity. Finally, it is important to mention that our approach avoids the use of *O*-protecting groups, the latter being used in all previously reported procedures for the synthesis of related compounds.[46-48]

Table 3.4. Synthesis of *anti*-2-amino-1,3-diols 12 and 13.

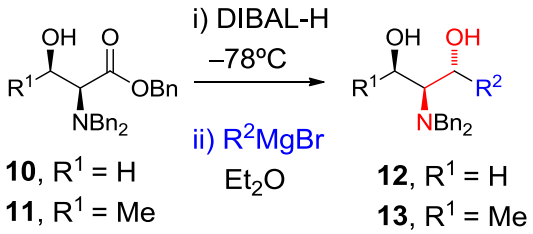

10, R^1 = H
11, R^1 = Me

12, R^1 = H
13, R^1 = Me

Entry	Compound	R^1	R^2	*anti*/*syn*[a]	Yield (%)
1	**12a**	H	Et	>95/1	60
2	**12b**	H	Vinyl	>95/1	70
3	**12c**	H	Ethynyl	>95/1	63
4	**13a**	Me	Et	>95/1	60
5	**13b**	Me	Vinyl	>95/1	63
6	**13c**	Me	Ethynyl	>95/1	58

[a] Diastereoisomeric ratio determined by ^{1}H NMR analysis of the crude products.

In order to determine the relative configuration of the obtained 1,3-diols, the six-membered acetonides **14a-c** and **15a-c** were synthesized (Figure 3.3) by treatment of diols **12a-c** and **13a-c**, respectively, with 2,2-dimethoxypropane (DMP) in the presence of pyridinium *p*-toluensulfonate (PPTS) in DCM (Figure 3.3).

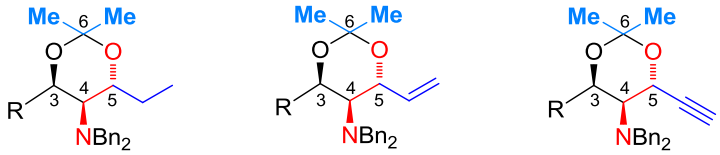

14a, R = H
15a, R = Me

14b, R = H
15b, R = Me

14c, R = H
15c, R = Me

Figure 3.3. Acetonides prepared to assign the relative configuration.

The acetonides **14a-c** showed a $J_{4,5}$ value of approximately 9.8 Hz which is in agreement with the *anti*-configuration reported.[49-51] Moreover, in acetonides **15a** and **15b** the 1,3-*anti* relation was established by ^{13}C NMR analysis of methyl (marked in bold blue face, Figure 3.3) signals (24.5 and 24.8 ppm for **15a** and 24.6 and 24.9 ppm for **15b**), and C-6 (100.3 and 100.4 ppm for **15a** and **15b**, respectively). In addition, the *anti*-relation of H-4 and H-5 was determined by the value of the coupling constant ($J_{4,5}$ = 7.4 Hz for both) which is in agreement with previous data reported.[52] The relative configuration of compound **15c** was determined by the $J_{5,6}$ = 4.8 Hz value, which is in agreement with the *anti*-configuration data reported.[53]

3.2.3. Synthesis of *anti*-3-amino-1,4-diols.

In a third application of the methodology, we examined the addition of EtMgBr to lactone **16** previously treated with DIBAL-H (Table 3.5). Lactone **16** was synthesized using $_{L}$-methionine as starting material.[54] For the synthesis of **17a** we decided to test the same one-pot methodology as for the compounds **3a-c** and **4a-c** (1.4 equiv of DIBAL-H, at –78 ºC for 2 h and subsequently addition of EtMgBr). Under the reaction conditions, the desired product **17a** was obtained in high yield and stereoselectivity (95% yield and *anti*/*syn* >95/1, Table 3.5). Furthermore, we tested this reaction with diverse Grignard reagents, allowing the synthesis of **17b** and **17c**.

The relative configuration of **17a-c** was determined by converting them to the lactones **18a-c** with tetrapropylammonium perruthenate (TPAP) and *N*-methylmorpholine *N*-oxide (NMO) (Figure 3.4). The ^{1}H NMR vicinal coupling constant between the protons H-3 and H-4 in the lactones **18a-c** showed a $J_{3,4}$ = 4.3 Hz, indicating an *anti*-configuration.[31,55,56]

Table 3.5. Synthesis of *anti*-3-amino-1,4-diols 17a-c.

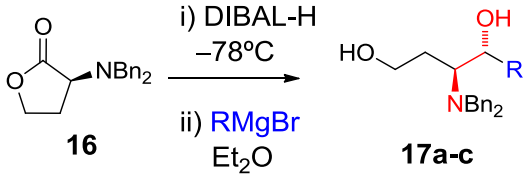

Entry	Compound	R	*anti*/*syn*[a]	Yield (%)
1	**17a**	Et	>95/1	95
2	**17b**	Vinyl	>95/1	96
3	**17c**	Ethynyl	>95/1	80

[a] Diastereoisomeric ratio determined by ^{1}H NMR analysis of the crude products.

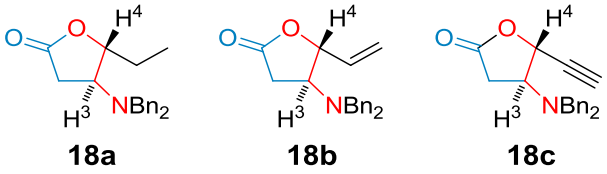

Figure 3.4. Lactones prepared to assign the relative configuration.

3.2.4 Synthetic applications.

In order to assess the wider application of our methodology, we turned our attention to spisulosine (**2c**). Using the same experimental procedure described above for the synthesis of *anti*-*β*-amino alcohols, **2c** could be prepared in just two steps from **4a** using pentadecynylmagnesium bromide as the Grignard reagent (Scheme 3.2). We observed that our one-pot methodology provided **19** as only one diastereomer (within limits of ^{1}H NMR detection in the crude reaction mixture) in good yield. The *N*-deprotection and reduction of the triple bond using hydrogenation with Pearlman's catalyst provided spisulosine (**2c**), in 42% overall yield.[6,57,58]

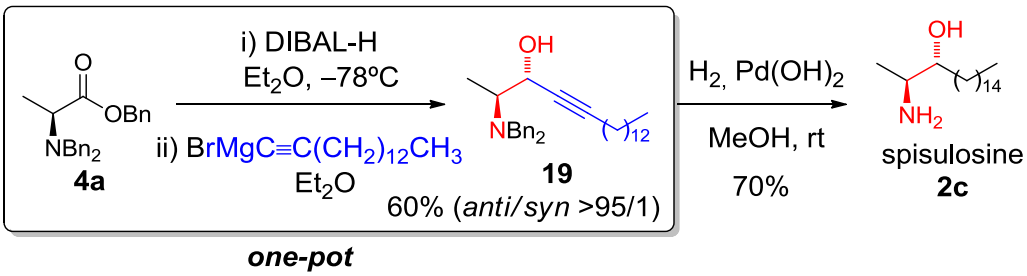

Scheme 3.2. Synthesis of spisulosine (2c).

Similarly, the synthesis of sphinganine (**1b**) was carried out using the same experimental procedure described for the synthesis of compounds **12a-c** and it is shown in Scheme 3.3. First, we obtained product **20** by the addition of pentadecynylmagnesium bromide to the aldehyde previously formed from **10**, in 75% yield and with high diastereoselectivity (*anti*/*syn* >95/1), without using protecting groups.[36] Further hydrogenation of **20** with Pearlman's catalyst provided sphinganine (**1b**) in 45% overall yield.[59]

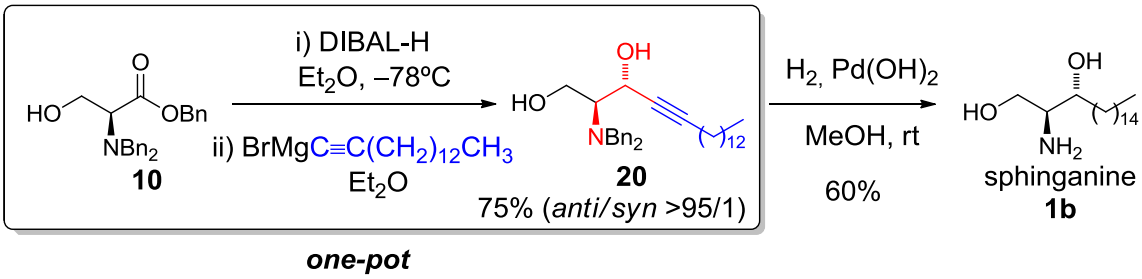

Scheme 3.3. Synthesis of sphinganine (1b).

3.3. Conclusion

In summary, a new general one-pot methodology has been developed for the synthesis of enantiopure *anti*-*β*-amino alcohols from *α*-dibenzylamino esters having their origin in *α*-amino acids, in good yields and excellent diastereoselectivity. Our results showed that optically active *α*-dibenzylamino esters can be reduced and converted into *β*-amino alcohols by subsequent addition of diverse Grignard reagents avoiding the problem of instability of the aldehydes. Presumably, these additions proceed under nonchelation control involving the aldehyde formed in situ using DIBAL-H at –78 ºC. Similarly, *anti*-2-amino-1,3-diols and *anti*-

3-amino-1,4-diols were obtained. Our technique is compatible with free hydroxyl groups present in the substrate. Considering the simplicity of preparing these products, we tested this methodology synthesizing spisulosine and sphinganine. Further studies on the synthesis of other derivatives and related natural products are in progress. The in vitro antiproliferative activity against human solid tumor cells is being evaluated with promising results and will be reported in due course.

3.4. References

1. Anaya de Parrodi, C.; Juaristi, E. *Synlett* **2006**, 2699.
2. Ager, D. J.; Prakash, I.; Schaad, D. R. *Chem. Rev.* **1996**, *96*, 835.
3. Métro, T.-X.; Gomez-Pardo, D, Cossy, J. *J. Org. Chem.* **2008**, *73*, 707.
4. Weinstein, A. B.; Schuman, D. P.; Tan, Z. X.; Stahl, S. S. *Angew. Chem. Int. Ed.* **2013**, *52*, 11867.
5. Bergmeier, S. C. *Tetrahedron*, **2000**, *56*, 2561.
6. Choi, Jae-Hoon.; Yoshida, M.; Suzuki, T.; Harada, E.; Kawade, M.; Yazawa, K.; Nishimoto S.; Hirai, H, Kawagishi, H. *Tetrahedron*, **2013**, *69*, 8609.
7. Abad, J. L.; Nieves, I.; Rayo, P.; Casas, J.; Fabriàs, G.; Delgado, A. *J. Org. Chem*. **2013**, *78*, 5858.
8. Menna, M. *Phytochem. Rev*. **2009**, *8*, 461.
9. Padrón, J. M. *Curr. Med. Chem*. **2006**, *13*, 755.
10. Aiello, A.; Fattorusso, E.; Giordano, A.; Menna, M.; Navarrete, C.; Muñoz, E. *Bioorg. Med. Chem*. **2007**, *15*, 2920.
11. Aiello, A.; Fattorusso, E.; Giordano, A.; Menna, M.; Navarrete, C.; Muñoz, E. *Tetrahedron* **2009**, *65*, 4384.
12. Reiehart, K. L.; Fregau, N. L.; Warwick, R. A.; Garcia Gravalos, D.; Avila, J.; Faircloth, G. T. PCT WO9952521 A1 19991021, **1999**.
13. Sanchez, A. M.; Malagarie-Cazenave, S.; Olea, N.; Vara, D.Cuevas, C.; Diaz-Laviada, I. *Eur. J. Pharmacol*. **2008**, *584*, 237.
14. Williams, R. *Expert Opin. Invest. Drugs*, **2009**, *18*, 1581.
15. Garrido, L.; Zubia, E.; Ortega, M. J.; Naranjo, S.; Salva, J. *Tetrahedron*. **2001**, *57*, 4579.
16. Jares-Erijman, E. A.; Bapat, C. P.; Lithgow-Bertelloni, A.; Rinehart, K. L.; Sakai, R. *J. Org. Chem.* **1993**, *58*, 5732.
17. Jimenez, C.; Crews, P. *J. Nat. Prod*. **1990**, *53*, 978.
18. Kokotos, G.; Padrón, J. M..; Noula, C.; Gibbons, W. A.; Martín, V. S. *Tetrahedron: Asymmetry* **1996**, *7*, 857.
19. Padrón, J. M.; Kokotos, G.; Martín, T.; Markidis, T.; Gibbons, W. A.; Martín, V. S. *Tetrahedron: Asymmetry* **1998**, *9*, 3381.
20. Kokotos, G.; Padrón, J. M.; Martín, T.; Gibbons, W. A.; Martín, V. S. *J. Org. Chem.* **1998**, *63*, 3741.
21. Padrón, J. M.; Martín, V. S.; Hadjipavlou-Litina, D.; Noula, C.; Constantinou-Kokotou, V.; Peters, G. J.; Kokotos, G. *Bioorg. Med. Chem. Lett.* **1999**, *9*, 821.

22. Markidis, T.; Padrón, J.M.; Martín, V.S.; Peters, G.J.; Kokotos, G. *Anticancer Res.* **2001**, *21*, 2835.
23. Padrón, J. M.; Peters, G. J. *Invest. New Drugs* **2006**, *24*, 195.
24. Reetz, M. T.; Drewes, M. W.; Schmitz, A. *Angew. Chem. Int. Ed.* **1987**, *26*, 1141.
25. Reetz, M. T.; Rölfing, K.; Griebenow, N. *Tetrahedron Lett.* **1994**, *35*, 1969.
26. Reetz, M. T. *Chem. Rev.* **1999**, *99*, 1121.
27. Bolis, G.; Fung, A. K.; Greer, J.; Kleinert, H. D.; Marcotte, P. A.; Perun, T. J.; Plattner, J. J.; Stein, H. H. *J. Med. Chem*. **1987**, *30*, 1729
28. Kano, S.; Yusa, Y.; Yokomatsu, T.; Shibuya, S. *Chem. Pharm. Bull*. **1989**, *37*, 2867.
29. Ibuka, T.; Habashita, H.; Otaka, A.; Fujii, N. *J. Org. Chem.* **1991**, *56*, 4370.
30. Bonar-Law, R. P.; Davis, A. P.; Dorgan, B. J.; Reetz, M. T.; Wehrsig, A. *Tetrahedron Lett*. **1990**, *31*, 6725.
31. Andrés, J. M.; Barrio, R.; Martínez M. A.; Pedrosa, R.; Pérez-Encabo, A. *J. Org. Chem.* **1996,** *61*, 4210.
32. Concellón, J. M.; Bernad, P. L.; Pérez-Andres, J. A. *J. Org. Chem.* **1997,** *62*, 8902.
33. Oppolzer, W.; Tamura, O.; Sundarababu, G.; Singer, M. *J. Am. Chem. Soc.* **1992**, *114*, 5900.
34. Andrés, J. M.; Muñoz, E. M.; Pedrosa, R.; Pérez-Encabo, A. *Eur. J. Org. Chem.* **2003**, 3387.
35. Andrés, J. M.; Pedrosa, R.; Pérez-Encabo, A. *Eur. J. Org. Chem*. **2006**, 3442.
36. Masuda, Y.; Tashiro, T.; Mori, K. *Tetrahedron: Asymmetry* **2006**, *17*, 3380.
37. Andrés, J. M.; Pedrosa, R.; Pérez-Encabo, A. *Tetrahedron Lett.* **2006**, *47*, 5317.
38. Andrés, J. M.; Pedrosa, R.; Pérez-Encabo, A.; Ramírez, M. *Tetrahedron,* **2006**, *62*, 7783.
39. Reetz, M. T.; Drewes, M. W.; Schwickardi, R. *Org. Synth.* **1999**, *76*, 110.
40. Ordóñez, M.; de la Cruz, R.; Fernandez-Zertuche, M.; Muñoz-Hernández, M.-A. *Tetrahedron: Asymmetry,* **2002**, *13*, 559.
41. Polt, R.; Peterson, M. A.; De Yung, L. *J. Org. Chem.* **1992**, *57*, 5469.
42. Cherest, M.; Felkin, H.; Prudent, N. *Tetrahedron Lett*. **1968**, 18, 2199.
43. Brook, M. A.; Chan, T. H. *Synthesis* **1983**, 201.
44. Mei, D.; Zhang, W.; Li, Y.; *Synthetic Comm*. **2010**, *40*, 1099.
45. Higgins, G.; Slassi, A.; Isaac, M.; *US2010/0016403*.
46. Andrés, J. M.; Pedrosa, R. *Tetrahedron: Asymmetry* **1998**, *9*, 2493.
47. Laïb, T.; Chastanet, J.; Zhu, J. *J. Org. Chem.* **1998,** *63*, 1709.

48. Bi-Shuang, C.; Long-He, Y.; Jian-Liang Y.; Tao, H.; Yuan-Ping, R.; Jin, F.; Pei-Qiang, H. *Eur. J. Med. Chem.* **2011**, *46*, 5480.
49. Boutin, R. H.; Rapoport, H. *J. Org. Chem.* **1986**, *51*, 5320.
50. Hafner, A.; Duthaler, R. O.; Marti, R.; Rihs, G.; Rothe-Streit, P.; Schwarzenbach, F. *J. Am. Chem. Soc***. 1992**, *114*, 2321.
51. Van Overmeire, I.; Boldin, S. A.; Dumont, F.; Van Calenbergh, S.; Slegers, G.; De Keukeleire, D.; Futerman, A. H.; Herdewijn, P. *J. Med. Chem.* **1999**, *42*, 2697.
52. Rychnovsky S. D.; Rogers, B.; Yang, G. *J. Org. Chem.* **1993**, *58*, 3511.
53. Marshall, J. A.; Seletsky, B. M.; Coant, P. S. *J. Org. Chem.* **1994**, 59, 5139.
54. White, J. D.; Hansen, J. D. *J. Org. Chem.* **2005**, *70*, 1963.
55. Hauser, F. M.; Rhee, R. P.; Ellenberger, S. R. *J. Org. Chem.* **1984**, *49*, 2236.
56. Davies, S. G.; Smyth, G. D.; Chippindale, A. M. *J. Chem. Soc*., *Perkin Trans.* **1999**, *1*, 3089.
57. Ghosal, P.; Shaw, A. K. *Tetrahedron Lett*. **2010**, *51*, 4140.
58. Xu, K.; Lai, G.; Zha, Z.; Pan, S.; Chen, H.; Wang, Z. *Chem. Eur. J*. **2012**, *18*, 12357.
59. Kobayashi, S.; Furuta, T. *Tetrahedron* **1998**, *54*, 10275.

3.5. Experimental Section

3.5.1. General Remarks

Reactions were performed using oven-dried glassware under an atmosphere of argon. Reagent-grade chemicals were obtained from diverse commercial suppliers and were used as received. Optical rotations were measured with a polarimeter at the sodium line at different temperatures in $CHCl_3$. $^1H/^{13}C$ NMR spectra of the samples as $CDCl_3$ solutions were recorded at 400/100 MHz or at 500/125 MHz or 600/150 MHz respectively at 298 K. Chemical shifts (δ) are quoted in ppm and referenced to internal TMS (δ = 0 ppm) for ^1H NMR and $CDCl_3$ (δ = 77.0 ppm) for ^{13}C NMR; coupling constants (*J*) are quoted in Hz. Data are reported as follows: s, singlet; d, doublet; t, triplet; q, quartet; quin, quintet, sex, sextet, sep, septet, m, multiplet; br, broad. 2D NMR techniques were used to assist in structure elucidation. IR spectra were recorded neat on a FT-ATR IR system and the data are reported in reciprocal centimeters (cm^{-1}). Accurate mass (HRMS) were determined by electrospray ionization (ESI-TOF) and electronic impact (EI-TOF). Reactions were monitored using thin-layer chromatography (TLC) on aluminum packed percolated Silica Gel 60 F_{254} plates. Flash column chromatography was carried out with silica gel 60 (particle size less than 0.020 mm) by using appropriate mixtures of ethyl acetate and hexanes as eluent. Compounds were visualized by use of UV light and 2.5% phosphomolybdic acid in ethanol. All reactions involving air- or moisture-sensitive materials were carried out under Argon atmosphere. Anhydrous magnesium sulfate was used for drying solutions. Melting points were measured with micro melting point apparatus. Chemical nomenclature was generated using Chem Bio Draw Ultra 13.0.

3.5.2. Synthetic procedures and characterization for the glutamic acid derivatives

(2*S*,3*R*)-2-(dibenzylamino)pentan-3-ol (5a).[28-30] To a cooled (–78 ºC) solution of **4a** (100 mg, 0.28 mmol) in dry Et_2O (3 mL) under argon was added DIBAL-H (0.4 mL, 0.4 mmol, 1 M in hexane). After stirring for 2 h, ethylmagnesium bromide solution (0.3 mL, 0.84 mmol, 3 M in Et_2O) was carefully added at –78 ºC, and the mixture was allowed to warm to –10 ºC and stirred for 18 h. Then, the mixture was warmed up to 0 ºC and quenched with saturated NH_4Cl (8 mL). The mixture was extracted with Et_2O (10 mL × 3). The combined organic phases were washed with brine, dried over $MgSO_4$, filtered and concentrated in vacuum. The residue was purified by flash chromatography on silica gel (eluent AcOEt/PE, 98:2), to give **5a** (56.6 mg, 0.20 mmol, 70% yield) as a colorless oil. $[\alpha]^{25}_D$ +48.1 (*c*, 1.0, $CHCl_3$).

(3*R*,4*S*)-4-(dibenzylamino)pent-1-en-3-ol (5b). The procedure described above was applied to **4a** on a 0.28 mmol (100 mg) scale with vinylmagnesium bromide solution (0.84 mL, 0.84 mmol, 1 M in THF), to give **5b** (47 mg, 0.17 mmol, 60% yield) as a colorless oil. $[\alpha]^{25}_D$ = +5.99

(*c*, 1.03, $CHCl_3$); ^{1}H NMR (400 MHz, $CDCl_3$): δ = 1.05 (d, 3H, *J* = 6.9 Hz), 2.76 (br, 1H), 2.87 (q, 1H *J* = 6.6 Hz), 3.33 (d, 2H, *J* = 13.7 Hz), 3.73 (d, 2H, *J* = 13.7 Hz), 3.94 (br, 1H), 5.07 (d, 1H, *J* = 10.4 Hz), 5.26 (dd, 1H, J_1 = 17.3, J_2 = 1.3 Hz), 5.90 (ddd, 1H, J_1 = 16.2, J_2 = 10.5, J_3 = 5.5 Hz); ^{13}C NMR (100 MHz, $CDCl_3$): δ = 139.8, 139.2, 128.9, 128.4, 127.1, 115.2, 73.8, 57.1, 54.9, 9.0; IR (ATR-neat) ν_{max} = 3409, 3031, 1644, 1605, 1455, 924; HRMS (ESI-TOF) (m/z) [M + H^+] = calcd for $C_{19}H_{24}NO$ 282.1858, found 282.1861.

(3*R*,4*S*)-4-(dibenzylamino)pent-1-yn-3-ol (5c).[32] The procedure described above was applied to **4a** on a 0.28 mmol (100 mg) scale with ethynylmagnesium bromide solution (1.68 mL, 0.84 mmol, 0.5 M in THF), to give **5c** (50.8 mg, 0.18 mmol, 65% yield) a solid. mp = 54-55 ºC; $[\alpha]^{25}_D$ = +31.0 (*c*, 0.6, $CHCl_3$).

(2*S*,3*R*)-2-(dibenzylamino)-1-phenylpentan-3-ol (7a).[28,29] The procedure described for the synthesis of compound **5a** was applied to **6** (100 mg, 0.23 mmol) using DIBAL-H (0.32 mL, 0.32 mmol, 1 M in hexane) and ethylmagnesium bromide solution (0.23 mL, 0.69 mmol, 3 M in Et_2O), to give **7a** (59.4 mg, 0.17 mmol, 72% yield) as a colorless oil. $[\alpha]^{25}_D$ = +21.0 (*c*, 1.0, $CHCl_3$).

(3*R*,4*S*)-4-(dibenzylamino)-5-phenylpent-1-en-3-ol (7b). The procedure described for the synthesis of compound **7a** was applied to **6** (100 mg, 0.23 mmol) using vinylmagnesium bromide solution (0.69 mL, 0.69 mmol, 1 M in THF), to give **7b** (51.8 mg, 0.15 mmol, 63% yield) as a colorless oil. $[\alpha]^{25}_D$ = +3.6 (*c*, 1.0, $CHCl_3$); ^{1}H NMR (400 MHz, $CDCl_3$): δ = 2.76 (dd, 1H, J_1 = 13.7, J_2 = 8.1 Hz), 2.92 (d, 1H, *J* = 7.3 Hz), 3.10 (dd, 1H, J_1 = 13.7, J_2 = 6.5 Hz), 3.17-3.21 (m, 1H), 3.52 (d, 2H, *J* 13.6 Hz), 3.86 (d, *J* = 13.6 Hz), 4.04-4.05 (m, 1H), 5.17 (d, *J* = 10.5 Hz), 5.38 (d, *J* = 17.3 Hz), 6.06 (ddd, 1H, J_1 = 15.9, J_2 = 10.5, J_3 = 5.0 Hz), 7.17-7.31 (m, 15H); ^{13}C NMR (100 MHz, $CDCl_3$): δ = 139.8, 139.5, 138.5, 129.3, 128.9, 128.5, 128.4, 127.2, 126.2, 115.5, 71.0, 63.2, 55.3, 31.7; IR (ATR-neat) ν_{max} = 3435, 3026, 1641, 1602, 1453, 922, 920*;* HRMS (ESI-TOF) (m/z) [M + H^+] = calcd for $C_{25}H_{28}NO$ 358.2171, found 358.2160.

(3*R*,4*S*)-4-(dibenzylamino)-5-phenylpent-1-yn-3-ol (7c).[32] The procedure described for the synthesis of compound **7a** was applied to **6** (100 mg, 0.23 mmol), with ethynylmagnesium bromide solution (1.38 mL, 0.69 mmol, 0.5 M in THF), to give **7c** (57.2 mg, 0.161 mmol, 70% yield) as a colorless solid. mp = 131-132 ºC; $[\alpha]^{25}_D$ = +63.1.0 (*c*, 1.0, $CHCl_3$).

(2*S*,3*R*)-2-aminopentan-3-ol (8).[28] To a solution of **5b** (100 mg, 0.36 mmol), in 5 mL of dry MeOH were added 10 mg of 20% Pd $(OH)_2$-C in one portion. The mixture was stirred under 1 atm of H_2, at room temperature for 18 h. After completion of the reaction, the catalyst was removed by filtration through Celite and washed with 20 mL of MeOH. The solvent was

evaporated under reduced pressure to afford **8** (36.2 mg, 0.32 mmol, 90% yield) as colorless oil. $[\alpha]^{25}_{D}$ = +14.6 (*c*, 1.0, $CHCl_3$).

(2*S*,3*R*)-2-amino-1-phenylpentan-3-ol (9).[28] The procedure described above was applied to **7b** on a 0.28 mmol (100 mg) scale, to give **9** (42.5 mg, 0.26 mmol, 92% yield) as a colorless solid**;** mp = 104-106 ºC; $[\alpha]^{25}_{D}$ = +39.0 (*c*, 1.0, $CHCl_3$).

(2*S*,3*R*)-2-(dibenzylamino)pentane-1,3-diol (12a). To a cooled (–78 ºC) and stirred solution of *N*,*N*-amino benzyl ester **10** (100 mg, 0.27 mmol) in dry Et_2O (3 mL), under argon was added DIBAL-H in two portions (0.38 mL, 0.38 mmol, 1 M in hexane; and 1 h later 0.19 mL, 0.19 mmol). One hour after the addition of the second portion of DIBAL-H, ethylmagnesium bromide solution (0.27 mL, 0.81 mmol, 3 M in Et_2O) was carefully added and the mixture was allowed to warm to –10 ºC and stirred for 18 h. Then, the mixture was warmed to 0 ºC and quenched with saturated NH_4Cl (8 mL). The mixture was extracted with Et_2O (10mL × 3), the combined organic phases were washed with brine, dried over $MgSO_4$, filtered and concentrated in vacuum. The residue was purified by flash chromatography on silica gel flash (eluent gradient AcOEt/PE, 8:2 to 7:3), to give **12a** (48.5 mg, 0.16 mmol, 60% yield) as a colorless oil. $[\alpha]^{25}_{D}$ = –7.5 (*c*, 1.2, $CHCl_3$); ^{1}H NMR (400 MHz, $CDCl_3$): δ = 0.82 (t, 3H, *J* = 7.4 Hz), 1.34 (sep, 1H, *J* = 7.5 Hz), 1.67 (m, 1H), 2.63 (q, 1H, *J* = 5.8 Hz), 3.64 (d, 2H, *J* = 13.7 Hz), 3.72-3.75 (m, 3H), 3.82 (m, 1H), 7.18-7.27 (m, 10H); ^{13}C NMR (100 MHz, $CDCl_3$): δ = 139.6, 129.0, 128.4, 127.1, 72.7, 61.9, 59.0, 54.6, 28.6, 9.9; IR (ATR-neat) ν_{max} = 3371, 3062, 3028, 2962, 1493, 1453, 1365; HRMS (ESI-TOF) (m/z) [M + H^+] = calcd for $C_{19}H_{25}NO_2$ 300.1964, found 300.1968.

(2*S*,3*R*)-2-(dibenzylamino)pent-4-ene-1,3-diol (12b). The procedure described above for the synthesis of compound **12a** was applied to **10** on a 0.27 mmol (100 mg) scale using vinylmagnesium bromide solution (0.81 mL, 0.81 mmol, 1 M in THF) to give **12b** (56 mg, 0.19 mmol, 70% yield) as a colorless oil. $[\alpha]^{25}_{D}$ = –23.0 (*c*, 1.2, $CHCl_3$); ^{1}H NMR (400 MHz, $CDCl_3$): δ = 2.80 (q, 1H, *J* = 5.8 Hz), 3.67-3.79 (m, 5H), 3.84-3.87 (m, 1H), 4.41 (t, 1H, *J* = 5.8 Hz), 5.14 (d, 1H, *J* = 10.4 Hz), 5.25 (d, 1H, *J* = 17.3 Hz), 5.88 (ddd, J_1 = 16.8, J_2 = 10.4*;* J_3 = 6.1 Hz), 7.18-7.27 (m, 10H); ^{13}C NMR (100 MHz, $CDCl_3$): δ = 139.9, 139.5, 129.0, 128.6, 128.4, 127.2, 115.7, 72.0, 62.4, 59.0, 54.6; IR (ATR-neat) ν_{max} =3361, 3063, 3027, 1602, 1493, 1452, 1365; HRMS (ESI-TOF) (m/z) [M + H^+] = calcd for $C_{19}H_{23}NO_2$ 298.1807, found 298.1816.

(2*S*,3*R*)-2-(dibenzylamino)pent-4-yne-1,3-diol (12c). The procedure described above for the synthesis of compound **12a** was applied to **10** on a 0.27 mmol (100 mg) scale using ethynylmagnesium bromide solution (1.62 mL, 0.81 mmol, 0.5 M in THF) to give **12c** (50.2

mg, 0.17 mmol, 63% yield) as a colorless oil. $[\alpha]^{25}_{D}$ = –18.8 (*c*, 0.83, $CHCl_3$); ^{1}H NMR (400 MHz, $CDCl_3$): δ = 2.46 (d, 1H, *J* = 1.9 Hz), 3.04 (t, 1H, *J* = 6.1 Hz), 3.17 (br, 1H), 3.72 (d, 2H, *J* = 13.3 Hz), 3.81-3.84 (m, 1H), 3.92-3.98 (m, 3H), 4.46 (br, 1H), 7.19-7.27 (m, 10H); ^{13}C NMR (100 MHz, $CDCl_3$): δ = 139.1, 129.2, 128.5, 127.4, 83.8, 74.8, 61.8, 60.3, 59.6, 54.8; IR (ATR-neat) ν_{max} =3371, 3292, 3062, 3028, 1602, 1494, 1452, 1366; HRMS (ESI-TOF) (m/z) [M + Na^+] = calcd for $C_{19}H_{21}NO_2$ 318.1470, found 318.1474.

(2*R*,3*S*,4*R*)-3-(dibenzylamino)hexane-2,4-diol (13a). The procedure described above for the synthesis of compound **12a** was applied to **11** on a 0.26 mmol (100 mg) scale using ethylmagnesium bromide solution (0.26 mL, 0.78 mmol, 3 M in Et_2O) to give **13a** (50.1 mg, 0.16 mmol, 60% yield) as a colorless oil. $[\alpha]^{25}_{D}$ = –43.0 (*c*, 1.0, $CHCl_3$); ^{1}H NMR (400 MHz, $CDCl_3$): δ = 0.91 (t, 3H, *J* = 7.6 Hz), 1.18 (d, 3H, *J* = 6.1 Hz), 1.67-1.58 (m, 2H), 2.10 (br, 1H), 2.36 (dd, 1H, J_1 = 7.1, J_2 = 1.9 Hz), 3.48 (d, 2H, *J* = 13.5 Hz), 3.93-3.96 (m, 1H), 4.01 (d, 2H, *J* = 13.5 Hz), 4.13 (quin, 1H, *J* = 6.2 Hz), 7.16-7.29 (m, 10H); ^{13}C NMR (100 MHz, $CDCl_3$): δ = 139.4, 129.1, 128.4, 127.2, 70.9, 65.8, 64.9, 55.1, 30.2, 20.9, 18.8; IR (ATR-neat) ν_{max} = 3415, 3062, 3026, 2968, 2922, 1496, 1455, 1374; HRMS (ESI-TOF) (m/z) [M + H^+] = calcd for $C_{20}H_{27}NO_2$ 314.2120, found 314.2118.

(2*R*,3*S*,4*R*)-3-(dibenzylamino)hex-5-ene-2,4-diol (13b). The procedure described above for the synthesis of compound **12a** was applied to **11** on a 0.26 mmol (100 mg) scale using vinylmagnesium bromide solution (0.78 mL, 0.78 mmol, 1 M in THF) to give **13b** (50.9 mg, 0.16 mmol, 63% yield) as a colorless oil. $[\alpha]^{25}_{D}$ = –42.7 (*c*, 0.93, $CHCl_3$); ^{1}H NMR (400 MHz, $CDCl_3$): δ = 1.14 (d, 3H, *J* = 6.1 Hz), 2.52 (dd, 1H, J_1 = 7.6, J_2 =2.2 Hz), 3.60 (d, 2H, *J* = 13.5 Hz), 4.03 (d, 2H, *J* = 13.5 Hz), 4.12 (quin, 1H, *J* = 6.3 Hz), 4.56 (br, 1H), 5.11 (d, 1H, *J* = 10.5), 5.27 (d, 1H, *J* = 17.2 Hz) 5.86 (ddd, 1H, J_1 =16.7, J_2 = 10.5, J_3 = 5.2 Hz), 7.17-7.31 (m 10H); ^{13}C NMR (100 MHz, $CDCl_3$): δ = 140.4, 139.2, 129.1, 128.9, 128.5, 127.3, 114.8, 69.9, 66.4, 65.2, 55.3, 21.0; IR (ATR-neat) ν_{max} =3391, 3063, 3026, 1603, 1494, 1454; HRMS (ESI-TOF) (m/z) [M + H^+] = calcd for $C_{20}H_{25}NO_2$ 312.1964, found 312.1972.

(2*R*,3*S*,4*R*)-3-(dibenzylamino)hex-5-yne-2,4-diol (13c). The procedure described above for the synthesis of compound **12a** was applied to **11** on a 0.26 mmol (100 mg) scale using ethynylmagnesium bromide solution (1.56 mL, 0.78 mmol, 1 M in THF) to give **13c** (46 mg, 0.15 mmol, 58% yield) as a colorless oil. $[\alpha]^{25}_{D}$ = –33.8 (*c*, 1.02, $CHCl_3$); ^{1}H NMR (400 MHz, $CDCl_3$): δ = 1.25 (d, 3H, *J* = 6.0 Hz), 2.49 (d, 1H, *J* = 1.7 Hz), 2.77 (dd, 1H, J_1 =8.9, J_2 =4.9 Hz), 4.01 and 4.06 (2 x 2H, AB system, *J* = 13.1 Hz), 4.34-4.44 (m, 2H), 7.23-7.34 (m, 10H); ^{13}C NMR (100 MHz, $CDCl_3$): δ = 139.2, 129.5, 128.5, 127.3, 83.7, 74.7, 66.8, 65.6, 59.5, 55.5, 21.2; IR (ATR-neat) ν =3379, 3224, 3063, 3025, 1495, 1454, 1364; HRMS (ESI-TOF) (m/z)

[M + H^+] = calcd for $C_{20}H_{23}NO_2$ 310.1807, found 310.1805.

(4*R*,5*S*)-*N*,*N*-dibenzyl-4-ethyl-2,2-dimethyl-1,3-dioxan-5-amine (14a). To a solution of **12a** (20.0 mg, 0.07 mmol) were added DMS (0.8 mL, 0.85 mmol) and PPTS (5 mg, 0.02 mmol) in 2 mL of dry DCM. The solution was stirred for 18 h at room temperature. The solvent was then evaporated and the residue was chromatographed on silica gel flash (eluent AcOEt/PE, 95:5) to give **14a** (19.0 mg, 0.06 mmol, 80% yield) as a colorless oil. $[\alpha]^{25}_D$ = +68.1. (*c*, 0.93, $CHCl_3$); ^{1}H NMR (500 MHz, $CDCl_3$): δ = 0.75 (t, 3H, *J* = 7.4 Hz), 1.22 (s + m 4H), 1.29 (s, 3H), 1.83 (dsext, 1H, J_1 = 7.4, J_2 = 2.6 Hz), 2.64 (td, 1H, J_1 = 9.6, J_2 = 5.6 Hz), 3.45 (d, 2H, *J* = 14.3 Hz) 3.62 (dt, 1H, J_1 = 9.6, J_2 = 2.6 Hz), 3.76 (dd, 1H, J_1 = 11.9, J_2 = 5.6 Hz), 3.83 (d + dd, 3H, J_1 = 14.3, J_2 = 11.9, J_3 = 5.6 Hz) 7.13-7.26 (m, 10H); ^{13}C NMR (100 MHz, $CDCl_3$): δ = 139.7, 128.7, 128.0, 127.0, 99.0, 71.3, 58.2, 57.8, 54.8, 26.6, 25.6, 21.7, 9.7; IR (ATR-neat) ν_{max} = 3068, 2938, 2880, 1457, 1379, 1227, 1204, 1116; HRMS (ESI-TOF) (m/z) [M + H^+] = calcd for $C_{22}H_{30}NO_2$ 340.2277, found 340.2271.

(4*R*,5*S*)-*N*,*N*-dibenzyl-2,2-dimethyl-4-vinyl-1,3-dioxan-5-amine (14b). The procedure described above for the synthesis of compound **14a** was applied to **12b** (20 mg, 0.067 mmol) to give **14b** (18.5 mg, 0.05 mmol, 82% yield) as a colorless oil. $[\alpha]^{25}_D$ = +19.7 (*c*, 1.01, $CHCl_3$); ^{1}H NMR (500 MHz, $CDCl_3$): δ = 1.37 (s, 3H), 1.47 (s, 3H), 2.88 (ddd, 1H, J_1 =9.5, J_2 = 7.8, J_3 = 5.6 Hz), 3.66 (d, 2H, *J* = 13.8 Hz), 3.88 (dd, 1H, J_1 = 11.7, J_2 = 5.6 Hz), 3.93 (d, 2H, *J* = 13.8 Hz), 3.97 (dd, 1H, J_1 = 11.7, J_2 = 7.8 Hz), 4.40 (dd, 1H, J_1 = 9.8, J_2 = 6.5 Hz), 5.32 (d, 1H, *J* = 10.5 Hz), 5.42 (d, 1H, *J* = 17.1 Hz), 5.93 (ddd, 1H, J_1 = 17.1, J_2 = 10.5, J_3 = 6.5 Hz), 7.24-7.37 (m, 10H); ^{13}C NMR (100 MHz, $CDCl_3$): δ = 139.5, 137.7, 128.7, 127.1, 117.5, 98.8, 71.4, 59.1, 57.4, 54.7, 27.6; IR (ATR-neat) ν_{max} = 3503, 3063, 3027, 2989, 2936, 2887, 1602, 1493, 1453, 1200; HRMS (ESI-TOF) (m/z) [M + H^+] = calcd for $C_{22}H_{27}NO_2$ 338.2120, found 338.2117.

(4*R*,5*S*)-*N*,*N*-dibenzyl-4-ethynyl-2,2-dimethyl-1,3-dioxan-5-amine (14c). The procedure described above for the synthesis of compound **14a** was applied to **12c** (20 mg, 0.068 mmol) to give **14c** (18.2 mg, 0.05 mmol, 80% yield) as a colorless oil. $[\alpha]^{25}_D$ = +29.2 (*c*, 0.96, $CHCl_3$); ^{1}H NMR (500 MHz, $CDCl_3$): δ = 1.36 (s, 3H), 1.39 (s, 3H), 2.59 (d, 1H, *J* =2.1 Hz), 3.18 (ddd, 1H, J_1 = 9.8, J_2 = 7.5, J_3 = 5.6 Hz), 3.74 (d, 2H, *J* = 13.9 Hz), 3.79 (dd, 1H, J_1 = 10.4, J_2 = 5.6 Hz), , 3.84 (dd, 1H, J_1 = 10.4, J_2 = 7.5 Hz), 3.97 (d, 1H, *J* = 13.9 Hz), 4.66 (dd, 1H, J_1 = 9.8, J_2 = 2.1 Hz), 7.22-7.40 (m, 10H); ^{13}C NMR (100 MHz, $CDCl_3$): δ = 139.4, 128.7, 128.3, 127.1, 99.4, 82.6, 74.3, 61.3, 60.2, 57.6, 54.7, 27.1, 20.8; IR (ATR-neat) ν_{max} = 3288, 3062, 3028, 2991, 2124, 1703; HRMS (ESI-TOF) (m/z) [M + H^+] = calcd for $C_{22}H_{25}NO_2$ 336.1964, found 336.1969.

(4*R*,5*S*,6*R*)-*N*,*N*-dibenzyl-4-ethyl-2,2,6-trimethyl-1,3-dioxan-5-amine (15a). The procedure

described above for the synthesis of compound **14a** was applied to **13a** (20 mg, 0.064 mmol) to give **15a** (18.1 mg, 0.05 mmol, 80% yield) as a colorless oil. $[\alpha]^{25}_{D}$ = +27.2 (*c*, 0.3, $CHCl_3$); ^{1}H NMR (600 MHz, $CDCl_3$): δ = 0.83 (s, 3H), 1.26 (s, 3H), 1.33 (s, 3H), 1.27 (m, 1H), 1.40 (d, 1H, *J* =7.0 Hz), 1.69 (dsext, 1H, J_1 = 7.4, J_2 = 2.8 Hz), 2.60 (dd, 1H, J_1 = 7.4, J_2 = 5..0 Hz), 3.68 (td, 1H, J_1 = 7.4, J_2 = 2.8 Hz), 4.01-4.03 (br + m, 3H), 7.19-7.27 (m, 10H); ^{13}C NMR (100 MHz, $CDCl_3$): δ = 140.5, 128.6, 128.2, 126.8, 100.3, 70.9, 68.6, 61.0, 55.8, 24.8, 24.5, 17.8, 10.3; IR (ATR-neat) ν_{max} = 3067, 2987, 2936, 2855, 1458, 1380, 1228; HRMS (ESI-TOF) (m/z) [M + H^+] = calcd for $C_{23}H_{31}NO_2$ 354.2433, found 354.2437.

(4*R*,5*S*,6*R*)-*N*,*N*-dibenzyl-2,2,4-trimethyl-6-vinyl-1,3-dioxan-5-amine (15b). The procedure described above for the synthesis of compound **14a** was applied to **13b** (20 mg, 0.057 mmol) to give **15b** (15.8 mg, 0.05 mmol, 79% yield) as a colorless oil. $[\alpha]^{25}_{D}$ = –7.5 (*c*, 0.30, $CHCl_3$); ^{1}H NMR (600 MHz, $CDCl_3$): δ = 1.29 (s, 3H), 1.39 (s, 3H), 1.37 (d, 3H, *J* =6.9 Hz), 2.79 (dd, 1H, J_1 = 7.4, J_2 = 5.3 Hz), 3.89 (br, 2H), 4.07-4.11 (br + m, 3H), 4.46 (t, 1H, *J* = 7.4 Hz), 5.21 (d,1H, *J* = 10.4 Hz), 5.32 (d, 1H, *J* = 17.2 Hz), 5.88 (ddd, 1H, J_1 = 17.2, J_2 = 10.4, J_3 = 6.6 Hz), 7.19-7.37 (m, 10H); ^{13}C NMR (100 MHz, $CDCl_3$): δ = 140.1, 139.1, 128.6, 128.2, 126.8, 116.7, 100.4, 69.7, 67.9, 60.7, 55.4, 29.7, 25.0, 24.6, 17.4; IR (ATR-neat) ν_{max} = 3330, 3063, 3027, 2925, 2852, 1603, 1494, 1454, 1224; HRMS (ESI-TOF) (m/z) [M + H^+] = calcd for $C_{23}H_{29}NO_2$ 352.2277, found 352.2268.

(4*R*,5*S*,6*R*)-*N*,*N*-dibenzyl-4-ethynyl-2,2,6-trimethyl-1,3-dioxan-5-amine (15c). The procedure described above for the synthesis of compound **14a** was applied to **13c** (20 mg, 0.065 mmol), to give **15c** (18.8 mg, 0.05 mmol, 83% yield) as a colorless oil. **[**$\alpha]^{25}_{D}$ = +3.5 (*c*, 0.34, $CHCl_3$); ^{1}H NMR (600 MHz, $CDCl_3$): δ = 1.34 (d, 3H, *J* =6.5 Hz), 1.37 (s, 3H), 1.48 (s, 3H), 2.54 (d, 1H, *J* = 2.4 Hz), 2.87 (1H, t, *J* = 4.8 Hz), 3.70 (d, 2H, *J* = 13.4 Hz), 4.16 (br, 2H), 4.29 (dq, 1H, J_1 = 6.6, J_2 = 4.8 Hz), 4.94 (dd, 1H, *J*1 = 4.8, *J*2 = 2.4 Hz), 7.20-7.36 (m, 10H); ^{13}C NMR (100 MHz, $CDCl_3$): δ = 139.8, 128.7, 128.3, 126.9, 100.7, 84.4, 74.6, 66.5, 59.6, 58.8, 55.3, 27.2, 23.4, 17.4; IR (ATR-neat) ν_{max} =3400, 3063, 3028, 2925, 2336, 2963, 1734; HRMS (ESI-TOF) (m/z) [M + H^+] = calcd for $C_{23}H_{27}NO_2$ 350.2120, found 350.2129.

(3*S*,4*R*)-3-(dibenzylamino)hexane-1,4-diol (17a). The procedure described for the synthesis of compound **5a** was applied to **16** on a 0.7 mmol (200 mg) scale using ethylmagnesium bromide solution (0.7 mL, 2.1 mmol, 3 M in Et_2O). The residue was purified by flash chromatography on silica gel (eluent gradient AcOEt/PE, 8: 2 to 7:3) to give **17a** (203.9 mg, 0.65 mmol, 95% yield) as a colorless oil. **[**$\alpha]^{25}_{D}$ = –34.0 (*c*, 1.18, $CHCl_3$); ^{1}H NMR (400 MHz, $CDCl_3$): δ = 0.82 (t, 3H, *J* = 7.4 Hz), 1.30 (sep, 1H, *J* = 7.4 Hz), 1.43-1.56 (m, 1H), 1.96-2.05 (m, 1H), 2.60-2.64 (m, 1H), 3.46 (d, 2H, *J* = 13.6 Hz), 3.58 (br, 2H), 3.72-3.74 (d + m, 3H, *J* = 13.6 Hz), 7.50-7.24 (m,

10H); ^{13}C NMR (100 MHz, $CDCl_3$): δ = 139.4, 129.1, 128.4, 127.2, 71.4, 62.4, 61.1, 54.5, 28.7, 27.2, 10.4; IR (ATR-neat) ν_{max} =3314, 3063, 3028, 2930, 2960, 1494, 1453, 1365; HRMS (ESI-TOF) (m/z) [M + H^+] = calcd for $C_{20}H_{27}NO_2$ 314.2120, found 314.2119.

(3*S*,4*R*)-3-(dibenzylamino)hex-5-ene-1,4-diol (17b). The procedure described for the synthesis of compound **5a** was applied to **16** on a 0.7 mmol (200 mg) scale using vinylmagnesium bromide solution (2.1 mL, 2.1 mmol, 1 M in THF) to give **17b** (209.1 mg, 0.67 mmol, 96% yield) as a colorless oil. **[**$\alpha]^{25}_D$ = –31.4 (*c*, 1.26, $CHCl_3$); ^{1}H NMR (400 MHz, $CDCl_3$): δ = 1.59-1.68 (m, 1H), 2.10-2.19 (m, 1H), 2.88-2.92 (m, 1H), 3.68-3.72 (d + m, 4H, *J* = 13.5 Hz), 3.83 (d, 2H, *J* = 13.5 Hz), 4.45 (br, 1H), 5.2 (d, 1H, *J* = 10.4 Hz), 5.33 (d, 1H, *J* = 17.2 Hz), 5.93 (ddd, 1H, J_1 = 16.4, J_2 = 10.4, J_3 = 5.4 Hz), 7.28-7.37 (m, 10H); ^{13}C NMR (100 MHz, $CDCl_3$): δ = 140.1, 139.3, 129.1, 128.5, 127.3, 115.1, 70.9, 62.0, 60.8, 54.7, 27.2; IR (ATR-neat) ν_{max} =3337, 3063, 3027, 1602, 1494, 1452; HRMS (ESI-TOF) (m/z) [M + H^+] = calcd for $C_{20}H_{25}NO_2$ 312.1964, found 312.1964.

(3*S*,4*R*)-3-(dibenzylamino)hex-5-yne-1,4-diol (17c). The procedure described for the synthesis of compound **5a** was applied to **16** on a 0.7 mmol (200 mg) scale using ethynylmagnesium bromide solution (4.2 mL, 2.1 mmol, 0.5 M in THF) to give **17c** (173.1 mg, 0.56 mmol, 80% yield) as a colorless oil. **[**$\alpha]^{25}_D$ = –13.7. (*c*, 1.03, $CHCl_3$); ^{1}H NMR (400 MHz, $CDCl_3$): δ = 1.78-1.86 (m, 1H), 2.01-2.09 (m, 1H), 2.40 (d, 1H, *J* = 6.2 Hz), 3.55-3.57 (d + m, 3H, *J* = 13.3 Hz), 3.62-3.69 (m, 1H), 3.92 (d, 2H, *J* = 13.3 Hz), 4.38 (d, 1H, *J* = 4.4 Hz), 7.18-7.25 (m, 10H); ^{13}C NMR (100 MHz, $CDCl_3$): δ = 139.0, 129.3, 128.6, 127.4, 84.1, 74.6, 60.9, 60.7, 58.8, 54.8, 28.2; IR (ATR-neat) ν_{max} =3379, 3296, 3066, 3032, 1498, 1456, 1370; HRMS (ESI-TOF) (m/z) [M + H^+] = calcd for $C_{20}H_{23}NO_2$ 310.1807, found 310.1813.

(4*S*,5*R*)-4-(dibenzylamino)-5-ethyldihydrofuran-2(3H)-one (18a).[31] TPAP (32.0 mg, 0.09 mmol) was added to a stirred mixture of **17a** (278.7 mg, 0.89 mmol), NMO (320.0 mg, 2.67 mmol) and activated powdered molecular sieves (60 mg) in dry DCM (1 mL) at room temperature under argon. After stirring for 2 h, the reaction mixture was purified by column chromatography flash (eluent AcOEt/PE, 8:2) to give **18a** (137.6 mg, 0.45 mmol, 50% yield) as a colorless oil. **[**$\alpha]^{25}_D$ = +84.3 (*c*, 0.4, $CHCl_3$).

(4*S*,5*R*)-4-(dibenzylamino)-5-vinyldihydrofuran-2(3H)-one (18b). The procedure described for the synthesis of compound **18a** was applied to **17b** (50 mg, 0.16 mmol) to give **18b** (26.0 mg, 0.08 mmol, 51% yield) as a colorless oil. **[**$\alpha]^{25}_D$ = +27.8 (*c*, 0.7, $CHCl_3$); ^{1}H NMR (500 MHz, $CDCl_3$): δ = 2.60.(d, 2H, *J* = 7.1 Hz), 3.53 (ddd, 1H, J_1 = 7.3, J_2 = 6.7, J_3 = 4.6 Hz), 3.57 (d, 2H, *J* = 13.8 Hz), 3.71 (d, 2H, *J* =13.8 Hz), 4.98 (ddd, 1H, J_1 = 5.4, J_2 = 4.6, J_3 = 1.4 Hz), 5.24 (dd, 1H, J_1 = 10.5, J_2 = 1.0), 5.34 (dt, 1H, J_1 = 17.2, J_2 = 1.0 Hz), 5.76 (ddd, 1H, J_1 = 5.4,

J_2 = 4.6, J_3 = 1.4 Hz), 7.25-7.34 (m, 10H); ^{13}C NMR (100 MHz, $CDCl_3$): δ = 175.6, 138.2, 134.8, 128.5, 127.5, 117.3, 81.7, 60.6, 54.3, 29.7; IR (ATR-neat) ν_{max} = 3029, 2921, 1778, 1646, 1184, 1163, 987, 738, 700; HRMS (ESI-TOF) (m/z) [M + H^+] = calcd for $C_{20}H_{21}NO_2$ 308,1651, found 308.1651.

(4*S*,5*R*)-4-(dibenzylamino)-5-ethynyldihydrofuran-2(3H)-one (18c). The procedure described for the synthesis of compound **18a** was applied to **17c** (50 mg, 0.16 mmol) to give **18c** (24.4 mg, 0.08 mmol, 49% yield) as a colorless oil. **[**$\alpha]^{25}_D$ = +25.0 (*c*, 0.3, $CHCl_3$); ^{1}H NMR (500 MHz, $CDCl_3$): δ = 2.57 (dd, 1H, , J_1 = 18.4, J_2 = 4.4 Hz), 2.65 (d, 1, H, J = 2.2 Hz), 2.79 (dd, J_1 = 18.4, J_2 = 8.8 Hz), 3.63 2×2AB system, 4H, J = 13.8 Hz), 3.89 (qd, 1H, J_1 = 4.3, J_2 = 4.3 Hz), 5.13 (dd, J_1 = 4.3, J_2 = 2.2 Hz), 7.26-7.34 (m, 10H); ^{13}C NMR (100 MHz, $CDCl_3$) δ: = 174.7, 137.7, 128.7, 128.6, 127.6, 79.4, 70.3, 62.6, 54.1, 29.7; IR (ATR-neat) ν_{max} = 3283, 2925, 2123, 1787, 1453, 1194, 970, 911, 736, 631 ; HRMS (ESI-TOF) (m/z) [M + Na^+] = calcd for $C_{20}H_{19}NO_2$ 328.1313 found.328.1316.

(2*S*,3*R*)-2-(dibenzylamino)octadec-4-yn-3-ol (19). To a solution of 1-nonyne (0.14 mL, 0.84 mmol) in dry Et_2O (10 mL) was added ethylmagnesium bromide solution (0.28 mL, 0.84 mmol, 3 M in THF). The mixture was refluxed for 2.5 h and then it was allowed to cool down to room temperature. In parallel, to a cooled (–78 ºC) solution of **4a** (100 mg, 0.28 mmol) in dry Et_2O (3 mL) was added DIBAL-H (0.4 mL, 0.4 mmol, 1M in hexane) under argon atmosphere. After stirring for 2 h, a solution of alkynyl magnesium bromide previously formed was carefully added at –78 ºC. The mixture was allowed to warm to –10 ºC and stirred for 18 h. Then, the mixture was warmed to 0 ºC and quenched with saturated NH_4Cl (8 mL). The mixture was extracted with Et_2O (10 mL × 3), the organic phases were washed with brine, dried over $MgSO_4$, filtered and concentrated in vacuum. The residue was purified by flash chromatography on silica gel (eluent AcOEt/PE, 9:1) to give **19** (77.5 mg, 0.17 mmol, 60% yield) as a colorless oil $[\alpha]^{25}_D$ = –10.2 (*c*, 0.89, $CHCl_3$); ^{1}H NMR (400 MHz, $CDCl_3$): δ = 0.83 (t, 3H, J = 7.0 Hz), 1.14-1.25 (m, 23H), 1.39 (quin, 2H, J = 7.0 Hz), 2.13 (td, 2H, J_1 = 7.0, J_2 = 2.0 Hz), 2.95 (quin, 1H, J =6.6 Hz), 3.32 (d, 2H, J = 13.3 Hz), 3.89 (br, 1H), 4.14 (d + m, 3H, J = 13.3 Hz), 7.17-7.27 (m, 10H); ^{13}C NMR (100 MHz, $CDCl_3$): δ = 139.4, 129.1, 128.4, 127.2, 86.8, 80.0, 63.2, 56.0, 54.7, 31.9, 29.7, 29.5, 29.4, 29.1, 28.9, 28.6, 22.7, 18.8, 14.1, 9.5*;* IR (ATR-neat) ν = 3425, 2925, 2853, 1332, 747, 699; HRMS (EI-TOF) (m/z) [M - H_2O^+] = calcd for $C_{32}H_{47}NO$ 443, 3552, found 443.3541.

(2*S*,3*R*)-2-(dibenzylamino)octadec-4-yne-1,3-diol (20).[36] To a solution of 1-nonyne (0.13 mL, 0.81 mmol) in dry Et_2O (10 mL) was added ethylmagnesium bromide solution (0.27 mL, 0.81 mmol, 3 M in THF). The mixture was refluxed for 2.5 h and then it was allowed to cool down to

room temperature. In parallel, to a cooled (–78ºC) solution of **10** (100 mg, 0.27 mmol) in dry Et_2O (3 mL), under argon was added DIBAL-H in two portions (0.38 mL, 0.38 mmol, 1 M in hexane; and 45 min later 0.19 mL, 0.19 mmol). After additional stirring for 40 min at –78 ºC, a solution of the alkynyl magnesium bromide previously formed was carefully added at –78 ºC and the mixture was allowed to warm to –10 ºC and stirred for 18 h. Then, the mixture was cooled to 0 ºC and quenched with saturated NH_4Cl (8 mL). The mixture was extracted with Et_2O (10 mL × 3), the organic phases were washed with brine, dried over $MgSO_4$, filtered and concentrated in vacuum. The residue was purified by flash chromatography on silica gel flash (eluent AcOEt/PE, 8:2) to give **20** (90.2 mg, 0.19 mmol, 70% yield) as a colorless oil $[\alpha]^{25}_D$ = –37.6 (*c*, 0.94, $CHCl_3$).

(2*S*,3*R*)-2-aminooctadecan-3-ol (spisulosine, 2c).[6,53,54] The procedure described for the synthesis of compound **8** was applied to **19** (50 mg, 0.11 mmol) to give **2c** (25,1 mg, 0.09 mmol, 70% yield) as a white solid. mp = 65-67 ºC; $[\alpha]^{25}_D$.= +25.3 (*c*, 0.94, $CHCl_3$).

(2*S*,3*R*)-2-aminooctadecane-1,3-diol (sphinganine, 1b).[55] The procedure described for the synthesis of compound **8** was applied to **20** (50 mg, 0.10 mmol) to give **1b** (19.0 mg, 0.06 mmol, 60% yield) as a white solid. mp = 70-72 ºC; $[\alpha]^{25}_D$.= +0.62 (*c*, 0.57, EtOH).

3.5.3. High-performance liquid chromatography (HPLC)

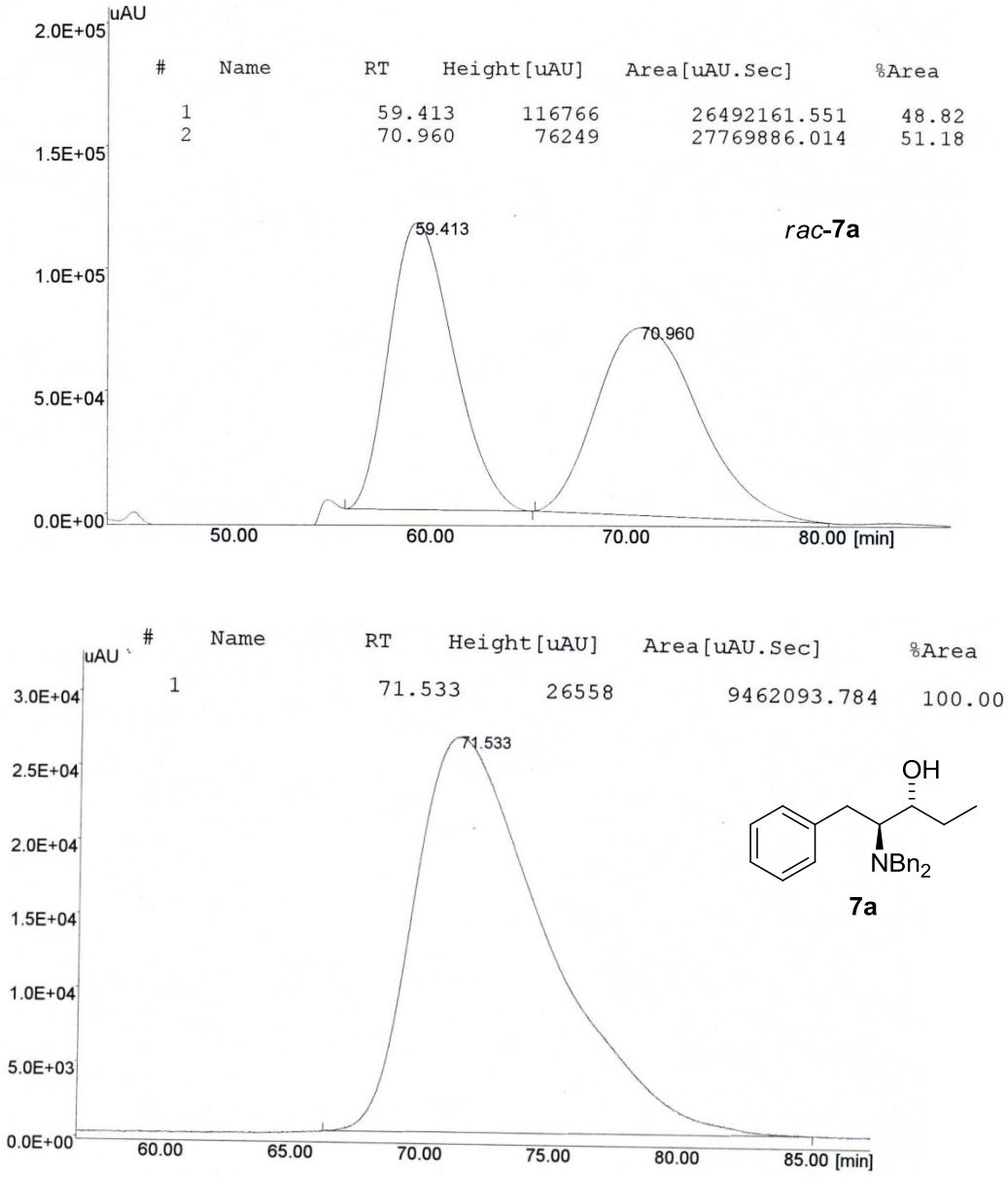

Figure S39. HPLC analysis of *rac*-7a and 7a. Chiral The enantiomeric ratio was determined by HPLC analysis in comparison with racemic material (CHIRALCEL OJ-H column, 99.0/1.0 *n*-hexane/2-propanol, 0.5 mL/min, major isomer: t_R = 71.53 min, UV detection at 254.0 nm, 25°C).

3.5.4. NMR data comparison with literature data

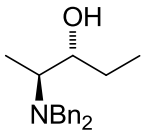

Table S1. ^{1}H NMR data ($CDCl_3$) comparison with literature data for 5a.

This work **400 MHz**	**Ref 1** **300 MHz**	**Ref 2** **300 MHz**	**Ref 3** **200 MHz**
0.89 **(t, 3H, *J* = 7.3 Hz)**	0.87 (t, 3H, *J* =7.4 Hz)	0.89 (d, 3H, *J* = 7.3 Hz)	0.87 (t, 3H, *J* = 7.4 Hz)
1.13 **(d, 3H, *J* = 6.8 Hz)**	1.11 (d, 3H, *J* = 6.8 Hz)	1.11 (d, 3H, *J* = 6.9 Hz)	1.11 (d, 3H, *J* = 7.4 Hz)
1.28-1.39 **(m, 1H)**	1.30 (m, 1H)	1.23-1.42 (m, 1H)	1.32 (m, 1H)
1.76-1.82 **(m, 2H)**	1.77 (m, 2H)	1.69-1.93 (m, 2H)	1.60 (br, 1H) 1.76 (m, 1H)
2.74 **(quint, 1H, *J* = 6.7 Hz)**	2.71 (m, 1H)	2.75 (m, 1H)	2.72 (m, 1H)
3.50 **(d, 2H, *J* = 13.9 Hz)**	3,47 (d, 2H, *J* = 13.8 Hz)	3.50 (AB syst, 2H, *J* = 13.4 Hz)	3.47 (d, 2H, *J* = 14.0 Hz)
3.55 **(m, 1H)**	3.52 (m,1H)	3.52 (m, 1H)	3.52 (m, 1H)
3.79 **(d, 2H, *J* = 13.9 Hz)**	3.76 (d, 2H, *J* = 13.8 Hz)	3.79 (AB syst, 2H, *J* = 13.4 Hz)	3.76 (d, 2H, *J* = 13.6 Hz)
7.23-7.37 **(m, 10H)**	7.15-7.40 (m, 10H)	7.23-7.51 (m, 10H)	7.23 (m, 2H) 7.32 (m, 8H)

Table S2. ^{13}C NMR data ($CDCl_3$) comparison with literature data for 5a.

This work **100 MHz**	**Ref 1** **75 MHz**	**Ref 2** **75 MHz**	**Ref 3** **50 MHz**
140.2	140.0	140.0	140.1
128.8	128.6	128.7	128.8
128.2-126.9	128.1-126.8	128.2-126.8	128.2-126.9
75.3	75.0	75.1	75.2
57.1	56.9	57.0	57.1
54.8	54.6	54.7	54.8
27.2	27.1	27.1	27.2
10.4	10.2	10.3	10.3
8.6	8.5	8.6	8.6

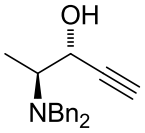

Table S3. **^{1}H NMR data ($CDCl_3$) comparison with literature data for 5c.**

This work **400 MHz**	**Ref 4** **300 MHz**
1.16 **(d, 3H, *J* = 6.8 Hz)**	1.27 (d, 3H, *J* = 6.9 Hz)
2.37 **(m, 1H)**	2.48 (d, 1H, *J* = 1.3 Hz)
2.97 **(quint, 1H, *J* = 6.6 Hz)**	3.08 (m, 1H)
3.31 **(d, 2H, *J* =13.3 Hz)**	3.42 (d, 2H, *J* = 13.3 Hz)
4.01 **(m, 1H (OH))**	
4.10 **(m, 1H)**	4.19 (m, 1H)
4.09 **(d, 3H, *J* = 13.3 Hz)**	4.21 (d, 2H, *J* = 13.3 Hz)
7.18-7.27 **(m, 10H)**	7.25.7.50 (m, 10H)

Table S4. **^{13}C NMR data ($CDCl_3$) comparison with literature data for 5c.**

This work **100 MHz**	**Ref 4** **75 MHz**
139.1	139.0
129.2	129.0
128.5	128.4
127.3	127.2
83.9	83.8
74.3	74.2
62.8	62.6
55.6	-----
54.7	54.5

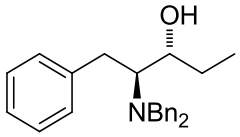

Table S5. ^{1}H NMR data ($CDCl_3$) comparison with literature data for 7a.

This work **400 MHz**	**Ref 1** **300 MHz**	**Ref 2** **300 MHz**
0.90 **(t, 3H, *J* = 7.3 Hz)**	0.88 (t, 3H, *J* = 7.3 Hz)	1.00 (t, 3H, *J* = 7.3Hz)
1.35-1.44 **(m, 1H)**	1.37 (m, 1H)	1.39-1.59 (m, 1H)
1.66-1.74 **(m, 1H)**	1.68 (m, 1H)	1.69-1.82 (m, 1H)
1.87 **(d, 1H, *J* = 6.9 Hz)**	1.90 (br, s, 1H)	
2.82 **(dd, 1H, J_1 = 12.9, J_2 = 5.8 Hz)**	2.80 (dd, 1H, J_1 = 12.7, J_2 = 5.8 Hz)	2.85-2.96 (m, 1H)
3.01-3.12 **(m, 2H)**	3.05 (m, 2H)	3.05-3.13 (m, 2H)
3.63 **(m, 1H)**	3.60 (m, 1H)	3.62-3.65 (m,5H)
3.67 **(d, 2H, *J* = 13.8 Hz)**	3.65 (d, 2H, *J* = 13.8 Hz)	
3.77 **(d, 2H, *J* = 13.8 Hz)**	3.77 (d, 2H, *J* = 13.8 Hz)	
7.16-7.31 **(m, 15H)**	7.10-7.40 (m, 15H)	7.12-7.45 (m, 15H)

Table S6. **^{13}C NMR data ($CDCl_3$) comparison with literature data for 7a.**

This work **100 MHz**	**Ref 1** **75 MHz**	**Ref 2** **75 MHz**
140.7	140.6	140.4
139.8	139.7	139.4
129.4	129.3	129.1
128.8	128.7	128.4
128.4	128.3	127.9
128.3	128.2	126.6
126.9	126.9	126.5
125.9	125.9	-----
73.4	73.2	72.6
63.1	63.0	62.6
55.1	55.0	54.5
32.0	31.9	31.6
27.8	27.6	27.4
10.9	10.9	10.6

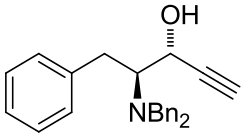

Table S7. **^{1}H NMR data ($CDCl_3$) comparison with literature data for 7c.**

This work **400 MHz**	**Ref 4** **300 MHz**
2.49 **(d, 1H, *J* = 1.7 Hz)**	2.60 (d, 1H, *J* = 2.0 Hz)
2.92 **(dd, 1H, J_1 = 12.4, J_2 = 10.2 Hz)**	3.03 (dd, 1H, J_1 = 12.2, J_2 = 9.7 Hz)
3.03-3.08 **(m, 1H)**	3.16 (m, 1H)
3.12 **(dd, 1H, J_1 = 4.2, J_2 = 12.7 Hz)**	3.24 (dd, 1H, J_1 =1 2.2, J_2 = 4.1 Hz)
3.43 **(d, 2H, *J* = 13.2 Hz)**	3.53 (d, 2H, *J* = 13.2 Hz)
3.97 **(br, 1H)**	4.07 (m, 1H)
4.03 **(m, 1H)**	4.19 (brs, 1H)
4.25 **(d, 2H, *J* = 13.2 Hz)**	4.36 (d, 1H, *J* = 13.2 Hz)
7.13-7.28 **(m, 15H)**	7.20-7.50 (m, 15H)

Table S8. **^{13}C NMR data ($CDCl_3$) comparison with literature data for 7c.**

This work 100 MHz	Ref 4 75 MHz
138.9	138.8
138.5	138.3
129.3	129.2
129.2	129.1
128.7	128.6
128.6	128.5
127.5	127.4
126.5	126.4
83.9	83.8
75.2	75.1
62.3	62.1
60.2	60.0
55.1	54.9
31.6	31.4

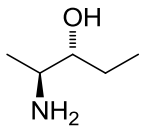

Table S9. **^{1}H NMR data ($CDCl_3$) comparison with literature data for 8.**

This work **400 MHz**	**Ref 4** **300 MHz**
1.01 **(t, 3H, *J* = 7.2 Hz)**	0.98 (t, 3H, *J* = 7.4 Hz)
1.24 **(d, 3H, *J* = 6,3 Hz)**	1.04 (d, 3H, *J* = 6,6 Hz)
1.52 **(m, 2H)**	1.42 (m, 2H)
3.33 **(brs, 1H)**	2.91 (brs, 3H)
3.59 **(brs, 3H)**	3.01 (dq, 1H, J_1 = 6.6, J_2 = 3.2 Hz)
3.76 **(m, 1H)**	3.44 (m, 1H)

Table S10. **^{13}C NMR data ($CDCl_3$) comparison with literature data for 8.**

This work **400 MHz**	**Ref 4** **75 MHz**
73.2	75.4
51.2	50.2
25.7	25.4
13.3	16.1
10.5	10.5

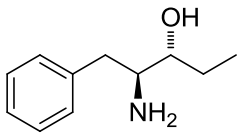

Table S11. **^{1}H NMR data ($CDCl_3$) comparison with literature data for 9.**

This work **400 MHz**	**Ref 4** **300 MHz**
1.04 **(t, 3H, *J* = 5.6 Hz)**	1.05 (t, 3H, *J* = 7.4 Hz)
1.57 **(brs, 2H)**	1.56 (m, 2H)
	1.85 (brs, 3H)
2.61 **(t, 1H, *J* = 9.2 Hz)**	2.45 (dd, 1H, J_1 = 13,5, J_2 = 10.5 Hz)
2.91 **(d, 1H, *J* = 10.4 Hz)**	2.89 (dq, 1H, J_1 = 13.5, J_2 = 3.4 Hz)
3.17 **(brs, 1H)**	3.07 (m, 1H)
3.66 **(brs, 4 H)**	3.51 (m, 1H)
7.22-7.32 **(m, 5H)**	7.20-7.40 (m, 5H)

Table S12. **^{13}C NMR data ($CDCl_3$) comparison with literature data for 9.**

This work **100 MHz**	**Ref 4** **75 MHz**
138.6	139.3
129.3	129.1
128.7	128.5
126.6	126.2
74.5	75.3
56.7	56.4
36.4	37.6
25.3	25.3
10.6	10.6

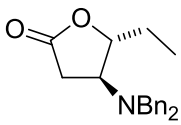

Table S13. ^{1}H NMR data ($CDCl_3$) comparison with literature data for 18a.

This work **500MHz**	**Ref 5** **300 MHz**
0.90 **(t, 3H, *J* = 7.4 Hz)**	0.90 (t, 3H, *J* = 7.4 Hz)
1.52-1.66 **(m, 2H)**	1.59 (m, 2H)
2.56 **(dd, 1H, J_1 = 18.2, J_2 = 8.8 Hz)**	2.55 (dd, 1H, J_1 = 18.2, J_2 = 8.6 Hz)
2.65 **(dd, 1H, J_1 = 18.2, J_2 = 5.5 Hz)**	2.65 (dd, 1H, J_1 = 18.2, J_2 = 5.7 Hz)
3.40 **(ddd, 1H, J_1 = 8.6, J_2 = 5.7, J_3 = 4.6 Hz)**	3.39 (ddd, 1H, J_1 = 8.6, J_2 = 5.7, J_3 = 4.6 Hz)
3.47 **(d, 2H, *J* = 13.8 Hz)**	3.46 (d, 2H, *J* = 13.7 Hz)
3.73 **(d, 2H, *J* = 13.7 Hz)**	3.72 (d, 2H, *J* = 13.7 Hz)
4.44 **(ddd, 1H, J_1 = 7.2, J_2 = 5.7, J_3 = 4.6 Hz)**	4.43 (m, 1H)
7.25-7.35 **(m, 10H)**	7.20-7.40 (m, 10H)

Table S14. **^{13}C NMR data ($CDCl_3$) comparison with literature data for 18a.**

This work **125 MHz**	**Ref 5** **75 MHz**
175.9	175.9
138.4	138.3
128.6	128.5
128.5	128.4
127.4	127.3
84.0	83.9
59.4	59.2
54.3	54.1
28.9	28.8
27.5	27.4
9.4	9.4

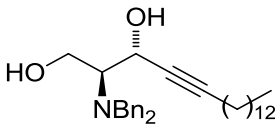

Table S15. ^{1}H NMR data ($CDCl_3$) comparison with literature data for 20.

This work **400 MHz**	**Ref 6** **300 MHz**
0.82 **(t, 3H, *J* = 7.0 Hz)**	0.89 (t, 3H, *J* = 7.0 Hz)
1.31-1.75 **(m, 20H)**	1.25 (m, 20H)
1.43 **(q, 2H, *J* = 7.5 Hz)**	1.48 (m, 2H)
2.15 **(app.t, 2H, *J* = 6.8 Hz,)**	2.22 (td, 2H, J_1 = 7.1, J_2 =2.0 Hz)
2.98 **(q, 1H, *J* = 6.3 Hz)**	3.04 (m, 1H)
3.74 **(d, 2H, *J* = 13.3 Hz)**	3.79 (d, 2H, *J* = 13.3 Hz)
3.81 **(dd, 1H, J_1=11.4, J_2 = 6.3 Hz)**	3.85 (dd, 1H, J_1 =11.0, J_2 =6.0 Hz)
3.88 **(dd, 1H, J_1 = 10.7, J2=7.7 Hz)**	3.94 (dd, 1H, J_1 = 11.0, J_2 = 7.7 Hz)
3.96 **(d, 2H, *J* = 13,3 Hz,)**	4.02 (d, 2H, *J* = 13.3 Hz)
4.47 **(app. d, 1H, *J* = 5.6 Hz)**	4.52 (dt, 1H, J_1 = 6.0, J_2 = 2.0 Hz)
7.17–7.28 **(m, 10H)**	7.20–7.40 (m, 10H)

Table S16. **^{13}C NMR data ($CDCl_3$) comparison with literature data for 20.**

This work 400 MHz	**Ref 6 75 MHz**
139.3	139.2
129.2	129.1
128.5	128.4
127.2	127.2
87.6	87.4
79.9	79.9
62.3	62.0
60.8	60.6
59.7	59.6
54.7	54.6
31.9	31.9
29.6	29.6
29.5	29.5
29.3	29.3
29.1	29.1
29.0	29.0
28.5	28.5
22.7	22.6
18.8	18.8
14.1	14.1

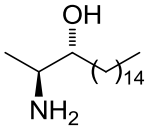

spisulosine

Table S17. **^{1}H NMR data ($CDCl_3$) comparison with literature data for spisulosine (2c).**

This work **400MHz**	**Ref 7** **300 MHz**	**Ref 8** **400 MHz**
0.88 **(t, 3H, *J* = 7.0 Hz)**	0.84-0.88 (m, 3H)	0.88 (t, 3H, *J* = 6.4Hz)
1.05 **(d, 3H, *J* = 6.2Hz)**	0.99 (d, 3H, *J* = 6.4 Hz)	1.00 (d, 3H, *J* = 6.4Hz)
1.25-1.49 **(m, 28H)**	1.24-1.37 (brm, 27H)	1.26-1.50 (m, 28H)
	1.46-1.48 (brm, 1H)	
2.62 **(brs, 3H)**	1.83 (brs, 3H)	1.65 (brs, 3H)
3.02 **(brs, 1H)**	2.94 (brm, 1H)	2.97 (m, 1H)
3.52 **(brs, 1H)**	3.42 (brm, 1H)	3.44 (m, 1H)

Table S18. **^{13}C NMR data ($CDCl_3$) comparison with literature data for spisulosine (2c).**

This work **100MHz**	**Ref 7** **75 MHz**	**Ref 8** **100 MHz**
74.0	75.1	74.9
50.6	50.8	50.5
32.5	32.9	32.6
31.9	32.3	32.1
29.7-29.4	30.2-29.7	29.9-29.5
26.2	26.6	26.4
22.7	23.1	22.8
16.0	17.3	17.3
14.1	14.5	15.2

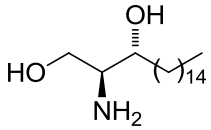

sphinganine

Table S19. ^{1}H NMR data (CD_3OD) comparison with literature data for sphinganine (1b).

This work **400 MHz**	**Ref 9** **400 MHz**
0.92-0.91 **(m, 3H)**	0.90 (t, 3H, *J* = 6.6 Hz)
1.31-1.55 **(m, 28H)**	1.28-1.67 (m, 28H)
2.78-2.82 **(m, 1H)**	2.78-2.82 (m, 1H)
3.51-3.57 **(m, 2H)**	3.47-3.57 (m, 2H)
3.75-3.78 **(m, 1H)**	3.74 (dd, 1H, , *J* = 6.6 Hz)

Table S20. ^{13}C NMR data (CD_3OD) comparison with literature data for sphinganine (1b).

This work **100 MHz**	**Ref 9** **100 MHz**
73.3	73.4
63.2	63.4
58.2	58.1
34.4	34.3
33.1	33.0
30.8	30.7
30.5	30.4
27.1	27.0
23.7	23.7
14.4	14.5

3.6. ^{1}H and ^{13}C NMR spectra

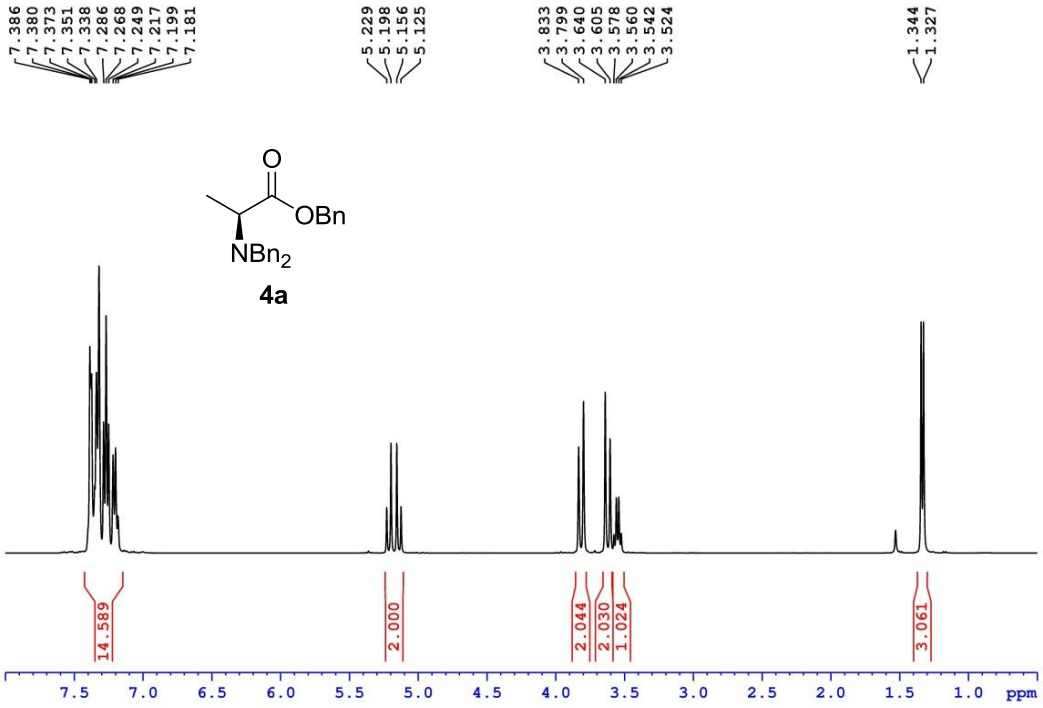

Figure S1. ^{1}H **(400 MHz) NMR spectrum of 4a in** $CDCl_3$**.**

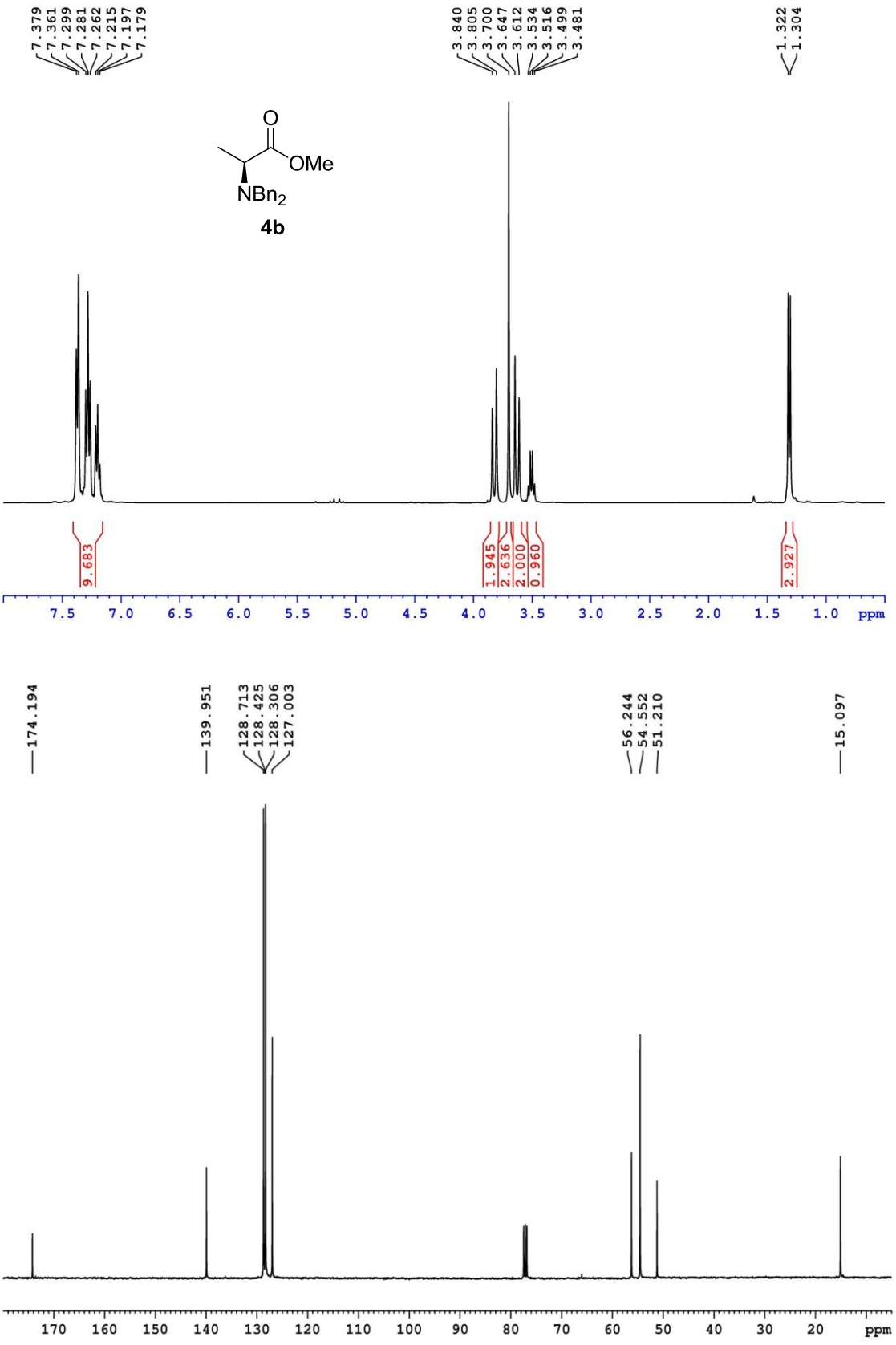

Figure S2. **^{1}H (400 MHz) and ^{13}C (100 MHz) NMR spectra of 4b in $CDCl_3$.**

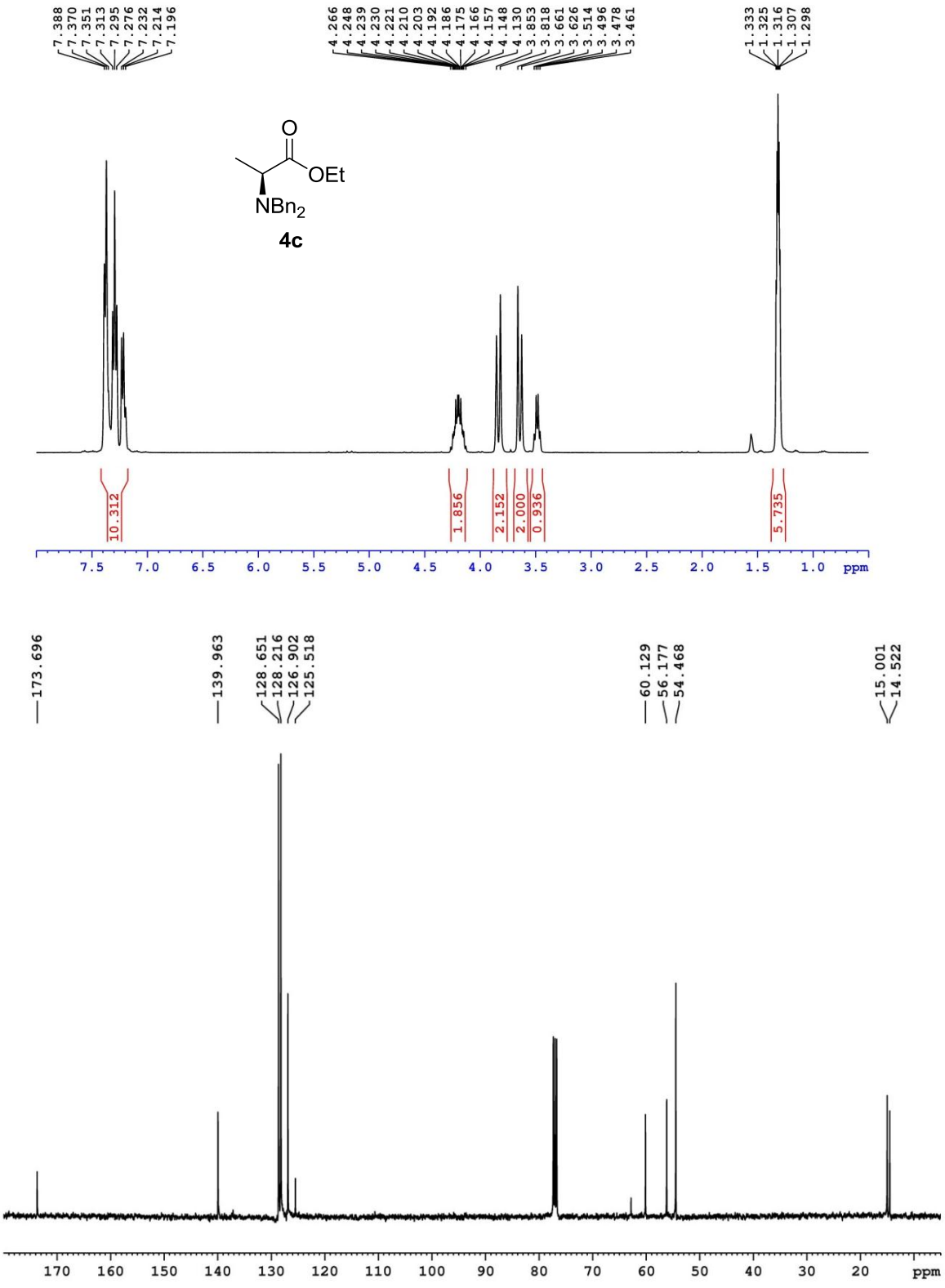

Figure S3. ^{1}H **(400 MHz) and** ^{13}C **(100 MHz) NMR spectra of 4c in** $CDCl_3$**.**

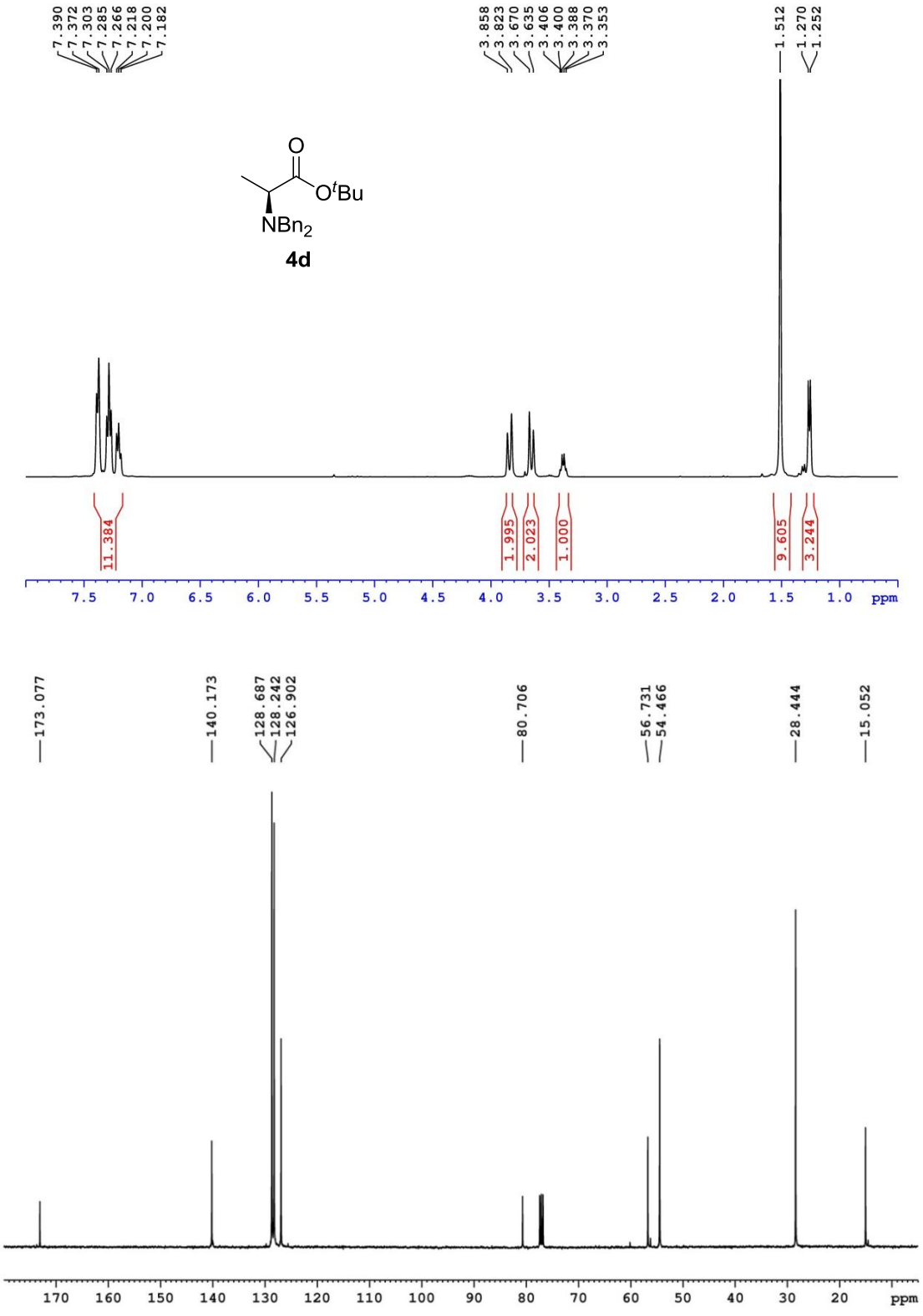

Figure S4. **^{1}H (400 MHz) and ^{13}C (100 MHz) NMR spectra of 4d in $CDCl_3$.**

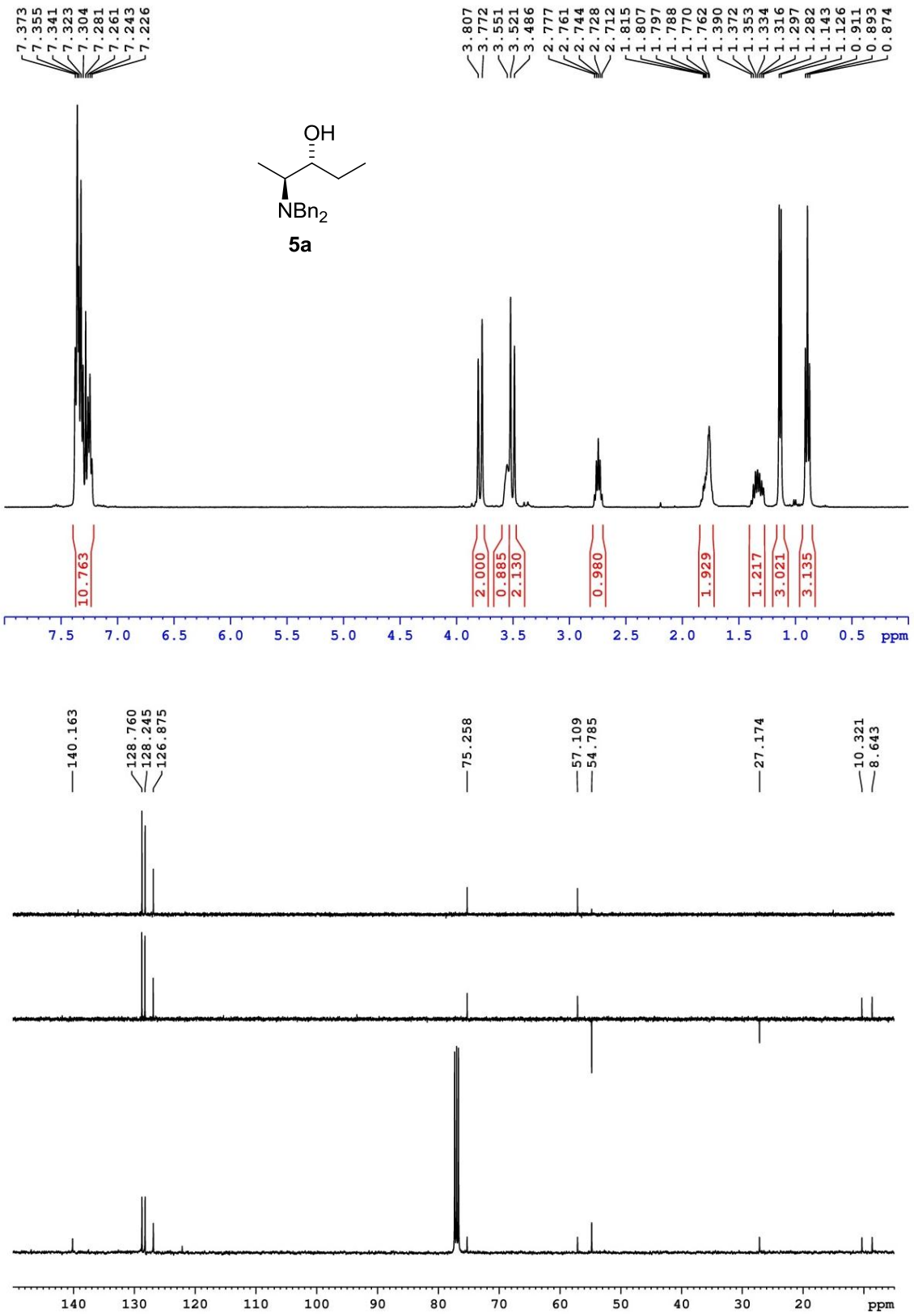

Figure S5. ^{1}H (400 MHz) and ^{13}C (100 MHz) NMR spectra of 5a in $CDCl_3$.

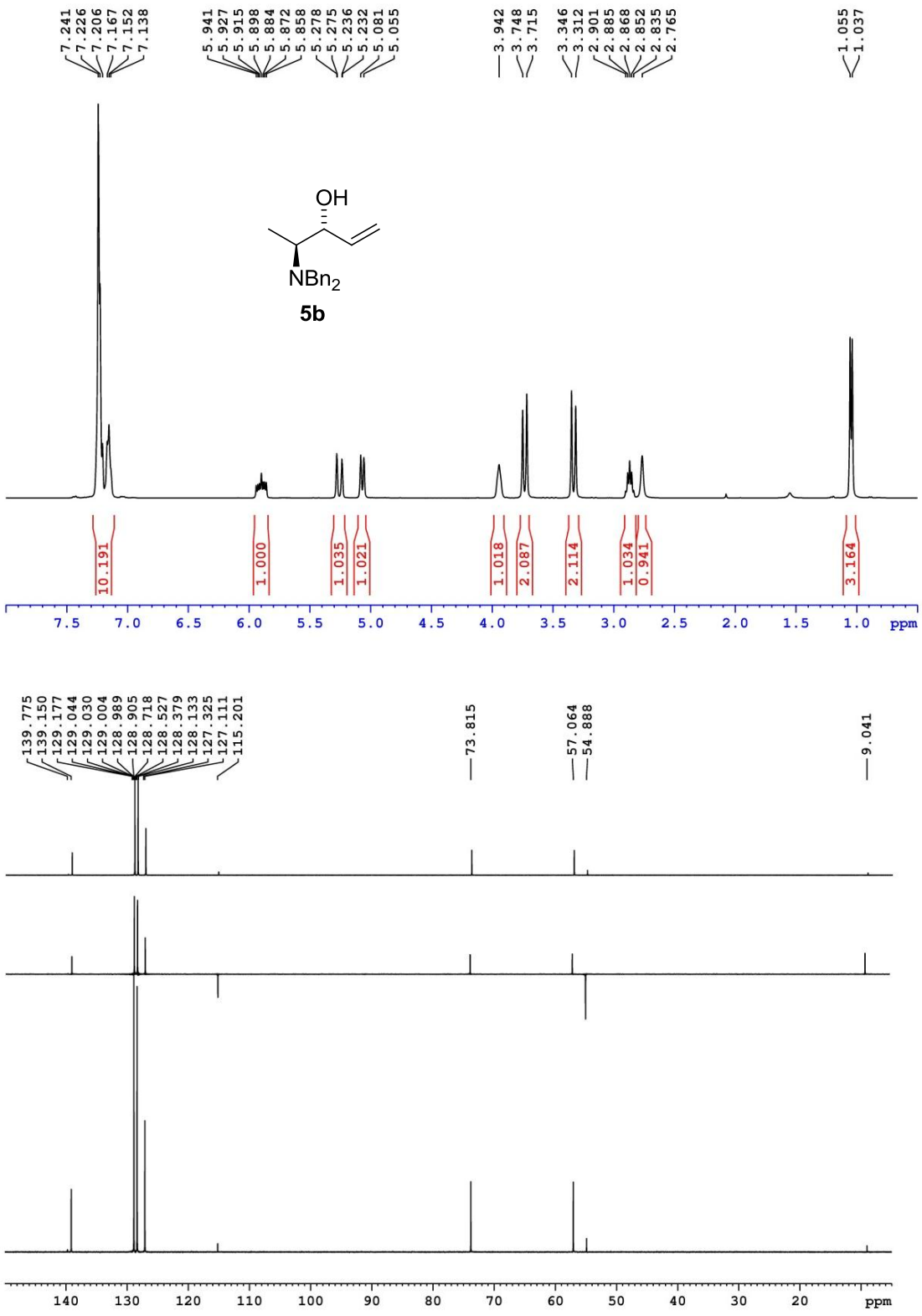

Figure S6. **^{1}H (400 MHz) and ^{13}C (100 MHz) NMR spectra of 5b in $CDCl_3$.**

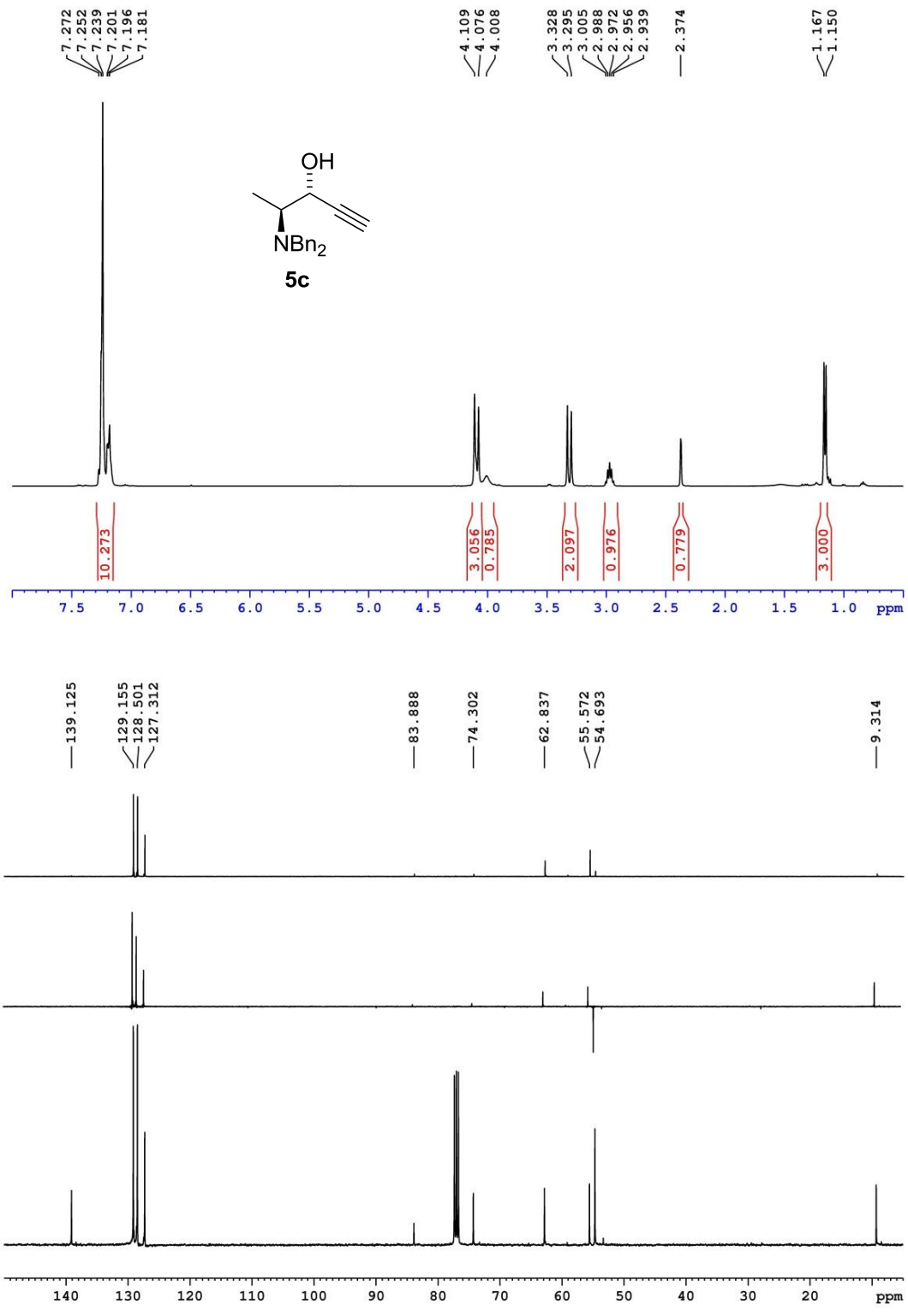

Figure S7. **^{1}H (400 MHz) and ^{13}C (100 MHz) NMR spectra of 5c in $CDCl_3$.**

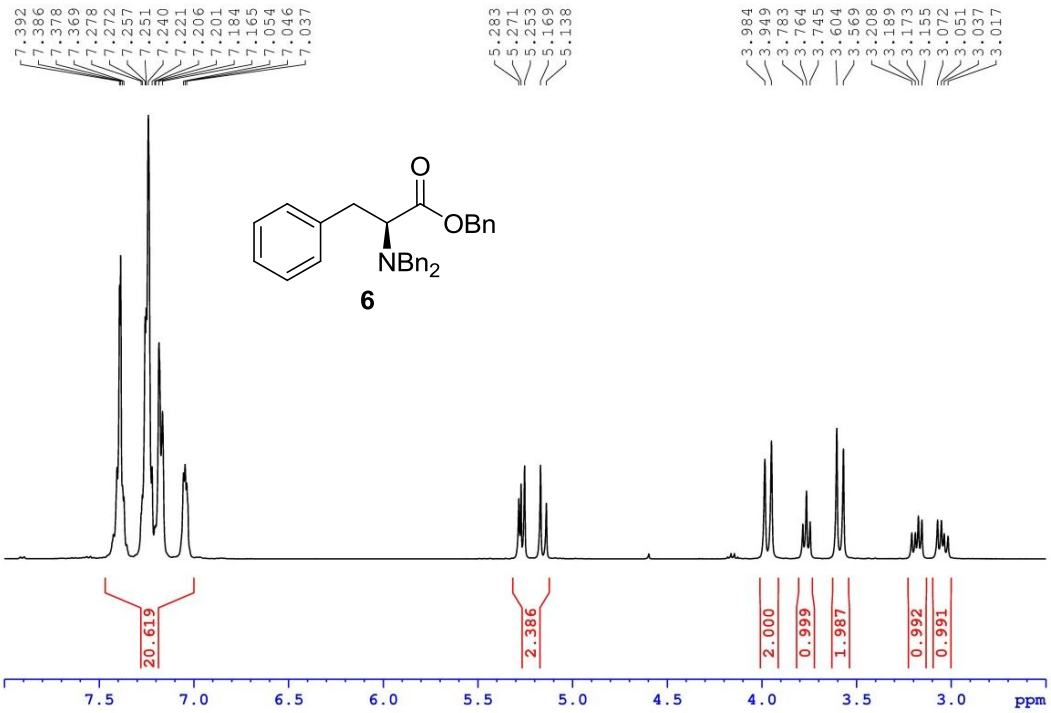

Figure S8. ^{1}**H (400 MHz) NMR spectrum of 6 in** $CDCl_3$**.**

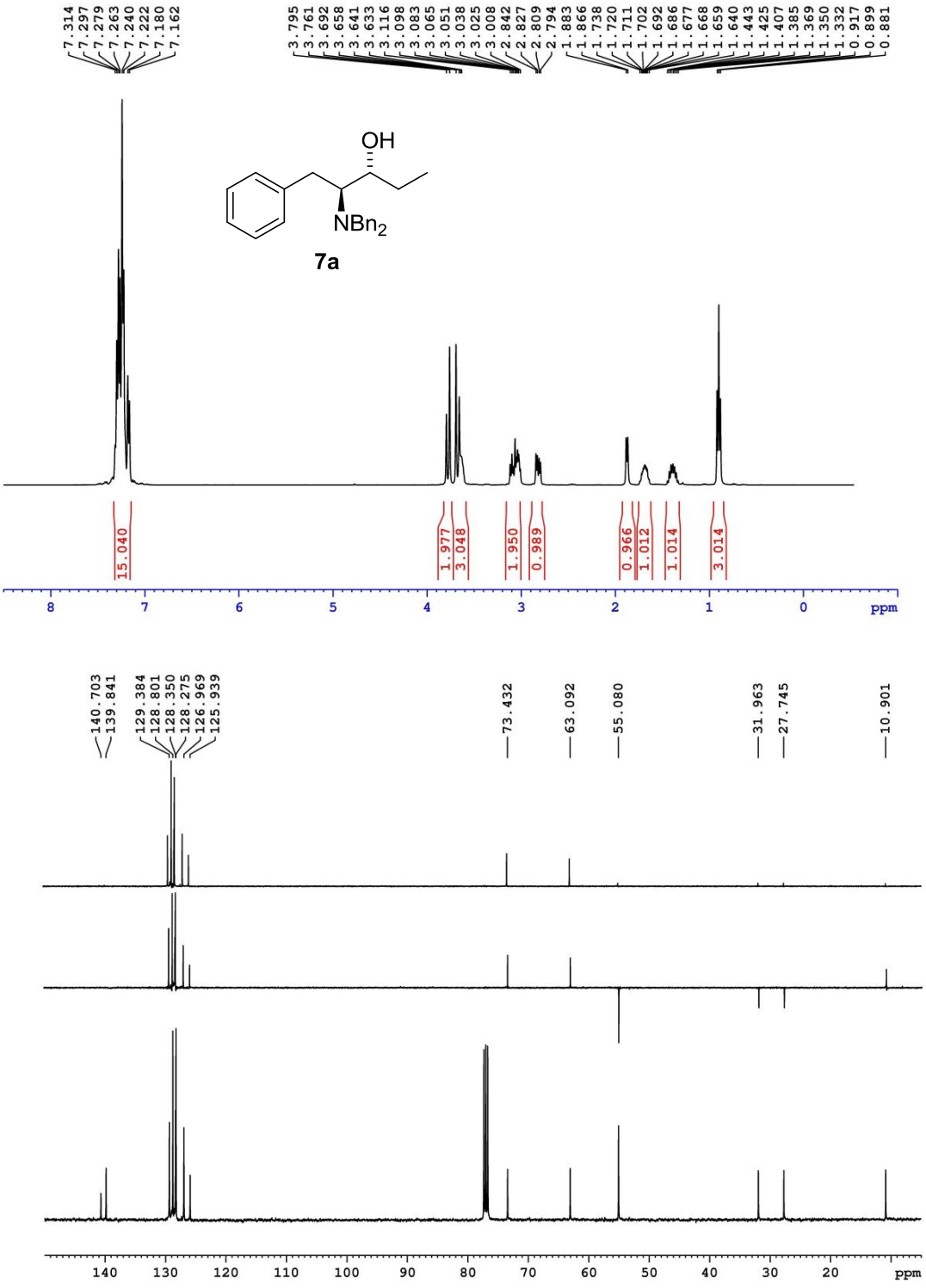

Figure S9. **^{1}H (400 MHz) and ^{13}C (100 MHz) NMR spectra of 7a in $CDCl_3$.**

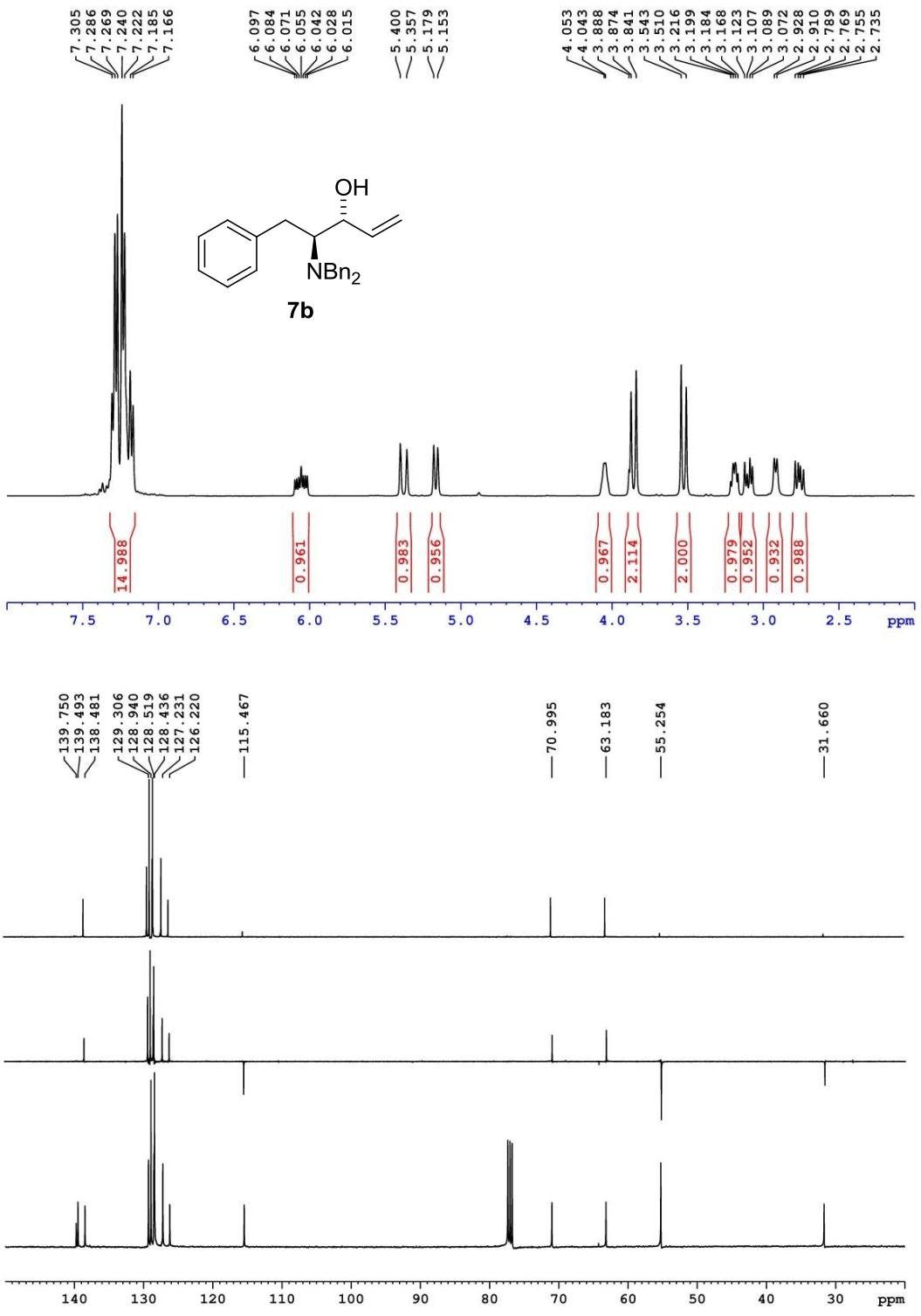

Figure S10. **^{1}H (400 MHz) and ^{13}C (100 MHz) NMR spectra of 7b in $CDCl_3$.**

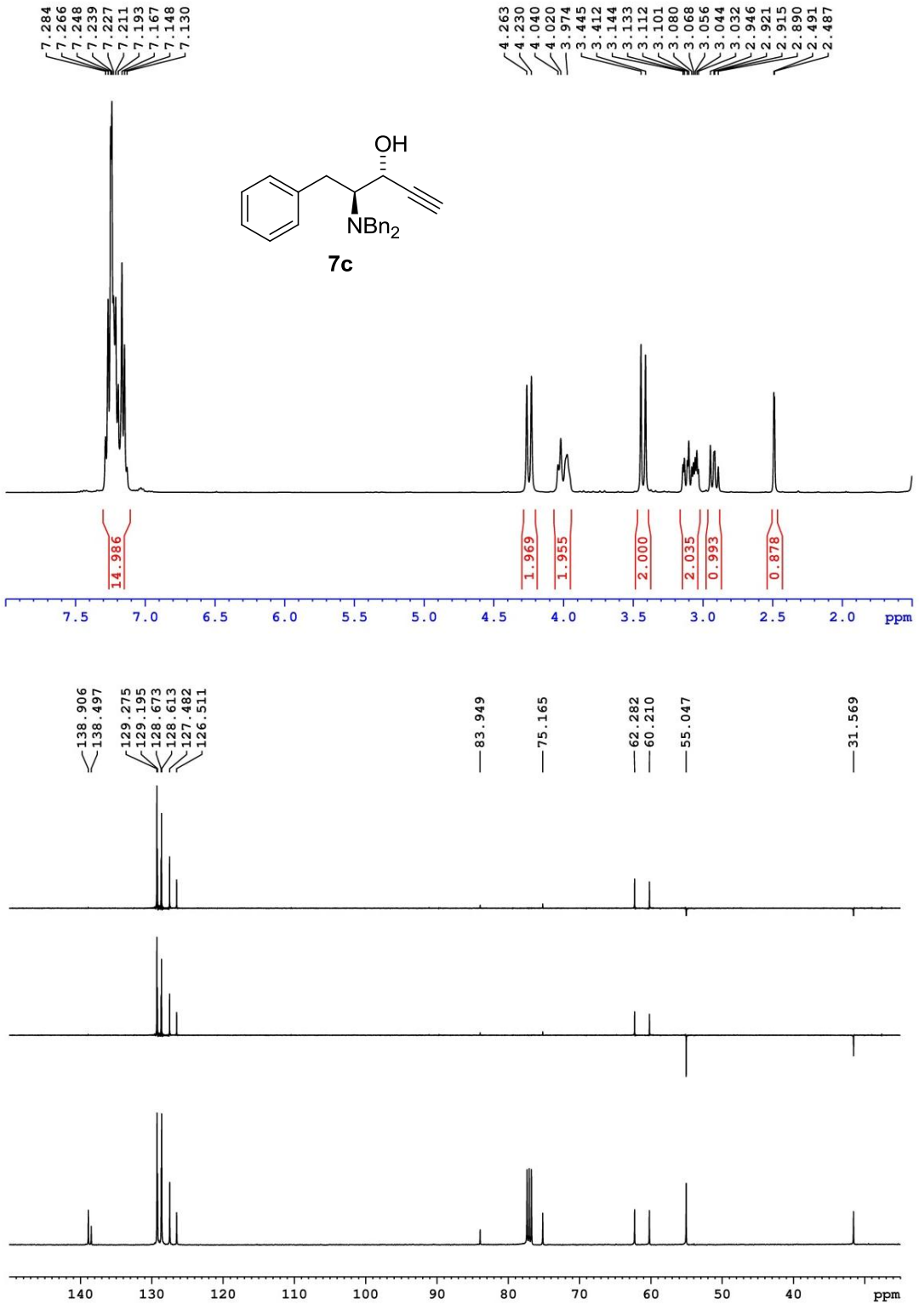

Figure S11. ^{1}H (400 MHz) and ^{13}C (100 MHz) NMR spectra of 7c in $CDCl_3$.

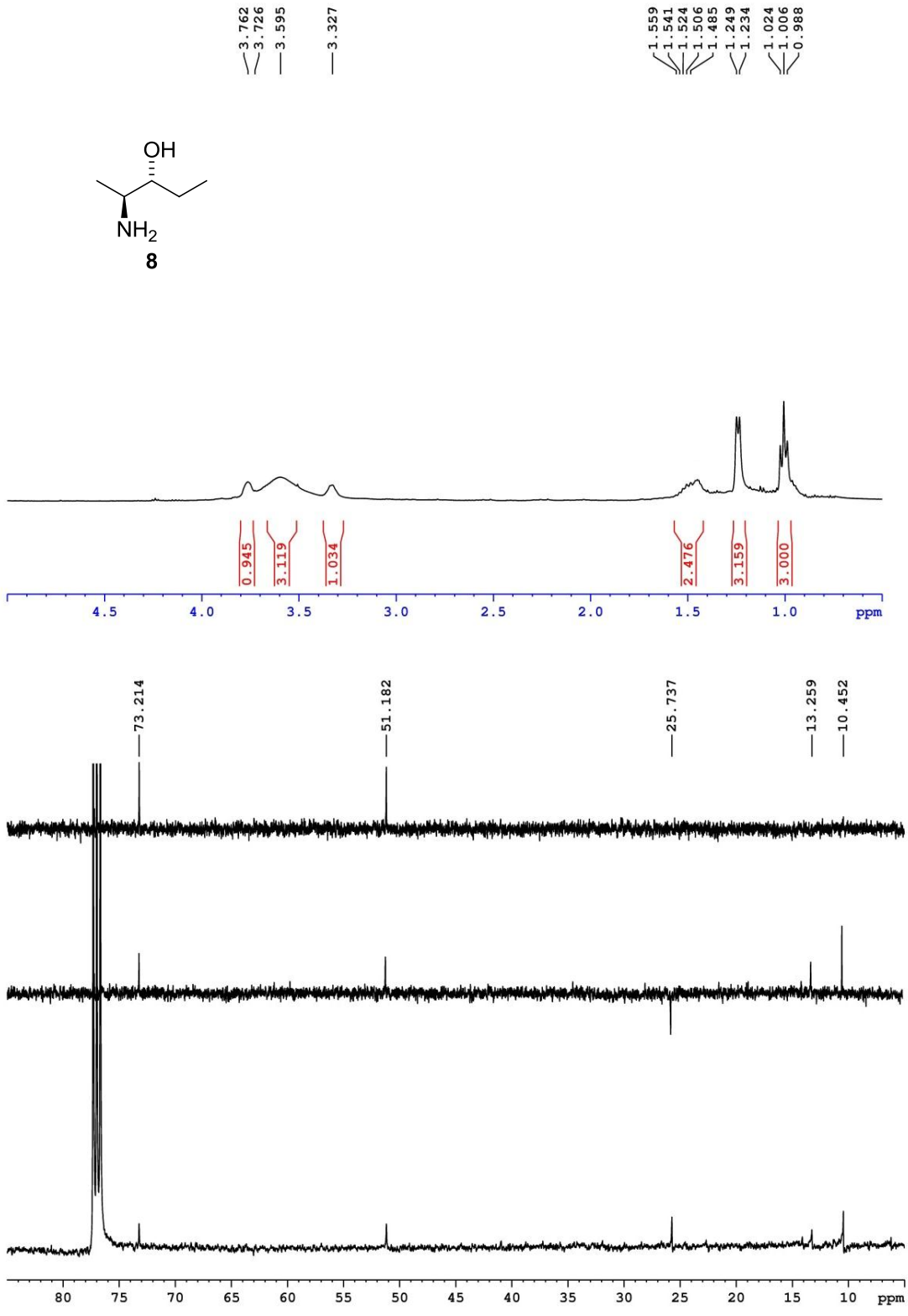

Figure S12. **^{1}H (400 MHz) and ^{13}C (100 MHz) NMR spectra of 8 in $CDCl_3$.**

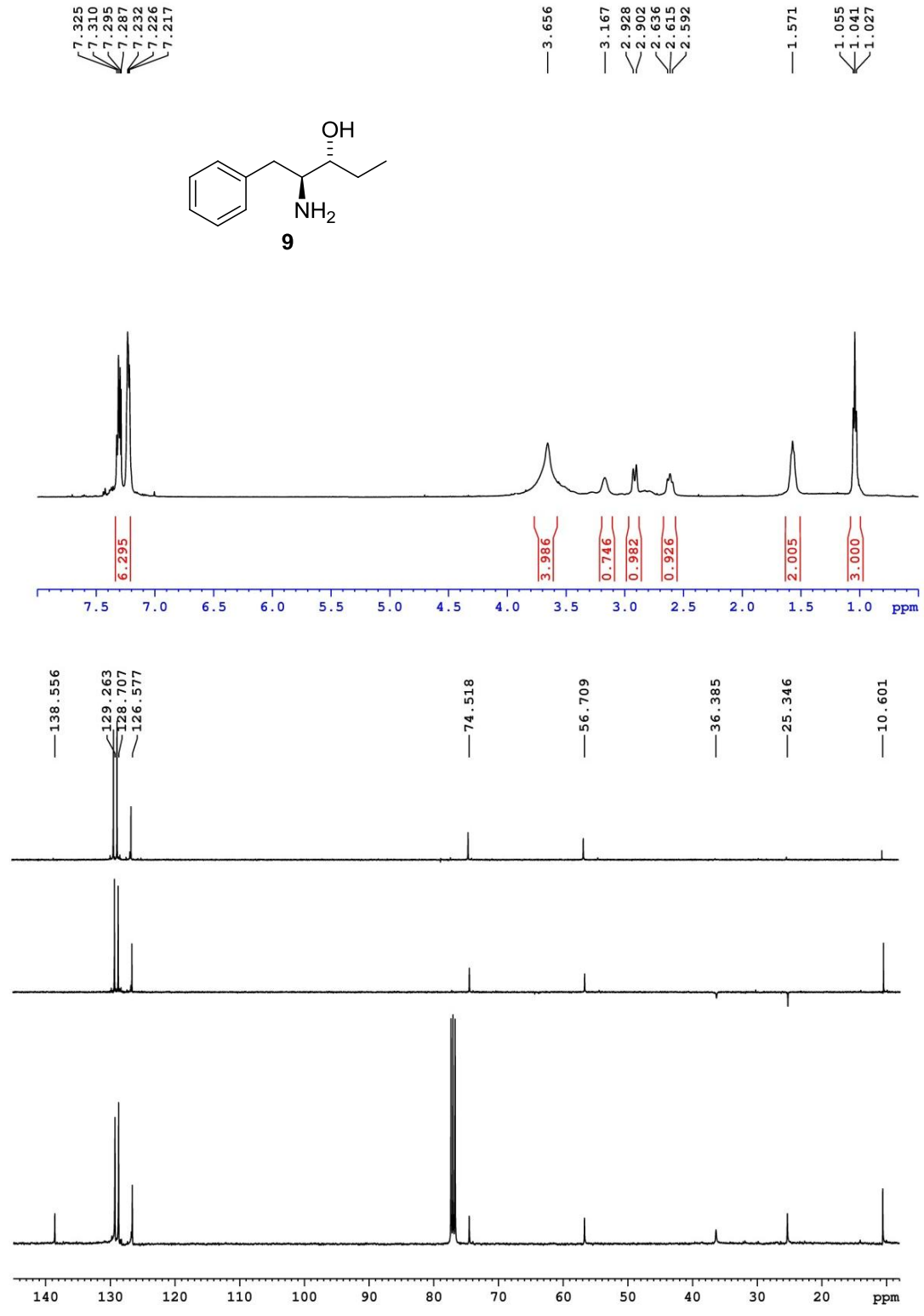

Figure S13. ^{1}H (400 MHz) and ^{13}C (100 MHz) NMR spectra of 9 in $CDCl_3$.

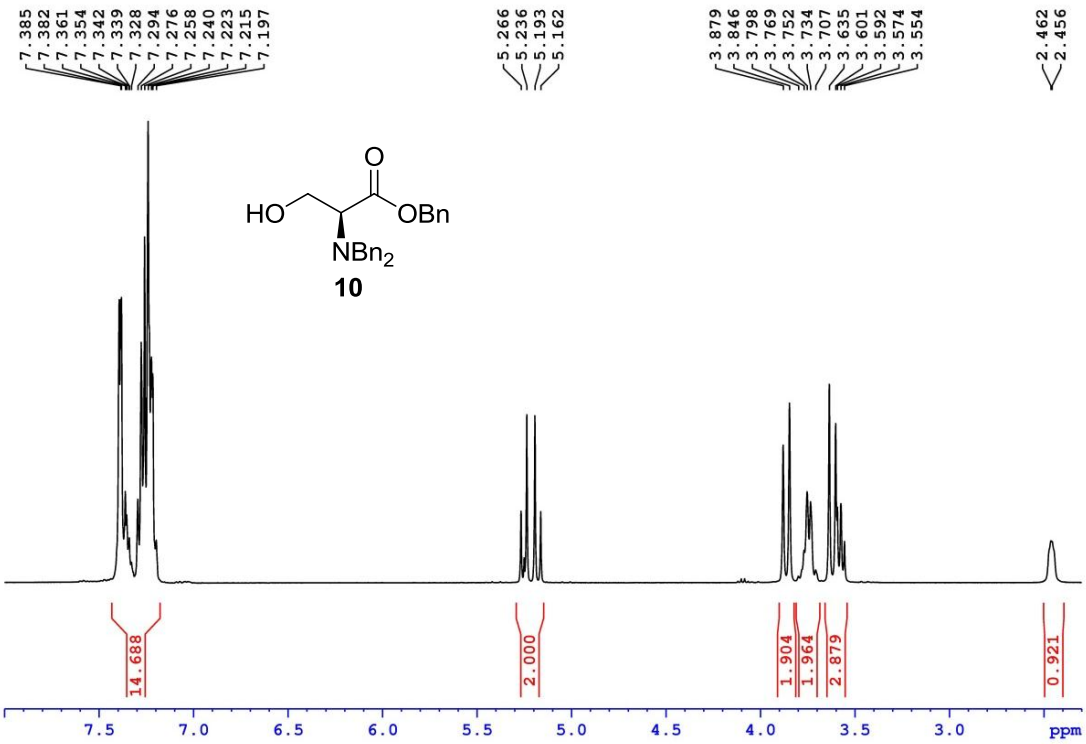

Figure S14. ^{1}**H (400 MHz) NMR spectrum of 10 in** $CDCl_3$**.**

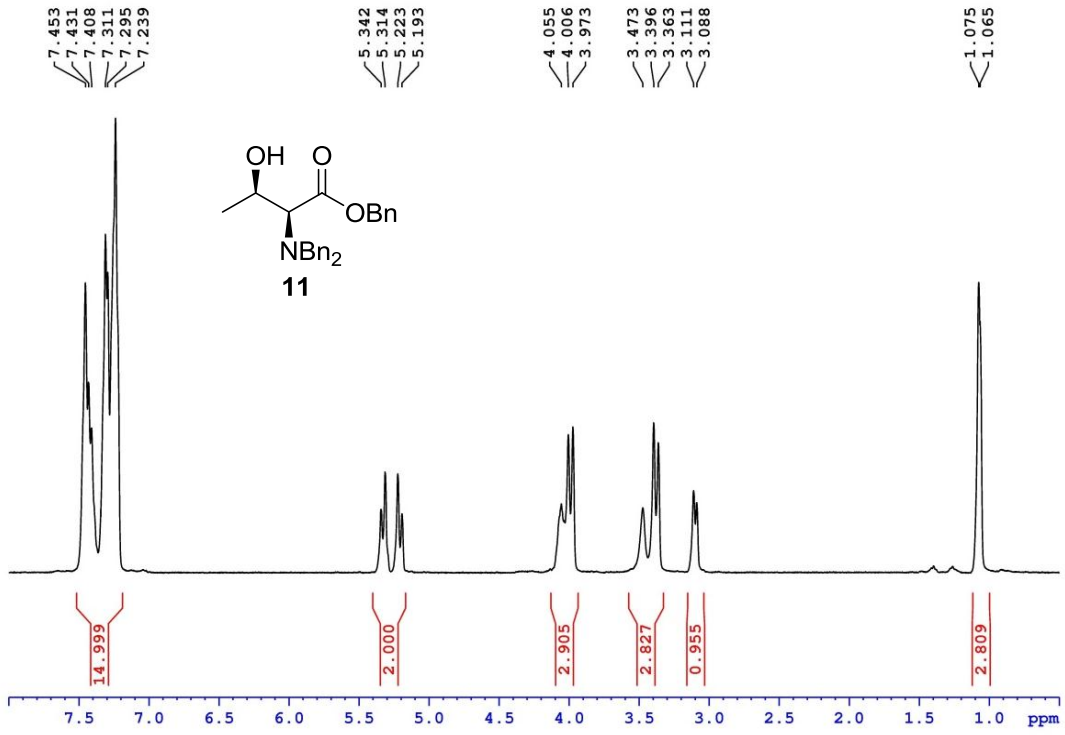

Figure S15. ^{1}**H (400 MHz) NMR spectra of 11 in** $CDCl_3$**.**

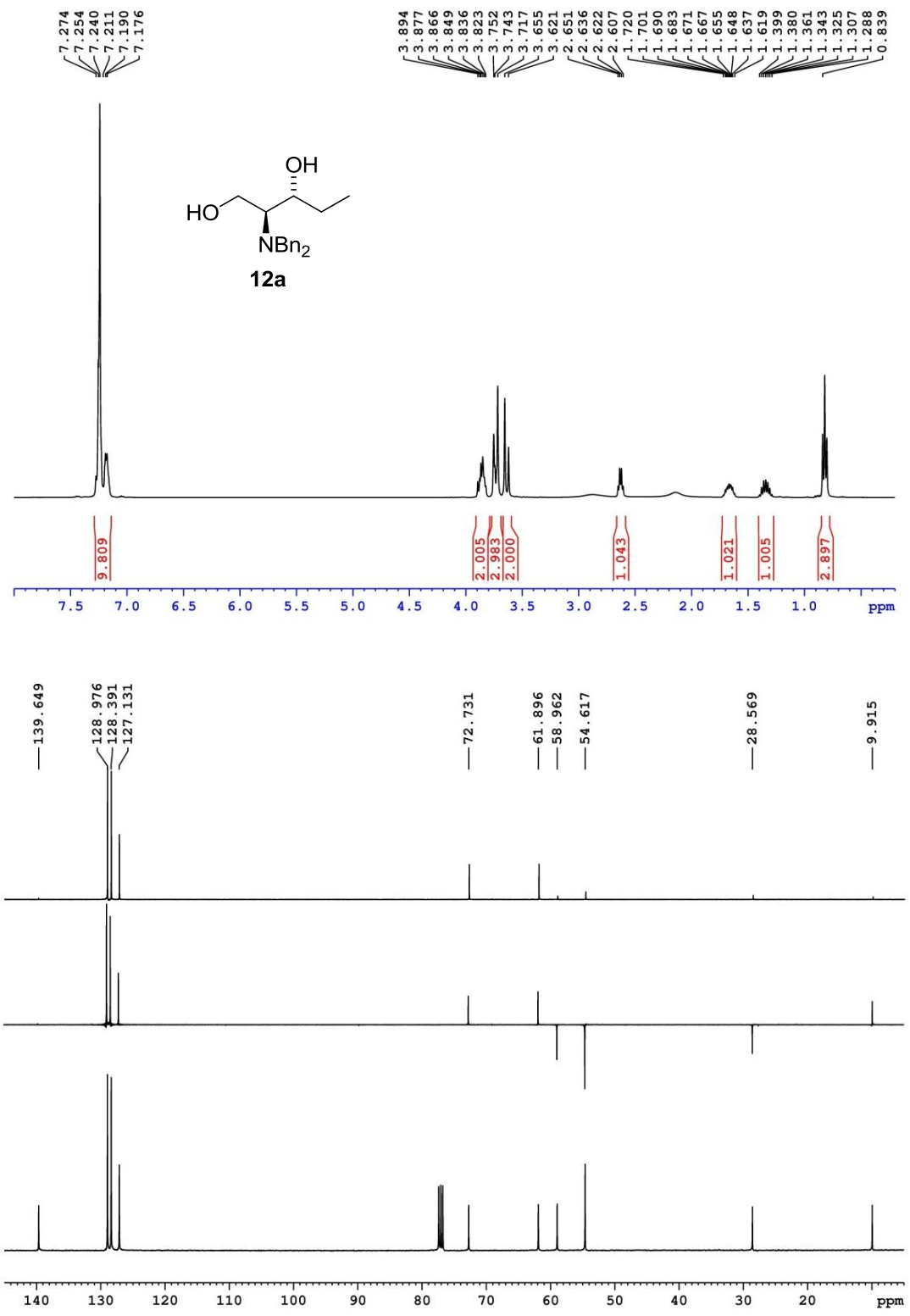

Figure S16. ^{1}H **(400 MHz) and** ^{13}C **(100 MHz) NMR spectra of 12a in** $CDCl_3$**.**

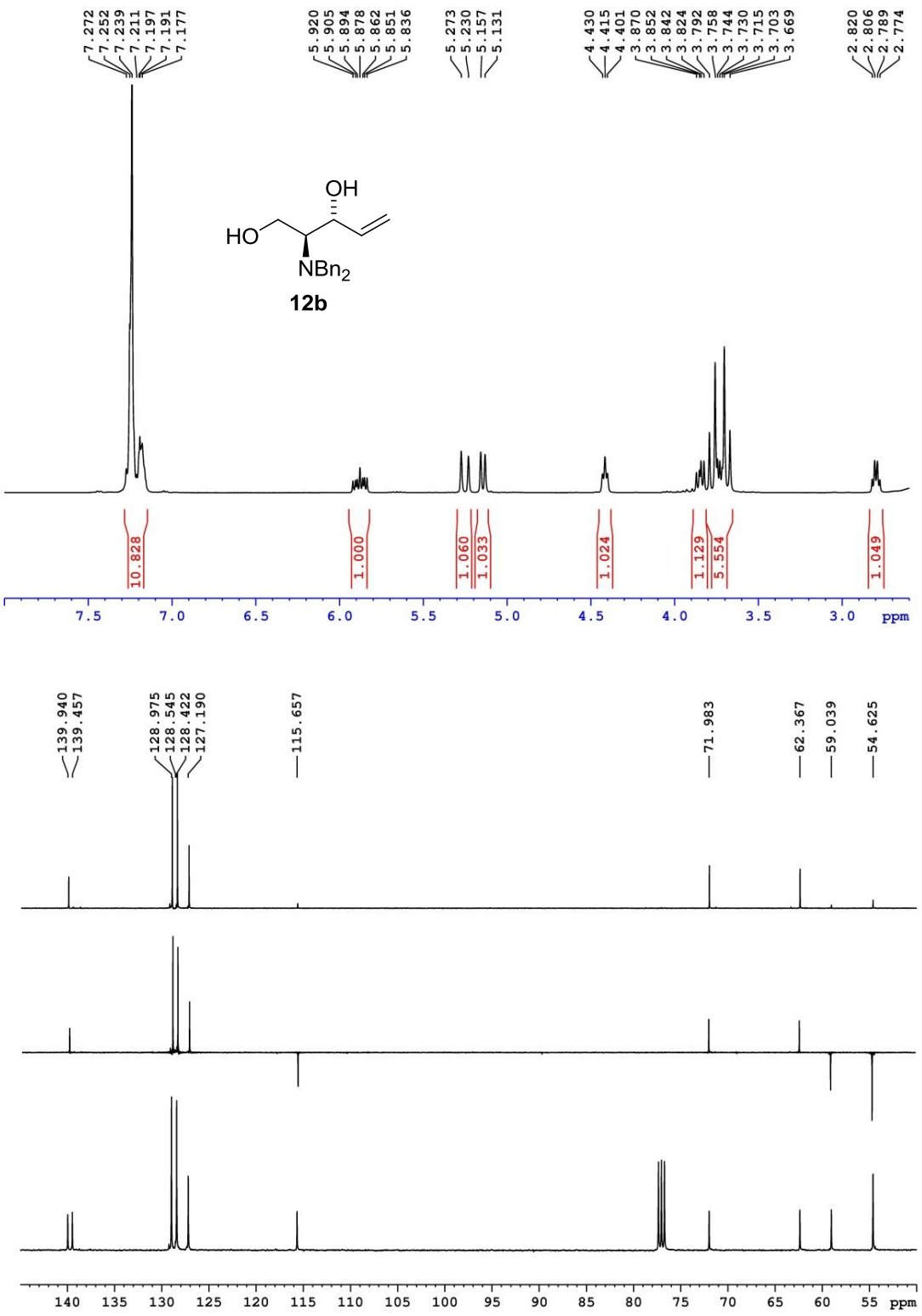

Figure S17. **^{1}H (400 MHz) and ^{13}C (100 MHz) NMR spectra of 12b in $CDCl_3$.**

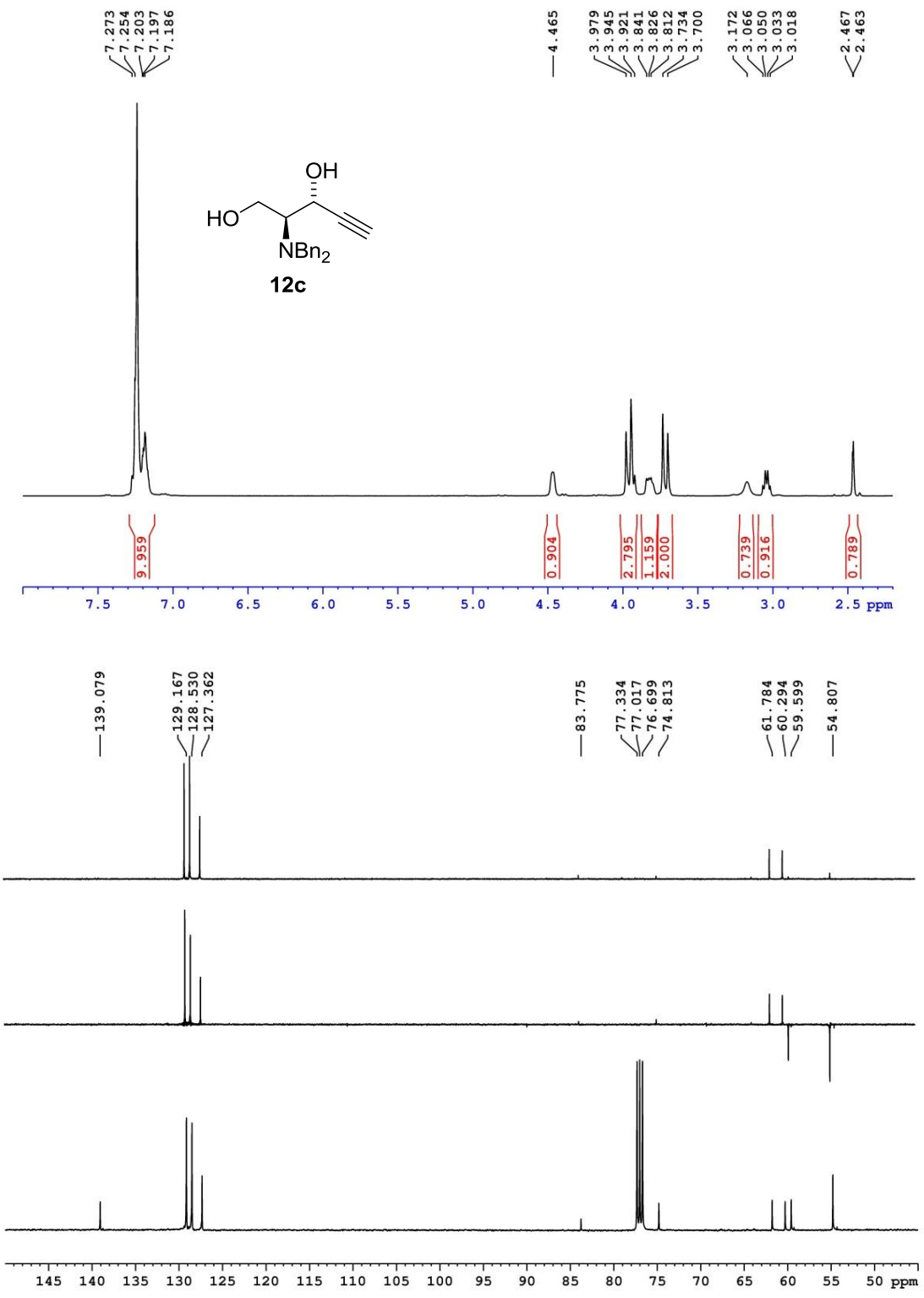

Figure S18. ^{1}H (400 MHz) and ^{13}C (100 MHz) NMR spectra of 12c in $CDCl_3$.

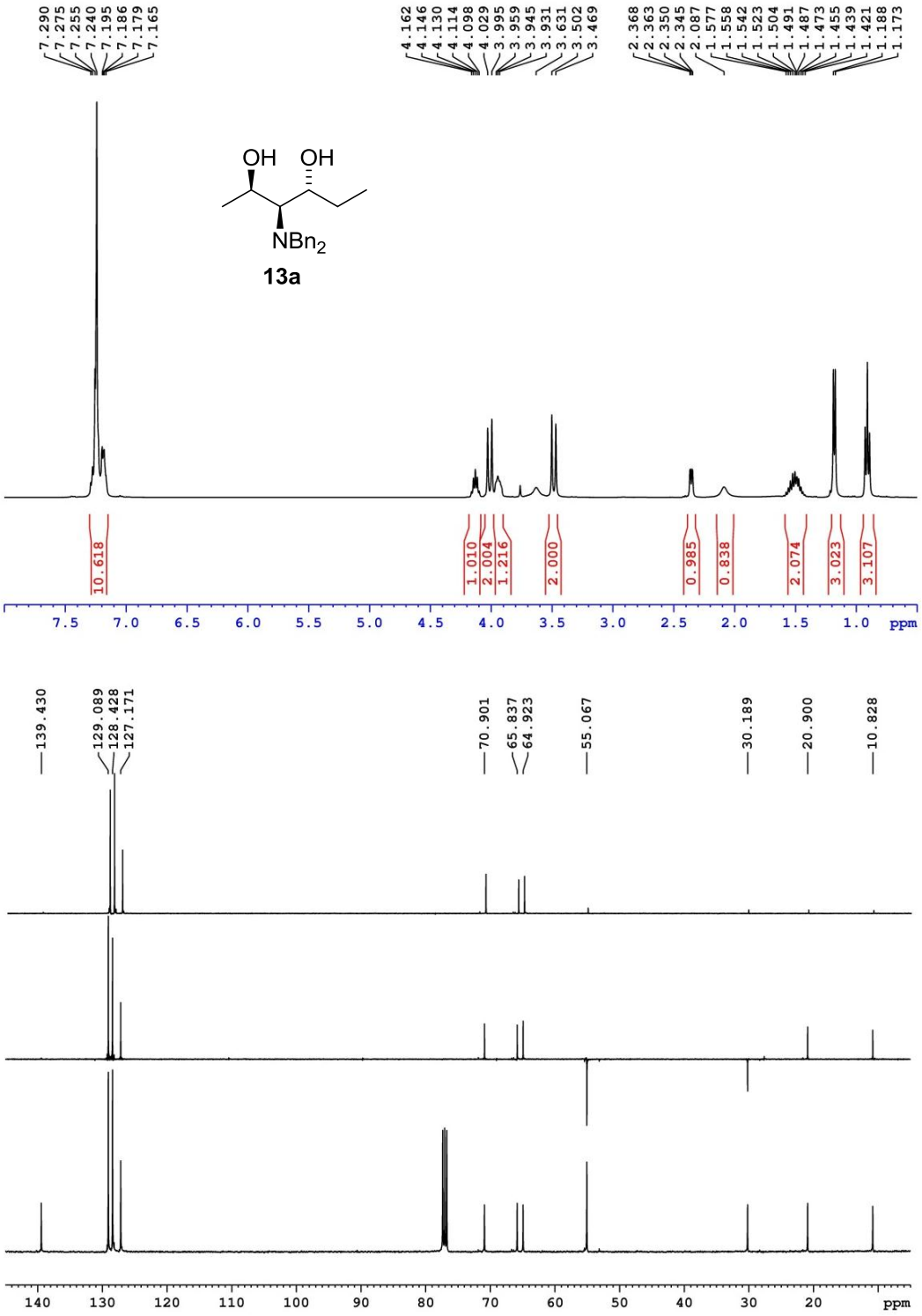

Figure S19. **^{1}H (400 MHz) and ^{13}C (100MHz) NMR spectra of 13a in $CDCl_3$.**

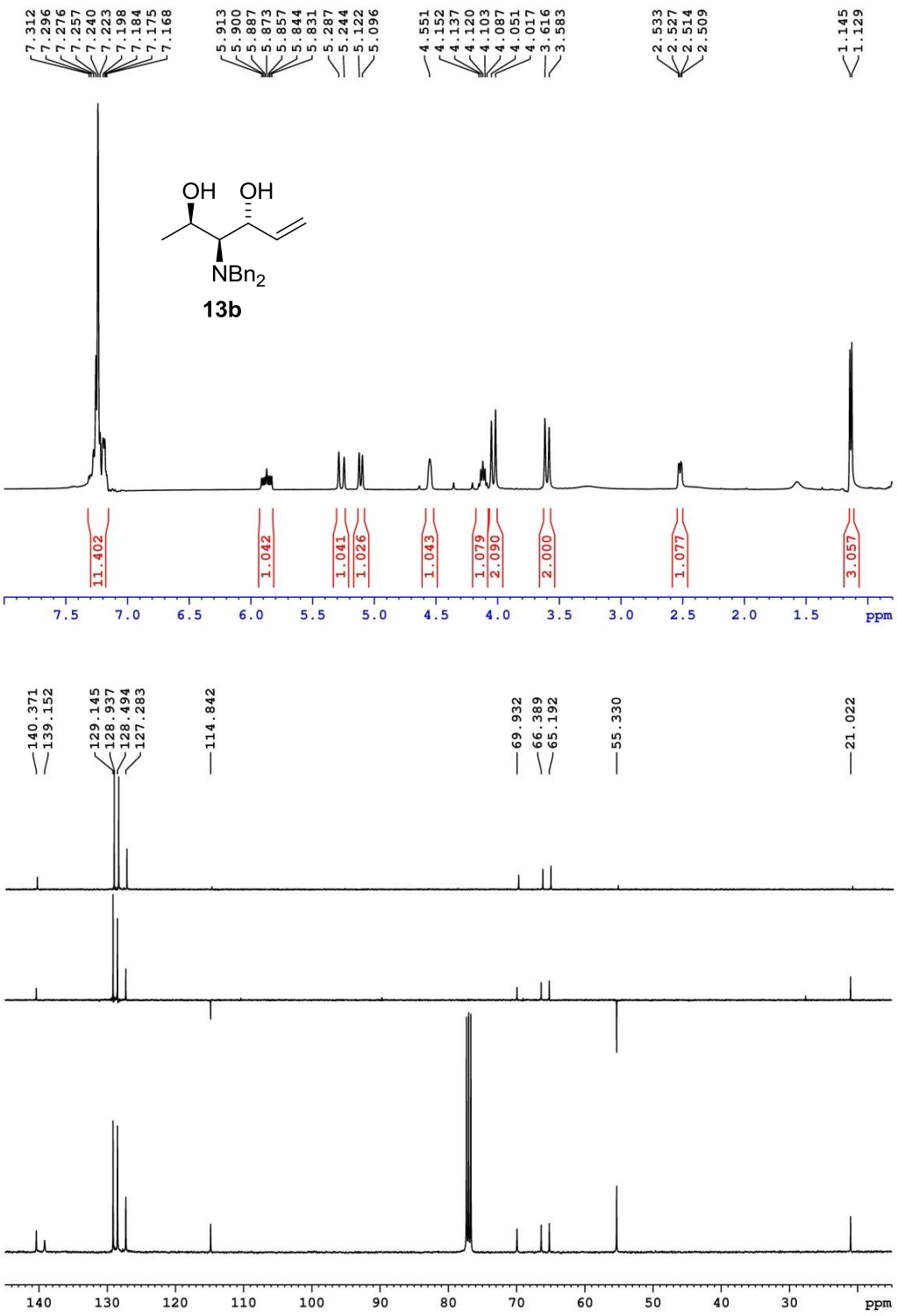

Figure S20. ^{1}H (400 MHz) and ^{13}C (100MHz) NMR spectra of 13b in $CDCl_3$.

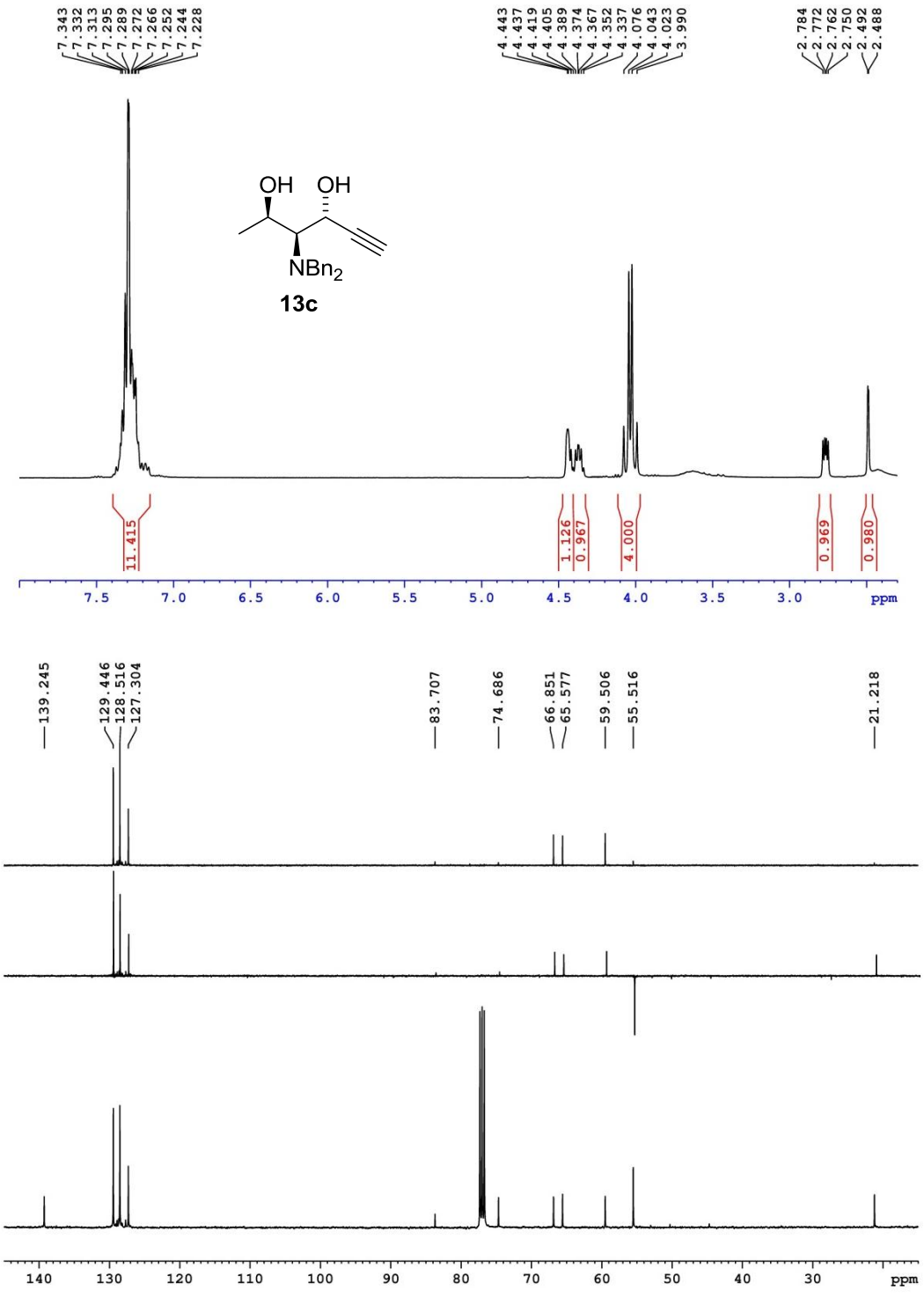

Figure S21. ^{1}**H (400 MHz) and 13C (100 MHz) NMR spectra of 13c in** $CDCl_3$**.**

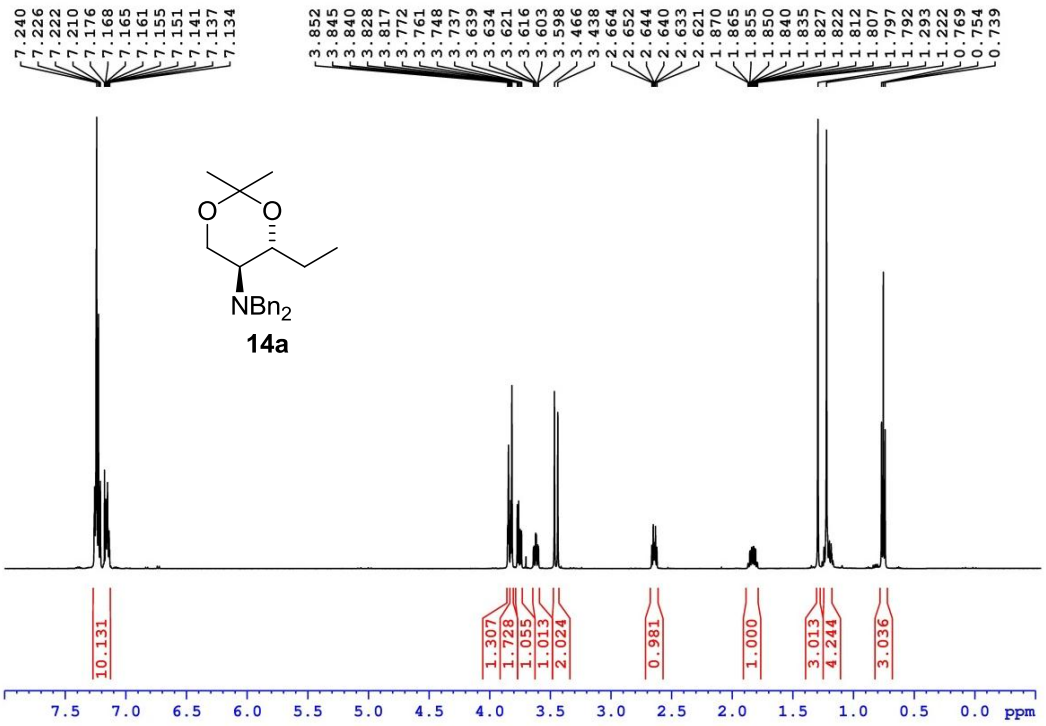
7.240
7.226
7.222
7.210
7.176
7.168
7.165
7.161
7.155
7.151
7.141
7.137
7.134
3.852
3.845
3.840
3.828
3.817
3.772
3.761
3.748
3.737
3.639
3.634
3.621
3.616
3.603
3.598
3.466
3.438
2.664
2.652
2.644
2.640
2.633
2.621
1.870
1.865
1.855
1.850
1.840
1.835
1.827
1.822
1.812
1.807
1.797
1.792
1.293
1.222
0.769
0.754
0.739
NBn2
14a
10.131
1.307
1.728
1.055
1.013
2.024
0.981
1.000
3.013
4.244
3.036
7.5
7.0
6.5
6.0
5.5
5.0
4.5
4.0
3.5
3.0
2.5
2.0
1.5
1.0
0.5
0.0
ppm

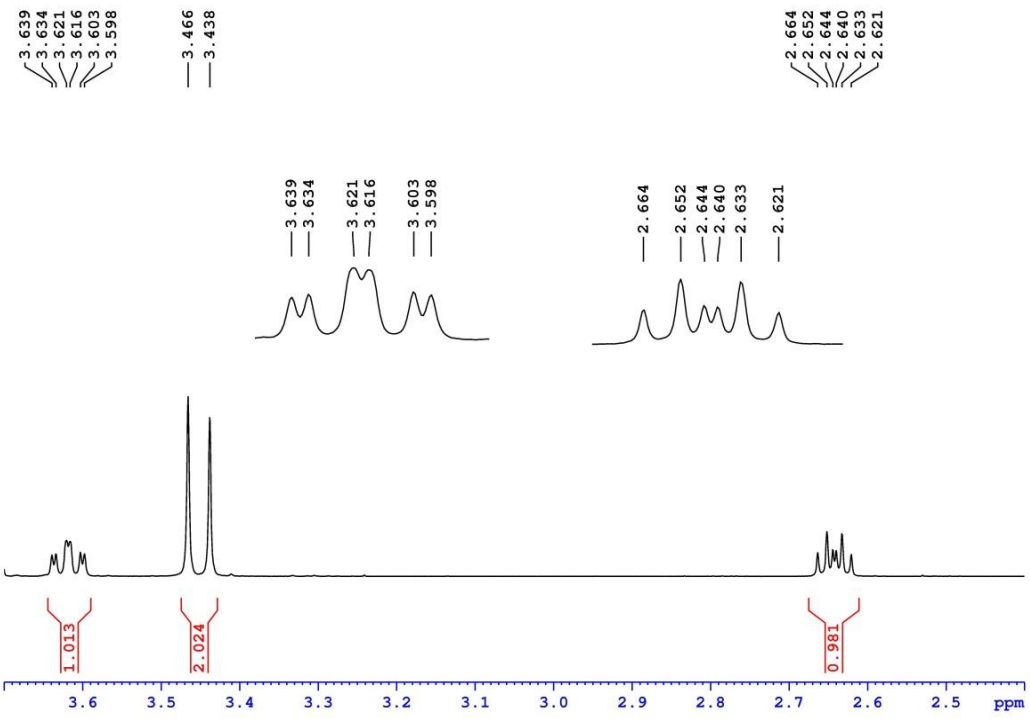
3.639
3.634
3.621
3.616
3.603
3.598
3.466
3.438
2.664
2.652
2.644
2.640
2.633
2.621
1.013
2.024
0.981
3.6
3.5
3.4
3.3
3.2
3.1
3.0
2.9
2.8
2.7
2.6
2.5
ppm

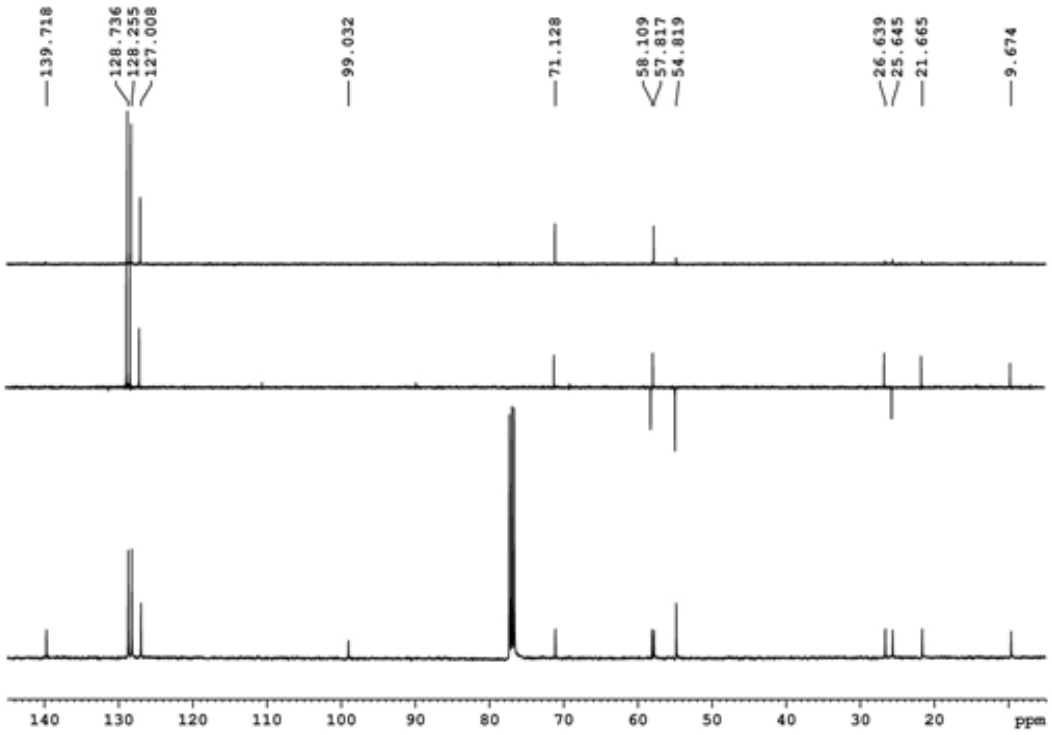

Figure S22. ^{1}**H (500 MHz) and** ^{13}**C (100 MHz) NMR spectra of 14a in** $CDCl_3$**.**

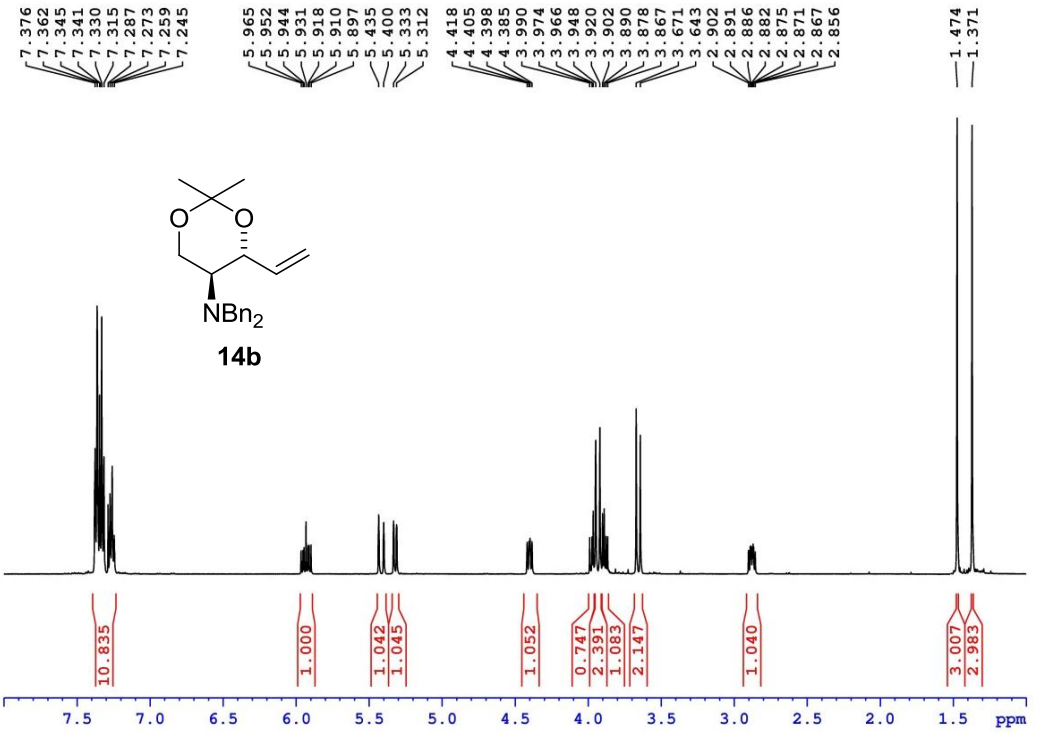
7.376
7.362
7.345
7.341
7.330
7.315
7.287
7.273
7.259
7.245
5.965
5.952
5.944
5.931
5.918
5.910
5.897
5.435
5.400
5.333
5.312
4.418
4.405
4.398
4.385
3.990
3.974
3.966
3.948
3.920
3.902
3.890
3.878
3.867
3.671
3.643
2.902
2.891
2.886
2.882
2.875
2.871
2.867
2.856
1.474
1.371
NBn2
14b
10.835
1.000
1.042
1.045
1.052
0.747
2.391
1.083
2.147
1.040
3.007
2.983
7.5
7.0
6.5
6.0
5.5
5.0
4.5
4.0
3.5
3.0
2.5
2.0
1.5
ppm

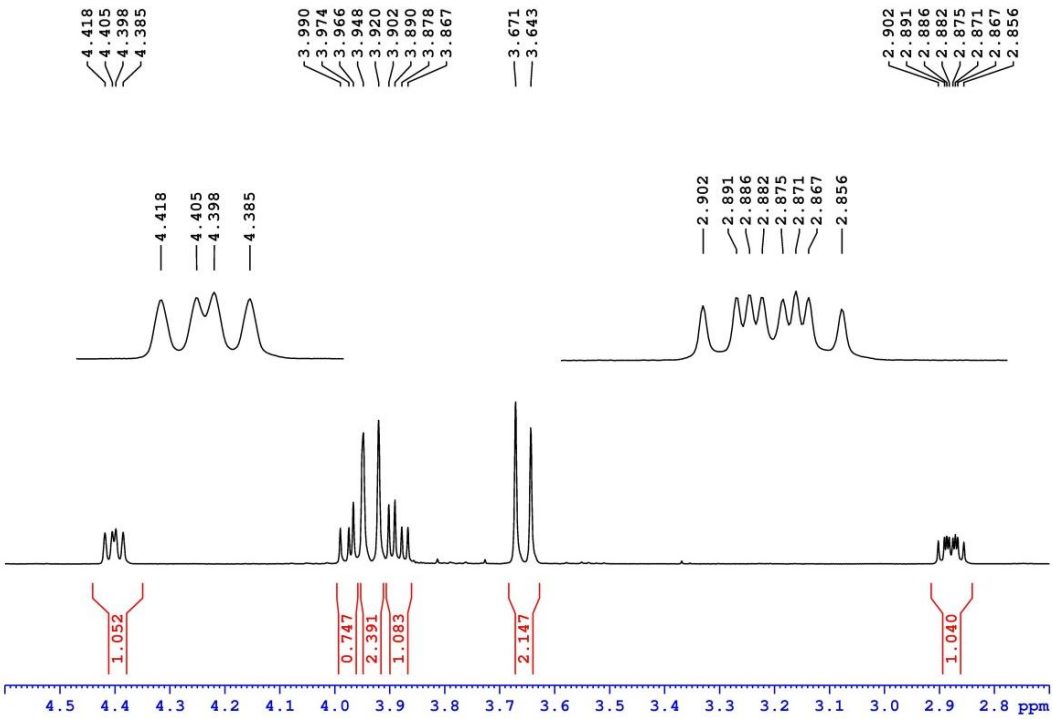
4.418
4.405
4.398
4.385
3.990
3.974
3.966
3.948
3.920
3.902
3.890
3.878
3.867
3.671
3.643
2.902
2.891
2.886
2.882
2.875
2.871
2.867
2.856
1.052
0.747
2.391
1.083
2.147
1.040
4.5
4.4
4.3
4.2
4.1
4.0
3.9
3.8
3.7
3.6
3.5
3.4
3.3
3.2
3.1
3.0
2.9
2.8
ppm

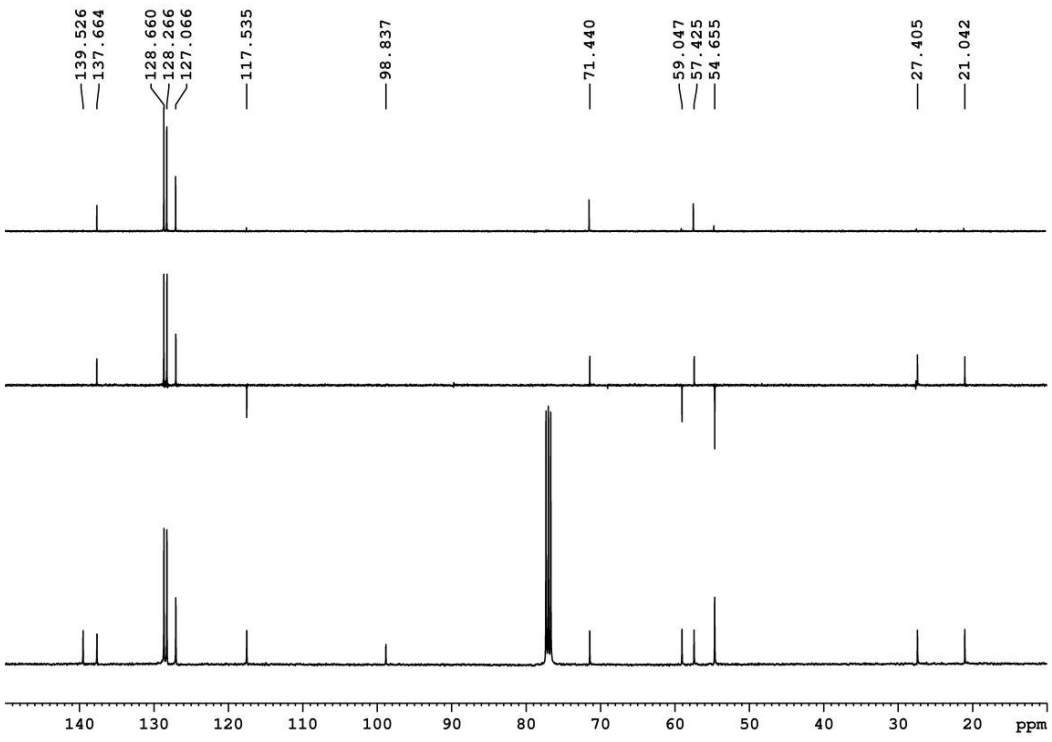

Figure S23. ^{1}**H (500 MHz) and** ^{13}**C (100 MHz) NMR spectra of 14b in** $CDCl_3$**.**

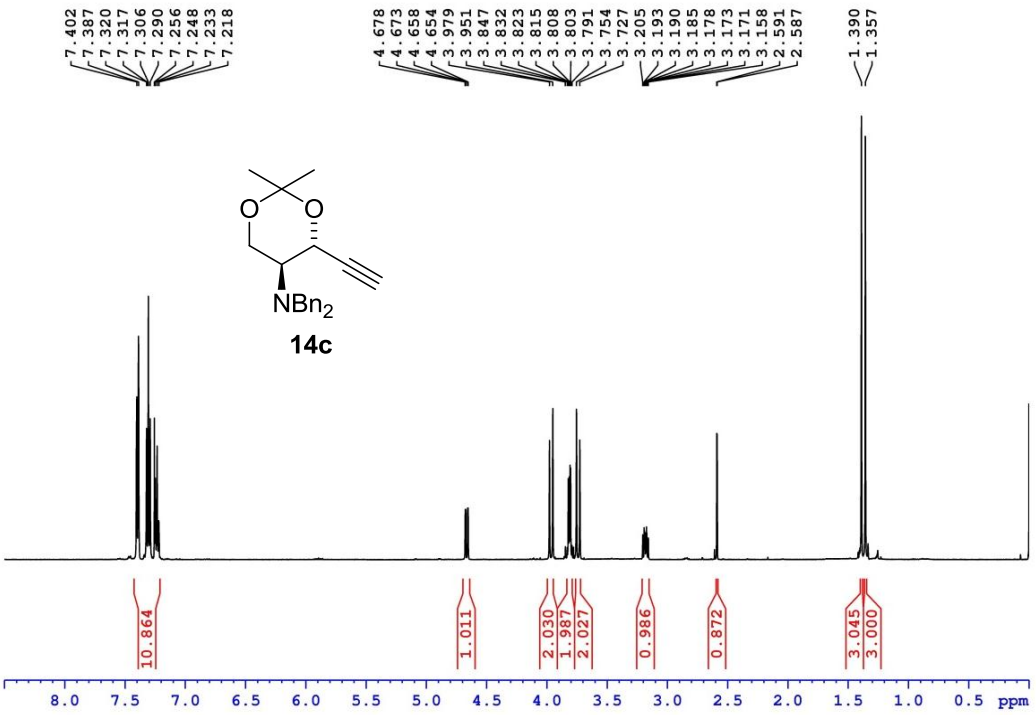
7.402
7.387
7.320
7.317
7.306
7.290
7.256
7.248
7.233
7.218
4.678
4.673
4.658
4.654
3.979
3.951
3.847
3.832
3.823
3.815
3.808
3.803
3.791
3.754
3.727
3.205
3.193
3.190
3.185
3.178
3.173
3.171
3.158
2.591
2.587
1.390
1.357
O
O
NBn2
14c
10.864
1.011
2.030
1.987
2.027
0.986
0.872
3.045
3.000
8.0 7.5 7.0 6.5 6.0 5.5 5.0 4.5 4.0 3.5 3.0 2.5 2.0 1.5 1.0 0.5 ppm

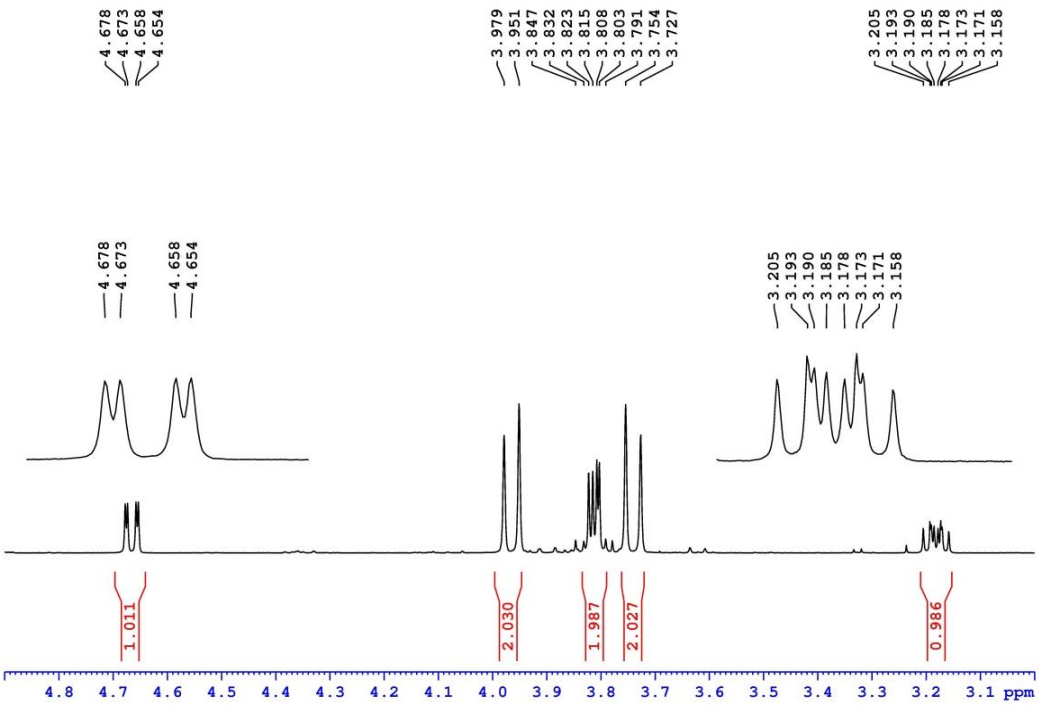
4.678
4.673
4.658
4.654
3.979
3.951
3.847
3.832
3.823
3.815
3.808
3.803
3.791
3.754
3.727
3.205
3.193
3.190
3.185
3.178
3.173
3.171
3.158
1.011
2.030
1.987
2.027
0.986
4.8 4.7 4.6 4.5 4.4 4.3 4.2 4.1 4.0 3.9 3.8 3.7 3.6 3.5 3.4 3.3 3.2 3.1 ppm

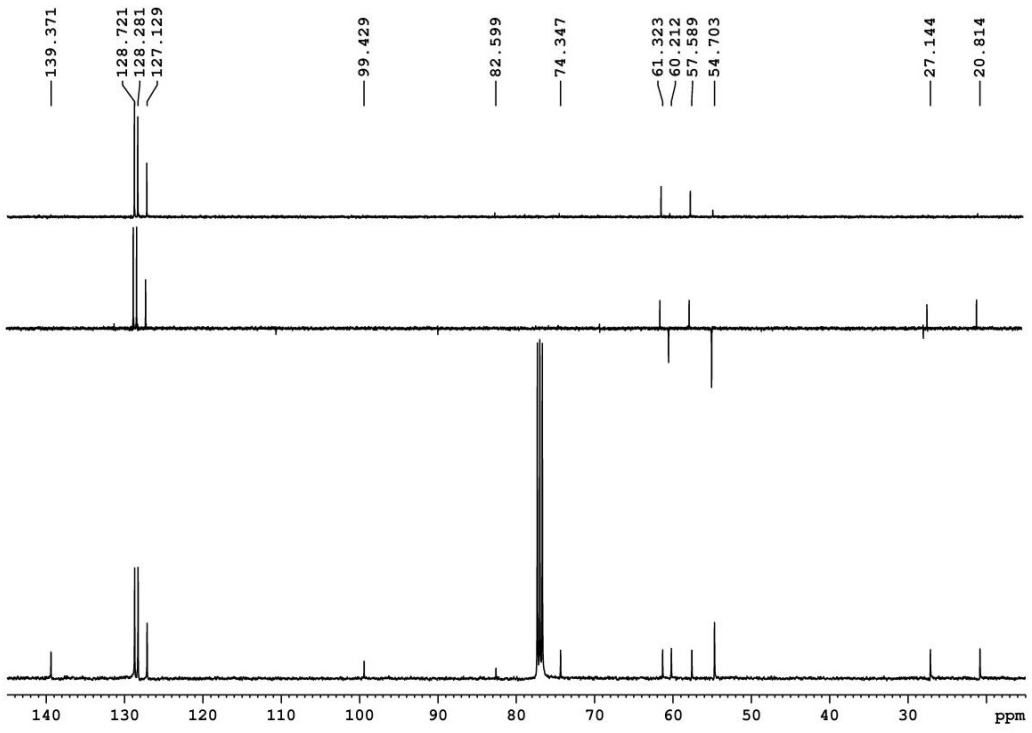

Figure S24. ^{1}H **(500 MHz) and** ^{13}C **(100 MHz) NMR spectra of 14c in** $CDCl_3$**.**

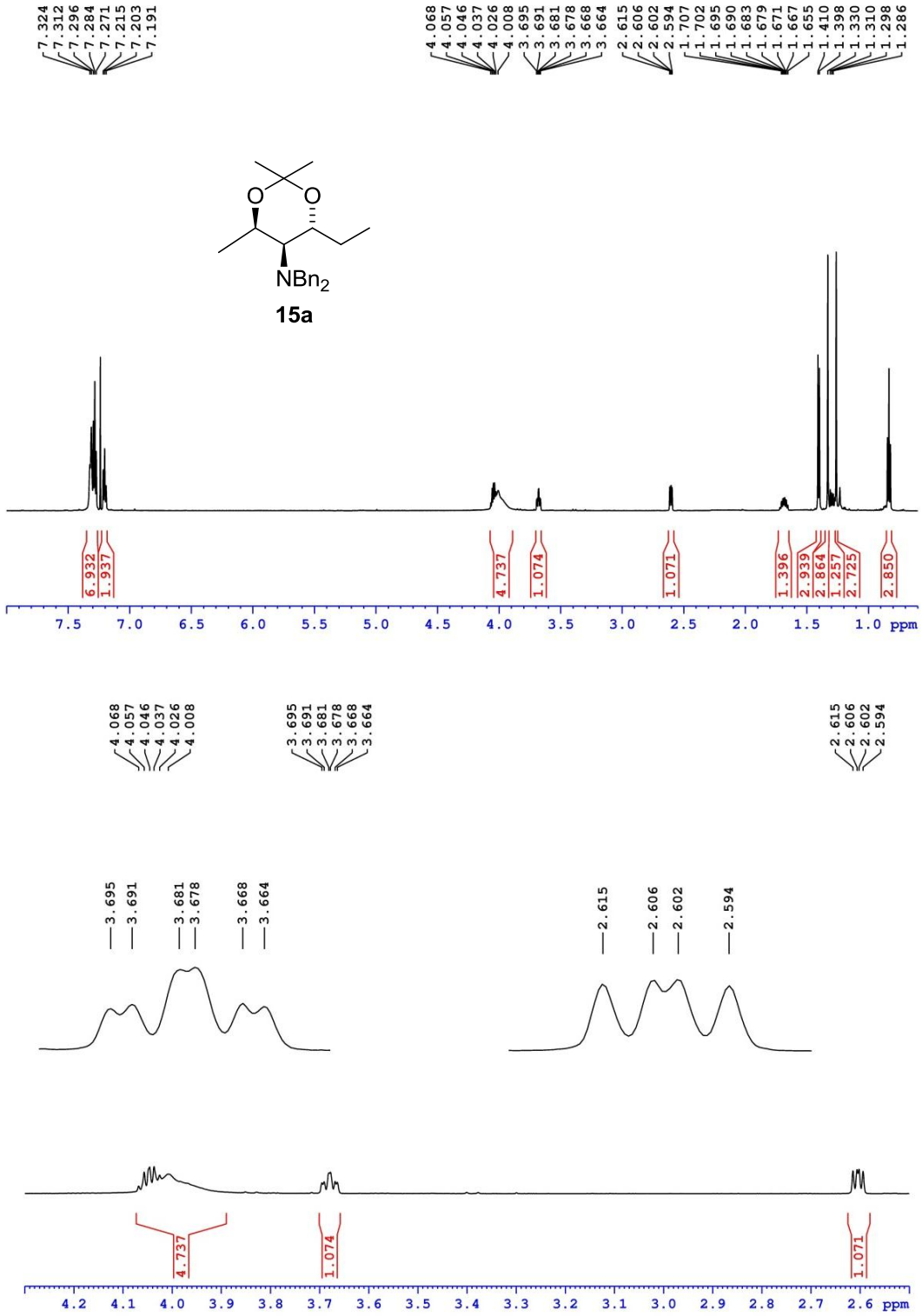
7.324
7.312
7.296
7.284
7.271
7.215
7.203
7.191
4.068
4.057
4.046
4.037
4.026
4.008
3.695
3.691
3.681
3.678
3.668
3.664
2.615
2.606
2.602
2.594
1.707
1.702
1.695
1.690
1.683
1.679
1.671
1.667
1.655
1.410
1.398
1.330
1.310
1.298
1.286
O
O
NBn2
15a
6.932
1.937
4.737
1.074
1.071
1.396
2.939
2.864
1.257
2.725
2.850
7.5 7.0 6.5 6.0 5.5 5.0 4.5 4.0 3.5 3.0 2.5 2.0 1.5 1.0 ppm
4.737
1.074
1.071
4.2 4.1 4.0 3.9 3.8 3.7 3.6 3.5 3.4 3.3 3.2 3.1 3.0 2.9 2.8 2.7 2.6 ppm

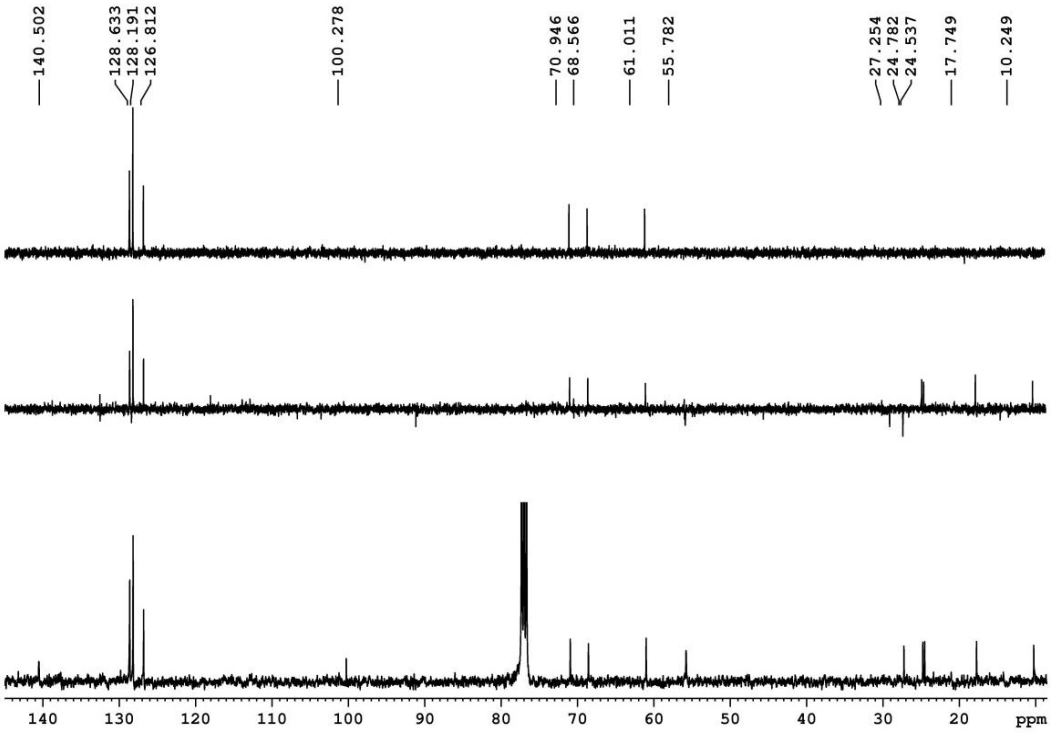

Figure S25. ^{1}H **(600 MHz) and** ^{13}C **(100 MHz) NMR spectra of 15a in** $CDCl_3$**.**

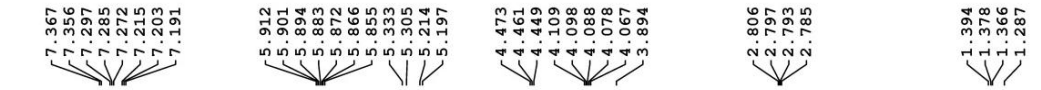
7.367
7.356
7.297
7.285
7.272
7.215
7.203
7.191
5.912
5.901
5.894
5.883
5.872
5.866
5.855
5.333
5.305
5.214
5.197
4.473
4.461
4.449
4.109
4.098
4.088
4.078
4.067
3.894
2.806
2.797
2.793
2.785
1.394
1.378
1.366
1.287

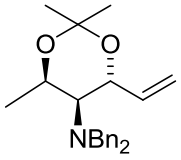
O
O
NBn2

15b

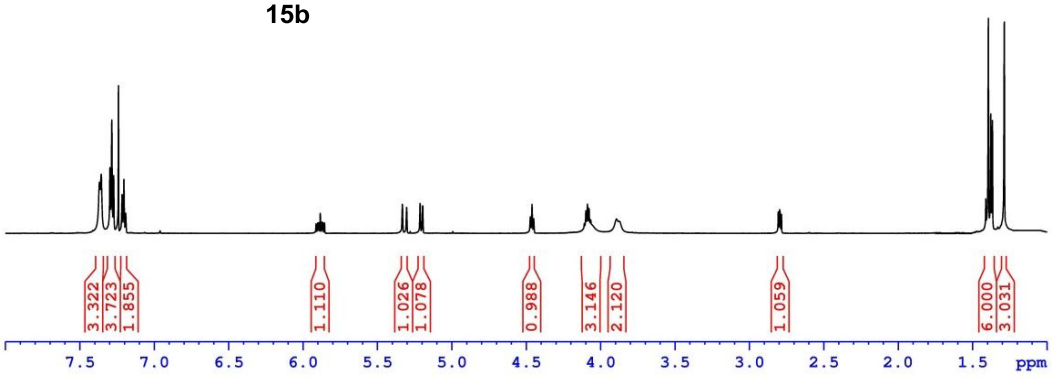
3.322
3.723
1.855
1.110
1.026
1.078
0.988
3.146
2.120
1.059
6.000
3.031
7.5
7.0
6.5
6.0
5.5
5.0
4.5
4.0
3.5
3.0
2.5
2.0
1.5
ppm

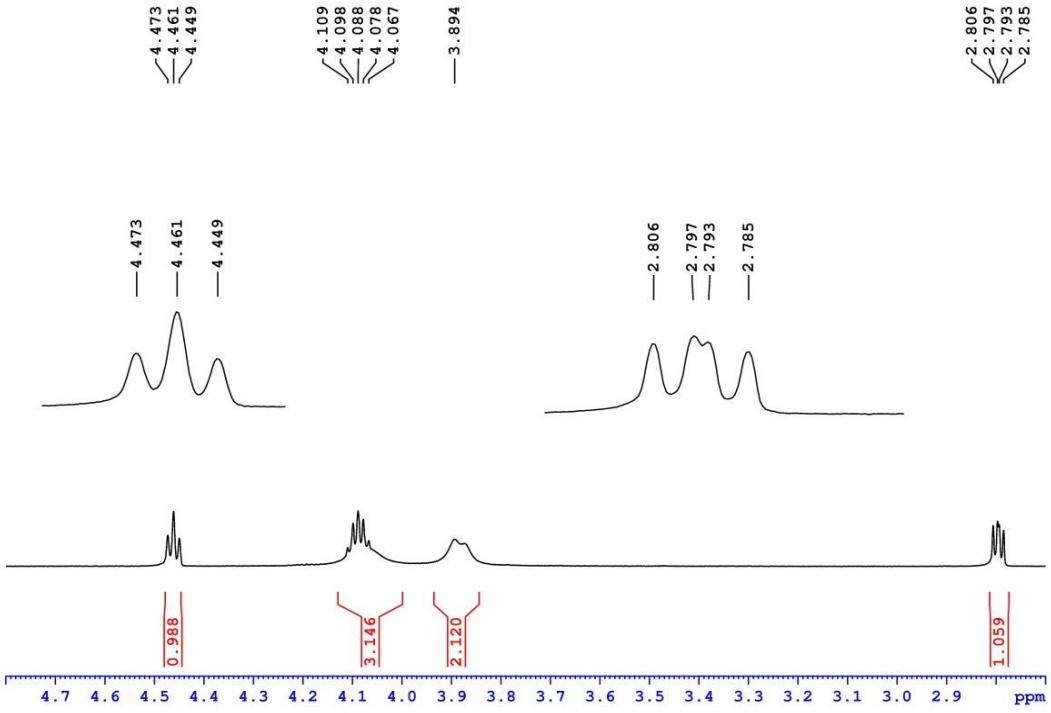
4.473
4.461
4.449
4.109
4.098
4.088
4.078
4.067
3.894
2.806
2.797
2.793
2.785
0.988
3.146
2.120
1.059
4.7
4.6
4.5
4.4
4.3
4.2
4.1
4.0
3.9
3.8
3.7
3.6
3.5
3.4
3.3
3.2
3.1
3.0
2.9
ppm

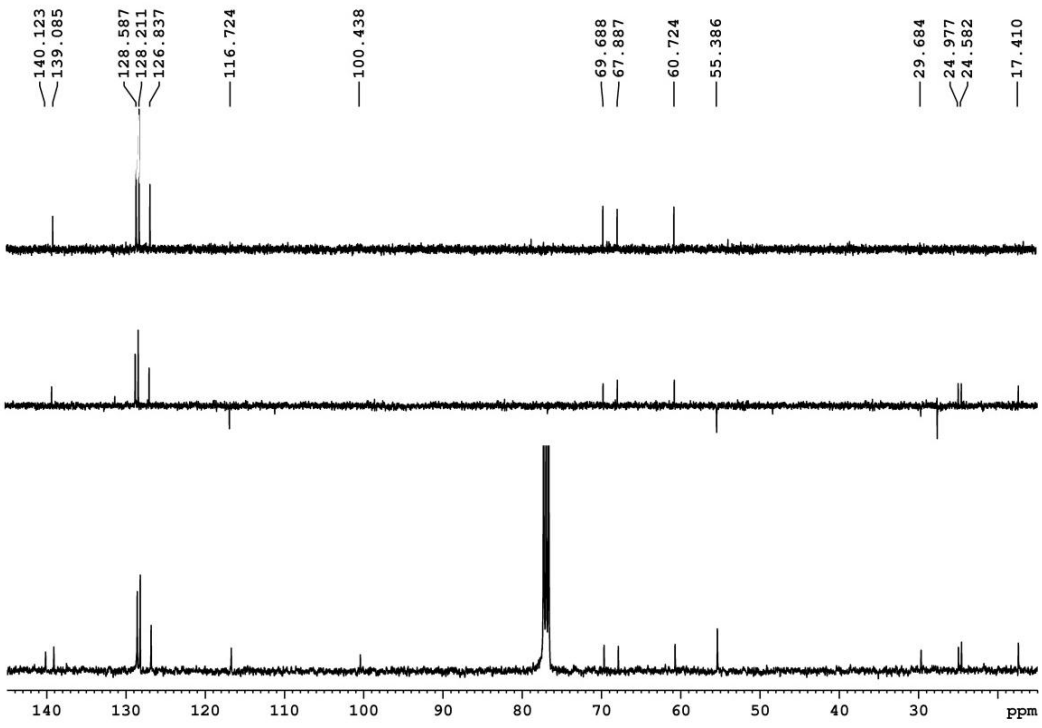

Figure S26. ^{1}H **(600 MHz) and** ^{13}C **(100 MHz) NMR spectra of 15b in** $CDCl_3$**.**

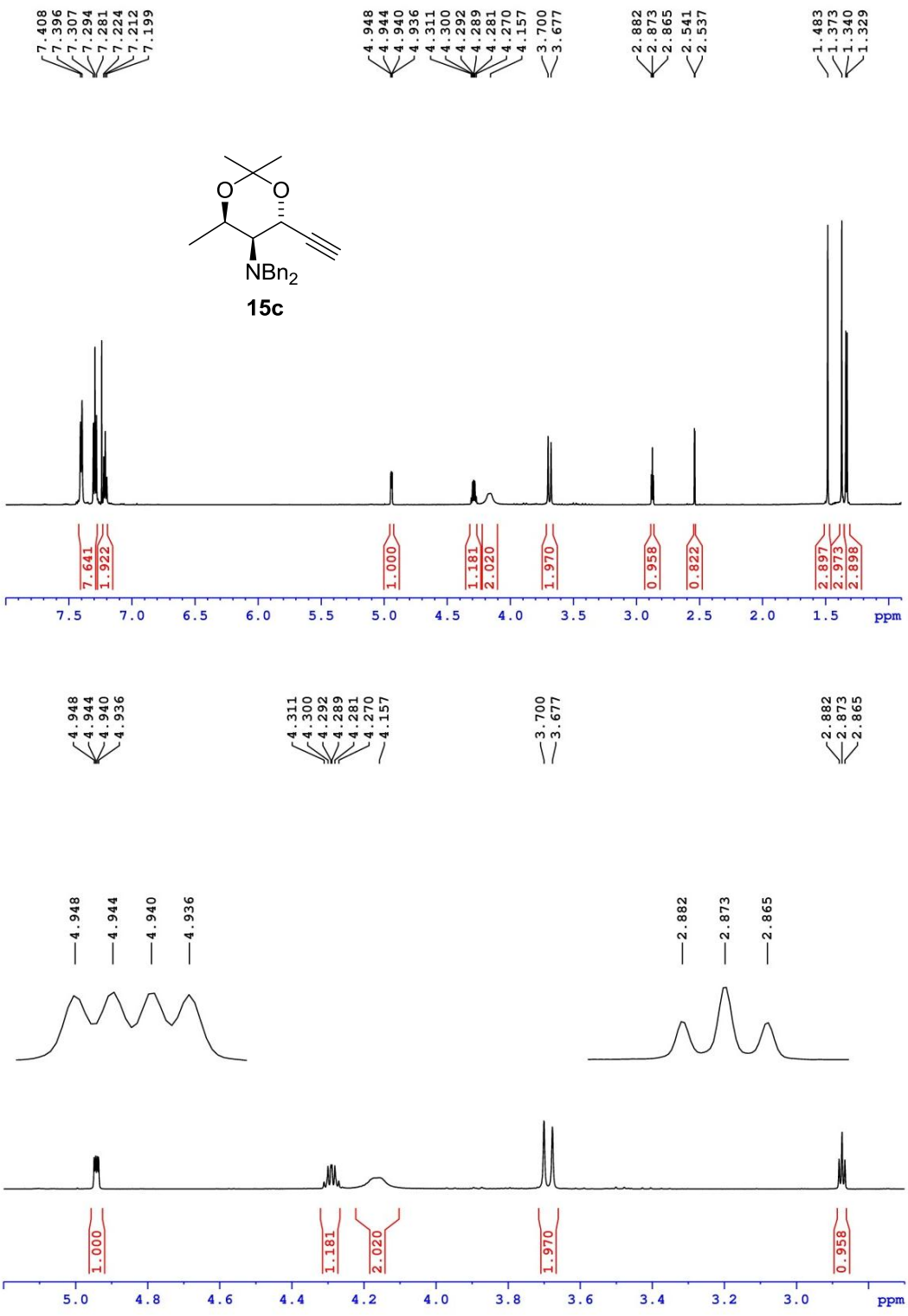
7.408
7.396
7.307
7.294
7.281
7.224
7.212
7.199
4.948
4.944
4.940
4.936
4.311
4.300
4.292
4.289
4.281
4.270
4.157
3.700
3.677
2.882
2.873
2.865
2.541
2.537
1.483
1.373
1.340
1.329
O
O
NBn2
15c
7.641
1.922
1.000
1.181
2.020
1.970
0.958
0.822
2.897
2.973
2.898
7.5
7.0
6.5
6.0
5.5
5.0
4.5
4.0
3.5
3.0
2.5
2.0
1.5
ppm
4.948
4.944
4.940
4.936
4.311
4.300
4.292
4.289
4.281
4.270
4.157
3.700
3.677
2.882
2.873
2.865
4.948
4.944
4.940
4.936
2.882
2.873
2.865
1.000
1.181
2.020
1.970
0.958
5.0
4.8
4.6
4.4
4.2
4.0
3.8
3.6
3.4
3.2
3.0
ppm

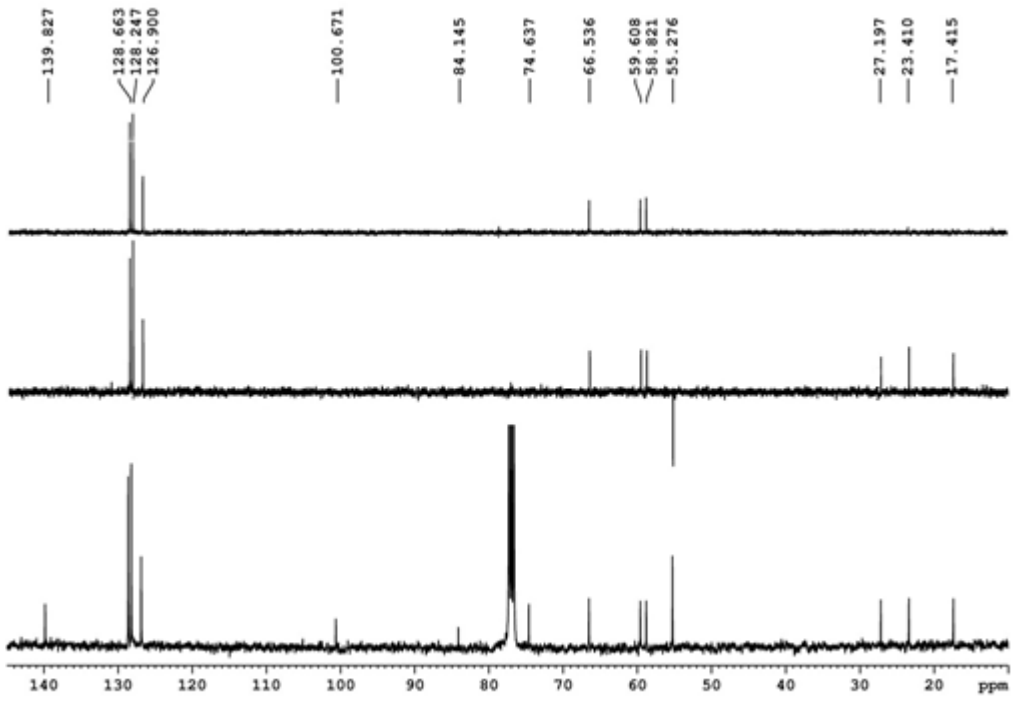

Figure S27. **^{1}H (600 MHz) and ^{13}C (100 MHz) NMR spectra of 15c in $CDCl_3$.**

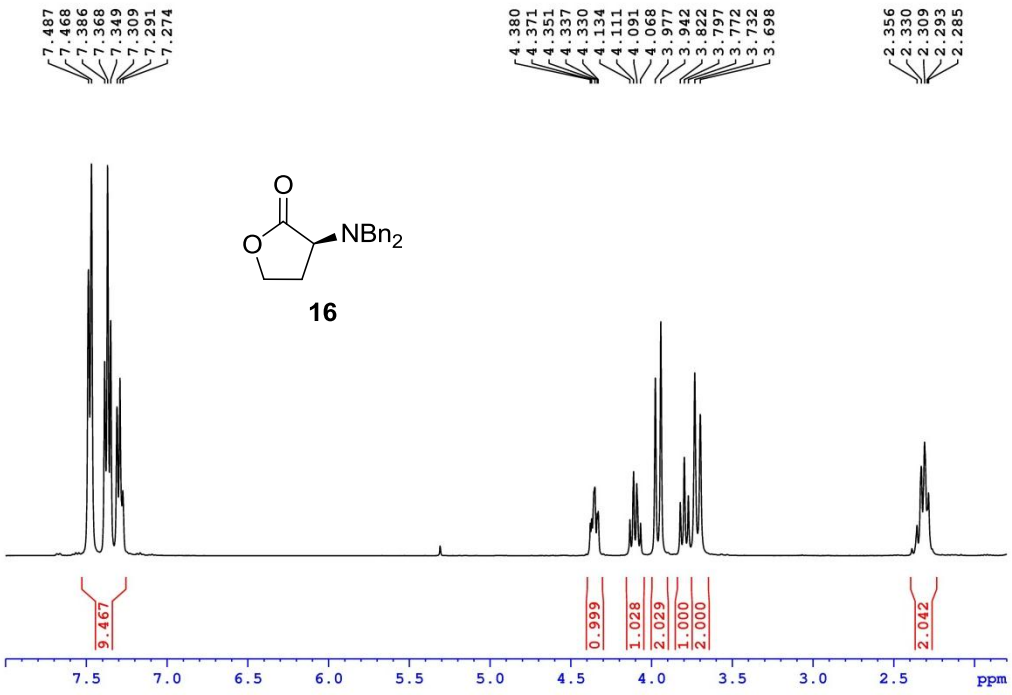

Figure S28. ^{1}**H (400 MHz) NMR spectrum of 16 in** $CDCl_3$**.**

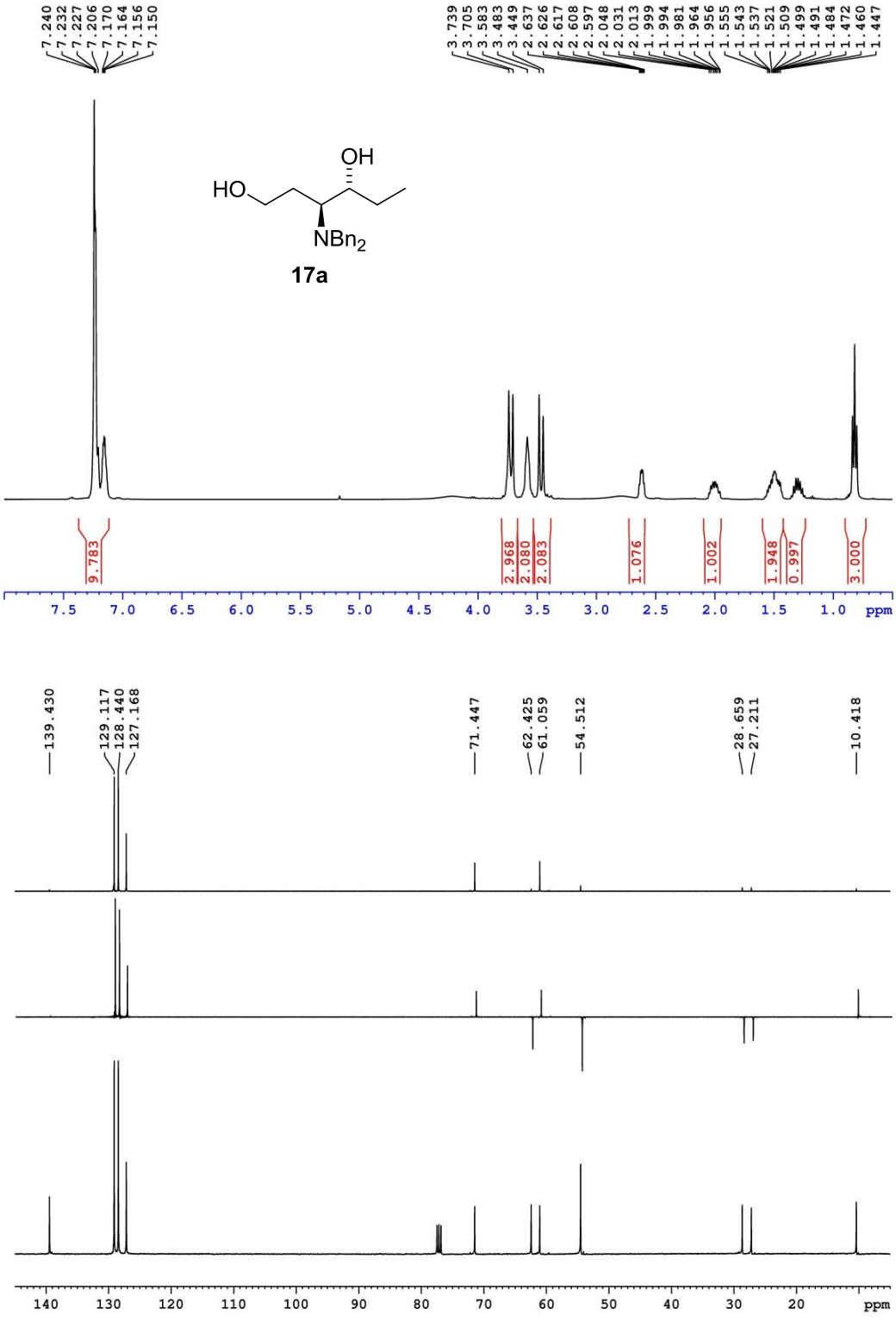

Figure S29. ^{1}H **(400 MHz) and** ^{13}C **(100 MHz) NMR spectra of 17a in** $CDCl_3$**.**

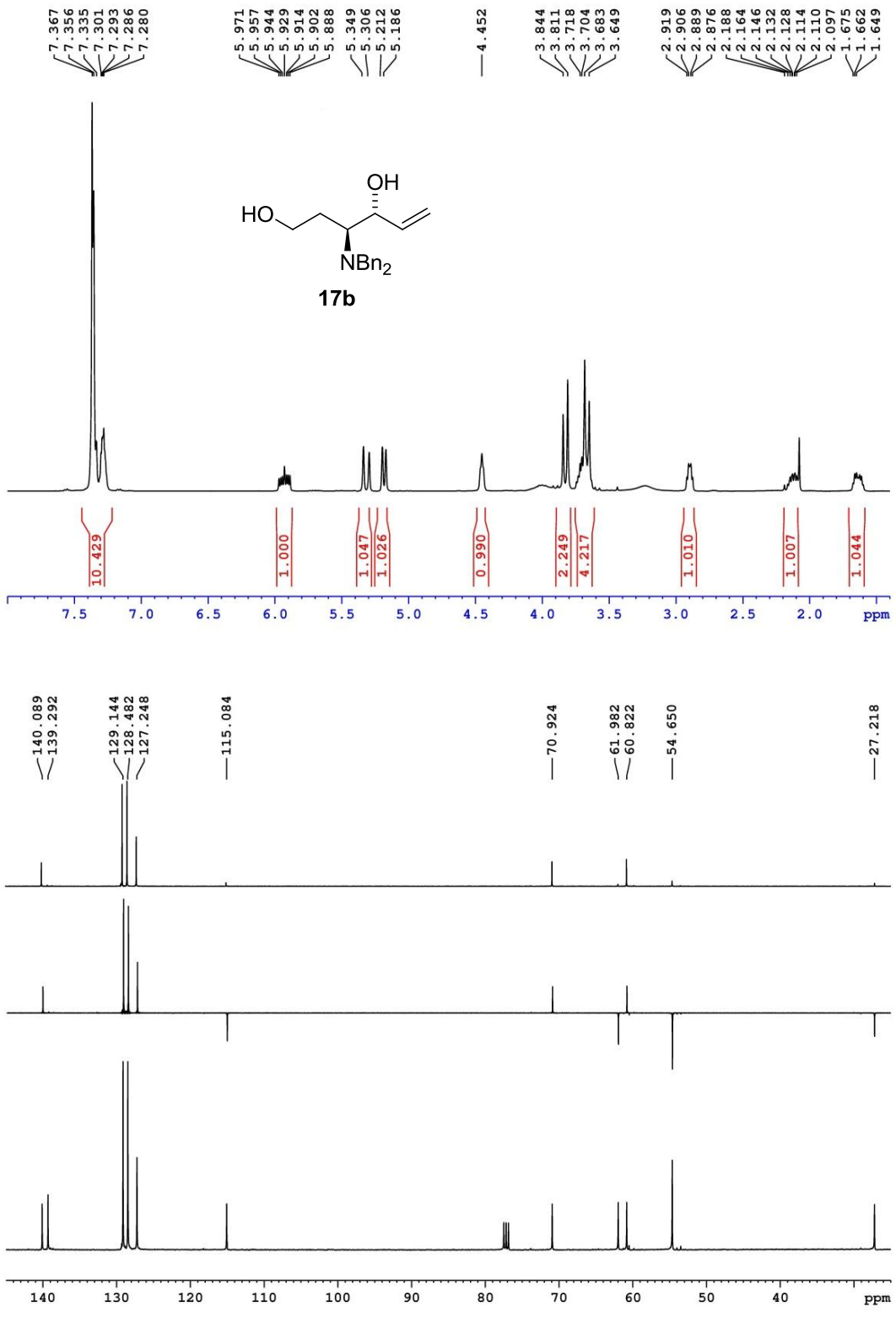

Figure S30. ^{1}**H (400 MHz) and** ^{13}**C (100 MHz) NMR spectra of 17b in** $CDCl_3$**.**

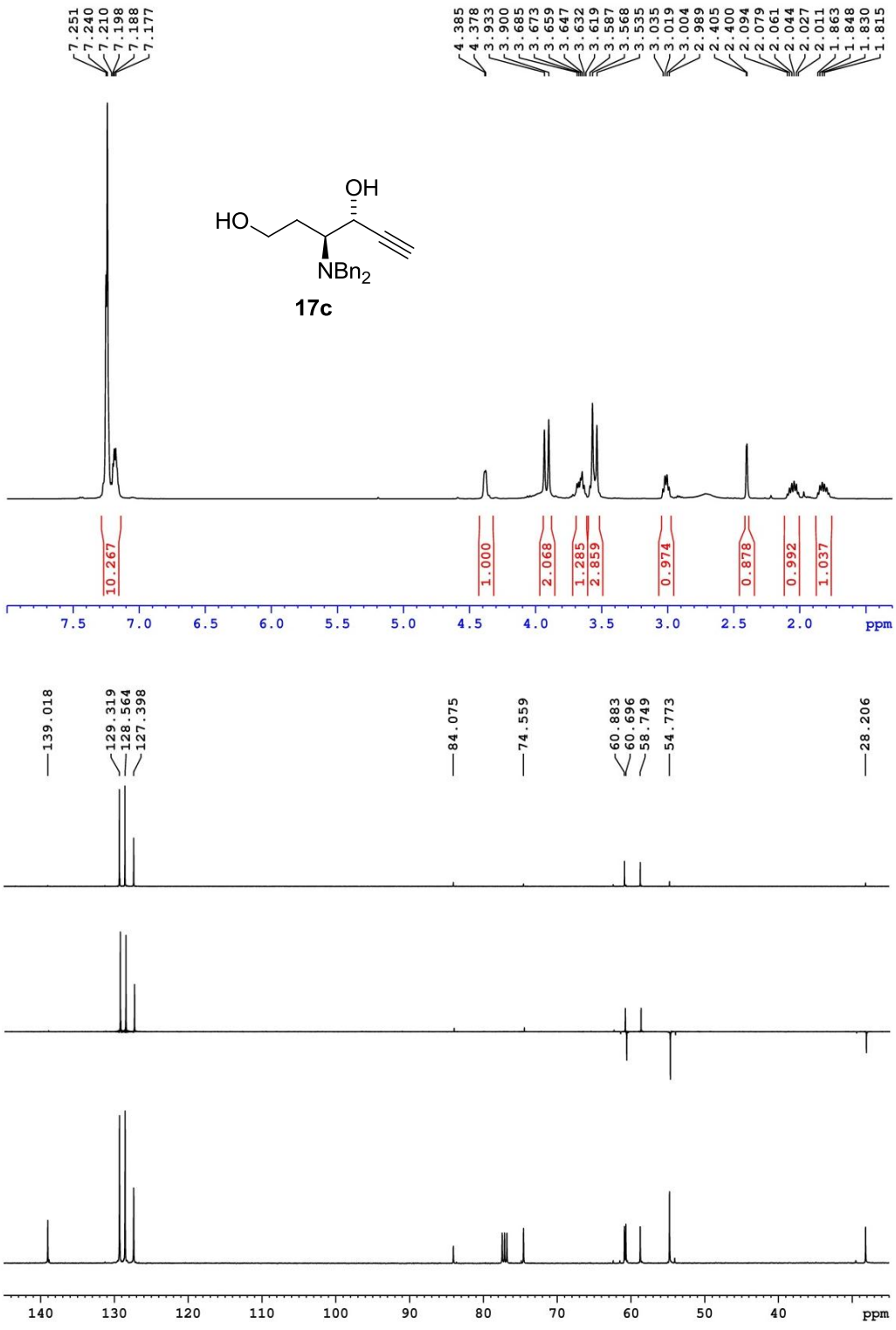

Figure S31. ^{1}H (400 MHz) and ^{13}C (100 MHz) NMR spectra of 17c in $CDCl_3$.

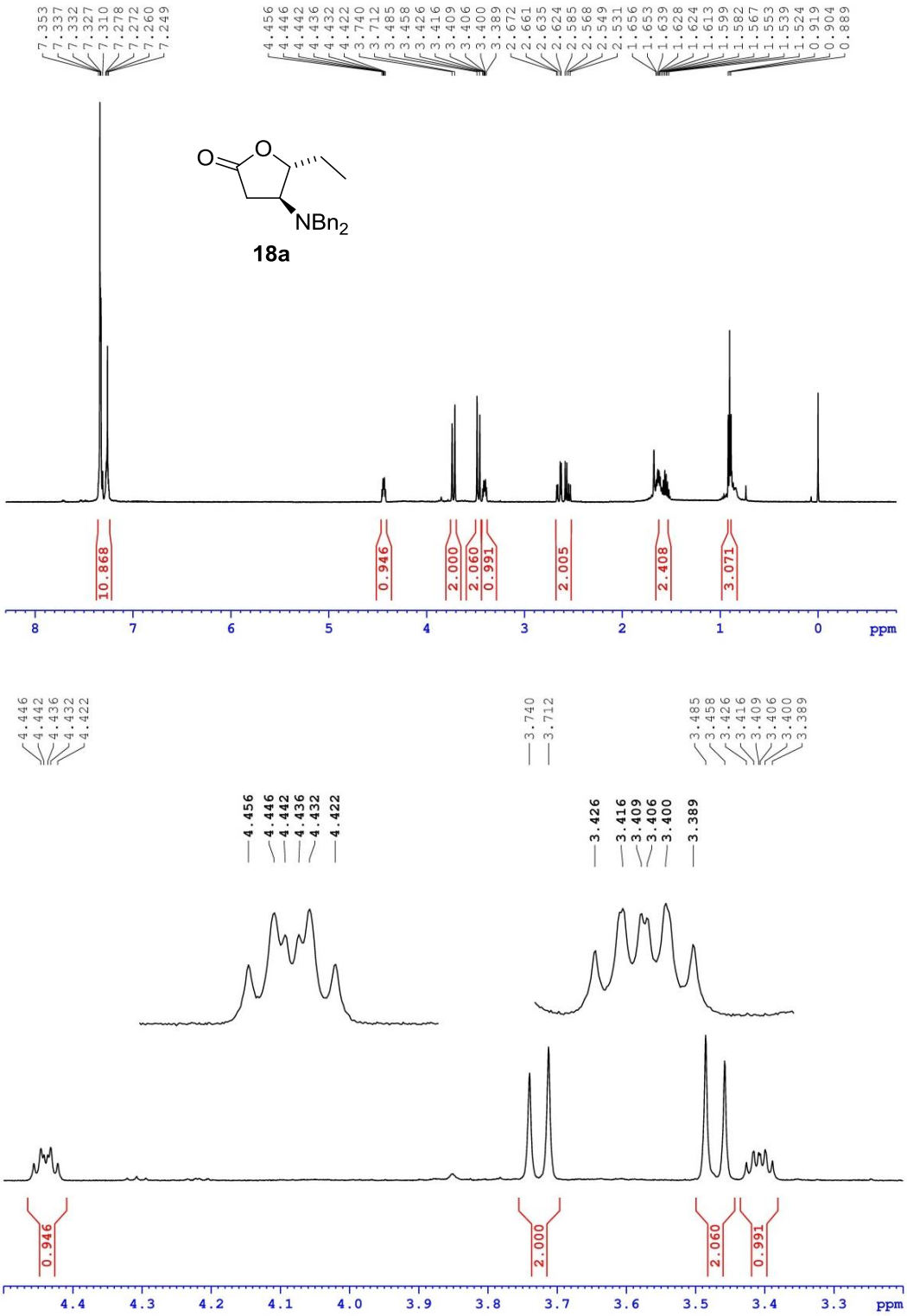
7.353
7.337
7.332
7.327
7.310
7.278
7.272
7.260
7.249
4.456
4.446
4.442
4.436
4.432
4.422
3.740
3.712
3.485
3.458
3.426
3.416
3.409
3.406
3.400
3.389
2.672
2.661
2.635
2.624
2.585
2.568
2.549
2.531
1.656
1.653
1.639
1.628
1.624
1.613
1.599
1.582
1.567
1.553
1.539
1.524
0.919
0.904
0.889
O
O
NBn2
18a
10.868
0.946
2.000
2.060
0.991
2.005
2.408
3.071
ppm
0.946
2.000
2.060
0.991
ppm

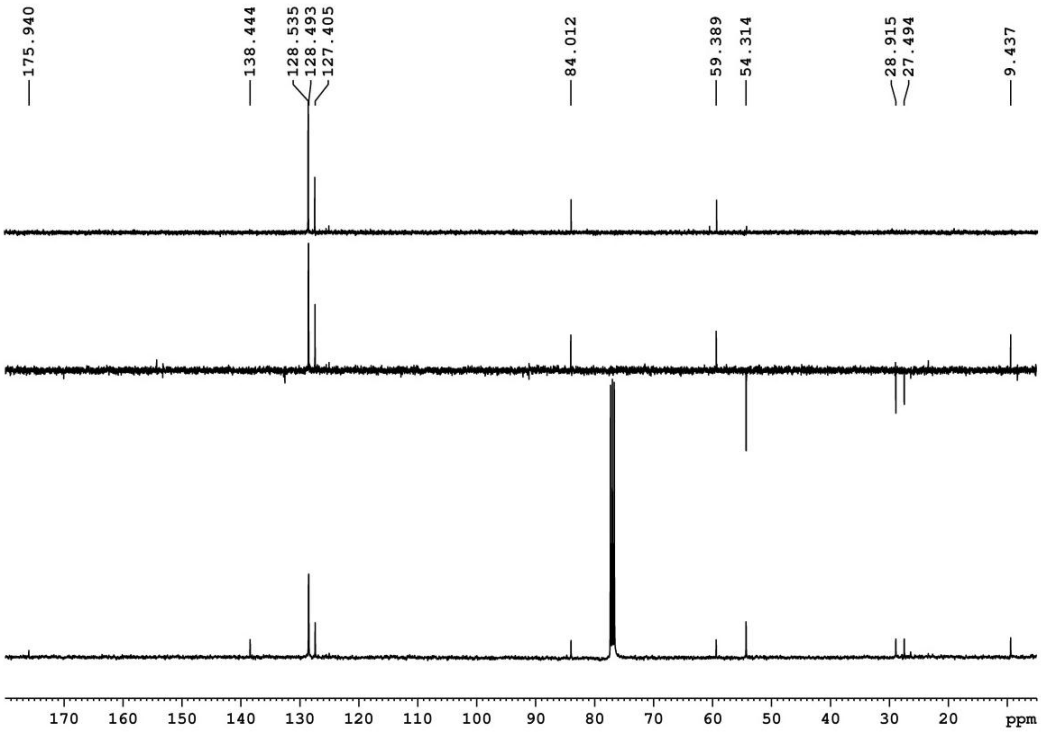

Figure S32. ^{1}H (500 MHz) and ^{13}C (100 MHz) NMR spectra of 18a in $CDCl_3$.

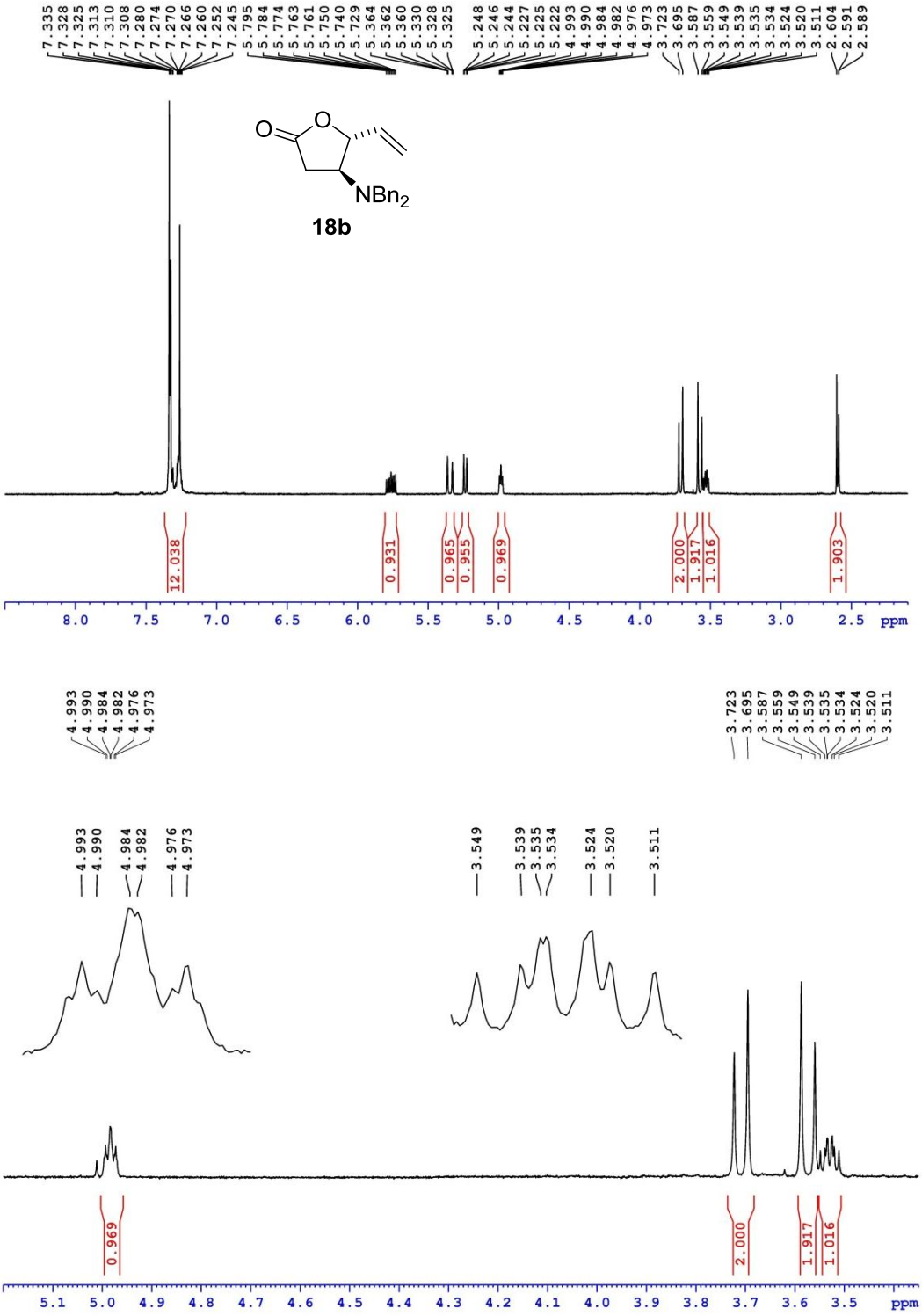
7.335
7.328
7.325
7.313
7.310
7.308
7.280
7.274
7.270
7.266
7.260
7.252
7.245
5.795
5.784
5.774
5.763
5.761
5.750
5.740
5.729
5.364
5.362
5.360
5.330
5.328
5.325
5.248
5.246
5.244
5.227
5.225
5.222
4.993
4.990
4.984
4.982
4.976
4.973
3.723
3.695
3.587
3.559
3.549
3.539
3.535
3.534
3.524
3.520
3.511
2.604
2.591
2.589
O
O
NBn2
18b
12.038
0.931
0.965
0.955
0.969
2.000
1.917
1.016
1.903
8.0
7.5
7.0
6.5
6.0
5.5
5.0
4.5
4.0
3.5
3.0
2.5
ppm
4.993
4.990
4.984
4.982
4.976
4.973
3.723
3.695
3.587
3.559
3.549
3.539
3.535
3.534
3.524
3.520
3.511
0.969
2.000
1.917
1.016
5.1
5.0
4.9
4.8
4.7
4.6
4.5
4.4
4.3
4.2
4.1
4.0
3.9
3.8
3.7
3.6
3.5
ppm

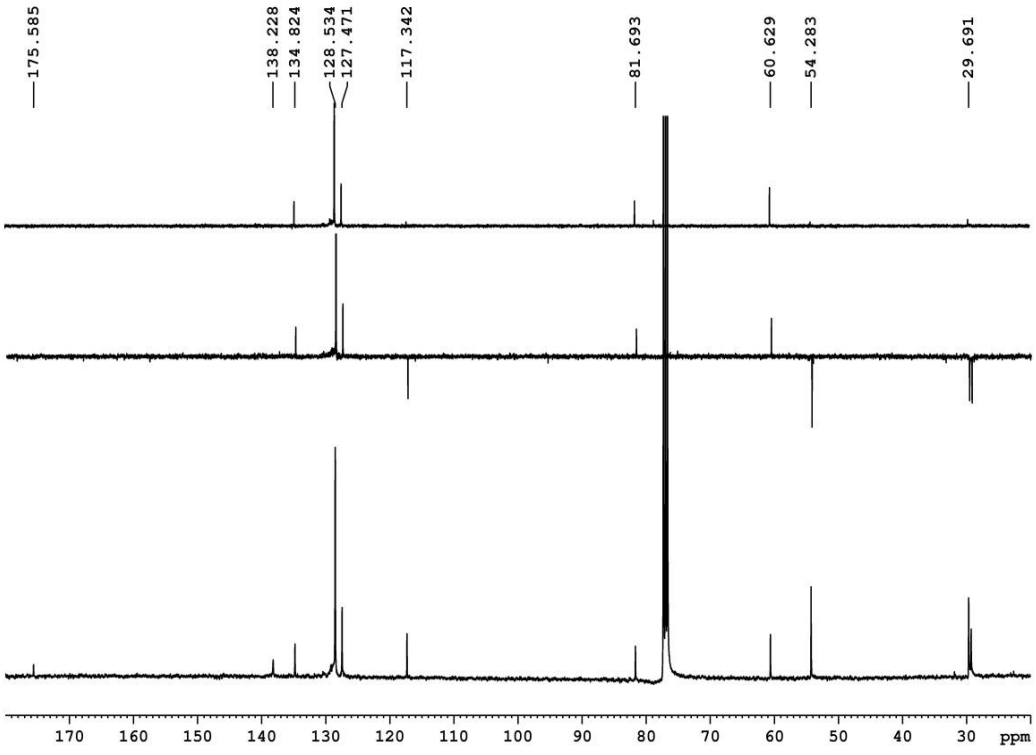

Figure S33. ^{1}H (500 MHz) and ^{13}C (100 MHz) NMR spectra of 18b in $CDCl_3$.

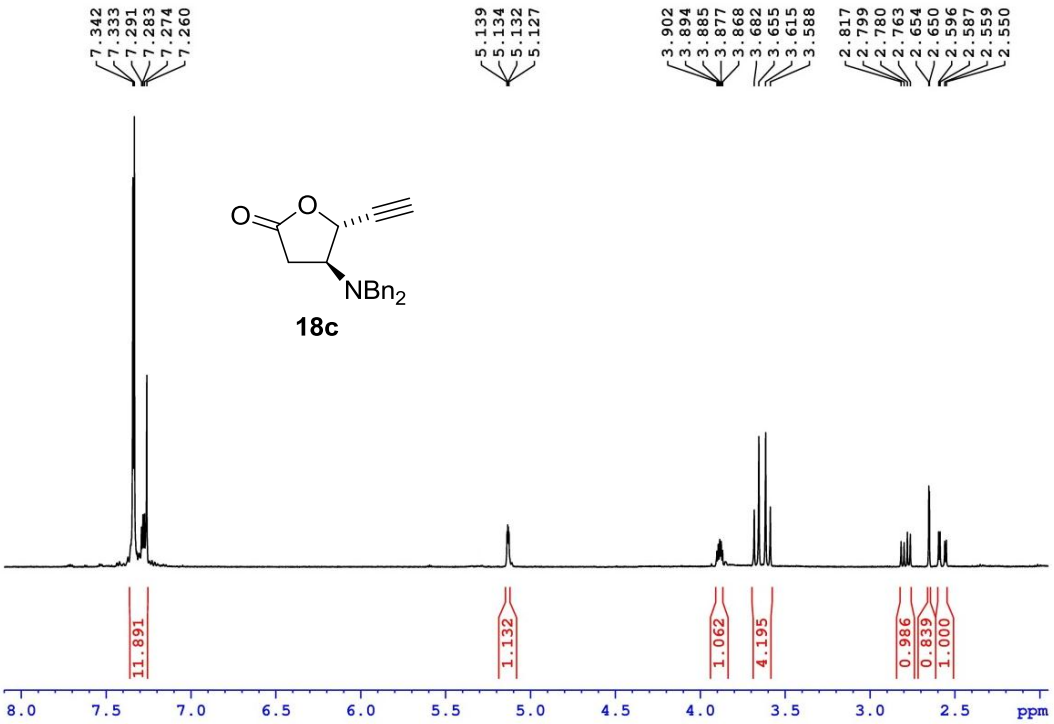
7.342
7.333
7.291
7.283
7.274
7.260
5.139
5.134
5.132
5.127
3.902
3.894
3.885
3.877
3.868
3.682
3.655
3.615
3.588
2.817
2.799
2.780
2.763
2.654
2.650
2.596
2.587
2.559
2.550
O
O
NBn2
18c
11.891
1.132
1.062
4.195
0.986
0.839
1.000
8.0
7.5
7.0
6.5
6.0
5.5
5.0
4.5
4.0
3.5
3.0
2.5
ppm

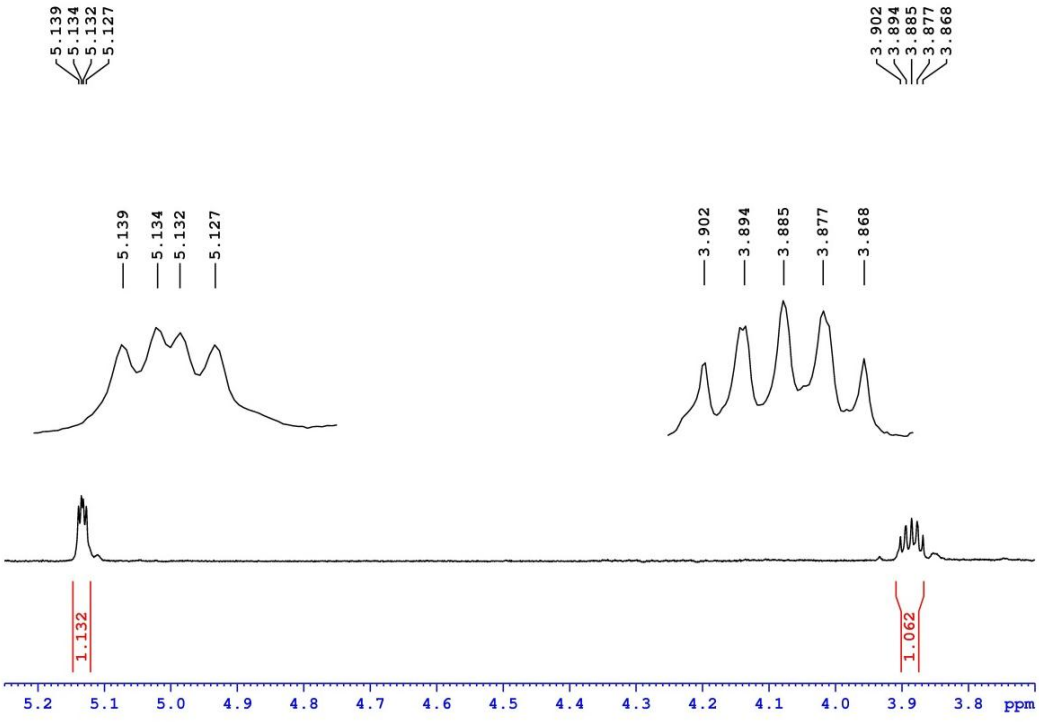
5.139
5.134
5.132
5.127
3.902
3.894
3.885
3.877
3.868
1.132
1.062
5.2
5.1
5.0
4.9
4.8
4.7
4.6
4.5
4.4
4.3
4.2
4.1
4.0
3.9
3.8
ppm

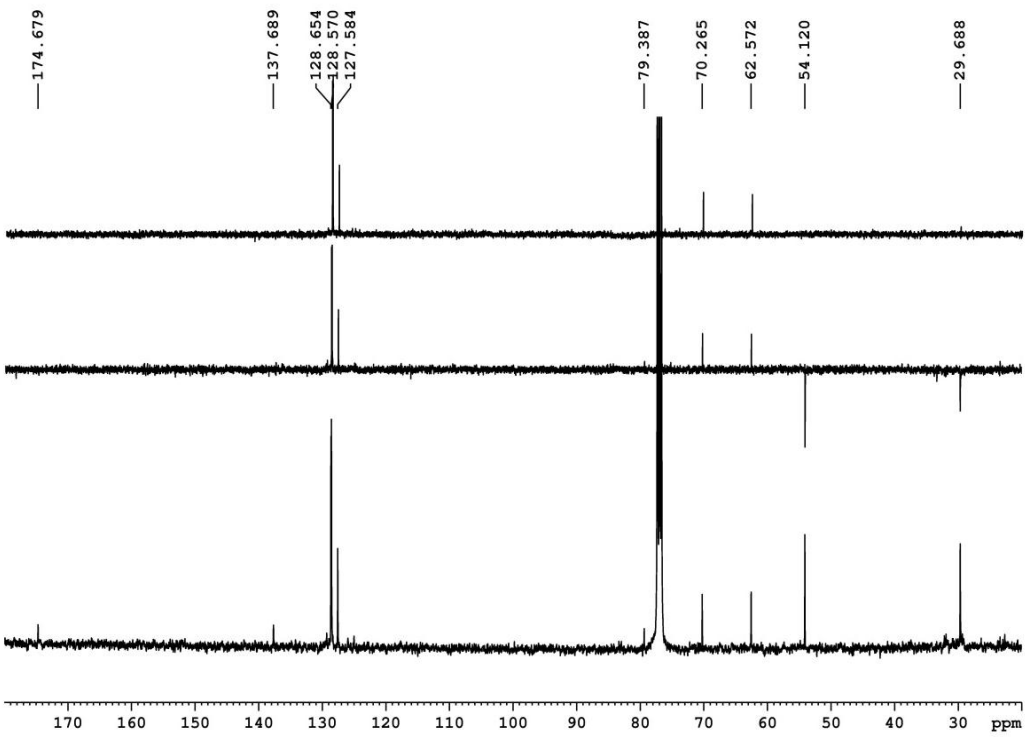

Figure S34. ^{1}**H (500 MHz) and** ^{13}**C (100 MHz) NMR spectra of 18c in** $CDCl_3$**.**

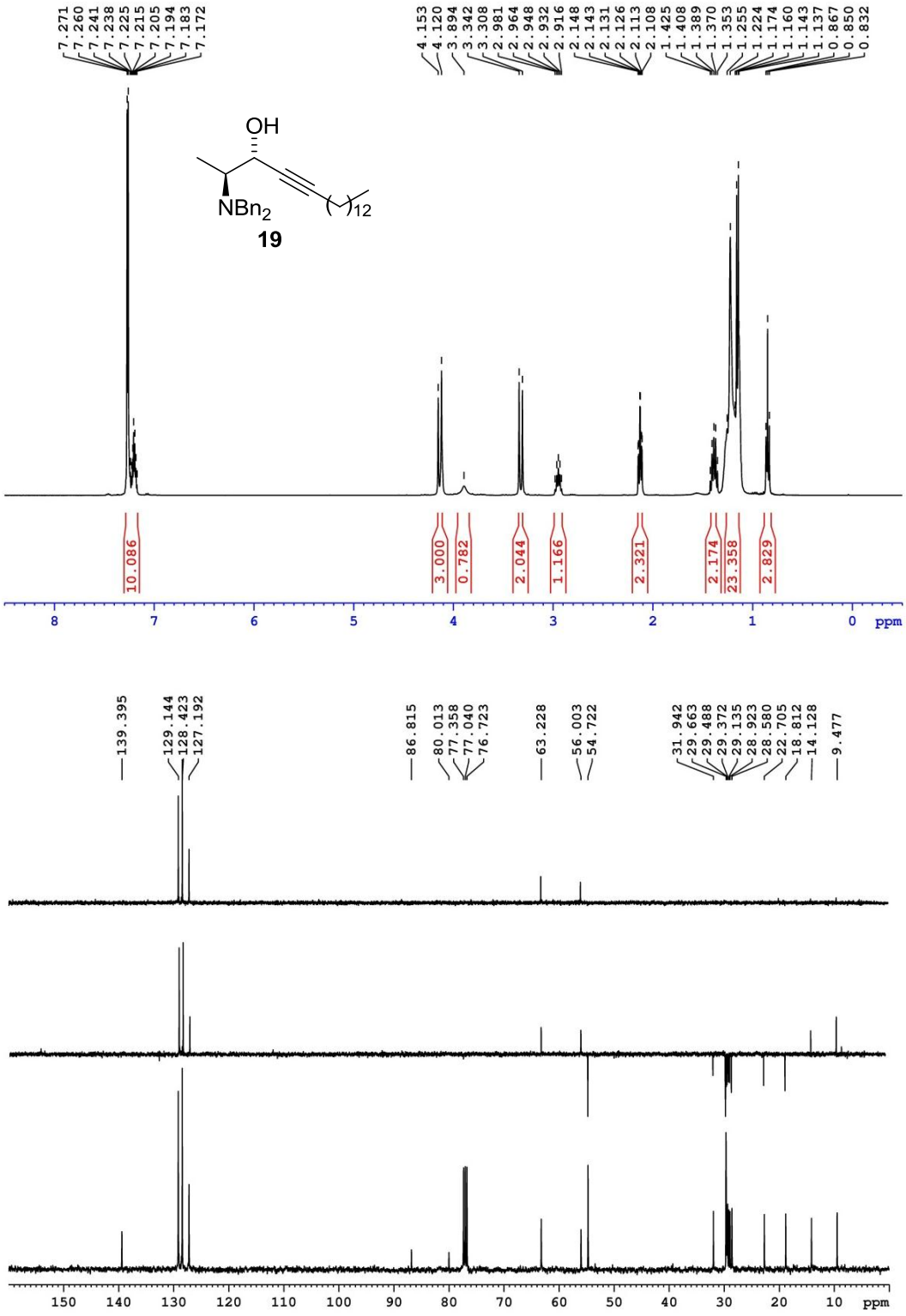

Figure S35. ^{1}H (400 MHz) and ^{13}C (100 MHz) NMR spectra of 19 in $CDCl_3$.

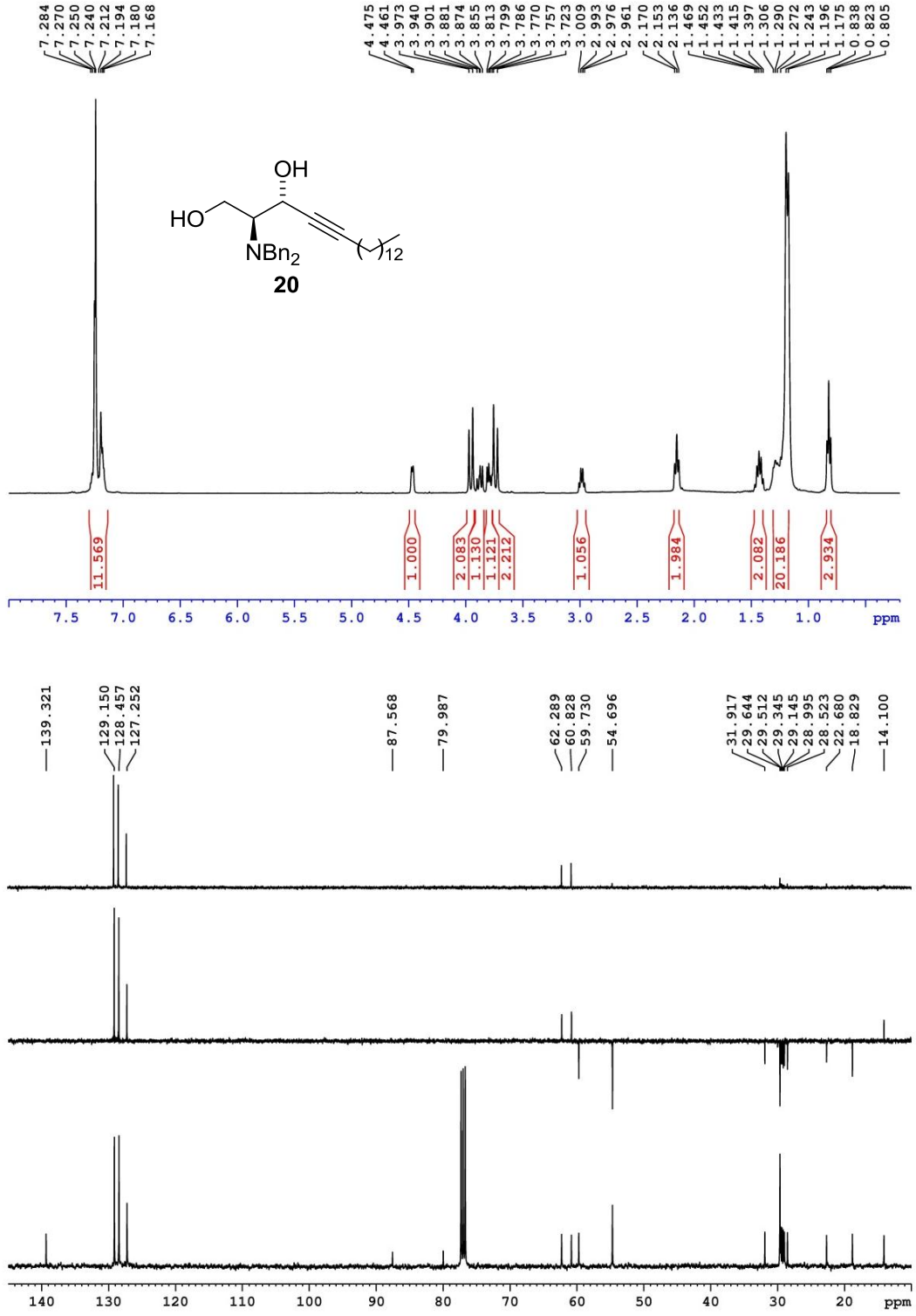

Figure S36. **^{1}H (400 MHz) and ^{13}C (100 MHz) NMR spectra of 20 in $CDCl_3$.**

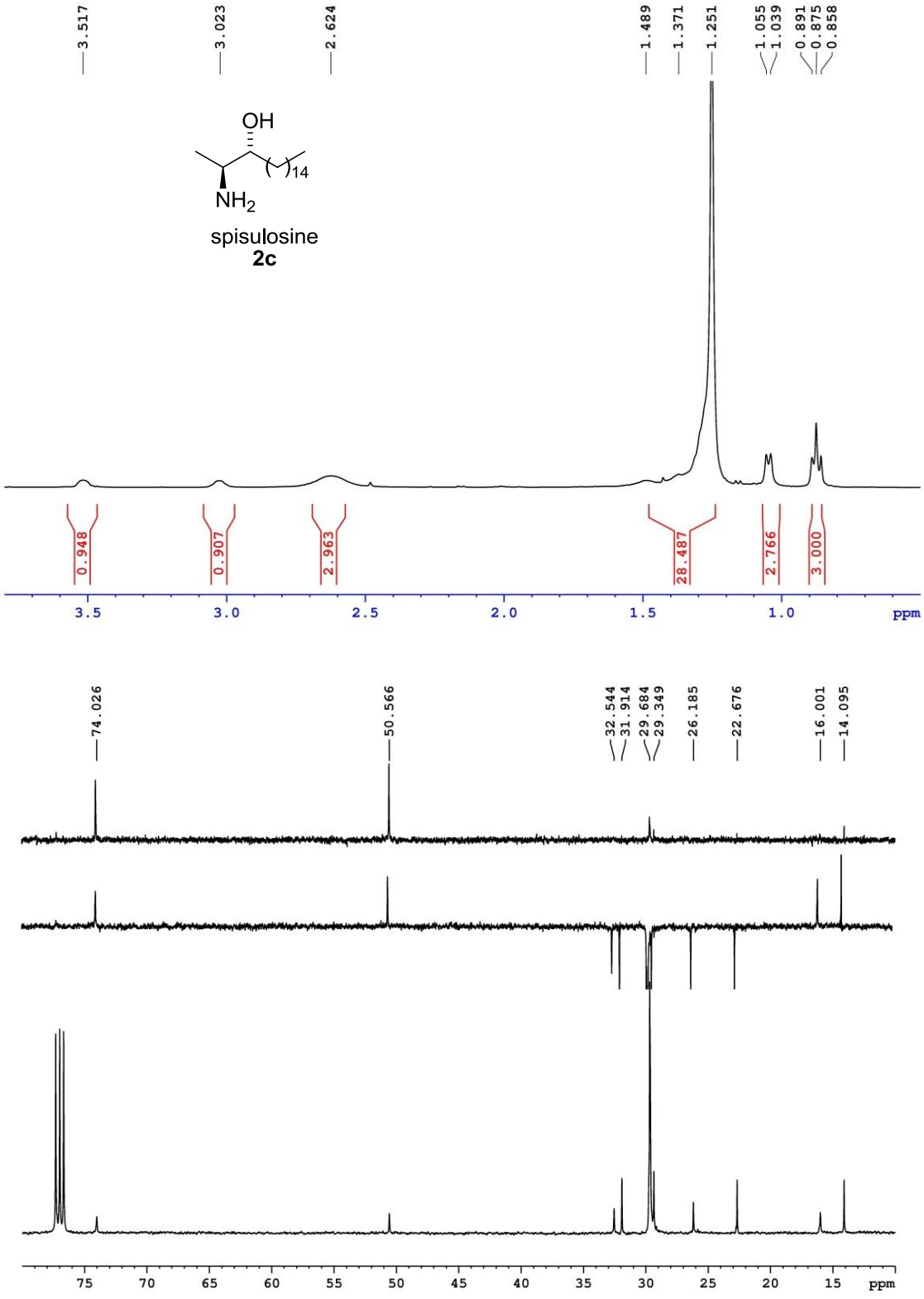

Figure S37. **^{1}H (400 MHz) and ^{13}C (100 MHz) NMR spectra of spisulosine (2c) in $CDCl_3$.**

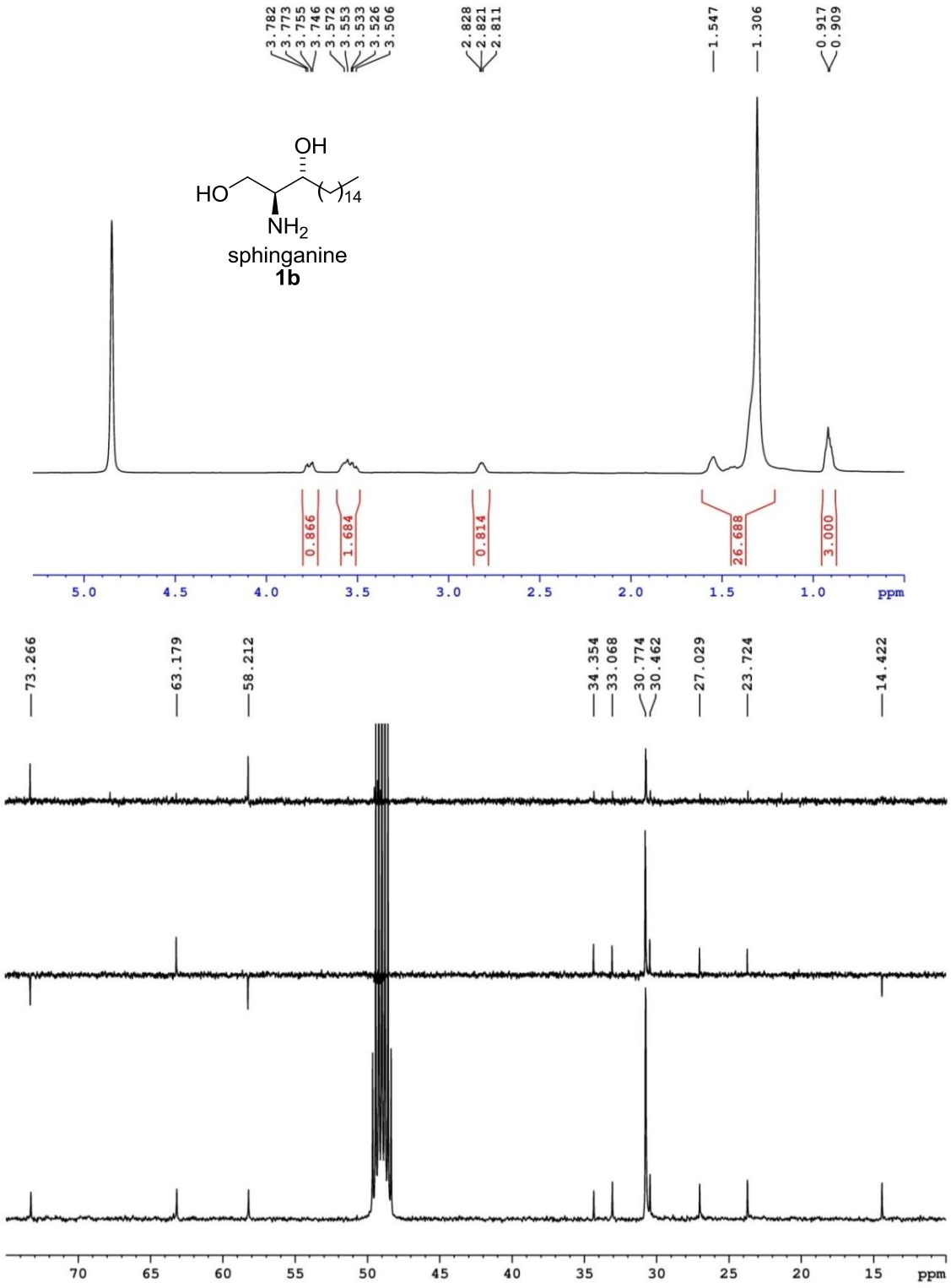

Figure S38. **^{1}H (400 MHz) and ^{13}C (100 MHz) NMR spectra of sphinganine (1b) in CD_3OD.**

CHAPTER 4

SYNTHESIS AND IDENTIFICATION OF UNPRECEDENTED SELECTIVE INHIBITORS OF CK1ε

4. Synthesis and identification of unprecedented selective inhibitors of CK1ε

4.1. Introduction

Naturally occurring sphingoid bases (sometimes referred to as "long chain bases" or "sphingosines", containing two or three hydroxyl groups)[1] have shown a number of relevant biological activities.[2] In particular, long chain amino alcohols from Nature have demonstrated significant activity as antitumor and cytotoxic drugs.[3] Representative examples include the marine compounds spisulosine (**1**),[4] pachastrissamine (**2**),[5] and clavaminols (**3**) (Figure 4.1).[6,7] Besides structural components of membranes, this family of compounds controls cellular processes such as migration, differentiation, proliferation, growth, senescence, and apoptosis. Therefore, they appear as promising structures for designing and developing new anticancer drugs.

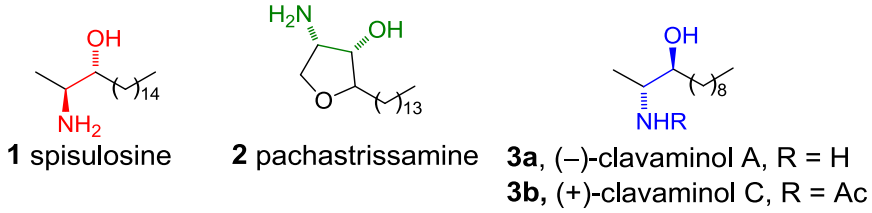

Figure 4.1. General structure of sphingoid bases with antiproliferative activity.

In the last decades, drug discovery has primarily been based on the search for drug leads against a preselected therapeutic target followed by subsequent testing of the derived drug candidates. While this so-called Targeted Drug Discovery (TDD) strategy has demonstrated useful in the discovery of new drugs, the unbiased identification of the molecular mechanism of action provided by empirical phenotypic approaches, i.e. Phenotypic Drug Discovery (PDD),[8] has proven more successful for small-molecules and first-in-class medicines.[9] In the particular scenario of antineoplastic drugs, a significant number of drugs whose discovery depended on phenotypic screening approaches have been identified.[10] Still, the discovery of new anticancer drugs remains a key factor to progress in cancer treatment. Anticancer therapy is the biggest area in drug development in terms of spending and number of clinical trials. Nonetheless, this disease class was reported to have 468 research targets versus 78 successful targets.[11] PDD measures the effect of compounds in cells as a whole, whereas TDD determines the potency of a molecule against one single target. In essence, a PDD screen generates additional data about that

molecule which is missed in a TDD screen. In spite the fact that cancer is a disease with multiple phenotypes or molecular mechanisms, a PDD strategy for anticancer drugs uses antiproliferative assays in tumor cell lines, which have a common phenotype of uncontrolled growth. With these premises in mind, we have applied successfully phenotypic assays that led to the discovery of an unprecedented family of human DNA topoisomerase IIα catalytic inhibitors.[12]

In an effort to enhance our PDD strategy, we have envisioned the use of computational methods in combination with the data obtained from the phenotypic screen. Noteworthy, computational methods have played a major role in the development of therapeutically important small molecules in the last decades.[13] Computational methods can be classified in two, virtual screening (VS) and reverse screening (RS), also known as computational target fishing.[14] In VS, large libraries of compounds are used to identify the molecules that are most likely to bind a specific target. In contrast, RS methods intend to identify the most probable target of a given molecule. While VS methods have been extensively used in TDD strategies, RS has not been linked to PDD. Recently, we have started the development of artificial neural networks (ANNs) modeling to correlate the chemical structure with the experimental data of the phenotypic assays in order to allow the prediction of activity, to run virtual screenings, or to anticipate pharmacokinetic and pharmacodynamics.[15]

As part of our interest in antiproliferative sphingoid bases, we have been involved in the synthesis and biological evaluation of diverse long chain amino alcohols.[16-21] More recently, we have described a more versatile and efficient methodology to synthesize *anti*-β-amino alcohols.[22] With this methodology in hand, we have prepared a small and structure-biased library of sphingoid bases, which was tested for antiproliferative activity against a representative panel of human solid tumor cell lines. Computational methods were applied subsequently to the resulting data in an effort to relate PDD and RS. Herein we report on our preliminary results on this searching, which successfully afforded an unprecedented selective inhibitor of casein kinase 1, epsilon (CK1ε).

4.2. Results

4.2.1. Chemistry

The synthesis of the enantiopure *anti*-β-amino alcohols included in this work was accomplished using an in-house one pot methodology.[22] The method is a simplified version of the well-known Reetz protocol[23] that avoids the three step sequence a) reduction of the ester to

alcohol, b) oxidation to aldehyde, and c) addition of the organometallic reagent. Scheme 4.1 depicts the general procedure. Briefly, optically active α-*N*,*N*- dibenzylamino esters (**4-11**) can be reduced and converted into β-*N*,*N*-dibenzylamino alcohols by subsequent addition of diverse Grignard reagents. The key step of the process is the one-pot sequential reduction to aldehyde with DIBAL-H at−78 °C and subsequent in situ addition of Grignard reagents. This one-pot procedure avoids the problem of instability of the aldehydes. Finally, hydrogenation allowed us to obtain the *anti*-β-amino alcohols for biological testing.

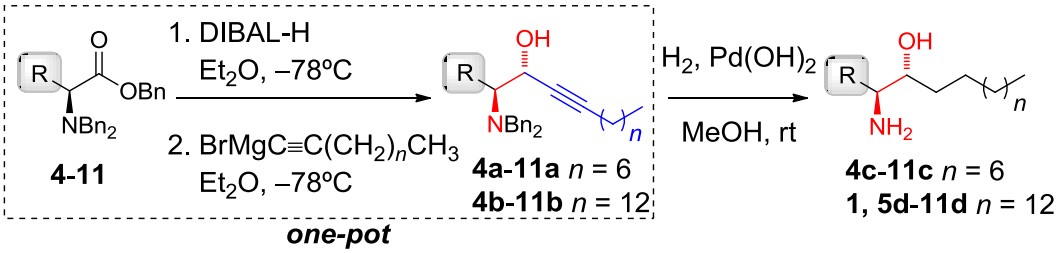

Scheme 4.1. General procedure for the synthesis of *anti*-β-amino alcohols.

With this tool in hand, we synthesized a small and structure-biased library of sphingoid bases. We selected L-alanine, L-valine, L-leucine, L-isoleucine, L-phenylalanine, L-tyrosine, L-serine and L-threonine as source to prepare by direct perbenzylation the corresponding α-*N*,*N*-dibenzylamino esters **4-11**, respectively.[24-28] In addition, we chose two Grignard reagents, 1-noninyl and 1-pentadecinylmagnesium bromide, to study the effect of short and long alkyl chains, respectively. As shown in Table 4.1, all the β-*N*,*N*-dibenzylamino alcohols (**4a-11a**, **4b-11b**) were obtained in 55-75% yield, with high diastereomeric excess. Compound **4a** was the only product obtained with lower diastereomeric excess. This decrease in selectivity was observed also when ethynylmagnesium bromide was used as Grignard reagent. However, when compound **4** was reacted, under the same one-pot conditions with ethyl-, and vinylmagnesium bromide solutions, the selectivity *anti*:*syn* of the process was reported to be >95:1.[17] Remarkably, our method can be applied to serine (**10**) and threonine (**11**) derivatives without the need to use protecting groups for the hydroxyl moiety. The removal of the benzyl groups and the reduction of the triple bond were carried out in one single step using standard hydrogenocatalytic conditions. With the exception of compound **9d** (decomposes under this hydrogenation conditions), all the corresponding *anti*-β-amino alcohols were obtained in 50-75% yield.

Table 4.1. Synthesis of *N,N*-dibenzylamino alcohols.

Entry	Reagent	Product	*n*	*anti*:*syn*[a]	Yield (%)
1	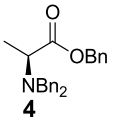 **4**	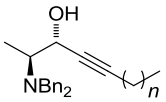 **4a** *n* = 6 **4b** *n* = 12	6	90:10	58
2			12	>95:1	60
3	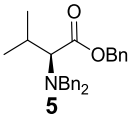 **5**	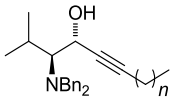 **5a** *n* = 6 **5b** *n* = 12	6	>95:1	65
4			12	>95:1	68
5	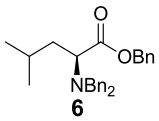 **6**	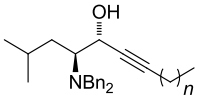 **6a** *n* = 6 **6b** *n* = 12	6	>95:1	62
6			12	>95:1	70
7	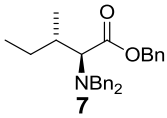 **7**	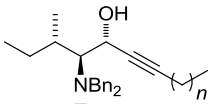 **7a** *n* = 6 **7b** *n* = 12	6	>95:1	59
8			12	>95:1	55
9	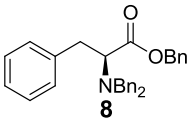 **8**	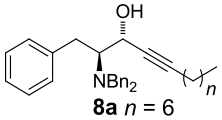 **8a** *n* = 6 **8b** *n* = 12	6	>95:1	63
10			12	>95:1	72
11	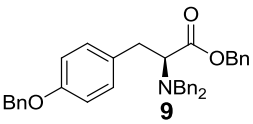 **9**	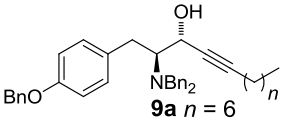 **9a** *n* = 6 **9b** *n* = 12	6	>95:1	68
12			12	>95:1	50
13	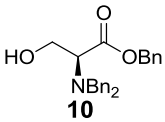 **10**	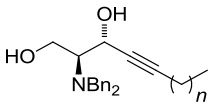 **10a** *n* = 6 **10b** *n* = 12	6	>95:1	73
14			12	>95:1	70
15	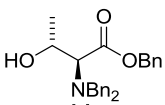 **11**	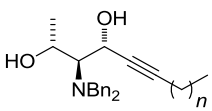 **11a** *n* = 6 **11b** *n* = 12	6	>95:1	75
16			12	>95:1	69

[a] Diastereomeric ratio determined by ^{1}H NMR analysis of the crude products.

4.2.2. Antiproliferative activity

The *in vitro* antiproliferative activity was determined in HBL-100, HeLa, SW1573, T-47D and WiDr human solid tumor cells. Table 4.2 shows the results (expressed as GI_{50}) using the SRB assay.[29] In addition, Figure 4.2 shows the mean graph derived from the obtained dose-response data given in Table 4.2. Overall, the data on antiproliferative activity show that all tested compounds exhibited growth inhibition in all cell lines of the panel. All compounds showed similar GI_{50} values when compared to the standard anticancer drugs cisplatin (CDDP) and etoposide (VP-16) that were used as positive controls. The most active compound of the series was spisulosine (**1**) and exhibited GI_{50} values against all cells in the range 0.7-2.6 μM. When compared to CDDP and VP-16, compounds **1** and **8d** showed an improved biological activity in the resistant cell lines T-47D and WiDr.

The structure-activity relationship (SAR) study revealed that the side chain R (Scheme 4.1) is not a critical factor for modulating the activity. The analysis of the GI_{50} values showed that in SW1573 cells the analogs with larger alkyl chain (**1**, **5d**-**11d**) are more active than their corresponding derivatives with short alkyl chain (**4c**-**11c**). This trend is not observed in the other cell lines. The *anti*-2-amino-1,3-diols (sphinganine analogs), derived from $_L$-serine (**10c**-**d**) and $_L$-threonine (**11c**-**d**), were in general less active than the *anti*-β-amino alcohols.

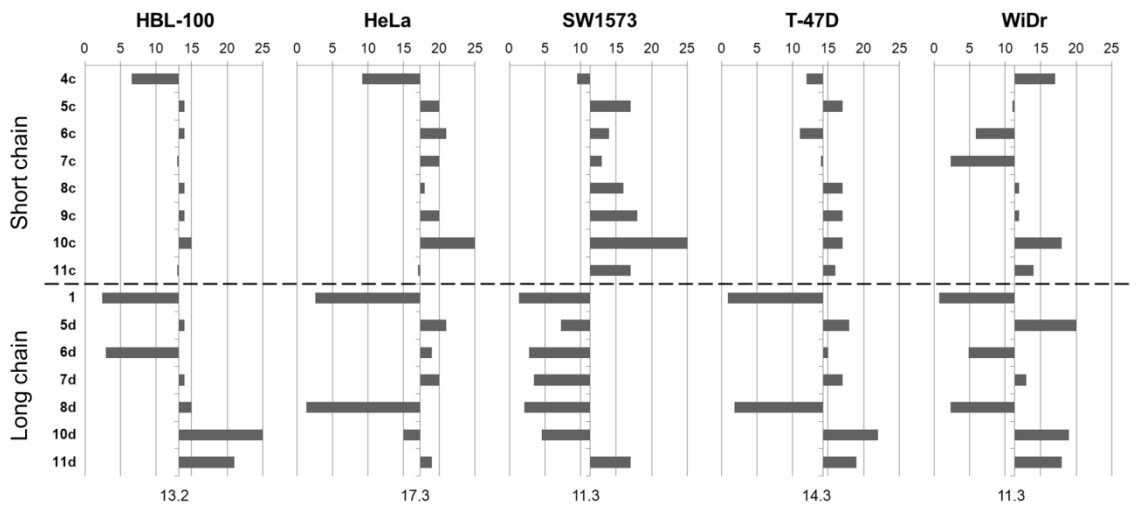

Figure 4.2. Mean graph profiles for *anti*-β-amino alcohols. The middle line represents the median GI_{50} (μM) value of the set of compounds against each individual cell line. The median GI_{50} (μM) value is given at the bottom.

Table 4.2. Antiproliferative activity (GI_{50}) against human solid tumor cells of compounds produced via Scheme 4.1.[a]

Compound	HBL-100 (breast)	HeLa (cervix)	SW1573 (lung)	T-47D (breast)	WiDr (colon)
4c	6.6 (± 0.2)	9.2 (± 1.7)	9.5 (± 3.7)	12 (± 5.3)	17 (± 3.9)
1	2.3 (± 0.3)	2.6 (± 0.7)	1.3 (± 0.6)	0.9 (± 0.4)	0.7 (± 0.3)
5c	14 (± 3.0)	20 (± 1.5)	17 (± 1.9)	17 (± 0.7)	11 (± 2.0)
5d	4.9 (± 2.4)	21 (± 6.2)	7.2 (± 2.4)	18 (± 6.4)	20 (± 5.6)
6c	14 (± 3.1)	21 (± 4.4)	14 (± 3.4)	11 (± 6.9)	5.9 (± 3.8)
6d	2.4 (± 0.8)	19 (± 4.2)	2.8 (± 0.9)	15 (± 1.2)	4.9 (± 3.1)
7c	13 (± 1.4)	20 (± 1.7)	13 (± 1.3)	14 (± 2.2)	2.3 (± 0.9)
7d	2.4 (± 0.5)	20 (± 4.5)	3.4 (± 0.7)	17 (± 5.5)	13 (± 0.9)
8c	14 (± 0.8)	18 (± 2.4)	16 (± 1.2)	17 (± 1.7)	12 (± 5.4)
8d	2.9 (± 0.2)	1.3 (± 0.2)	2.1 (± 0.1)	1.8 (± 0.1)	2.3 (± 0.1)
9c	14 (± 0.4)	20 (± 2.5)	18 (± 1.7)	17 (± 0.9)	12 (± 1.5)
10c	15 (± 1.7)	36 (± 10)	27 (± 10)	17 (± 5.2)	18 (± 6.8)
10d	25 (± 8.8)	15 (± 2.6)	4.5 (± 1.7)	22 (± 2.7)	19 (± 3.8)
11c	13 (± 2.4)	17 (± 0.6)	17 (± 1.1)	16 (± 1.5)	14 (± 0.5)
11d	21 (± 1.1)	19 (± 1.6)	17 (± 3.5)	19 (± 1.2)	18 (± 0.6)
CDDP	1.9 (±0.2)	2.0 (±0.3)	3.0 (±0.4)	15 (±2.3)	26 (±5.3)
VP-16	1.4 (±0.1)	3.3(±1.6)	15(±1.5)	22(±5.5)	23(±3.1)

[a] Values are given in μM and are means of two to three experiments; standard deviation is given in parentheses.

4.2.3. Computational calculations

After this initial identification, we attempted to predict the targets involved in the bioactivity of our compounds using molecular docking. To reach this goal we docked the series of lipidic amino alcohols **1** and **4c-11d** against 58 different targets involved in cancer (Experimental Section). The purpose of these docking calculations was to obtain the protein-ligand interaction energies and subsequently determine if any set of interaction energies between studied compounds and a particular protein target correlated with the biological activity experimental data (GI_{50}) of the same compounds for a particular cancer cell line. We considered that there was a correlation when R^2 between docking interaction energies and GI_{50} values was greater than 0.60 (meaning R observed > 0.77). Under these premises, we obtained the correlations shown in Table 4.3. With the exception of HeLa cells, correlations were obtained for the remaining cell lines. Although the obtained correlations point to several potential targets,

all of them share the characteristic of being kinases. Thus, we speculated that a kinase might be the therapeutic target responsible for the bioactivity of our compounds.

Table 4.3. Correlation between docking interaction energies and experimental GI_{50} values.

Cell line	Target	Correlation coefficient (R)
SW1573	HGFR (c-Met kinase domain)	0.87
T-47D	Tyrosine protein kinase receptor RET	0.83
HBL-100	Protein kinase C	0.80
HBL-100	HGFR (c-Met kinase domain)	0.78
T-47D	Casein kinase 1, epsilon	0.78
WiDr	IGF-1R kinase	0.78

4.2.4. Experimental target identification

To confirm experimentally the theoretical prediction that kinases were the targets of our compounds, we submitted **1**, **6d**, **8c**, and **11d** for testing. Since the biological activity was in the same range, these derivatives were selected on the basis of diversity in their molecular structure and the docking results. Besides the most active compound of the series **1**, we included analogs with long (**6d**, **11d**) and short (**8c**) side chain, derivatives bearing aromatic side chain (**8c**), and the amino diol framework (**11d**). The kinase selectivity of these compounds was evaluated using the KINOMEscan™ active site-directed competition-binding methodology (DiscoveRx Corporation). The compounds were assayed at a single concentration (10 μM) against a panel of 456 kinases (scanMAX℠) using the method described in the literature.[30] This scan revealed a single hit, compound **8c** as a selective inhibitor of CK1ε. In this method, interactions are reported as percent control (%Ctrl), where negative control (DMSO) means 100%Ctrl and the positive control denotes 0%Ctrl. The cut-off is set at 35%Ctrl, which represents 65% inhibition of kinase activity. Consequently, lower %Ctrl numbers indicate stronger hits. Table 4.4 summarizes the results obtained against casein kinases for comparison. Compound **8c** exhibited a 73% inhibition of CK1ε activity. To follow-up this discovery, the K_D (KdELECT™) of compound **8c** against CK1ε was determined experimentally and was found to be 29 μM.

Table 4.4. Percent control (%Ctrl) values obtained against casein kinases for selected compounds.

Gene Symbol	Kinase	1	6d	8c	11d
CSNK1A1	Casein kinase 1, alpha 1	100	93	95	100
CSNK1A1L	Casein kinase 1, alpha 1-like	100	91	88	100
CSNK1D	Casein kinase 1, delta	100	89	93	90
CSNK1E	Casein kinase 1, épsilon	60	48	27	43
CSNK1G1	Casein kinase 1, gamma 1	98	98	100	100
CSNK1G2	Casein kinase 1, gamma 2	100	94	96	87
CSNK1G3	Casein kinase 1, gamma 3	100	93	71	82
CSNK2A1	Casein kinase 2, alpha 1 polypeptide	87	84	70	71
CSNK2A2	Casein kinase 2, alpha prime polypeptide	98	100	100	100

4.2.5. CK1ε docking studies

Figure 4.3 shows the docked conformation of compound **8c** within the binding site of CK1ε. The predicted protein-ligand complex shows that the hydrophobic tail of compound **8c** inserts in the narrow and deep pocket of CK1ε binding site which is lined mostly of hydrophobic residues (Figure 4.3B). The polar atoms of compound **8c** establish 4 H-bonds with CK1ε residues Ser88, Asp91 and Asp132. We can also forecast that addition of substituents on the aromatic ring might improve the interaction with CK1ε since there is an unoccupied crevice in the protein structure available to establish interactions with the ligand straight along the direction pointed by compound **8c** aromatic ring.

4.3. Discussion

A major concern for PDD is that determining the relevant target(s) of molecules identified by phenotypic screening has often proven slow or impossible. However, the ability to identify the target is improving, and there will be additional technologies that come out to pinpoint the target, which will make researchers much more comfortable with PDD. In this particular context, we explored in this work the possibility of combining the phenotypic screen results on antiproliferative activity with computational methods and in particular with target fishing.[14]

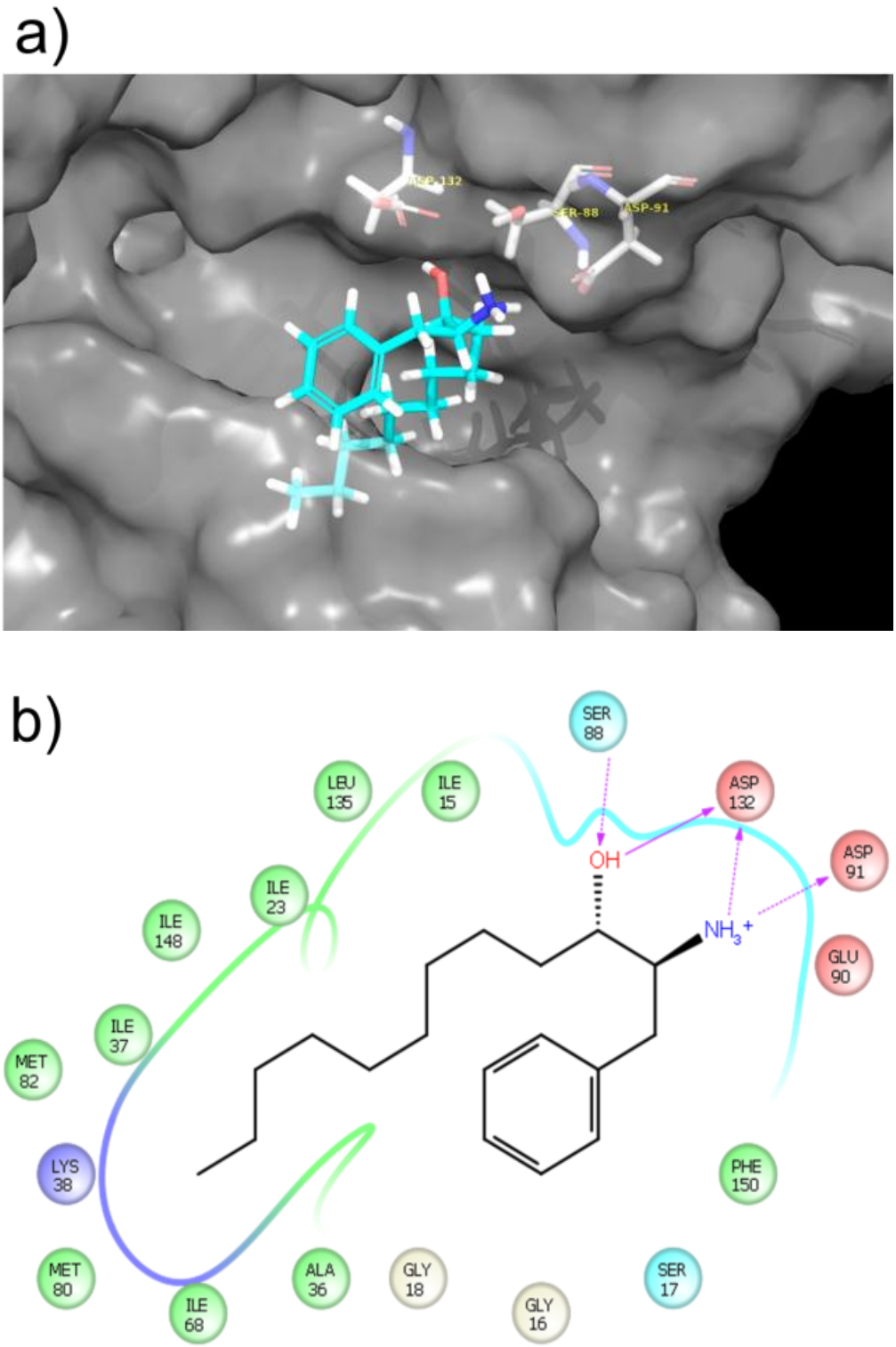

Figure 4.3. Docked conformation of compound 8c within the binding site of CK1ε (PDB ID: 4HNI): a) Binding mode of 8c. Only amino acids that establish H-bonds with inhibitor are specified; b) Predicted protein-ligand complex.

To test our hypothesis we designed a small but focused library of enantiopure *anti*-β-amino alcohols, which resemble the structure of sphingoid bases. Our previous SAR studies on lipidic 3-amino-1,2-diols, lipidic 2-amin-1-ols and lipidic 1,2-diamines revealed that active compounds should present a long aliphatic side chain and bear a free amino group.[21] That was set as the minimal structural requirements for the new analogs.

When considering the synthesis of the library, we avoided the use of our previous (lengthy) methods.[16-21] Thus, short synthetic routes were necessary in order to achieve our goal. In turn, we selected our recently described methodology for the synthesis of enantiopure *anti*-β-amino alcohols in three steps from readily available natural amino acids (Scheme 4.1).[22] Thus, the method was applied to amino acids with hydrophobic side chain ($_{L}$-alanine, $_{L}$-valine, $_{L}$-leucine, $_{L}$-isoleucine, $_{L}$-phenylalanine, $_{L}$-tyrosine). When compared to sphingoid bases, compounds **5-9** bring to mind an internalization of the polar groups (NH_2 and OH) present on the carbon chain. The new synthetic tool allowed us to prepare compounds belonging to a congeneric series. In addition, when amino acids $_{L}$-serine and L-threonine were used as starting material, sphinganine analogs were obtained.

Our PDD strategy starts with the study of *in vitro* antiproliferative activity in a panel of human solid tumor cell lines.[31] Ideally, the results allow obtaining 1 or 2 drug leads and establishing some SARs. Drug leads are further tested to unravel the mechanism of action, using more time-consuming and expensive techniques. The antiproliferative data from Table 4.2 shows that all compounds have moderate activity in the low micromolar range and this result is consistent with our past observations in terms of SAR.[19-21] In essence, all tested compounds could be considered initial hits for further testing. However, further experimental testing of all the compounds is not affordable. At this point, we considered introducing computational methods.

The combination of PDD with RS we described here, is based upon the assumption that a positive correlation between experimental GI_{50} values and calculated docking interactions may reveal a potential target. We are aware that, probably, in most cases this will not produce the positive outcome that we got. Phenomena such as cell membrane penetration, efflux mechanisms, and unique cellular responses cannot be incorporated in docking calculations that focus on a single therapeutic target. Since we did not test our compounds, either computationally or experimentally, against all available targets, we cannot discard that our compounds may have other targets that elicit the phenotypic response.

Therefore, we attempted to predict the targets involved in the bioactivity of our compounds using molecular docking. From the Protein Data Bank, we selected a set of 58

structures of proteins known to be research or successful targets in anticancer therapy.[11] Docking calculations predicted that the series of compounds would interact with kinases (Table 4.3). Since all the predicted targets, for which correlation with experimental GI_{50} values could be established, are kinases we safely assumed that the therapeutic target would be one (or more) of the kinases listed in the above table. Kinases regulate multiple cellular processes that contribute to tumor development and progression, and many human tumors are dependent on kinases activity for survival. In addition, sphingoid bases have been reported to inhibit kinases.[3] Therefore, the assumption that kinases could be the targets of these compounds is sensible.

In order to check experimentally the obtained correlations, we submitted a small subset of compounds (**1**, **6d**, **8c** and **11d**) for testing against the largest commercial kinase panel available, scanMAX™. The results showed that all four derivatives behave as inhibitors of CK1ε, being compound **8c** the most potent derivative (Table 4.4). More importantly, none of the compounds interact with other kinases, not even with those ones for which correlations were found. On the one hand, this could be regarded as a failure of our docking predictions that can be attributed to the fact that docking scoring functions tend to be "optimistic" when describing the protein-ligand interaction energy. That is, the scoring functions were not constructed to eliminate ligands that are poor binders but rather not to miss ligands that are good binders. On the other hand, we cannot neglect this approach since the predictions indicated a correlation between GI_{50} values and docking interaction with CK1ε in T-47D breast cancer cells. Nevertheless, docking studies (Figure 4.3) are in agreement with the experimental finding of CK1ε inhibition.

CK1ε belongs to a family of serine/threonine-specific kinases comprised of seven members (α, β, δ, ε, γ_1, γ_2 and γ_3). CK1ε activity is implicated in human pathologies such as neurodegenerative diseases, drug addiction and cancer. CK1ε plays a role in the cleavage of amyloid precursor protein, which makes it an attractive target for the treatment of Alzheimer's disease.[32] CK1ε along with CK1δ are involved in drug addiction induced behaviors by acting on the Darpp-32-PP1 signaling pathway to regulate AMPA receptor phosphorylation.[33] Regarding its role in cancer, CK1ε is required for the survival of breast cancer subtypes and myristoylated CK1ε is sufficient to provoke transformation via stabilization of β-catenin and activation of Wnt transcription targets.[34] RNAi screens showed that CK1ε knockdown slowed cancer cell growth,[35] and CK1ε play roles in breast,[36] ovarian[37] and oral cancers.[38]

CK1ε is the closest homologue to CK1δ (>98% sequence identity between these two kinases) and thus, reported inhibitors described in the literature behave as non-selective CK1δ/ε inhibitors.[39,40] However, CK1ε and CK1δ have roles distinct from each other as it was

confirmed with the selective CK1ε inhibitor PF-4800567 (Figure 4.4).[41] To the best of our knowledge, no other selective CK1ε inhibitor has been reported. It is noteworthy that PF4800567 (IC_{50} = 32 nM for CK1ε) does not inhibit human cancer cell growth at 1 μM, even after seven days of treatment.[42] Thus, our data demonstrate that compound **8c** represents the first selective CK1ε inhibitor with proven antiproliferative activity in cancer cell lines. Notably, we should highlight the identification of CK1ε as a selective target of our compounds. Should CK1ε not happen to be the single target of our compound, which leads to the phenotypic alterations experienced by the cancer cell lines, we would still have unraveled a therapeutic target for this class of compounds that holds a lot of potential to treat several pathologies that affect humans.

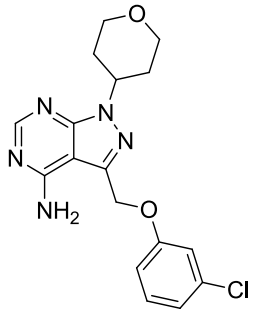

PF-4800567

Figure 4.4. Structure of selective CK1ε inhibitor PF-4800567.

4.4. Conclusion

In summary, we have described the synthesis of a small and biased library of enantiopure *anti*-β-amino alcohols. The compounds were tested against human solid tumor cell lines showing all of them the ability to inhibit cell growth, with GI_{50} values in the range 1-20 μM. A computational approach was designed to anticipate the molecular target(s) on the basis of the chemical structure and the antiproliferative activity. The methods pointed to kinases as plausible candidates. Experimental determination of the interaction with 456 kinases indicated that the *anti*-β-amino alcohols behave as selective CK1ε inhibitors. Docking studies agreed with these findings. Results from our study evidence that the combination of phenotypic drug discovery and computational studies to predict a therapeutic target might contribute to improve the efficiency of the drug discovery process.

With the pieces of information here presented, we will run an optimization program to improve the activity of our compounds against CK1ε. Additional experiments will be necessary to determine the exact mechanism of action of these *anti*-β-amino alcohols inside the cells and thus, whether CK1ε (or some other target) triggers the antiproliferative effect. Although preliminary, our combination of computational approach and PDD merits further exploration in order to be implemented as a tool in drug discovery processes. The outcome of all those studies stands outside the scope of this work and will be reported elsewhere.

4.5. References

1. Pruett, S. T.; Bushnev A.; Hagedorn, K.; Adiga, M.; Haynes C. A.; Sullards, M. C.; Liotta D. C.; Merrill, A. H. Jr. *J. Lipid Res.* **2008**, *49*, 1621.
2. Aguilera-Romero, A.; Gehin, C.; Riezman, H. *Biochim. Biophys. Acta* **2014**, *1841*, 647.
3. Padrón, J. M. *Curr. Med. Chem.* **2006**, *13* 755.
4. Butler, M. S. *Nat. Prod. Rep*. **2005**, *22*, 162.
5. Kuroda, I.; Musman, M.; Ohtani, I. I.; Ichiba, T.; Tanaka, J.; Gravalos, D. G.; Higa, T. *J. Nat. Prod.* **2002**, *65*, 1505.
6. Aiello, A.; Fattorusso, E.; Giordano, A.; Menna, M.; Navarrete, C.; Muñoz, E. *Bioorg. Med. Chem.* **2007**, *15*, 2920.
7. Aiello, A.; Fattorusso, E.; Giordano, A.; Menna, M.; Navarrete, C.; Muñoz, E. *Tetrahedron* **2009**, *65*, 4384.
8. Lee, J. A.; Berg, E. L. *J. Biomol. Screen*. **2013**, *18*, 1143.
9. Swinney, D. C. *Clin. Pharmacol. Ther.* **2013**, *93*, 299.
10. Moffat, J. G.; Rudolph, J.; Bailey, D. *Nature Rev. Drug Discov.* **2014**, *13*, 588.
11. Zheng, C. J.; Han, L. Y.; Yap, C. W.; Ji, Z. L.; Cao, Z. W.; Chen, Y. Z. *Pharmacol. Rev.* **2006**, *58*, 259.
12. León, L. G.; Ríos-Luci, C.; Tejedor, D.; Pérez-Roth, E.; Montero, J. C.; Pandiella, A.; García-Tellado, F.; Padrón, J. M. *J. Med. Chem.* **2010**, *53*, 3835.
13. Sliwoski, G.; Kothiwale, S.; Meiler, J.; Lowe Jr, E. W. *Pharmacol. Rev*. **2013**, *66*, 334.
14. Cereto-Massagué, A.; Ojeda, M. J.; Valls, C.; Mulero, M.; Pujadas, G.; Garcia-Vallve, S. *Methods* 2015, 71, 98.
15. Sousa, I. J.; Padrón, J. M.; Fernandes, M. X. *Neural Comput. Applic.* **2013**, *23*, 577.
16. Kokotos, G.; Padrón, J. M.; Noula, C.; Gibbons, W. A.; Martín, V. S. *Tetrahedron: Asymmetry* **1996**, *7*, 857.
17. Padrón, J. M.; Kokotos, G.; Martín, T.; Markidis, T.; Gibbons, W. A.; Martín, V. S. *Tetrahedron: Asymmetry* **1998**, *9*, 3381.
18. Kokotos, G.; Padrón, J. M.; Martín, T.; Markidis, T.; Gibbons, W. A.; Martín, V. S. *J. Org. Chem.* **1998**, *63*, 3741.
19. Padrón, J. M.; Martín, V. S.; Hadjipavlou-Litina, D.; Noula, C.; Constantinou-Kokotou, V.; Peters, G. J.; Kokotos, G. *Bioorg. Med. Chem. Lett*. **1999**, *9*, 821.
20. Markidis, T.; Padrón, J. M.; Martín, V. S.; Peters, G. J.; Kokotos, G. *Anticancer Res*. **2001**, *21*, 2835.
21. Padrón, J. M.; Peters, G. J. *Invest. New Drugs* **2006**, *24*, 195.

22. Silveira-Dorta, G.; Donadel, O. J.; Martín, V. S.; Padrón, J. M. *J. Org. Chem.* **2014**, *79*, 6775.
23. Reetz, M. T. *Chem Rev*. **1999**, *99*, 1121.
24. Reetz, M. T.; Drewes, M.W.; Schwickardi, R. *Org. Synth*. **1999**, *76*, 110.
25. Beaulieu, P. L.; Wernic, D. *J. Org. Chem.* **1996**, *61*, 3635.
26. Ordóñez, M.; de la Cruz, R.; Fernández-Zertuche, M.; Muñoz-Hernández, M.-A. *Tetrahedron: Asymmetry* **2002**, *13*, 559.
27. Higgins, G.; Slassi, A.; Isaac, M. Patent EP 2099444.
28. Menuel, S.; Joly, J. -P.; Courcot, B.; Elysée, J.; Ghermanid, N. -E.; Marsura, A. *Tetrahedron* **2007**, *63*, 1706.
29. Miranda, P. O.; Padrón, J. M.; Padrón, J. I.; Villar, J.; Martín, V.S. *ChemMedChem* **2006**, *1*, 323.
30. Fabian, M. A.; Biggs III, W. H.; Treiber, D. K.; Atteridge, C. E.; Azimioara, M. D.; Benedetti, M. G.; Carter, T. A.; Ciceri, P.; Edeen, P. T.; Floyd, M.; Ford, J. M.; Galvin, M.; Gerlach, J. L.; Grotzfeld, R. M.; Herrgard, S.; Insko, D. E.; Insko, M.A.; Lai, A. G.; Lélias, J. -M.; Mehta, S. A.; Milanov, Z. V.; Velasco, A. M.; Wodicka, L. M.; Patel, H. K.; Zarrinkar, P. P.; Lockhart, D. *J. Nat. Biotechnol.* **2005**, *23*, 329.
31. Ríos-Luci, C.; Domínguez-Kelly, R.; León, L. G.; Díaz-Rodríguez, E.; Freire, R.; Pandiella, A.; Cikotiene, I.; Padrón, J. M. *Bioorg. Med. Chem. Lett.* **2011**, *21*, 6641.
32. Köhler, C.; Dinekov. M.; Götz, *J. Neurobiol. Dis*. **2014**, *71*, 169.
33. Li, D.; Herrera, S.; Bubula, N.; Nikitina, E.; Palmer, A. A.; Hanck, D. A.; Loweth, J. A.; Vezina, P. *J. Neurochem.* **2011**, *118*, 237.
34. Swiatek, W.; Tsai, I. C.; Klimowski, L.; Pepler, A.; Barnette , J.; Yost, H. J.; Virshup, D. M. *J. Biol. Chem*. **2004**, *279*, 13011.
35. Shin, S.; Wolgamott, L.; Roux, P. P.; Yoon, S. O. *Cancer Res.* **2014**, *74*, 201.
36. Kim, S. Y.; Dunn, I. F.; Firestein, R.; Gupta, P.; Wardwell, L.; Repich, K.; Schinzel, A. C.; Wittner, B. Silver, S. J.; Root, D. E.; Boehm, J. S.; Ramaswamy, S.; Lander; E. S.; Hahn, W. C. *PLoS One* **2010**, *5*, e8979.
37. Rodriguez, N.; Yang, J.; Hasselblatt, K.; Liu, S.; Zhou, Y.; Rauh-Hain, J. A.; Ng, S. K.; Choi, P. W.; Fong, W.P.; Agar, N.Y.; Welch, W.R.; Berkowitz, R.S.; Ng, S. W. *EMBO Mol. Med.* **2012**, *4*, 952.
38. Lin, S. H.; Lin, Y. M.; Yeh, C. M.; Chen, C. J.; Chen, M. W.; Hung, H. F.; Yeh, K. T.; Yang, S. F. *Int. J. Mol. Sci*. **2014**, *15*, 2876.

39. Maiwald, F.; Benítez, D.; Charquero, D.; Dar, M.A.; Erdmann, H.; Preu, L.; Koch, O.; Hölscher, C.; Loaëc, N.; Meijer, L.; Comini, M. A.; Kunick, C. *Eur. J. Med. Chem.* **2014**, *83*, 274.

40. Diez-Cecilia, E.; Kelly, B.; Perez, C.; Zisterer, D. M.; Nevin, D. K.; Lloyd, D. G.; Rozas, I. *Eur. J. Med. Chem.* **2014**, *81*, 427.

41. Walton, K. M.; Fisher, K.; Rubitski, D.; Marconi, M.; Meng, Q. J.; Sladek, M.; Adams, J.; Bass, M.; Chandrasekaran, R.; Butler, T.; Griffor, M.; Rajamohan, F.; Serpa, M.; Chen Y.; Claffey, M.; Hastings, M.; Loudon, A.; Maywood, E.; Ohren, J.; Doran, A.; Wager, T. T. *J. Pharmacol. Exp. Ther*. **2009**, *330*, 430.

42. Cheong, J. K.; Nguyen, T. H.; Wang, H.; Tan, P.; Voorhoeve, P. M.; Lee, S. H.; Virshup, D. M.; *Oncogene* **2011**, *30*, 2558.

43. Kossuga, M. H.; MacMillan, J. B.; Rogers, E. W.; Molinski, T. F.; Nascimento, G. G. F.; Rocha, R. M.; Berlinck, R. G. S. *J. Nat. Prod*. **2004**, *67*, 1879.

44. Chen, B. -S.; Yang, L.-H.; Ye, J.-L.; Huang, T.; Ruan, Y.-P.; Fu, J.; Huang, P. -Q.; *Eur. J. Med. Chem.* **2011**, *46*, 5480.

45. Acena, J. L.; Adrio, J.; Cuevas, C.; Gallego, P.; Manzanares, I.; Munt, S.; Rodriguez, I. Patent WO 2001094357.

4.6. Experimental section

Chemistry

4.6.1. General remarks

Reactions were performed using oven-dried glassware under an atmosphere of argon. ^{1}H NMR spectra were recorded at 400 and 500 MHz at 298K, ^{13}C NMR spectra were recorded at 100 and 125 MHz respectively. Chemical shifts were reported in units (ppm) by assigning TMS resonance in the ^{1}H NMR spectrum as 0.00 ppm ($CDCl_3$, 7.26 ppm; C_6D_6, 7.2 ppm and CD_3OD, 3.35, 4.78 ppm). Data were reported as follows: chemical shift, multiplicity (s = singlet, d = doublet, t = triplet, q = quartet, quin = quintuplet, sex = sextet, dd = double doublet, ddd = double double doublet, m =multiplet and br = broad), coupling constant (*J* values) in Hz and integration. Chemical shifts for ^{13}C NMR spectra were recorded in ppm from tetramethylsilane as the internal standard. Using the central peak of $CDCl_3$ (77.0 ppm), C_6D_6 (128.0 ppm) and central peak of CD_3OD (49.3 ppm). Reagent-grade chemicals were obtained from diverse commercial suppliers and were used as received. Optical rotations were measured with a polarimeter at the sodium line at different temperatures in $CHCl_3$. Accurate mass (HRMS) were determined by electrospray ionization (ESI-TOF) and electronic impact (EI-TOF). Reactions were monitored using thin-layer chromatography (TLC) on aluminum packed percolated Silica Gel 60 F_{254} plates. Flash column chromatography was carried out with silica gel 60 (particle size less than 0.020 mm) by using appropriate mixtures of ethyl acetate and hexanes as eluent. Compounds were visualized by use of UV light and 2.5% phosphomolybdic acid in ethanol. All reactions involving air- or moisture-sensitive materials were carried out under Argon atmosphere. Anhydrous magnesium sulfate was used for drying solutions. Melting points were measured with micro melting point apparatus. Chemical nomenclature was generated using Chem Bio Draw Ultra 13.0.

Data for compounds **1**, **4b**, **10b** and **10d** have been described previously.[22]

4.6.2. General procedure and characterization for the preparation of 4a–11b.

To a solution of the alkyne (0.73 mmol) in dry Et_2O (10 mL) was added ethylmagnesium bromide solution (0.24 mL, 0.73 mmol, 3 M in THF). The mixture was refluxed for 2.5 h and then it was allowed to cool down to room temperature. In parallel, to a cooled (–78 ºC) solution of α-*N*,*N*-dibenzylamino ester (0.29 mmol) in dry Et_2O (3 mL) was added DIBAL-H (0.4 mL, 0.4 mmol, 1M in hexane) under argon atmosphere. For compounds **10**-**11** a second portion of DIBAL-H (0.2 mL, 0.2 mmol, 1M in hexane) was added 45 min later. After stirring for 2 h, the solution of alkynyl magnesium bromide previously formed was carefully added, at –78 ºC. The

mixture was warmed to –10 ºC. Then, the mixture was quenched with saturated NH_4Cl (8 mL). The mixture was extracted with Et_2O (10 mL × 3), the organic phases were washed with brine, dried over $MgSO_4$, filtered and concentrated in vacuum. After the evaporation of solvent under reduced pressure, the residue was purified by flash column chromatography eluting with hexane-ethyl acetate mixtures to give the corresponding β-*N*,*N*-dibenzylamino alcohol.

(2*S*,3*R*)-2-(dibenzylamino)dodec-4-yn-3-ol (4a). Colorless oil. Yield 58%. $[\alpha]^{25}_D$ –13.5 (*c* 0.96, $CHCl_3$). ^{1}H NMR (400 MHz, $CDCl_3$): δ = 0.79 (t, 3H, *J* = 7.2 Hz), 1.09-1.26 (m, 11H), 1.35 (m, 2H), 2.09-2.13 (m, 2H), 2.92 (q, 1H, *J* = 6.8 Hz), 3.29 (d, 2H, *J* = 13.4 Hz), 3.87 (br, 1H), 4.09 (d, 2H, *J* = 13.4 Hz), 7.16-7.23 (m, 10H) ppm. ^{13}C NMR (100 MHz, $CDCl_3$): δ = 9.5, 14.1, 18.8, 22.6, 28.6, 28.8, 28.9, 31.7, 54.7, 56.0, 63.2, 80.1, 86.8, 127.2, 128.4, 129.2, 139.4 ppm. HRMS (EI-TOF) (*m/z*) $[M - H]^+$ = calcd for $C_{26}H_{35}NO$ 377.2797, found 377.2728.

(3*S*,4*R*)-3-(dibenzylamino)-2-methyltridec-5-yn-4-ol (5a). Colorless oil. Yield 65%. $[\alpha]^{25}_D$ – 79.8 (*c* 0.99, $CHCl_3$). ^{1}H NMR (400 MHz, $CDCl_3$): δ = 0.76 (t, 3H, *J* = 6.9 Hz), 0.87 (d, 3H, *J* = 6.5 Hz), 1.04-1.36 (m, 13H), 2.07 (td, 2H, *J* = 6.9, 2.3 Hz), 2.27-2.36 (m, 1H), 2.42 (dd, 1H, *J* = 10.3, 5.0 Hz), 3.63 (d, 2H, *J* = 13.0 Hz), 4.05 (br, 1H), 4.23 (d, 2H, *J* = 13.0 Hz), 7.15-7.23 (m, 10H) ppm. ^{13}C NMR (100 MHz, $CDCl_3$): δ = 14.1, 18.8, 20.6, 22.6, 28.6, 28.8, 28.8, 29.3, 31.7, 55.9, 60.4, 66.7, 79.9, 85.8, 127.3, 129.6, 128.5, 139.7 ppm. HRMS (ESI-TOF) (m/z) $[M – H_2O]^+$ = calcd for $C_{28}H_{39}NO$ 387.2926, found 387.2939.

(3*S*,4*R*)-3-(dibenzylamino)-2-methylnonadec-5-yn-4-ol (5b). Colorless oil. Yield 68%. $[\alpha]^{25}_D$ –61.5 (*c* 1.05, $CHCl_3$). ^{1}H NMR (400 MHz, C_6D_6): δ = 0.92 (d, 3H, *J* = 6.3 Hz), 1.03 (t, 3H, *J* = 7.0 Hz), 1.21-1.46 (m, 25H), 2.11-2.14 (m, 2H), 2.48-2.58 (m, 1H), 2.69, (dd, 1H, *J* = 10.4; 5.6 Hz), 3.77 (d, 2H, *J* = 13.2 Hz), 4.15 (d, 1H, *J* = 8.9 Hz), 4.48 (d, 2H, *J* = 13.2 Hz), 4.53-4.56 (m, 1H), 7.17 (t, 2H, *J* = 7.2 Hz), 7.25-7.29 (m, 4H), 7.44 (d, 4H, *J* = 7.2 Hz) ppm. ^{13}C NMR (100 MHz, C_6D_6): δ = 14.3, 19.0, 20.6, 22.6, 23.1, 29.0, 29.21, 29.5, 29.8, 29.9, 30.0, 30.1, 32.3, 56.4, 60.9, 67.1, 81.6, 85.6, 127.5, 128.7, 129.9, 140.3 ppm. HRMS (ESI-TOF) (m/z) $[M + H]^+$ = calcd for $C_{34}H_{51}NO$ 490.4048, found 490.4046.

(4*S*,5*R*)-4-(dibenzylamino)-2-methyltetradec-6-yn-5-ol (6a). Colorless oil. Yield 62%. $[\alpha]^{25}_D$ –13.0 (*c* 1.01, $CHCl_3$). ^{1}H NMR (400 MHz, C_6D_6): δ = 0.87, (d, 2H, *J* = 5.6 Hz), 0.96-1.01 (m, 6H), 1.21-1.46 (m, 10H), 1.63-1.68 (m, 2H), 1.90 (t, 1H, *J* = 8.8 Hz), 2.09-2.12 (m, 2H), 3.08-3.11 (m, 1H), 3.47 (d, 2H, *J* = 13.4 Hz), 4.09 (d, 1H, *J* = 7.0 Hz), 4.34 (d, 2H, *J* = 13.4 Hz), 4.61 (br, 1H), 7.18 (t, 2H, *J* = 7.4 Hz), 7.30 (m, 4H), 7.48 (d, 4H, *J* = 7.4 Hz) ppm. ^{13}C NMR (100 MHz, C_6D_6): δ = 14.3, 18.9, 22.2, 22.9, 23.9, 25.0, 29.0, 29.1, 32.0, 34.6, 55.2, 58.6, 61.4, 81.5, 86.5, 127.5, 128.7, 129.6, 140.1 ppm. HRMS (ESI-TOF) (m/z) $[M + H]^+$ = calcd for $C_{29}H_{41}NO$ 420.3266, found 420.3268.

(4*S*,5*R*)-4-(dibezylamino)-2-methylicos-6-yn-5-ol (6b). Colorless oil. Yield 70%. $[\alpha]^{25}_{D}$ –10.5 (*c* 1.12, $CHCl_3$). ^{1}H NMR (400 MHz, C_6D_6): δ = 0.87, (d, 2H, *J* = 5.6 Hz), 1.00-1.05 (m, 6H), 1.21-1.46 (m, 22H), 1.62-1.68 (m, 2H), 1.91 (t, 1H, *J* = 9.0 Hz), 2.11-2.14 (m, 2H), 3.07-3.11 (m, 1H), 3.47 (d, 2H, *J* = 13.4 Hz), 4.08 (d, 1H, *J* = 5.8 Hz), 4.34 (d, 2H, *J* = 13.4 Hz), 4.61 (br, 1H), 7.19 (t, 2H, *J* = 7.4 Hz), 7.29 (m, 4H), 7.48 (d, 4H, *J* = 7.4 Hz) ppm. ^{13}C NMR (100 MHz, C_6D_6): δ = 14.3, 19.0, 22.3, 23.0, 23.9, 25.0, 29.0, 29.2, 29.5, 29.8, 29.9, 30.1, 32.3, 34.6, 55.2, 58.6, 61.4, 81.5, 86.5, 127.5, 128.7, 129.6, 140.1 ppm. HRMS (ESI-TOF) (m/z) $[M + H]^+$ = calcd for $C_{35}H_{53}NO$ 504.4205, found 504.4203.

(3*R*,4*S*,5*R*)-4-(dibenzylamino)-3-methyltetradec-6-yn-5-ol (7a). Colorless oil. Yield 59%. $[\alpha]^{25}_{D}$ –72.0 (*c* 1.12, $CHCl_3$). ^{1}H NMR (400 MHz, C_6D_6): δ = 0.92-1.04 (m, 9H), 1.19-1.46 (m, 11H), 1.91-2.01 (m, 1H), 2.10-2.13 (m, 2H), 2.34-2.40 (m, 1H), 2.35 (br, 1H), 2.80 (dd, 1H, *J* = 10.3, 5.3 Hz), 3.79 (d, 2H, *J* = 13.4 Hz), 3.97 (d, 1H, *J* = 8.9 Hz), 4.47 (d, 2H, *J* = 13.4 Hz), 4.56-4.59 (m, 1H), 7.18 (t, 2H, *J* = 7.5 Hz), 7.25-7.29 (m, 4H), 7.45 (d, 4H, *J* = 7.5 Hz) ppm. ^{13}C NMR (100 MHz, C_6D_6): δ = 10.9, 14.0, 15.7, 18.8, 22.7, 27.2, 28.8, 28.9, 31.8, 35.3, 56.3, 60.9, 65.5, 81.5, 85.5, 127.3, 128.5, 129.7, 140.2 ppm. HRMS (ESI-TOF) (m/z) $[M + H]^+$ = calcd for $C_{29}H_{41}NO$ 420.3266, found 420.3272.

(3*R*,4*S*,5*R*)-4-(dibenzylamino)-3-methyl-6-yn-5-ol (7b). Colorless oil. Yield 55%. $[\alpha]^{25}_{D}$ –62.8 (*c* 0.98, $CHCl_3$). ^{1}H NMR (400 MHz, C_6D_6): δ = 0.93 (d, 3H, *J* = 6.7 Hz) 1.01-1.04 (m, 6H), 1.23-1.47 (m, 23 H), 1.92-2.01 (m, 1H), 2.12-2.15 (m, 2H), 2.32-2.40 (m, 1H), 2.80 (dd, 1H, *J* = 10.3; 4.5 Hz), 3.79 (d, 2H, *J* = 13.4 Hz), 3.97 (d, 1H, *J* = 8.9 Hz), 4.47 (d, 2H, *J* = 13.4 Hz), 4.57-4.60 (m, 1H), 7.18 (t, 2H, *J* = 7.5 Hz), 7.27-7.30 (m, 4H), 7.46 (d, 4H, *J* = 7.5 Hz) ppm. ^{13}C NMR (100 MHz, C_6D_6): δ = 9.8, 14.5, 17.7, 21.7, 26.1, 27.7, 27.9, 28.2, 28.4, 28.6, 28.6, 28.7, 30.9, 34.2, 55.2, 59.8, 64.4, 80.4, 84.3, 126.1, 127.4, 128.5, 139.1 ppm. HRMS (ESI-TOF) (m/z) $[M + H]^+$ = calcd for $C_{35}H_{53}NO$ 504.4205, found 504.4193.

(2*S*,3*R*)-2-(dibenzylamino)-1-phenyldodec-4-yn-3-ol (8a). Colorless oil. Yield 63%. $[\alpha]^{25}_{D}$ +46.3 (*c* 1.03, $CHCl_3$). ^{1}H NMR (400 MHz, C_6D_6): δ = 0.98 (t, 3H, *J* = 6.9 Hz), 1.21-1.49 (m, 10H) 2.14 (td, 2H, *J* = 6.8, 1.6 Hz), 3.10-3.21 (m, 2H), 3.32-3.37 (m, 1H), 3.51 (d, 2H, *J* = 13.2 Hz), 3.96 (d, 1H, *J* = 8.3 Hz), 4.44-4.47 (m, 3H), 7.16-7.19 (m, 3H) 7.24-7.27 (m, 6H), 7.34 (d, 2H, *J* = 7.4 Hz), 7.43 (d, 4H, *J* = 7.2 Hz) ppm. ^{13}C NMR (100 MHz, C_6D_6): δ = 14.3, 19.0, 22.9, 28.9, 29.1, 32.0, 32.4, 55.3, 61.3, 63.2, 81.5, 87.2, 126.5, 127.5, 128.7, 128.8, 129.5, 130.5, 139, 8 ppm. HRMS (ESI-TOF) (m/z) $[M + H]^+$ = calcd for $C_{32}H_{39}NO$ 454.3110, found 454.3108.

(2*S*,3*R*)-2-(dibenzylamino)-1-phenyloctadec-4-yn-3-ol (8b). Colorless oil. Yield 72%. $[\alpha]^{25}_{D}$ +42.2 (*c* 1.03, $CHCl_3$). ^{1}H NMR (400 MHz, C_6D_6): δ = 1.03 (t, 3H, *J* = 7.4 Hz), 1.28-1.49 (m, 22H) 2.14-2.17 (m, 2H), 3.10-3.21 (m, 2H), 3.32-3.37 (m, 1H), 3.51 (d, 2H, *J* = 13.7 Hz), 3.96

(d, 1H, *J* = 8.7 Hz), 4.44-4.47 (m, 3H), 7.16-7.19 (m, 3H) 7.25-7.27 (m, 6H), 7.34 (d, 2H, *J* = 7.2 Hz), 7.43 (d, 4H, *J* = 7.2 Hz) ppm. ^{13}C NMR (100 MHz, C_6D_6): δ = 14.3, 19.0, 23.0, 29.0, 29.3, 29.6, 29.8, 29.9, 30.1, 32.1, 32.3, 32, 4, 55.4, 61.3, 63.2, 81.5, 87.2, 126.5, 127.5, 128.7, 128.8, 129.5, 130.0, 139, 8 ppm. HRMS (ESI-TOF) (m/z) $[M + H]^+$ = calcd for $C_{38}H_{51}NO$ 538.4049, found 538.4048.

(2*S*,3*R*)-1-(4-(benzyloxy)phenyl)-2-(dibenzylamino)dodec-4-yn-3-ol (9a). Colorless oil. Yield 68%. $[\alpha]^{25}_D$ +71.2 (*c* 1.03, $CHCl_3$). ^{1}H NMR (400 MHz, C_6D_6): δ = 0.94 (t, 3H, *J* = 8.0 Hz), 1.18-1.46 (m, 10H), 2.10-2.13 (m, 2H), 3.04, 3.15 (m, 2H), 3.27-3.32 (m, 1H), 3.49 (d, 2H, *J* = 12.7 Hz), 3.99 (d, 1H, *J* = 9.0 Hz), 4.43-4.48 (m, 3H), 4.82 (s, 2H), 6.93 (d, 2H, *J* = 8.4 Hz), 7.12-7.25 (m, 11H), 7.36 (d, 2H, *J* = 7.0 Hz), 7.41 (d, 4H, *J* = 7.5 Hz) ppm. ^{13}C NMR (100 MHz, C_6D_6): δ = 14.3, 19.0, 22.9, 29.0, 29.15, 29.2, 31.5, 32.0, 55.4, 61.3, 63.3, 70.1, 81.6, 87.1, 115.4, 127.5, 127.6, 128.7, 128.8, 129.5, 130.5, 131.7, 137.8, 139.8, 157.9 ppm. HRMS (ESI-TOF) (m/z) $[M + H]^+$ = calcd for $C_{39}H_{45}NO_2$ 560.3528, found 560.3522.

(2*S*,3*R*)-1-(4-(benzyloxy)phenyl)-2-(dibenzylamino)octadec-4-yn-3-ol (9b). Colorless oil. Yield 50%. $[\alpha]^{25}_D$ +67.3 (*c* 1.03, $CHCl_3$). ^{1}H NMR (400 MHz, C_6D_6): δ = 1.03 (t, 3H, *J* = 7.3 Hz), 1.28-1.53 (m, 22H), 2.16-2.20 (m, 2H), 3.09, 3.20 (m, 2H), 3.31-3.36 (m, 1H), 3.59 (d, 2H, *J* = 13.7 Hz), 4.03 (d, 1H, *J* = 8.4 Hz), 4.47-4.53 (m, 3H), 4.86 (s, 2H), 6.97 (d, 2H, *J* = 8.3 Hz), 7.17-7.21 (m, 3H), 7.25-7.30 (m, 8H), 7.40 (d, 4H, *J* = 7.5 Hz), 7.45 (d, 4Hz, *J* = 7.5 Hz) ppm. ^{13}C NMR (100 MHz, C_6D_6): δ = 14.3, 19.1, 23.1, 29.1, 29.3, 29.6, 29.8, 29.9, 30.1, 31.5, 32.3, 55.4, 61.3, 63.3, 70.0, 81.6, 87.1, 115.4, 127.5, 127.6, 128.7, 128.8, 129.5, 130.5, 131.7, 137.8, 139.8, 157.9 ppm. HRMS (ESI-TOF) (m/z) $[M + H]^+$ = calcd for $C_{45}H_{57}NO_2$ 644.4468, found 644.4458.

(2*S*,3*R*)-2-(dibenzylamino)dodec-4-yne-1,3-diol (10a). Colorless oil. Yield 73%. $[\alpha]^{25}_D$ –39.2 (*c* 0.91, $CHCl_3$). ^{1}H NMR (400 MHz, C_6D_6): δ = 0.98 (t, 3H, *J* = 7.0 Hz), 1.25-1.50 (m, 10H), 1.84 (br, 1H), 2.09-2.13 (m, 2H), 2.78 (br, 1H), 3.18-3.23 (m, 1H), 3.84-3.87 (m, 3H), 3.84-4.02 (dd, 1H, *J* = 11.1, 7.8 Hz) 4.14 (d, 2H, *J* = 13.4 Hz), 4.56 (br, 1H), 7.17-7.21 (m, 2H), 7.27-7.30 (m, 4H), 7.46 (d, 4H, *J* = 6.9 Hz) ppm. ^{13}C NMR (100 MHz, C_6D_6): δ = 14.3, 19.0, 22.9, 28.9, 29.1, 29.2, 32.0, 55.2, 60.2, 61.3, 62.8, 81.3, 86.7, 127.7, 128.7, 129.5, 140.1 ppm. HRMS (ESI-TOF) (m/z) $[M + H]^+$ = calcd for $C_{26}H_{35}NO_2$ 394.2668, found 394.2741.

(2*R*,3*S*,4*R*)-3-(dibenzylamino)tridec-5-yne-2,4-diol (11a). Colorless oil. Yield 75%. $[\alpha]^{25}_D$ – 53.1 (*c* 1.07, $CHCl_3$). ^{1}H NMR (400 MHz, C_6D_6): δ = 0.98 (t, 3H, *J* = 7.4 Hz), 1.20-1.47 (m, 10H), 2.07-2.10 (m, 1H), 2.17 (br, 3H), 2.93 (dd, 1H, *J* = 8.7, 4.8 Hz), 3.34 (d, 1H, *J* = 6.6 Hz), 4.23 (q, 4H, *J* = 13.2 Hz), 4.41-4.42 (m, 3H), 4.52 (br, 1H), 7.16-7.24 (m, 3H), 7.27-7.30 (m, 4H), 7.49 (d, 4H, *J* = 7.4 Hz) ppm. ^{13}C NMR (100 MHz, C_6D_6): δ = 14.3, 18.9, 22.9, 28.8, 28.9,

29.1, 32.0, 55.2, 59.2, 60.7, 61.8, 81.5, 86.5, 127.5, 128.7, 129.6, 139.9 ppm. HRMS (ESI-TOF) (m/z) $[M + H]^+$ = calcd for $C_{27}H_{37}NO_2$ 408.2903, found 408.2908.

(2*R*,3*S*,4*R*)-3-(dibenzylamino)nonadec-5-yne-2,4-diol (11b). Colorless oil. Yield 69%. $[\alpha]^{25}_D$ –43.7 (*c* 1.02, $CHCl_3$). ^{1}H NMR (400 MHz, $CDCl_3$): δ = 0.93 (t, 3H, *J* = 6.8 Hz), 1.25-1.31 (m, 22H), 1.49 (q, 2H, *J* = 7.4 Hz), 2.20-2.24 (m, 2H), 2.76 (dd, 1H, *J* = 8.8, 4.6 Hz), 2.91 (br, 1H), 3.52-3.56 (m, 1H), 4.05-4.11 (m, 4H) 4.31-4.35 (m, 1H), 4.52 (br, 1H), 7.28-7.36 (m, 10H) ppm. ^{13}C NMR (100 MHz, $CDCl_3$): δ = 14.1, 18.8, 21.1, 22.7, 28.5, 28.9, 29.1, 29.4, 29.5, 29.6, 29.7, 31.9, 55.5, 60.1, 66.2, 66.6, 80.1, 87.3, 127.2, 128.5, 129.5, 139.5. HRMS (ESI-TOF) (m/z) $[M + H]^+$ = calcd for $C_{33}H_{49}NO_2$ 492.3842 , found 492.3845.

4.6.3 General procedure for the hydrogenation of *N,N*-dibenzylamino alcohols 4a–11b.

To a solution of *N,N*-dibenzylamino alcohol (0.50 mmol) in dry MeOH (5 mL), were added in one portion 20 mg of 20% $Pd(OH)_2$/C. The mixture was stirred under 1 atm of H_2 at room temperature for 18 h. The reaction was monitored by TLC. After completion of the reaction, the catalyst was removed by filtration through celite and washed with 20 mL of MeOH. The solvent was evaporated under reduced pressure to afford the corresponding *anti*-β-amino alcohol.

(2*S*,3*R*)-2-aminododecan-3-ol (4c).[43,44] White solid; m.p. = 62-63 ºC. Yield 68%. $[\alpha]^{25}_D$ +4.5 (*c* 1.07, MeOH). ^{1}H NMR (400 MHz, CD_3OD): δ = 0.80 (t, *J* = 7.2 Hz, 3H), 0.99 (d, *J* = 6.7 Hz, 3H), 1.21-1.41 (m, 16H), 2.83 (br, 1H), 3.20-3.22 (m, 1H), 3.39-3.41 (m, 1H) ppm. ^{13}C NMR (100 MHz, CD_3OD): δ = 14.4, 15.6, 23.7, 27.2, 30.5, 30.7, 30.8, 33.1, 33.9, 52.3, 75.0 ppm. HRMS (ESI-TOF) (m/z) $[M + H]^+$ = calcd for $C_{12}H_{27}NO$ 202.2093; found 202.2095.

(3*S*,4*R*)-3-amino-2-methyltridecan-4-ol (5c). White solid; m.p. = 65-66 ºC. Yield 52%. $[\alpha]^{25}_D$ +32.2 (*c* 0.90, $CHCl_3$). ^{1}H NMR (400 MHz, $CDCl_3$): δ = 0.79-0.93 (m, 9H), 1.95-1.24 (m, 14H), 1.48-1.62 (m, 2H), 2.36-2.45 (m, 3H), 3.57 (br, 1H) ppm. ^{13}C NMR (100 MHz, $CDCl_3$): δ = 14.1, 19.3, 19.9, 22.6, 26.1, 29.3, 29.6, 29.7, 29.8, 30.5, 31.9, 61.8, 71.5 ppm. HRMS (ESI-TOF) (m/z) $[M + H]^+$ = calcd for $C_{14}H_{31}NO$ 230.2483, found 230.2484.

(3*S*,4*R*)-3-amino-2-methylnonadecan-4-ol (5d).[45] White solid; m.p. = 67-68 ºC. Yield 72%. $[\alpha]^{25}_D$ +10.7 (*c* 1.03, $CHCl_3$). ^{1}H NMR (400 MHz, $CDCl_3$): δ = 0.88-0.94 (m, 9H), 1.27-1.41 (m, 26H), 1.55-1.62 (m, 1H), 1.69-1.73 (m, 1H), 2.53-2.60 (m, 4H), 3.66 (br, 1H) ppm. ^{13}C NMR (100 MHz, $CDCl_3$): δ = 14.1, 19.5, 19.9, 22.7, 26.1, 29.4, 29.7, 30.6, 31.9, 62.3, 70.9 ppm. HRMS (ESI-TOF) (m/z) $[M + H]^+$ = calcd for $C_{20}H_{43}NO$ 314.3345; found 314.3343.

(4*S*,5*R*)-4-amino-2-methyltetradecan-5-ol (6c). White solid; m.p. = 67-69 ºC. Yield 55%. $[\alpha]^{25}_D$ –49.6 (*c* 0.67, $CHCl_3$). ^{1}H NMR (400 MHz, $CDCl_3$): δ = 0.67-1.08 (m, 9H), 0.91-0.93 (m, 1H), 1.08-1.57 (m, 20H), 2.43-2.67 (m, 3H) ppm. ^{13}C NMR (100 MHz, $CDCl_3$): δ = 14.1, 21.6,

22.7, 23.8, 24.7, 26.2, 26.4, 29.3, 29.6, 29.7, 29.8, 31.6, 31.9, 40.2, 53.3, 73.9 ppm. HRMS (ESI-TOF) (m/z) $[M + H]^+$ = calcd for $C_{15}H_{33}NO$ 244.2640; found 244.2642.

(4*S*,5*R*)-4-amino-2-methylicosan-5-ol (6d). White solid; m.p. = 69-70 ºC. Yield 60%. $[\alpha]^{25}_D$ –1.2 (*c* 0.81, $CHCl_3$). ^1H NMR (400 MHz, $CDCl_3$): δ = 0.79-0.90 (m, 9H), 1.18-1.68 (m, 31H), 3.34-3.62 (m, 3H) ppm. ^{13}C NMR (100 MHz, $CDCl_3$): δ = 14.1, 21.6, 22.7, 23.7, 24.5, 26.2, 29.3, 29.7, 31.9, 38.7, 53.8, 72.9 ppm. HRMS (ESI-TOF) (m/z) $[M + H]^+$ = calcd for $C_{21}H_{45}NO$ 328.3579 found 328.3577.

(3*R*,4*S*,5*R*)-4-amino-3-methyltetradecan-5-ol (7c). White solid; m.p. = 66-68 ºC. Yield 67%. $[\alpha]^{25}_D$ +44.3 (*c* 0.92, $CHCl_3$). ^1H NMR (400 MHz, $CDCl_3$): δ = 0.79-0.85 (m, 9H), 1.05-1.36 (m, 16H), 1.49-1.51 (m, 1H), 1.57-1.65 (m, 1H), 2.42 (br, 3H), 2.49-2.52 (m, 1H), 3.57-3.59 (m, 1H) ppm. ^{13}C NMR (100 MHz, $CDCl_3$): δ = ppm 10.8, 14.1, 15.6, 22.7, 25.4, 26.2, 29.3, 29.6, 29.7, 29.8, 30.2, 31.9, 37.2, 60.3, 71.3. HRMS (ESI-TOF) (m/z) $[M + H]^+$ = calcd for $C_{15}H_{33}NO$ 244.2640 found 244.2646.

(3*R*,4*S*,5*R*)-4-amino-3-methylicosan-5-ol (7d).[26] White solid; m.p. = 69-71 ºC. Yield 62%. $[\alpha]^{25}_D$ +14.1 (*c* 0.92, $CHCl_3$). ^1H NMR (400 MHz, $CDCl_3$): δ = 0.88-0.94 (m, 9H), 1.27-1.41 (m, 28H), 1.51-1.62 (m, 1H), 1.68-1.73 (m, 1H), 2.53-2.60 (m, 4H), 3.66-3.69 (m, 1H) ppm. ^{13}C NMR (100 MHz, $CDCl_3$): δ = ppm 10.8, 14.1, 15.6, 22.7, 25.4, 26.2, 29.3, 29.7, 30.2, 31.9, 37.1, 60.4, 71.2. HRMS (ESI-TOF) (m/z) $[M + H]^+$ = calcd for $C_{21}H_{45}NO$ 328.3579; found 328.3582.

(2*S*,3*R*)-2-amino-1-phenyldodecan-3-ol (8c). White solid; m.p. = 110-112 ºC. Yield 72%. $[\alpha]^{25}_D$ –10.8 (*c* 0.79, $CHCl_3$). ^1H NMR (400 MHz, $CDCl_3$): δ = 0.84 (t, 3H, *J* = 6.7 Hz), 1.19-1.23 (m, 14H), 1.41-1.48 (m, 2H), 2.15 (br, 3H), 2.38-2.44 (dd, 1H, *J* = 10.8; 13.1 Hz), 2.98-3.01 (m, 1H), 7.11-7.25 (m, 5H) ppm. ^{13}C NMR (100 MHz, $CDCl_3$): δ = 14.1, 22.7, 26.2, 29.3, 29.5, 29.6, 29.7, 29.8, 31.9, 32.3, 37.3, 56.7, 73.8, 126.4, 128.6, 129.2, 139.2 ppm. HRMS (ESI-TOF) (m/z) $[M + H]^+$ = calcd for $C_{18}H_{31}NO$ 277.2484; found 278.2486.

(2*S*,3*R*)-2-amino-1-phenyloctadecan-3-ol (8d). White solid; m.p. = 113-115 ºC. Yield 69%. $[\alpha]^{25}_D$ –11.5 (*c* 1.13, $CHCl_3$). ^1H NMR (400 MHz, $CDCl_3$): δ = 0.81 (t, 3H, *J* = 6.6 Hz), 1.19 (m, 24H), 1.44 (br, 2H), 2.57-2.60 (m, 1H), 2.81-2.84 (m, 1H), 3.12 (br, 1H), 3.71-3.79 (m, 5H) ppm. ^{13}C NMR (100 MHz, $CDCl_3$): δ = 14.1, 22.7, 26.2, 29.3, 29.6, 29.66, 29.7, 31.9, 126.7, 128.8, 129.29, 138.1 ppm. HRMS (ESI-TOF) (m/z) $[M + H]^+$ = calcd for $C_{24}H_{43}NO$ 362.3423; found 362.3432.

((2*S*,3*R*)-2-amino-3-hydroxydodecyl)phenol (9c). White solid; m.p. = 110-112 ºC. Yield 50%. $[\alpha]^{25}_D$ –5.8 (*c* 1.07, MeOH). ^1H NMR (400 MHz, CD_3OD): δ = 0.80 (t, 3H, *J* = 7.0 Hz), 1.20-

1.45 (m, 16H), 2.27 (br, 1H), 2.83-2.73 (m, 1H), 3.21 (br, 1 H), 3.40-3.38 (m, 1H), 6.64 (d, 2H, *J* = 8.4 Hz), 6.94 (d, J = 8.4 Hz, 2H) ppm. ^{13}C NMR (100 MHz, CD_3OD): δ = ppm 14.4, 23.7, 27.2, 30.5, 30.8, 33.1, 33.4, 38.1, 58.7, 74.6, 157.1 ppm. HRMS (ESI-TOF) (m/z) $[M + H]^+$ = calcd for $C_{18}H_{31}NO_2$ 294.2433 found 294.2434.

(2*S*,3*R*)-2-aminododecane-1,3-diol (10c). Colorless oil. Yield 56%. $[\alpha]^{25}_D$ –1.6 (c = 1.2 MeOH). ^{1}H NMR (400 MHz, $CDCl_3$): δ = 0.81 (t, *J* = 6.8 Hz, 3 H), 1.19-1.41 (m, 14 H), 3.34-3.41 (m, 1 H), 3.87-3.95 (m, 2 H), 5.50 (br, 2 H) ppm. ^{13}C NMR (100 MHz, $CDCl_3$): δ = ppm 14.1, 22.7, 26.3, 29.3, 29.4, 29.5, 29.7, 29.8, 31.9, 33.3, 58.4, 70.5 ppm. HRMS (ESI-TOF) (m/z) $[M + H]^+$ = calcd for $C_{12}H_{27}NO_2$ 218.2042; found 218.2121.

(2*R*,3*S*,4*R*)-3-aminotridecane-2,4-diol (11c). Colorless oil. Yield 50%. $[\alpha]^{25}_D$ +6.8 (*c* 1.07, $CHCl_3$). ^{1}H NMR (400 MHz, $CDCl_3$): δ = 0.81 (t, 3H, *J* = 7.6 Hz), 1.09 (d, 2H, *J* = 6.3Hz), 1.16-1.45 (m, 16H), 2.41 (br, 1H), 3.20 (br, 1H), 3.59-3.60 (m, 1H), 3.96-3.98 (m, 1H) ppm. ^{13}C NMR (100 MHz, $CDCl_3$): δ = ppm 14.0, 20.0, 22.6, 26.2, 29.3, 29.6, 29.7, 31.9, 33.5, 58.4, 64.8, 66.4, 74.5 ppm. HRMS (ESI-TOF) (m/z) $[M + H]^+$ = calcd for $C_{13}H_{29}NO_2$ 232.2277; found 232.2274.

(2*R*,3*S*,4*R*)-3-aminononadecane-2,4-diol (11d). Colorless oil. Yield 60%. $[\alpha]^{25}_D$ +1.4 (*c* 0.91, $CHCl_3$) ^{1}H NMR (400 MHz, $CDCl_3$): δ = 0.91 (t, 3H, *J* = 6.6 Hz), 1.14 (d, 2H, *J* = 6.1Hz), 1.29-1.49 (m, 30H), 2.42 (br, 1H), 3.23 (br, 2H), 3.66-3.69 (m, 1H), 4.02 (br, 1H) ppm. ^{13}C NMR (100 MHz, $CDCl_3$): δ = ppm 14.0, 20.0, 22.7, 26.2, 29.3, 29.7, 29.8, 31.9, 33.6, 58.3, 64.8, 66.4, 74.6 ppm. HRMS (ESI-TOF) (m/z) $[M + H]^+$ = calcd for $C_{19}H_{41}NO_2$ 316.3216; found 316.3211.

4.6.4. NMR data comparison with literature data

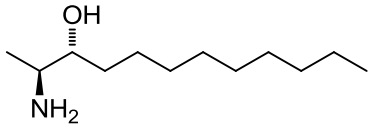

Table S1. ^{1}H NMR data (CD_3OD) for compound 4c and its comparison to literature.

This work **400 MHz**	**Ref 43** **400 MHz**	**Ref 44** **400 MHz**
3.39-3.41 (m, 1H)	3.64 (m, 1H)	3.44 (m, 1H)
3.20-3.22 (m, 1H)	3.18 (ddd, 1H, *J* = 2.9, 5.4, 10.6 Hz)	-----
2.83 (br, 1H)	-----	2.82 (ddd, *J* = 2.1, 4.2, 6.2 Hz , 1H)
-----	1.43 and 1.25 (m, 2H)	
-----	1.36 (m, 2H)	
1.21-1.41 (m, 16H)	1.22-1.20 (m, 10H)	1.28-1.60 (m, 16H)
0.99 (d, 3H, *J* = 6.7 Hz)	1.12 (d, 3H, *J* = 5.4 Hz)	1.05 (d, 3H, *J*=6.6 Hz)
0.80 (t, 3H, *J* = 7.2 Hz)	0.8 (t, 3H, J = 6.7 Hz)	0.90 (t, 3H, *J*=6.9 Hz)

Table S2. ^{13}C NMR data (CD_3OD) for compound 4c and its comparison to literature.

This work **100 MHz**	**Ref 43** **100 MHz**	**Ref 44** **100 MHz**
75.0	70.5	74.3
52.3	51.5	50.2
33.9	31.6	32.0
33.1	30.6	31.1
30.8	28.3	28.83
30.7	28.2	28.78
30.5	28.1	28.7
27.2	28.0	28.5
23.7	24.5	25.3
15.6	21.3	21.7
14.4	12.0	15.0
----	9.6	12.5

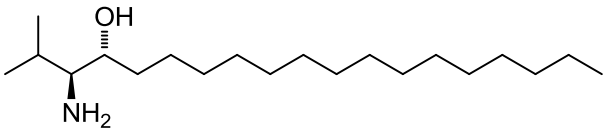

Table S3. ^{1}H NMR data ($CDCl_3$) for compound 5d and its comparison to literature.

This work **400 MHz**	**Ref 45** **300 MHz**
3.66 (br, 1H)	3.54-3.62 (m, 1H)
2.53-2.60 (m, 4H)	2.41 (dd, 1H, *J* = 7.9, 4.7 Hz)
1.69-1.73 (m, 1H)	2.02 (br s, 3H)
1.55-1.62 (m, 1H)	1.50-1.65 (m, 3H)
1.27-1.41 (m, 26H)	1.20-1.40 (m, 26H)
0.88-0.94 (m, 9H)	0.85 (t, 3H, *J* = 7.0 Hz); 0.88 (d, 3H, *J* = 6.7 Hz); 0.95 (d, 3H, *J* = 6.7 Hz)

Table S4. ^{13}C NMR data ($CDCl_3$) for compound 5d and its comparison to literature.

This work **100 MHz**	**Reference 45** **75 MHz**
70.9	71.5
62.3	61.7
31.9	31.9
30.6	30.8
29.7	30.4
29.4	29.7 (x 2); 29.6
26.1	26.1
22.7	22.6
19.9	19.8
19.5	19.2
14.1	14.1

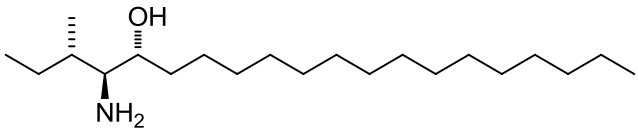

Table S5. **^{1}H NMR data ($CDCl_3$) for compound 7d and its comparison to literature.**

This work 400 MHz	**Reference 45 300 MHz**
	4.25-4.60 (m, 2H)
3.66-3.69 (m, 1H)	3.62-3.69 (m, 1H)
	2.68-2.72 (m, 1H)
2.53-2.60 (m, 4H)	2.45-2.51 (m, 2H)
1.68-1.73 (m, 1H)	1.65-1.69 (m, 1H)
1.51-1.62 (m, 1H)	
1.27-1.41 (m, 28H)	1.15-1.46 (m, 31H)
0.88-0.94 (m, 9H)	0.91-1.10 (m, 6H)

Biology

4.6.5. Biological assays. General remarks

All starting materials were commercially available research grade chemicals and used without further purification. RPMI 1640 medium was purchased from Flow Laboratories (Irvine, UK), fetal calf serum (FCS) was from Gibco (Grand Island, NY), trichloroacetic acid (TCA) and glutamine were from Merck (Darmstadt, Germany), and penicillin G, streptomycin, DMSO and sulforhodamine B (SRB) were from Sigma (St Louis, MO).

4.6.6. Cells, culture and plating

The human solid tumor cell lines HBL-100, HeLa, SW1573, T-47D and WiDr were used in this study. These cell lines were a kind gift from Prof. G. J. Peters (VU Medical Center, Amsterdam, The Netherlands). Cells were maintained in 25 cm^2 culture flasks in RPMI 1640 supplemented with 5% heat inactivated fetal calf serum and 2 mM L-glutamine in a 37 ºC, 5% CO_2, 95% humidified air incubator. Exponentially growing cells were trypsinized and re-suspended in antibiotic containing medium (100 units penicillin G and 0.1 mg of streptomycin per mL). Single cell suspensions displaying >97% viability by trypan blue dye exclusion were subsequently counted. After counting, dilutions were made to give the appropriate cell densities for inoculation onto 96-well microtiter plates. Cells were inoculated in a volume of 100 µL per well at densities of 10 000 (HBL-100, HeLa and SW1573), 15 000 (T-47D), and 20 000 (WiDr) cells per well, based on their doubling times.

4.6.7. Chemosensitivity testing

Compounds were initially dissolved in DMSO at 400 times the desired final maximum test concentration. Control cells were exposed to an equivalent concentration of DMSO (0.25% v/v, negative control). Each agent was tested in triplicate at different dilutions in the range of 1–100 µM. The drug treatment started on day 1 after plating. Drug incubation times were 48 h, after which cells were precipitated with 25 µL ice-cold TCA (50% w/v) and fixed for 60 min at 4ºC. Then the SRB assay was performed.[29] The optical density (OD) of each well was measured at 492 nm, using BioTek's PowerWave XS Absorbance Microplate Reader. Values were corrected for background OD from wells only containing medium

4.6.8. Computational calculations

All calculations were performed in commodity PCs running Windows 7 operating system. Open Babel was used to manipulate the various file formats of ligands. PyMol was used for visual inspection of results and graphical representations. All the tested compounds were drawn and minimized using AM1 semi-empirical method, using the Polak-Ribiere conjugate gradient energy minimization algorithm until the energy change between steps was lower than 0.01 kcal/mol using Hyperchem 8.0 (Hypercube, Inc., Florida, USA). The protein structures were downloaded from the Protein Data Bank and for the purpose of the docking calculations, we removed ligands and water molecules present in the crystal structure and added polar hydrogen atoms to the protein chain before running any docking calculations. AutoDock Vina was used to perform docking calculations. Docking was performed with the prepared ligand files against all the crystal structures with grid box dimensions of 30×30×30 Å. The docking accuracy, meaning the AutoDock Vina parameter 'exhaustiveness', was set to 100 and all the output files were visually inspected to check the correctness of obtained docked conformations. We used the MASC formula to correct the docking interaction energy results and subsequently calculated linear correlations between corrected interaction energy results and biological activity experimental data.

4.6.9. List of targets

Table S6. Anticancer targets used in the virtual screening of 1, 4c-11d.

Protein	PDB Code	Protein	PDB Code
26S Proteasome	1UOH	MET	3CCN
AURKA	1MQ4	MTAP	1SD1
β-tubulin	3E22	mTOR	2NPU
CAPN1	1ZCM	MYC	1NKP
CCNA2-CDK2	2C5O	PCAF	3GG3
CDC25A	1C25	PDF	3G5K
CDC25B	1QB0	PDK1	2R7B
CDK1	1LC9	PIK3CG	1E8Y
CDK4	3G33	PIN1	1PIN
Chk1	2HY0	PKB	1UNQ
COX-2	1V0X	PLAU	2O8T
CSNK1E	4HNI	Plk1	2OWB
EGFR	2RGP	PP2A	2IE4
FAK1	1MP8	PPAR-γ	3ET3
FLT-3	1RJB	PKC	2FK9
FNTB	1MZC	Rac GTPase	2OVJ
GART	1NJS	RAF-1	1C1Y
GLO1	1QIP	RET	2X2L
HDAC1	1TYI	RhoA	1KMQ
Hdm2	3LBL	ROC1	3DPL
HER2	2A91	SHIP2	2K4P
HIF1A	1H2K	SRC	1YOJ
HSP90A	1UYL	Tdp1	1JY1
hTERT	2BCK	TNKS-1	2RF5
IDO1	2D0T	TOP1	1K4T
IGF1R	3I81	TOP2A	1ZXN
KIF11	2PG2	TP53	2OCJ
MEK1	1S9J	TUBA	2E4H
MEK2	1S9I	TXNRD1	2CFY

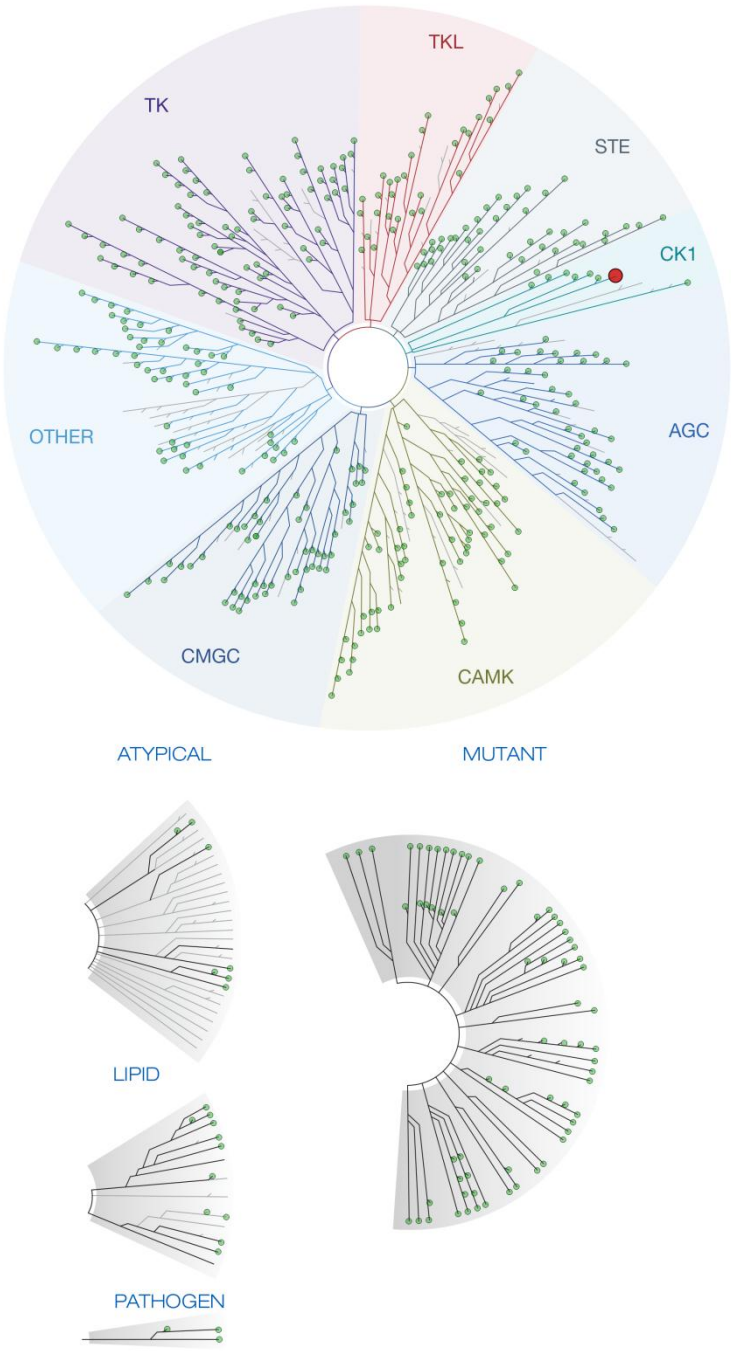

Figure S40. Kinome interaction map for 8c tested against 456 kinases in the DiscoveRx scanMAX™ panel. The red circle indicates CK1ε, found to bind to 8c tested at 10 µM. ***Image generated using TREEspot™ Software Tool and reprinted with permission from KINOMEscan®, a division of DiscoveRx Corporation, © DISCOVERX CORPORATION 2010.***

4.7 ^{1}H and ^{13}C NMR spectra

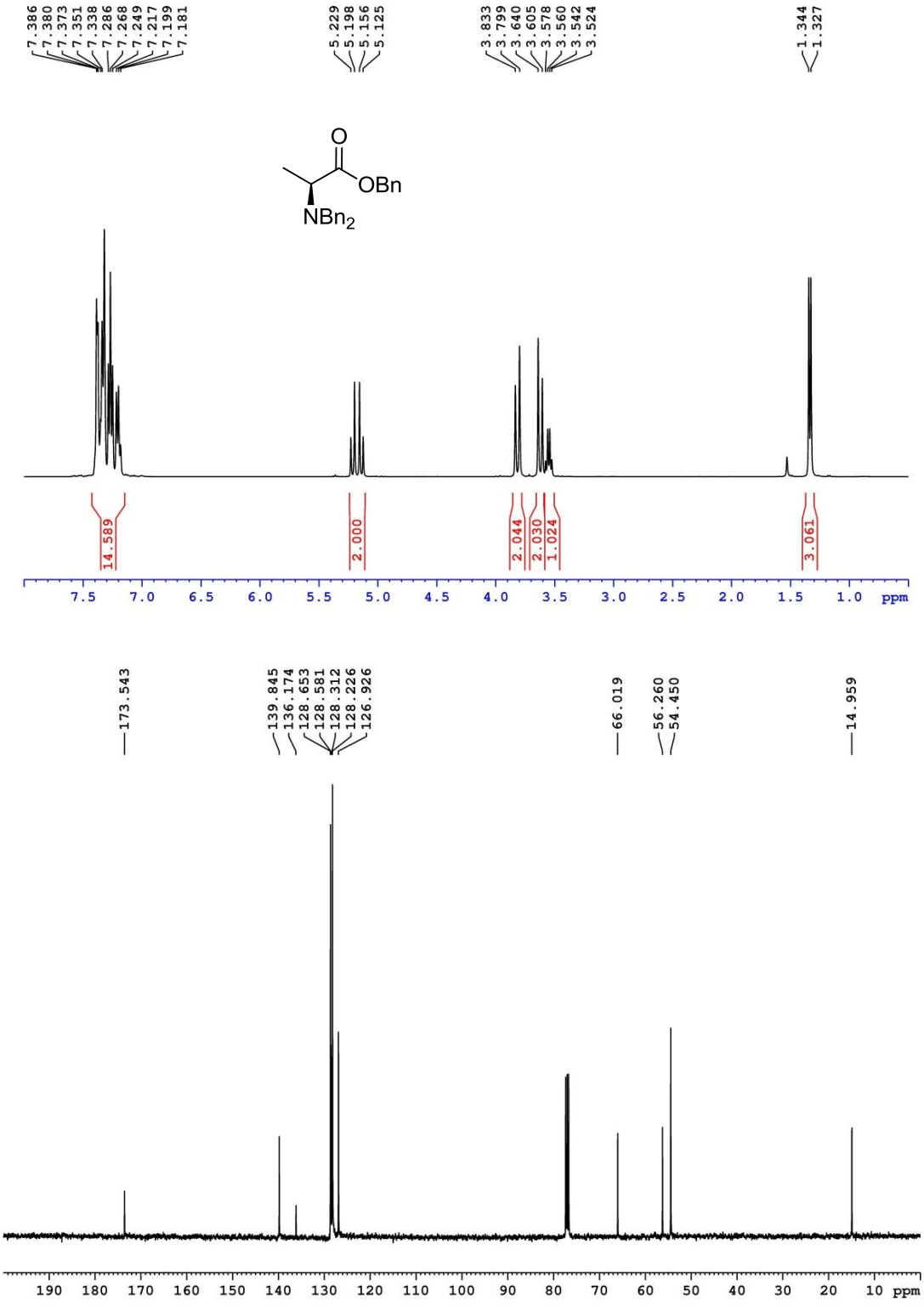

Figure S1. ^{1}H (400 MHz) and ^{13}C (100 MHz) NMR spectra of 4 in $CDCl_3$.

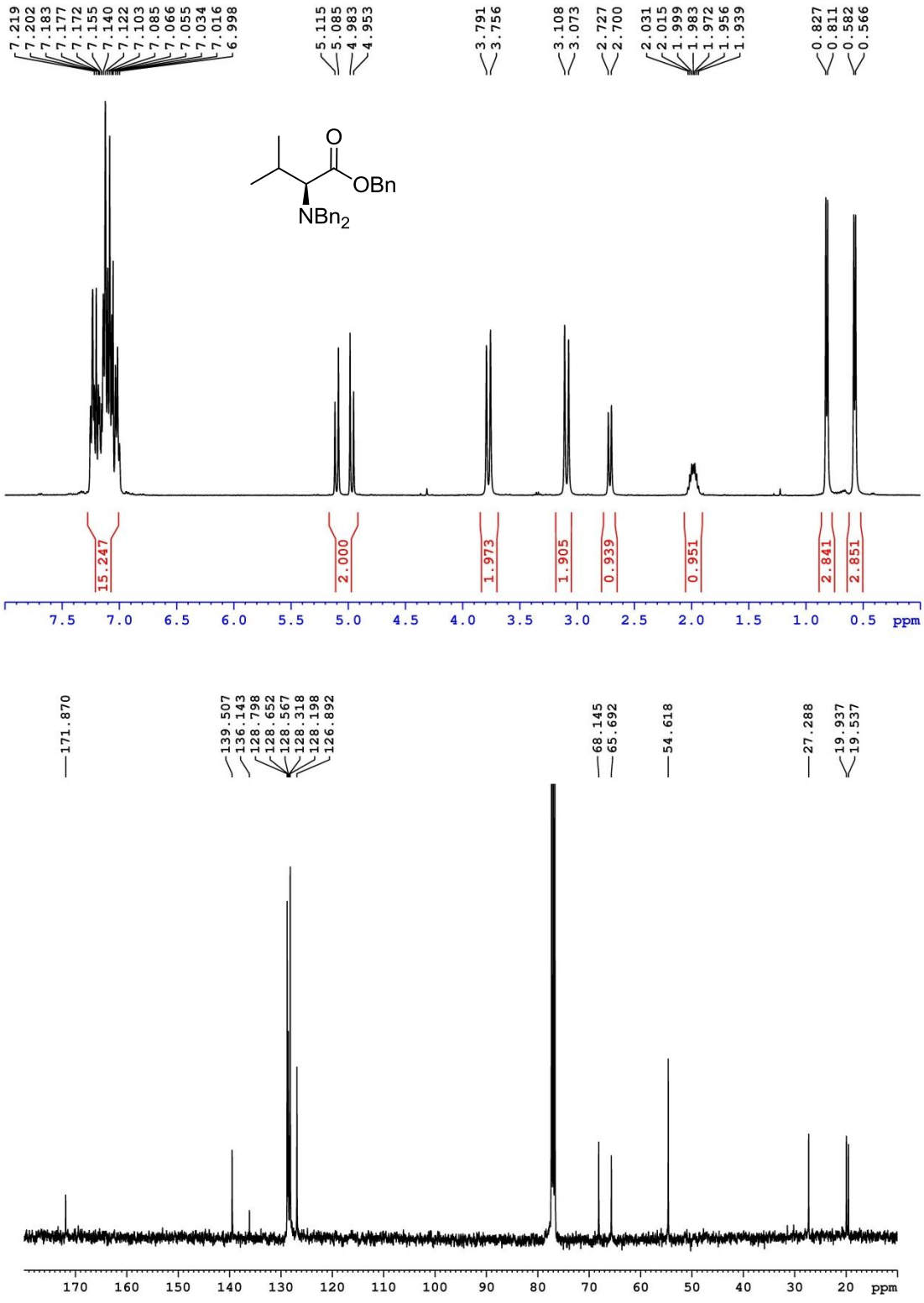

Figure S2. **^{1}H (400 MHz) and ^{13}C (100 MHz) NMR spectra of 5 in $CDCl_3$.**

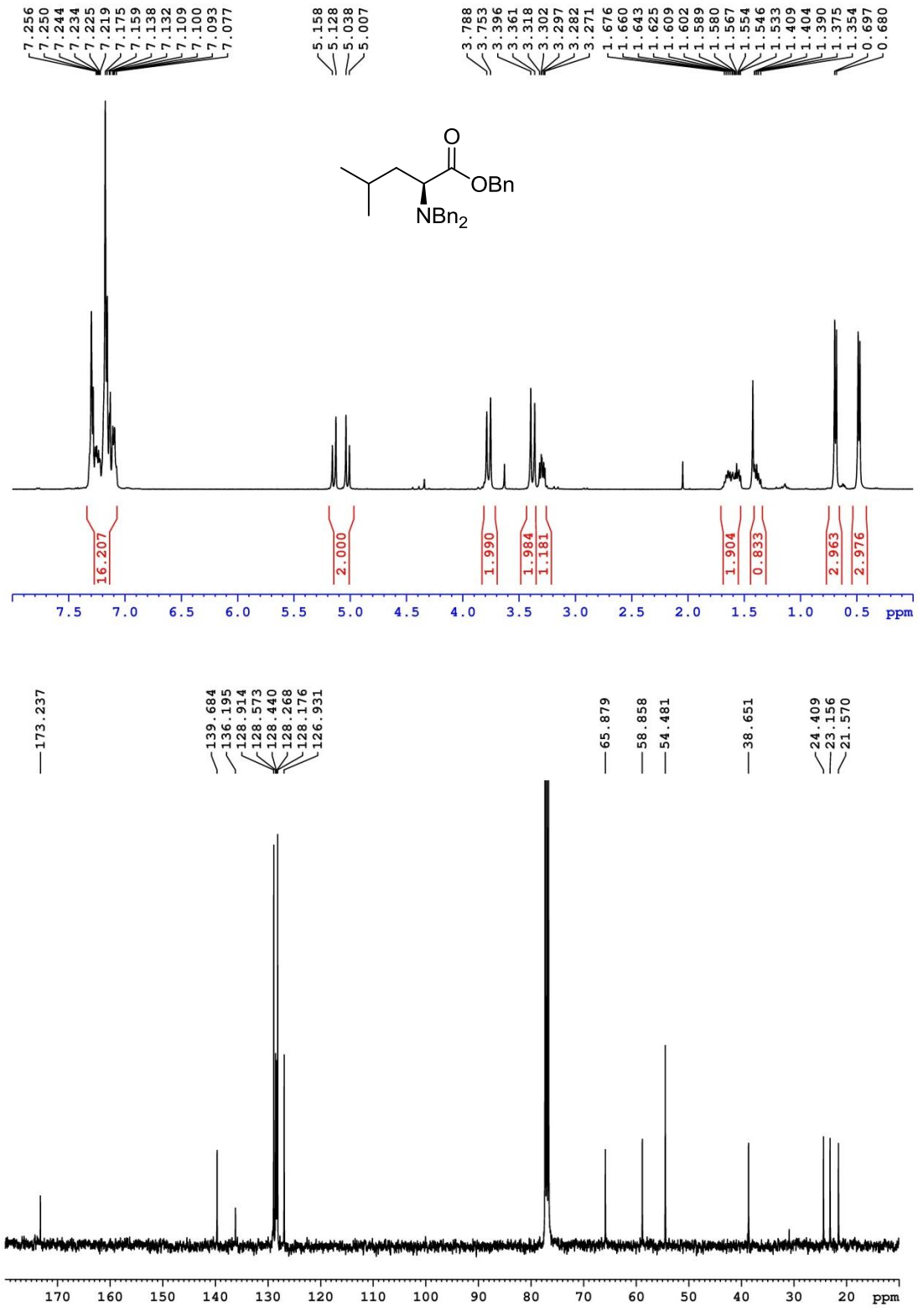

Figure S3. **^{1}H (400 MHz) and ^{13}C (100 MHz) NMR spectra of 6 in $CDCl_3$.**

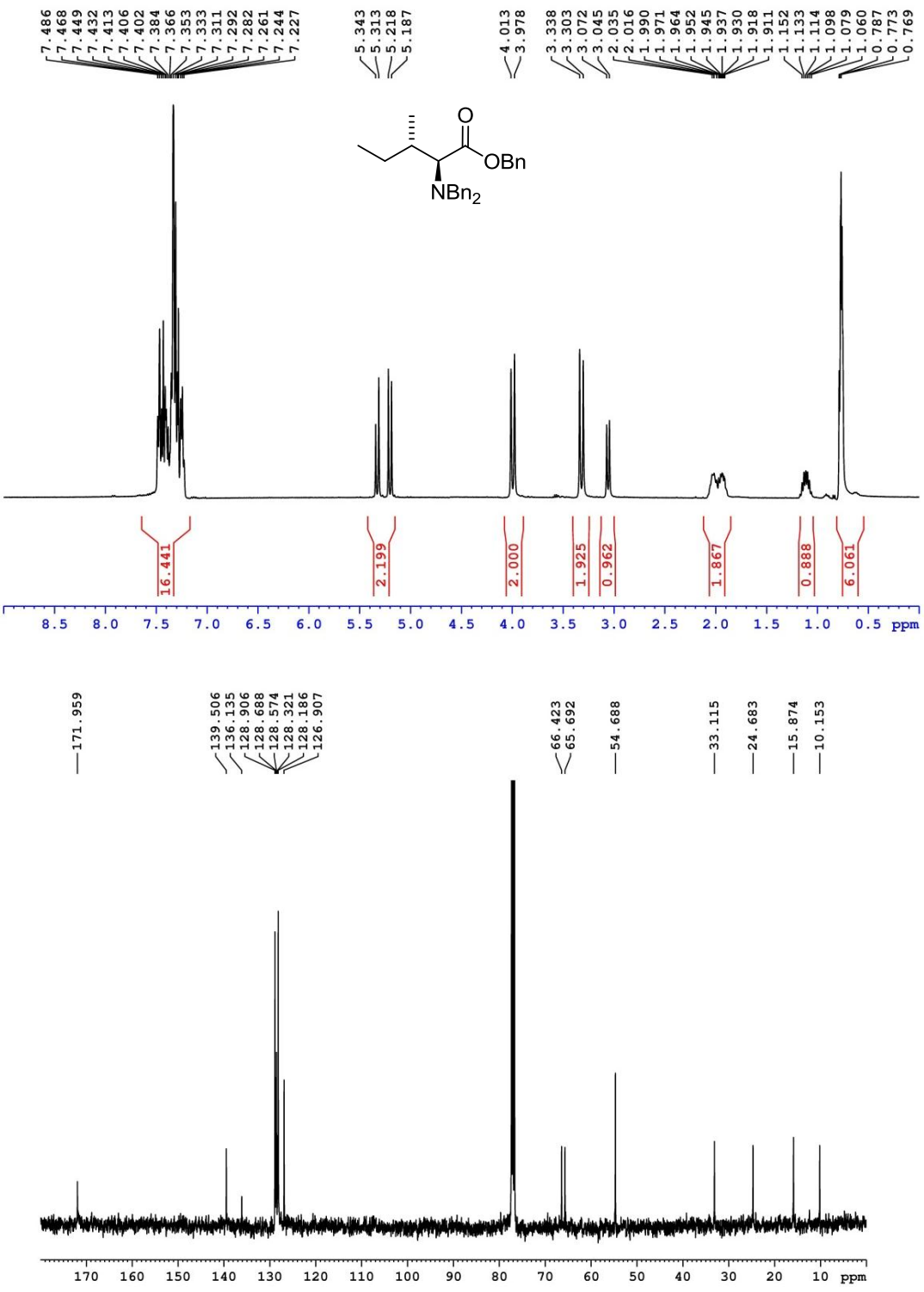

Figure S4. **^{1}H (400 MHz) and ^{13}C (100 MHz) NMR spectra of 7 in $CDCl_3$.**

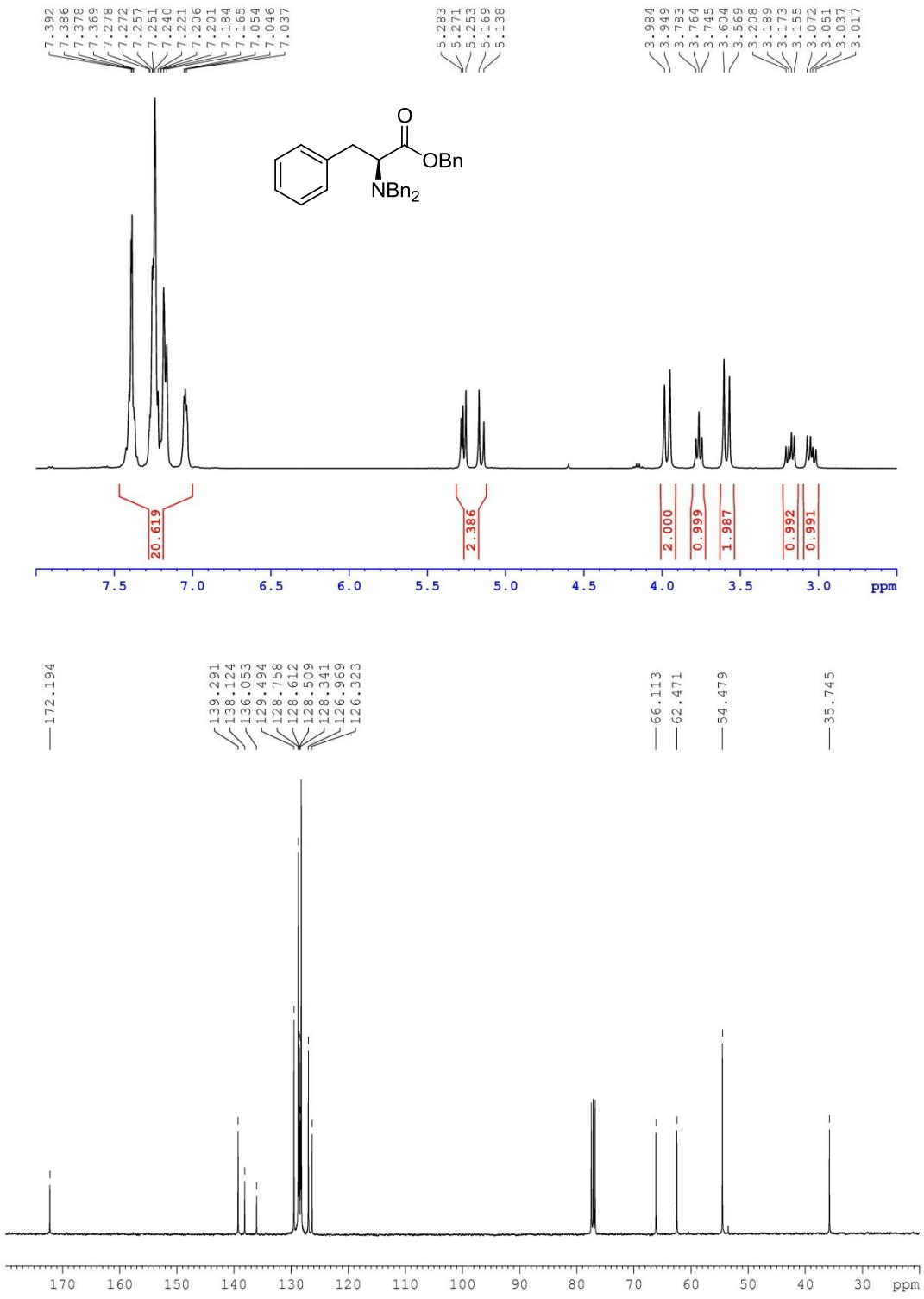

Figure S5. **^{1}H (400 MHz) and ^{13}C (100 MHz) NMR spectra of 8 in $CDCl_3$.**

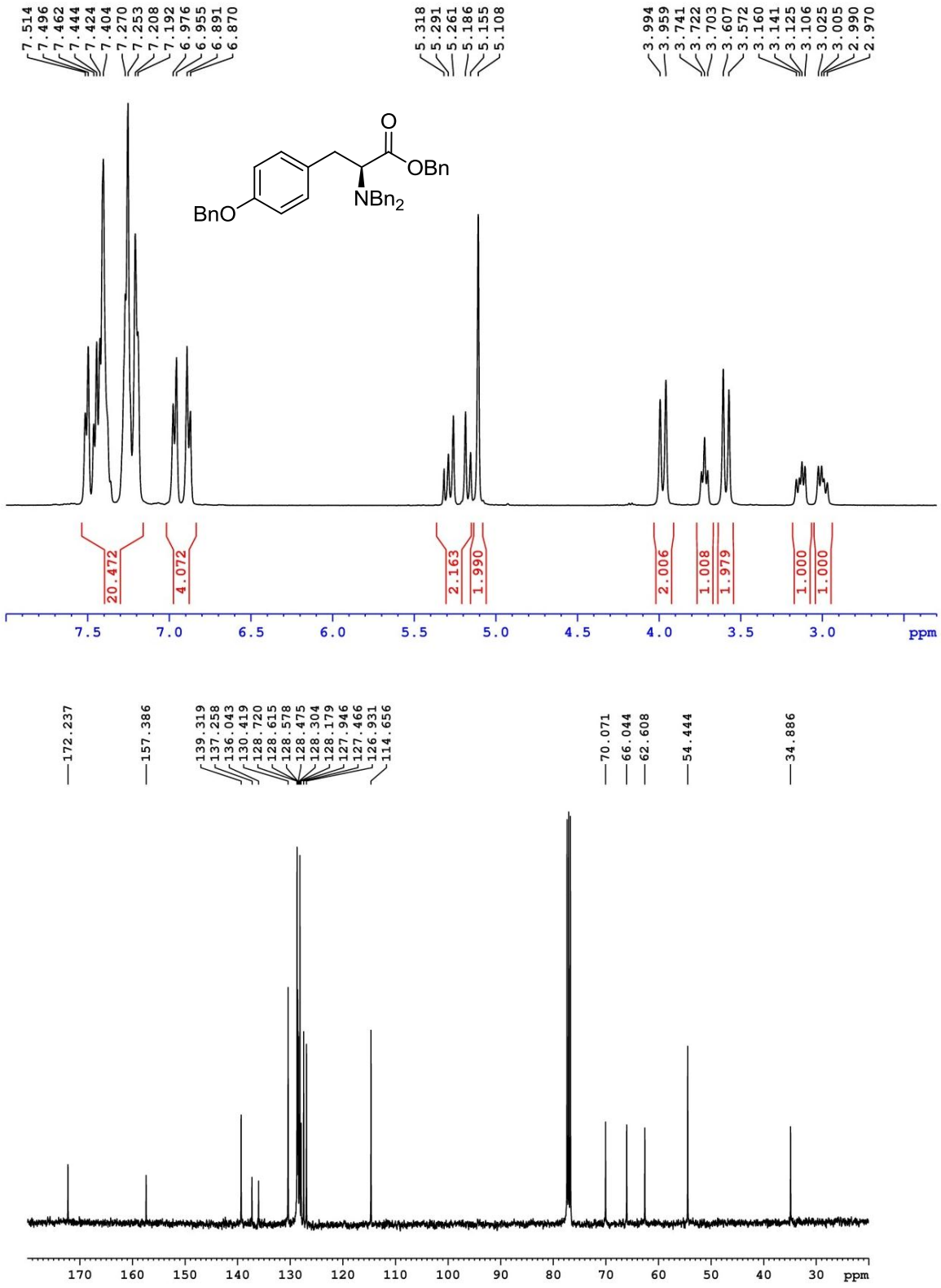

Figure S6. **^{1}H (400 MHz) and ^{13}C (100 MHz) NMR spectra of 9 in $CDCl_3$.**

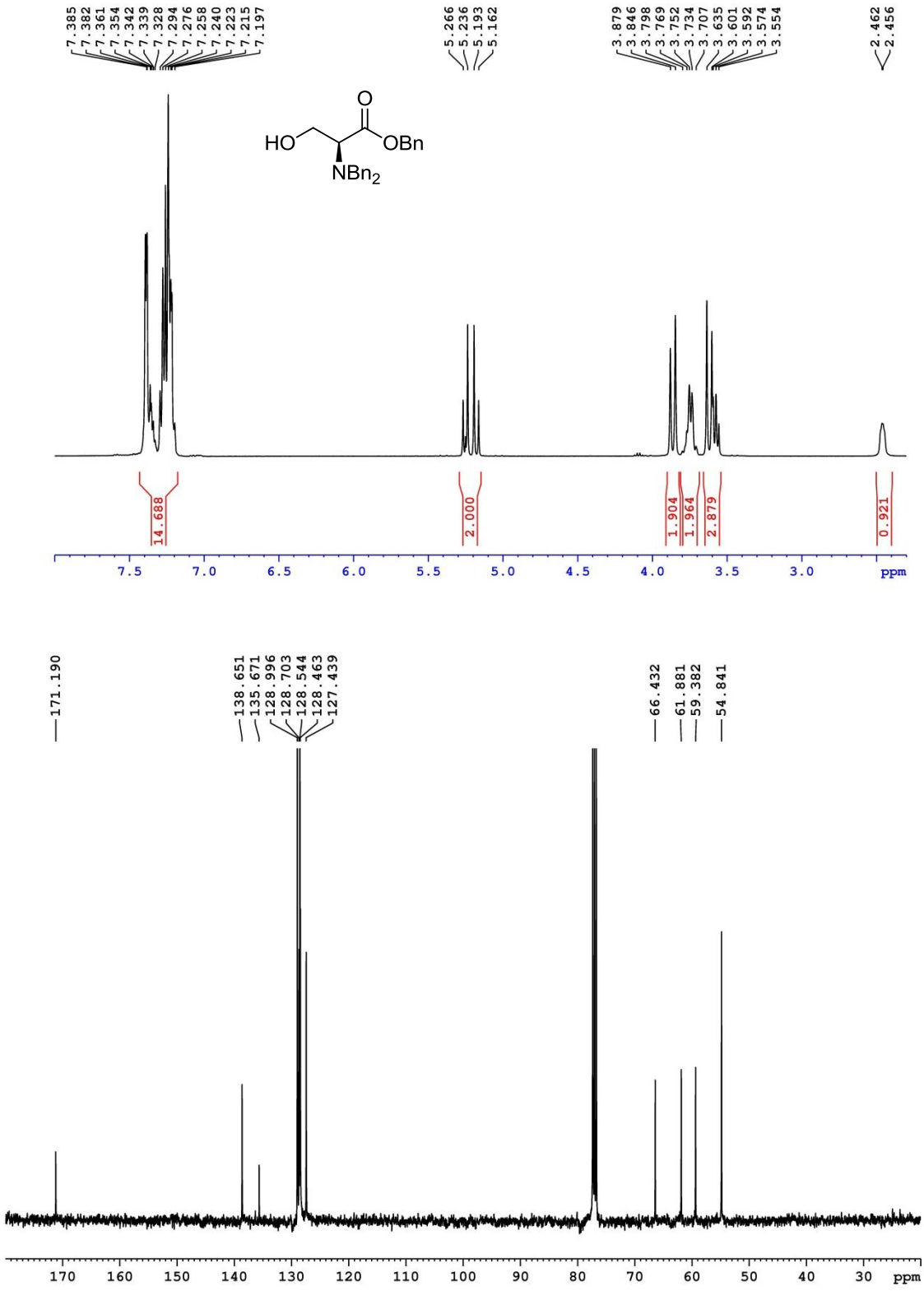

Figure S7. **^{1}H (400 MHz) and ^{13}C (100 MHz) NMR spectra of 10 in $CDCl_3$.**

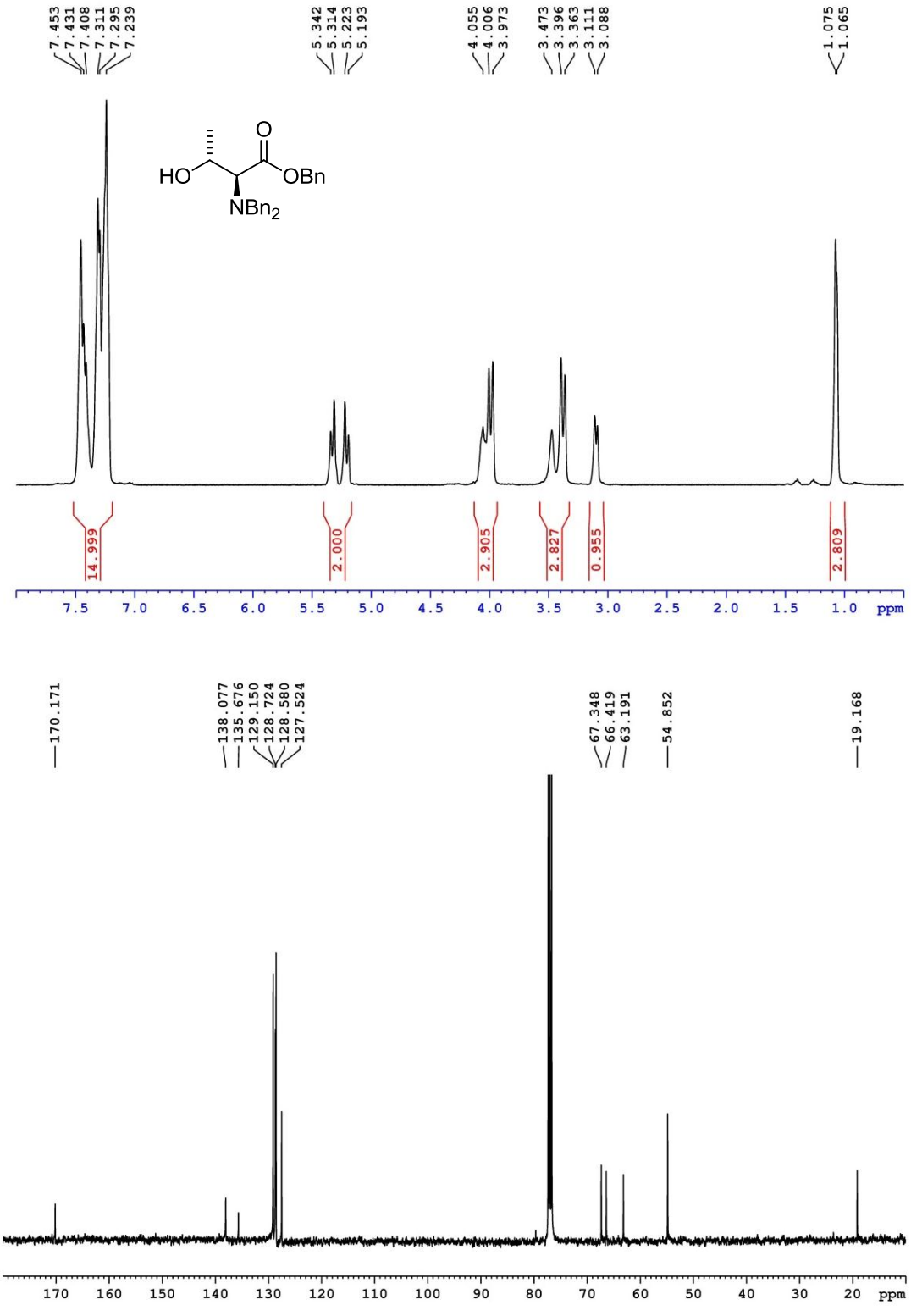

Figure S8. ^{1}H (400 MHz) and ^{13}C (100 MHz) NMR spectra of 11 in $CDCl_3$.

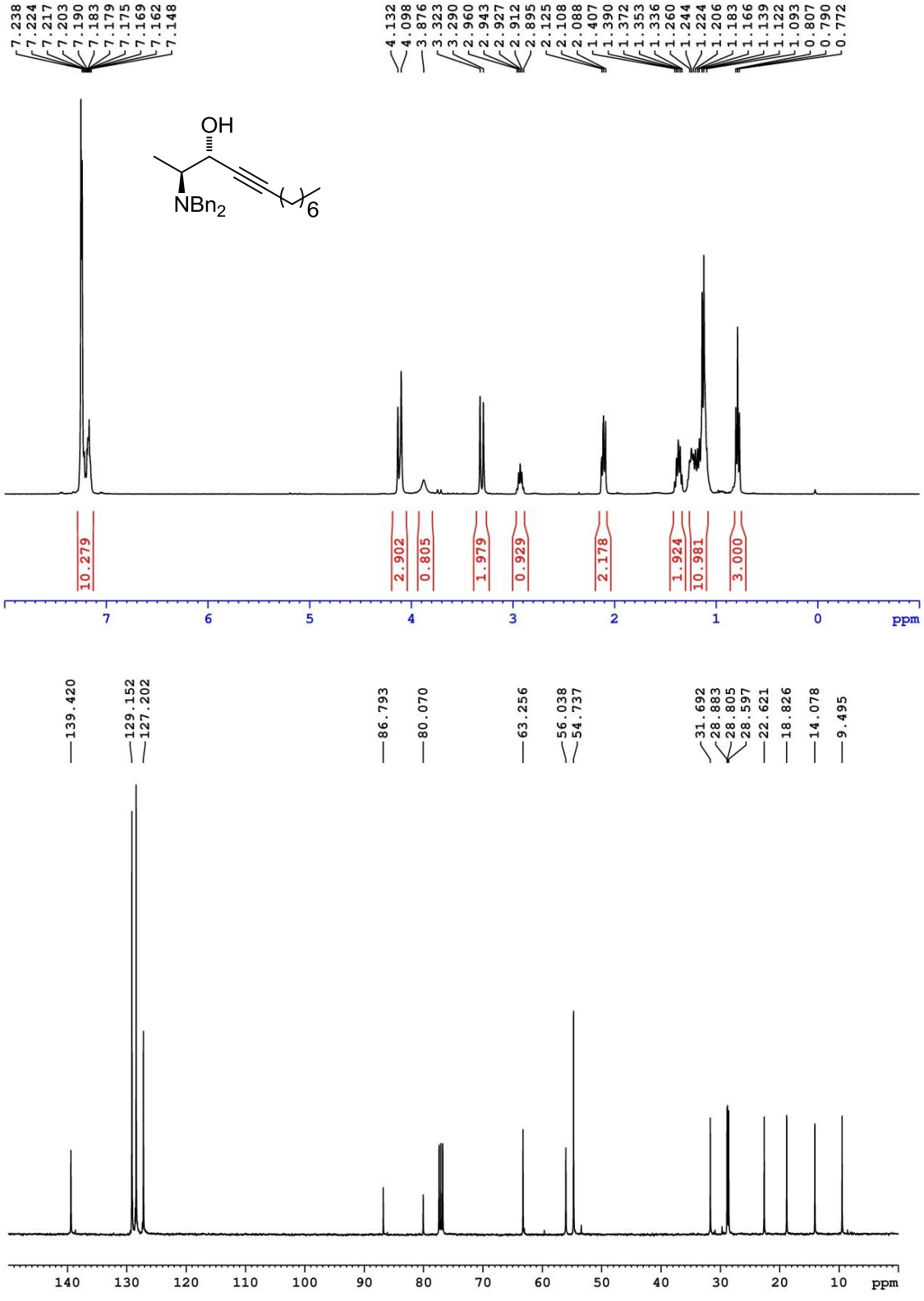

Figure S9. **^{1}H (400 MHz) and ^{13}C (100 MHz) NMR spectra of 4a in $CDCl_3$.**

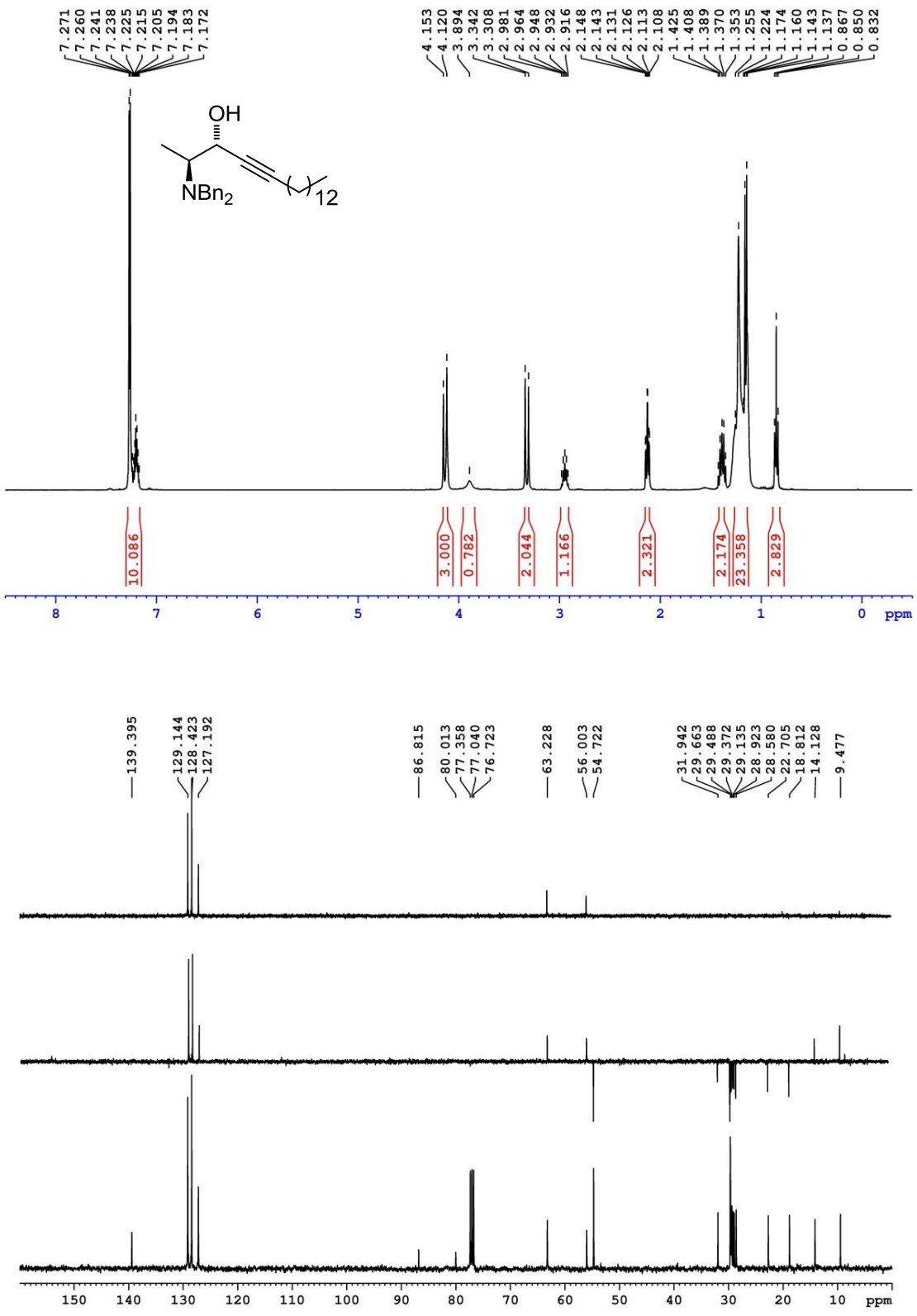

Figure S10. **^{1}H (400 MHz) and ^{13}C (100 MHz) NMR spectra of 4b in $CDCl_3$.**

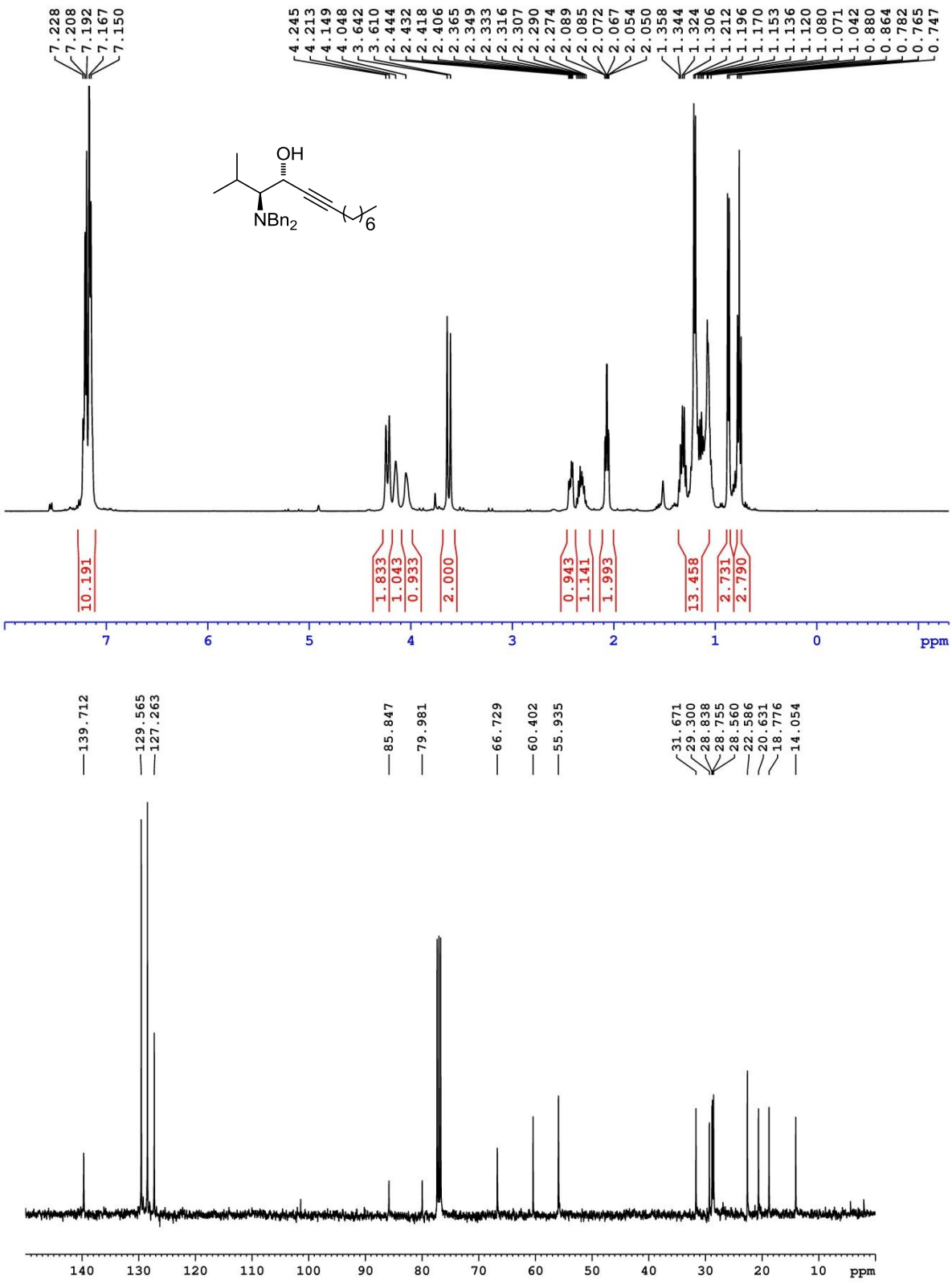

Figure S11. ^{1}H (400 MHz) and ^{13}C (100 MHz) NMR spectra of 5a in $CDCl_3$.

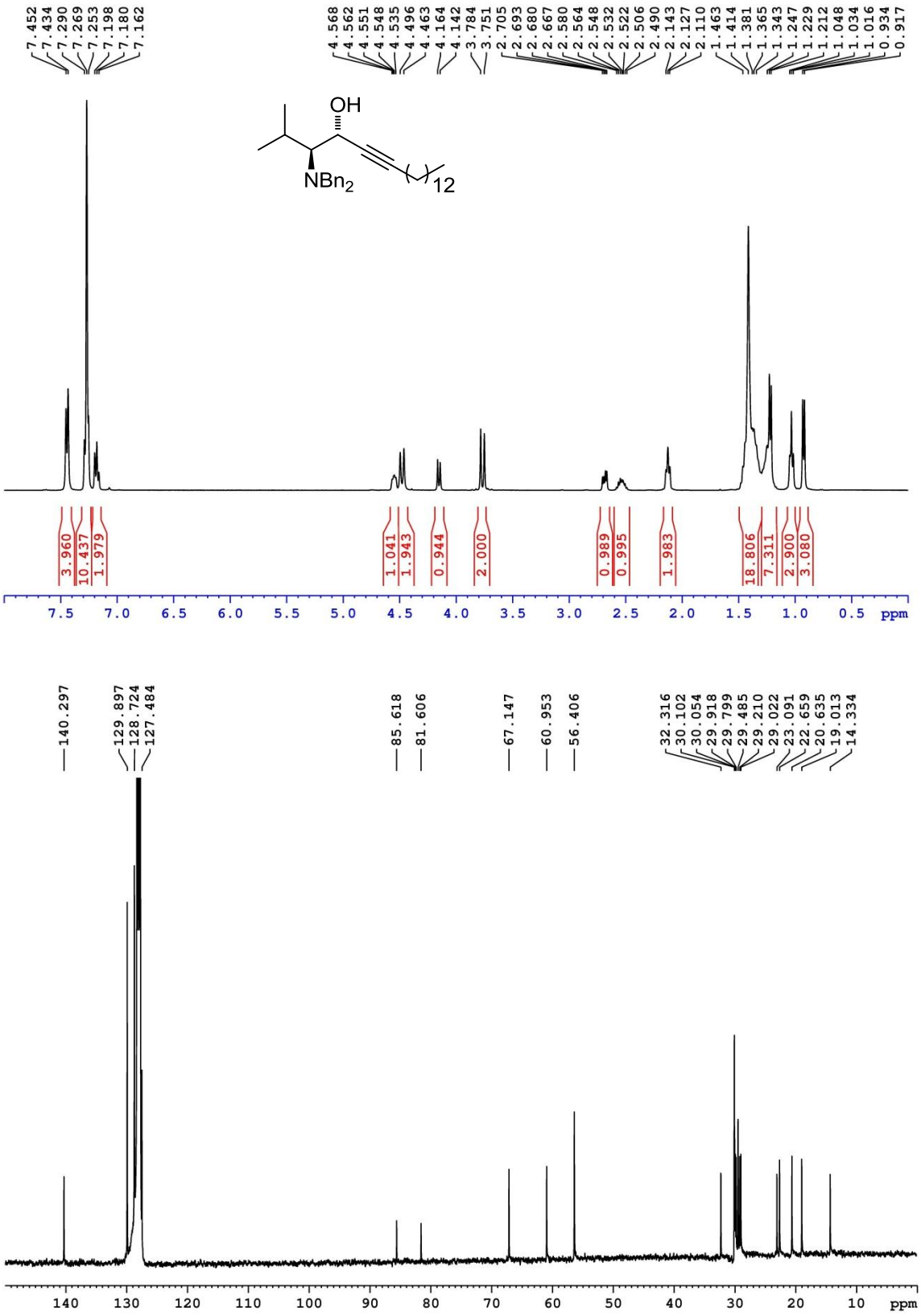

Figure S12. **^{1}H (400 MHz) and ^{13}C (100 MHz) NMR spectra of 5b in C_6D_6.**

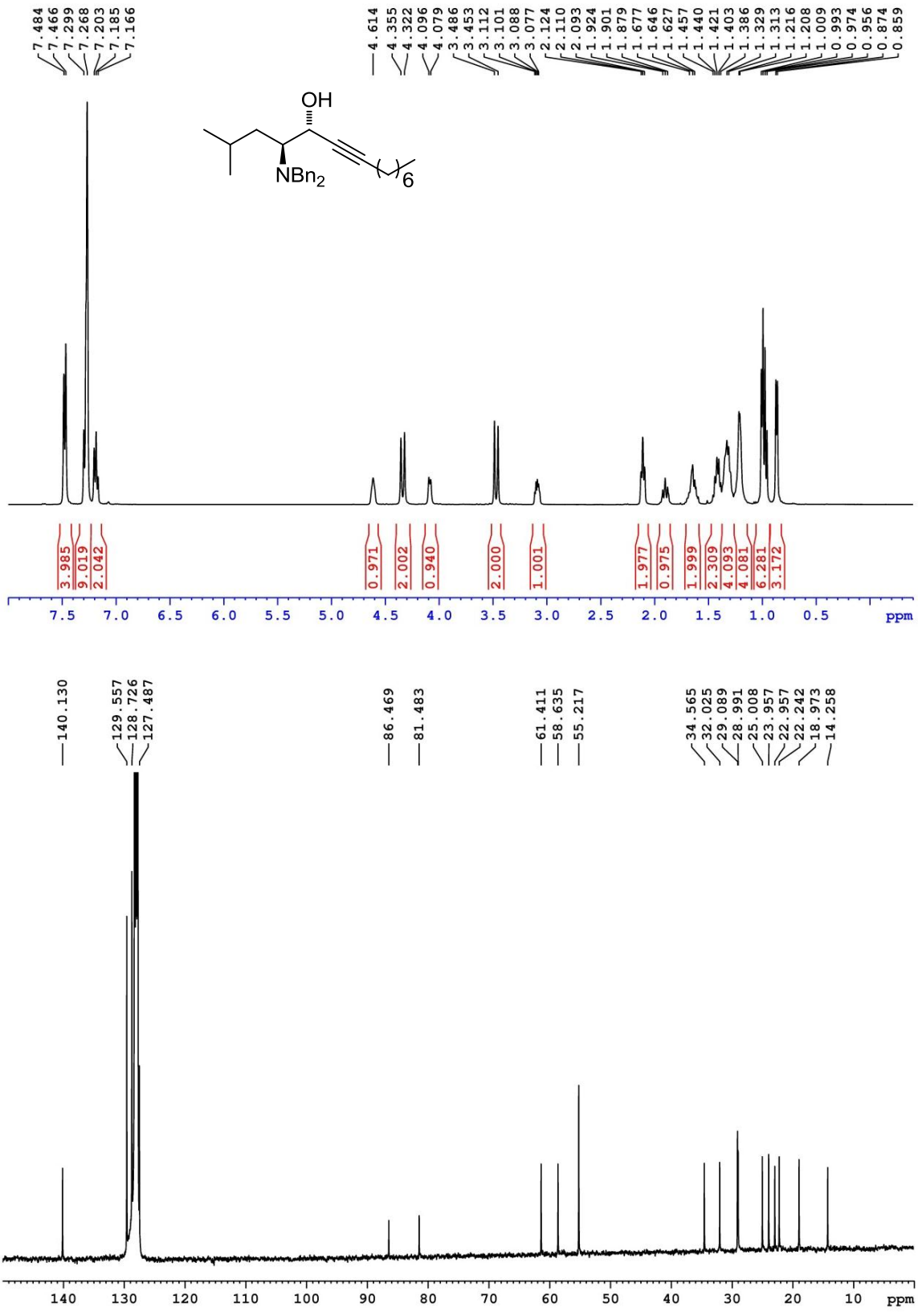

Figure S13. ^{1}H **(400 MHz) and** ^{13}C **(100 MHz) NMR spectra of 6a in** C_6D_6**.**

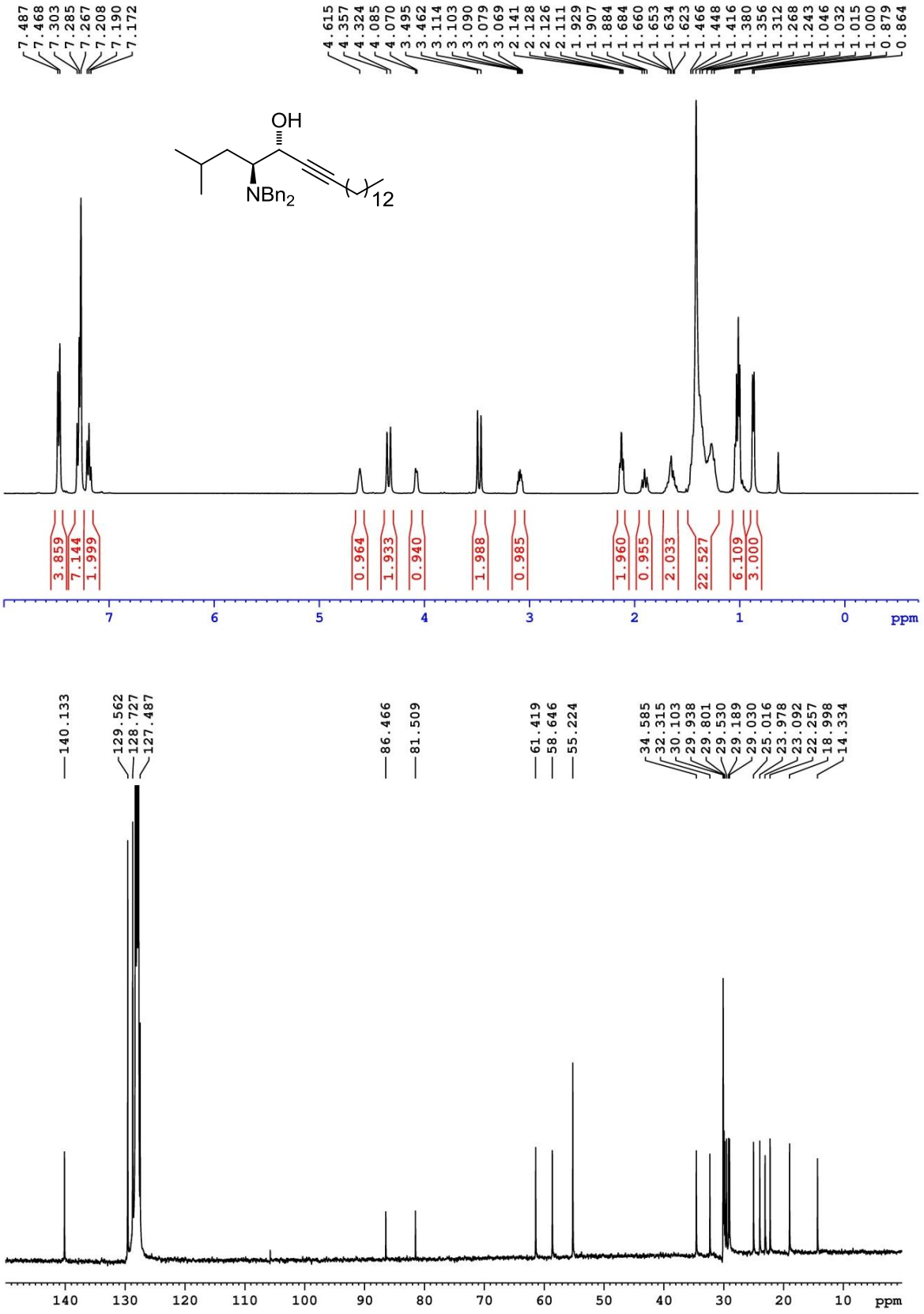

Figure S14. **^{1}H (400 MHz) and ^{13}C (100 MHz) NMR spectra of 6b in C_6D_6.**

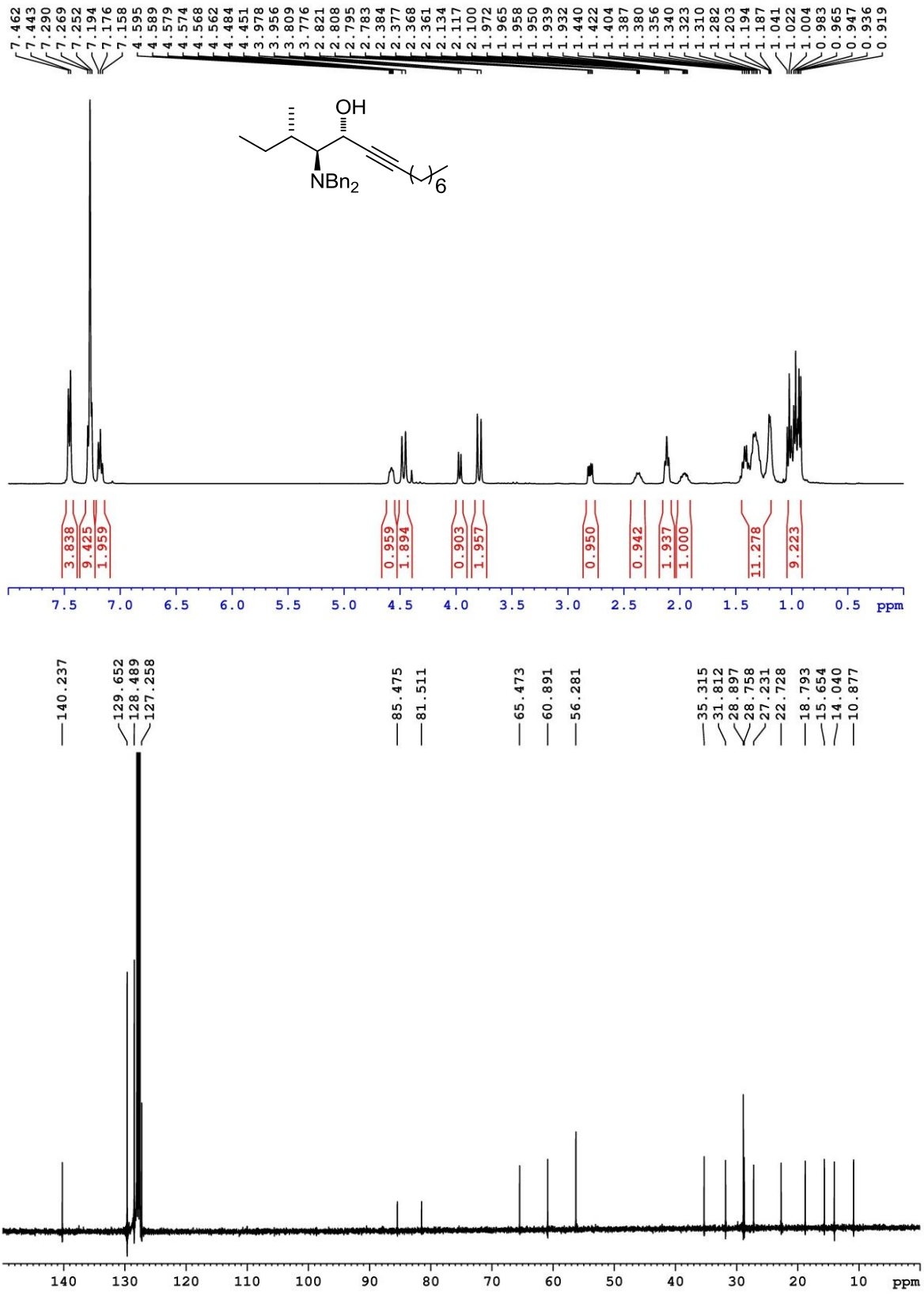

Figure S15. ^{1}H **(400 MHz) and** ^{13}C **(100 MHz) NMR spectra of 7a in** C_6D_6**.**

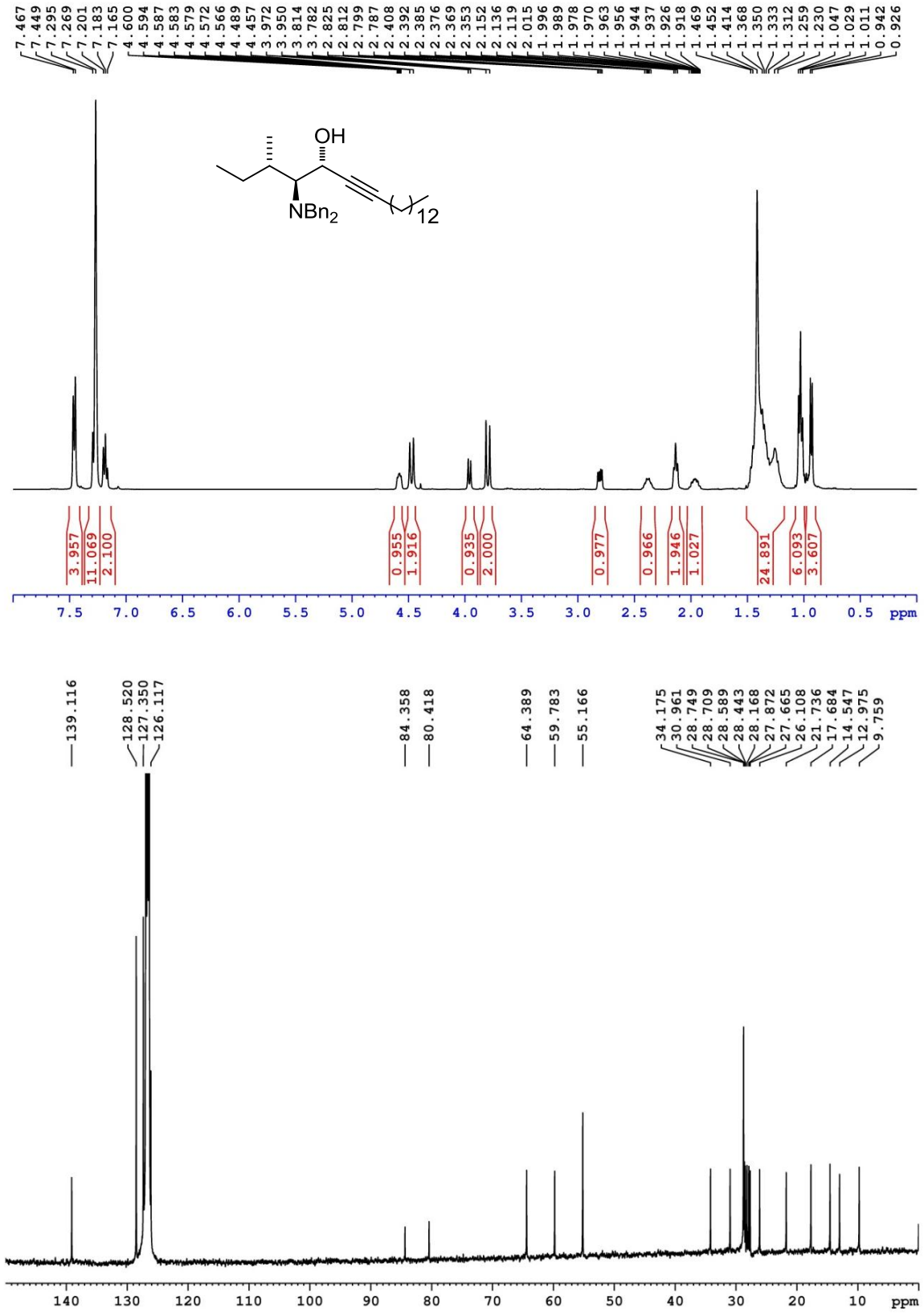

Figure S16. ^{1}H (400 MHz) and ^{13}C (100 MHz) NMR spectra of 7b in C_6D_6.

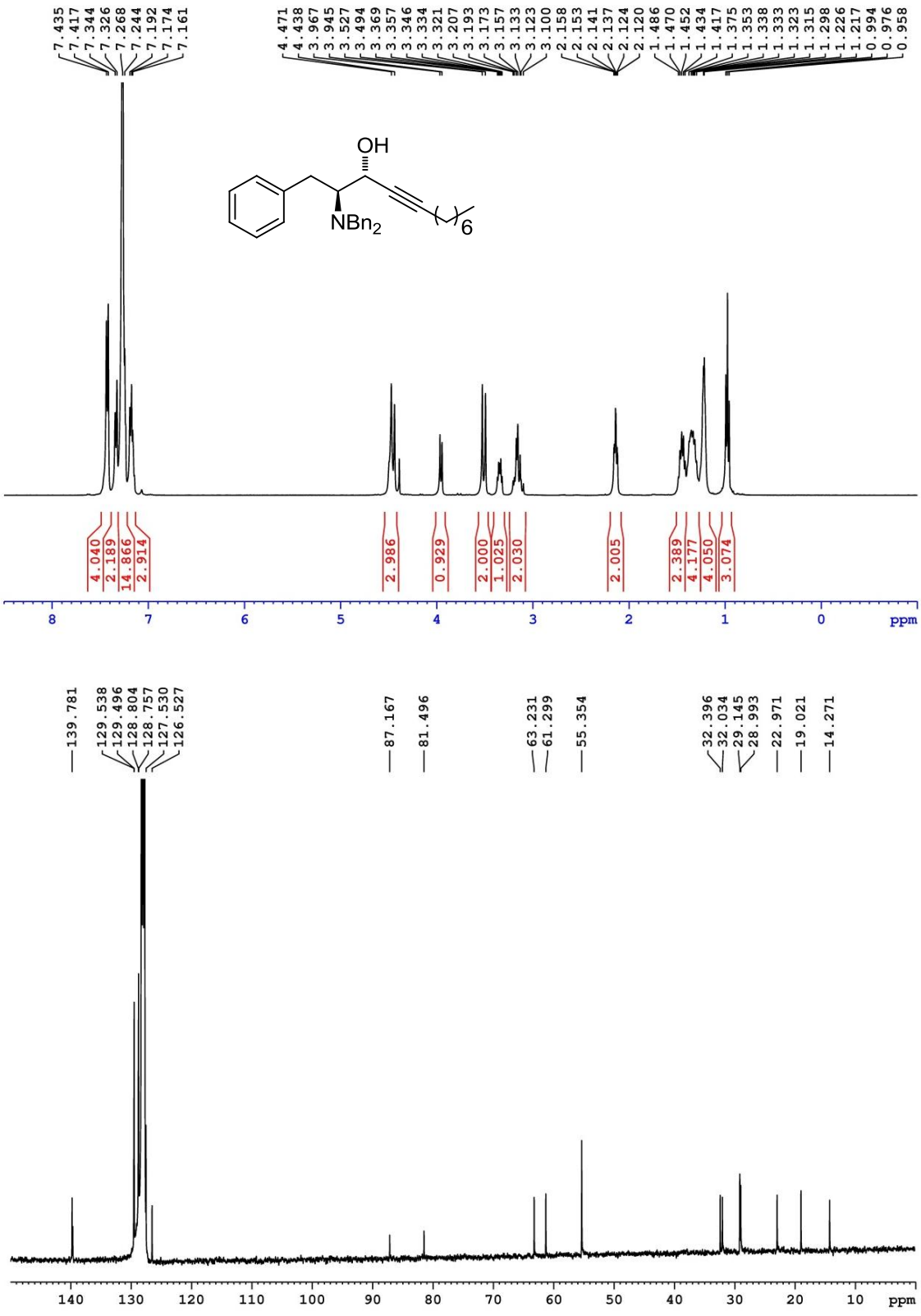

Figure S17. ^{1}H (400 MHz) and ^{13}C (100 MHz) NMR spectra of 8a in C_6D_6.

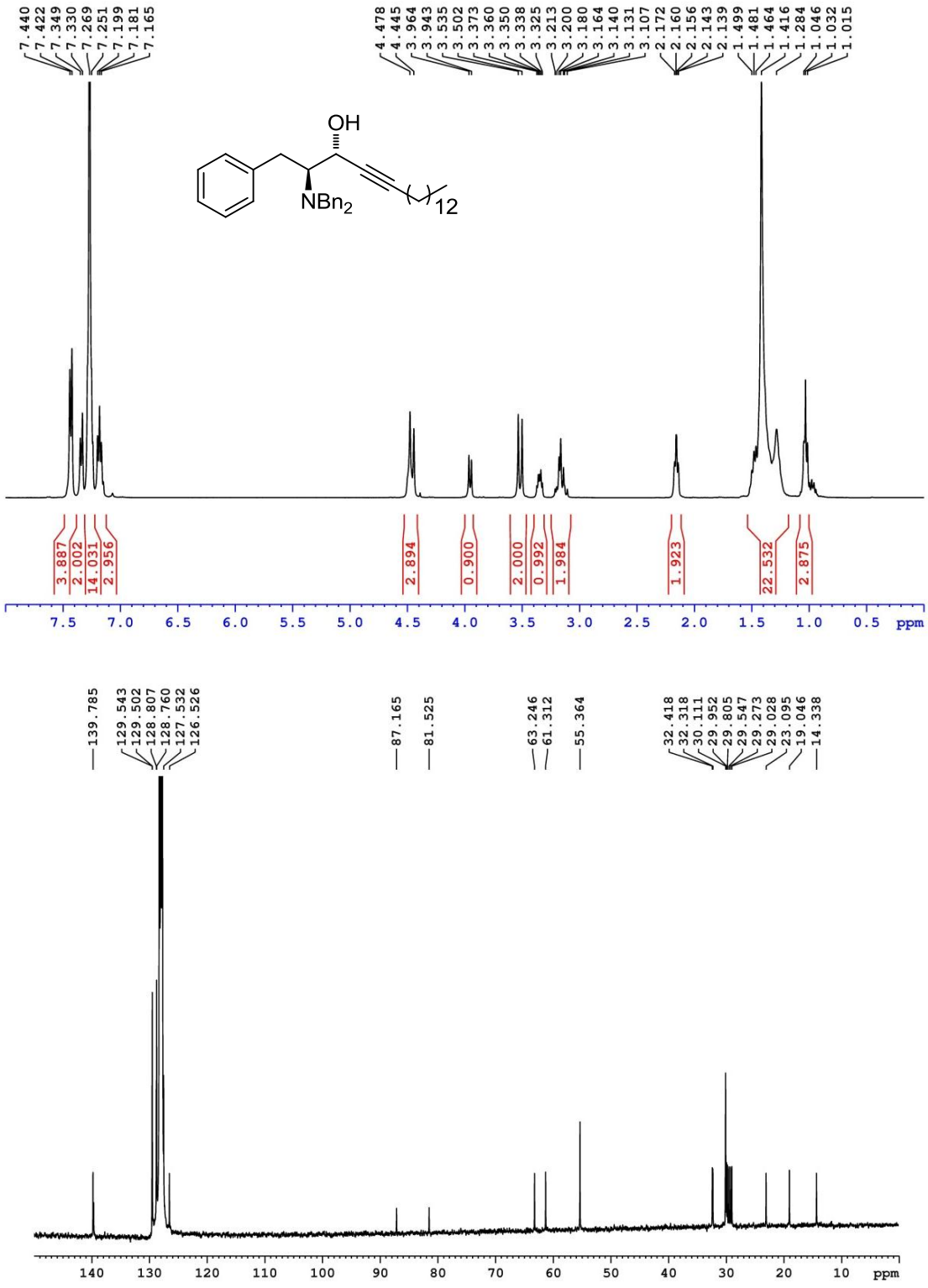

Figure S18. **^{1}H (400 MHz) and ^{13}C (100 MHz) NMR spectra of 8b in C_6D_6.**

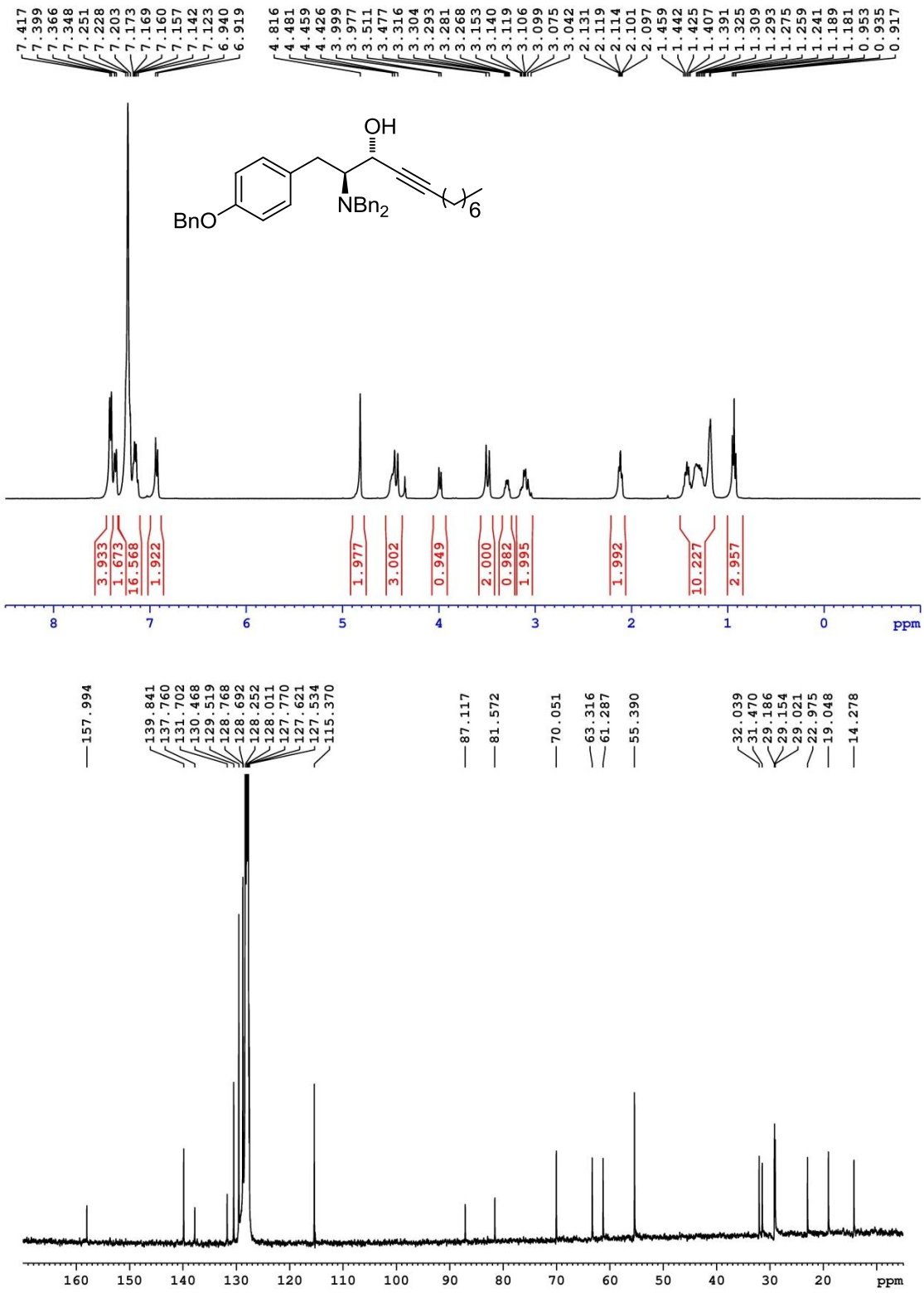

Figure S19. ^{1}H **(400 MHz) and** ^{13}C **(100 MHz) NMR spectra of 9a in** C_6D_6**.**

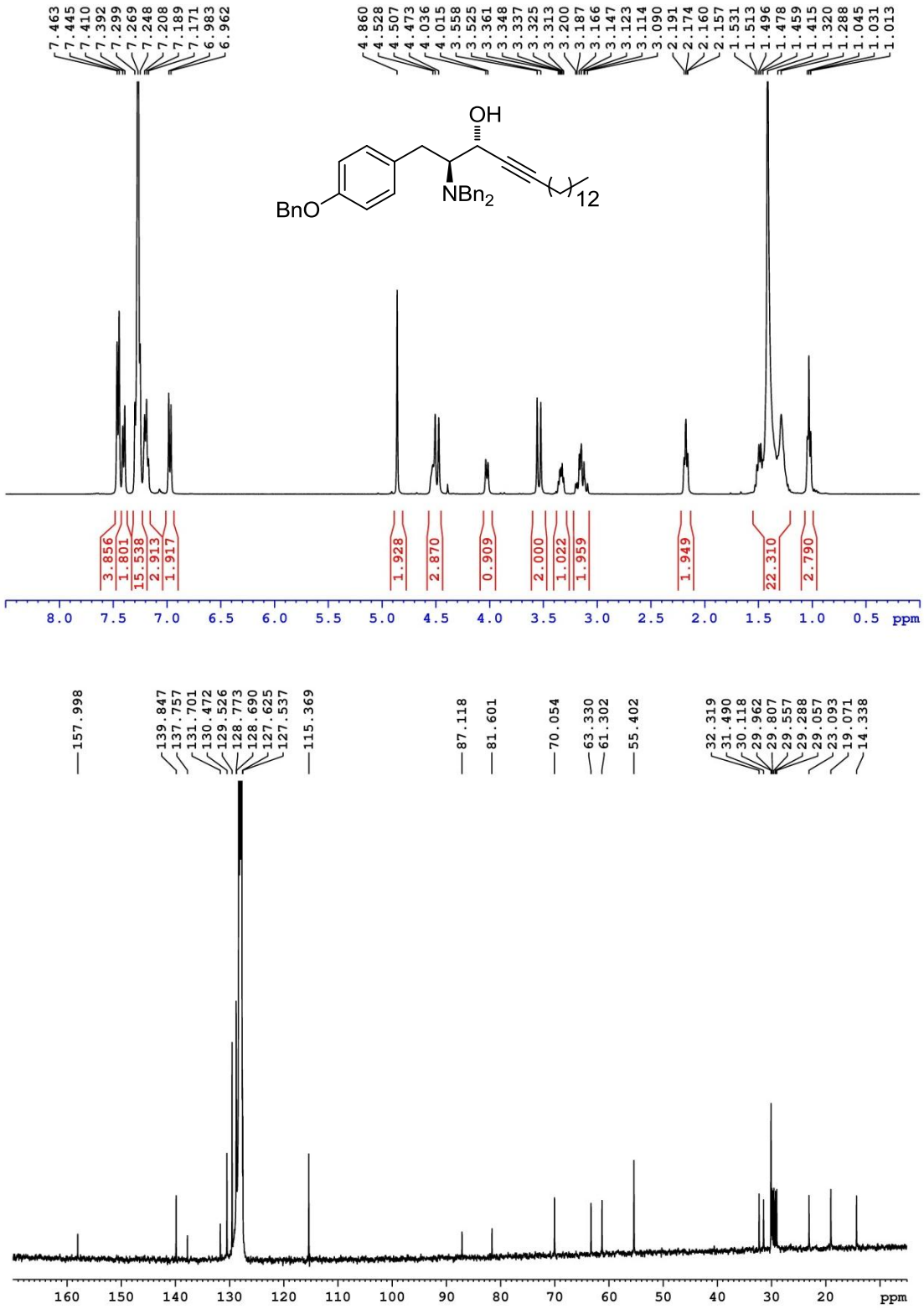

Figure S20. ^{1}H **(400 MHz) and** ^{13}C **(100 MHz) NMR spectra of 9b in** C_6D_6.

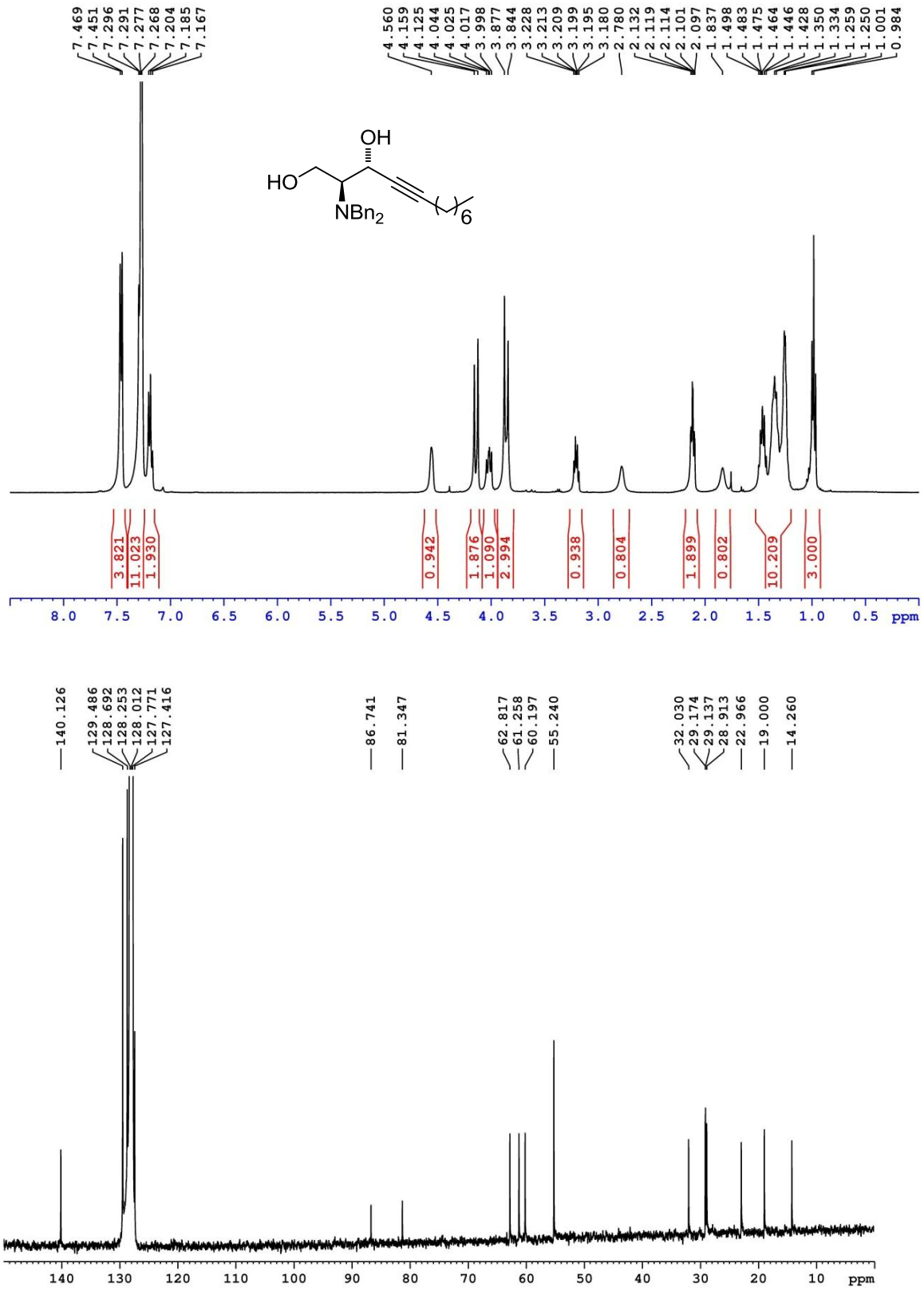

Figure S21. ^{1}H (400 MHz) and ^{13}C (100 MHz) NMR spectra of 10a in C_6D_6.

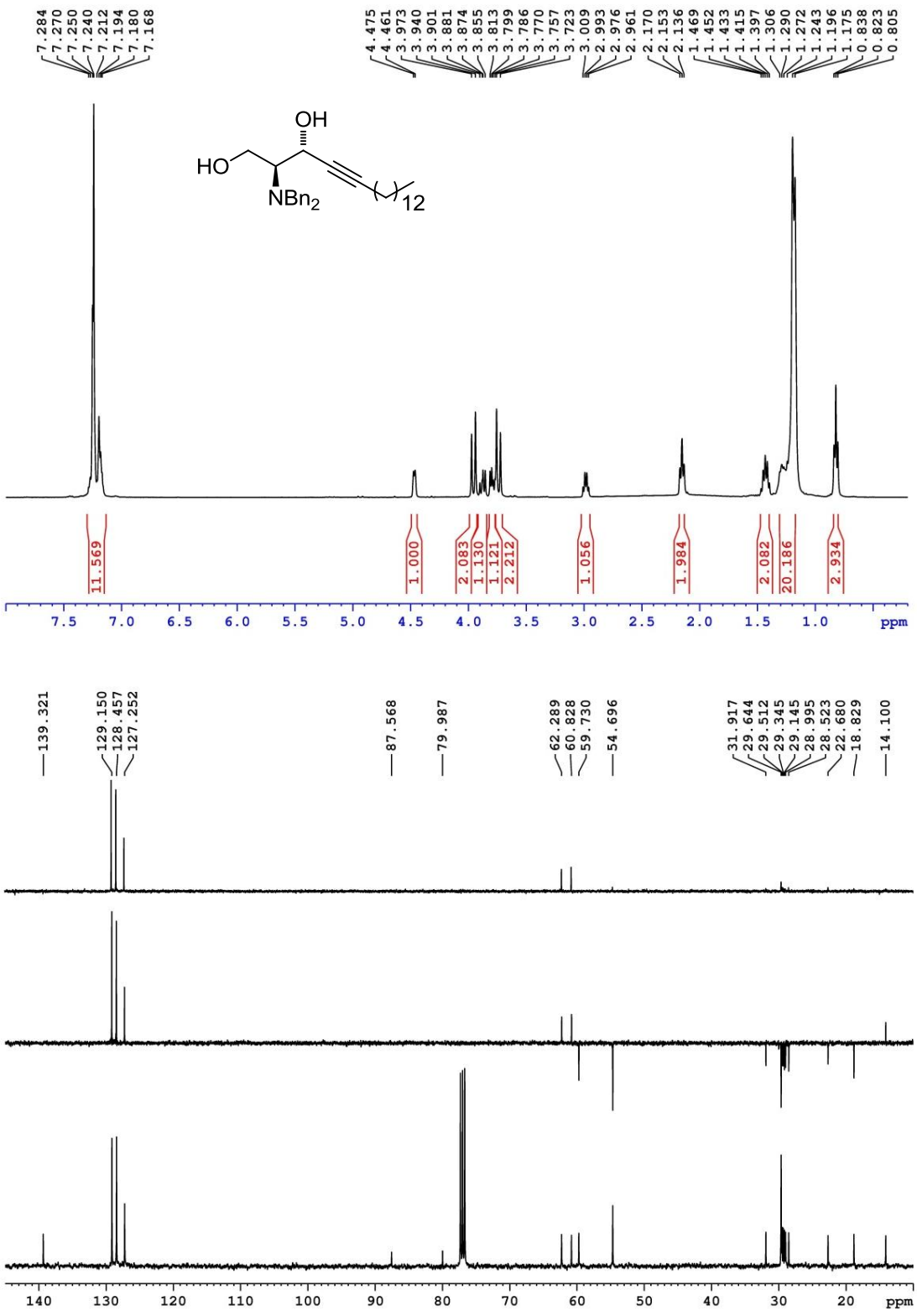

Figure S22. **^{1}H (400 MHz) and ^{13}C (100 MHz) NMR spectra of 10b in $CDCl_3$.**

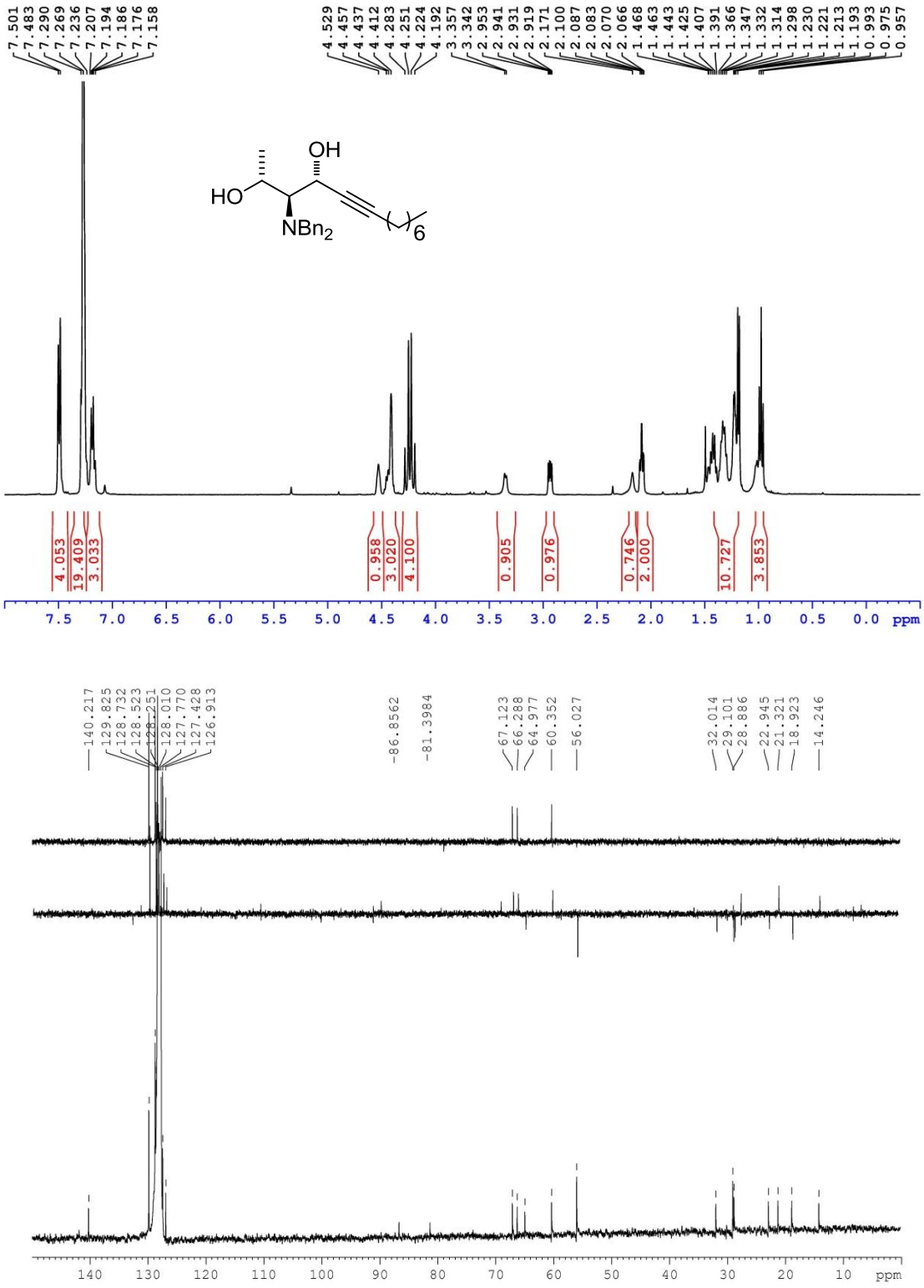

Figure S23. **^{1}H (400 MHz) and ^{13}C (100 MHz) NMR spectra of 11a in C_6D_6.**

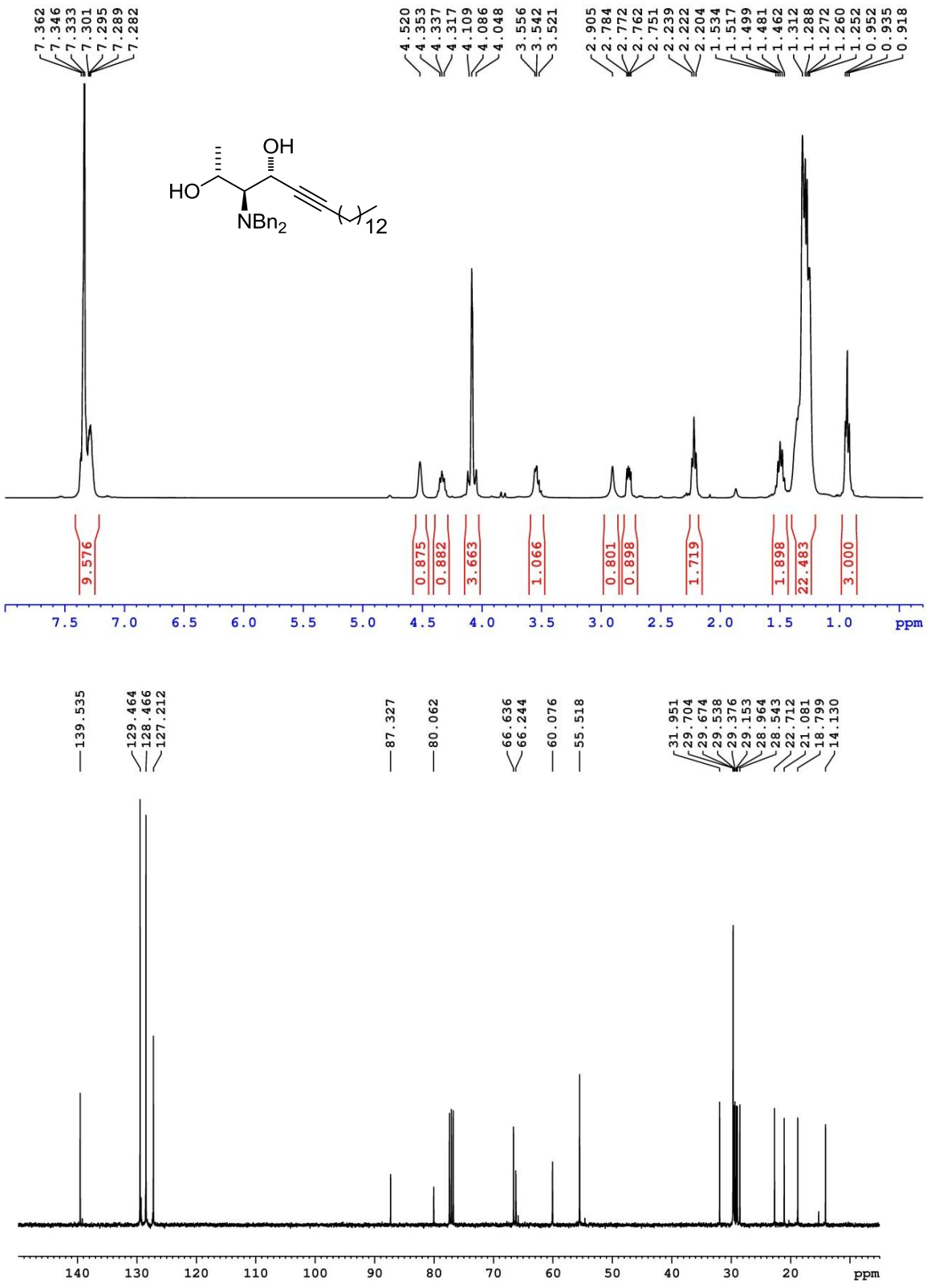

Figure S24. ^{1}**H (400 MHz) and** ^{13}**C (100 MHz) NMR spectra of 11b in** $CDCl_3$**.**

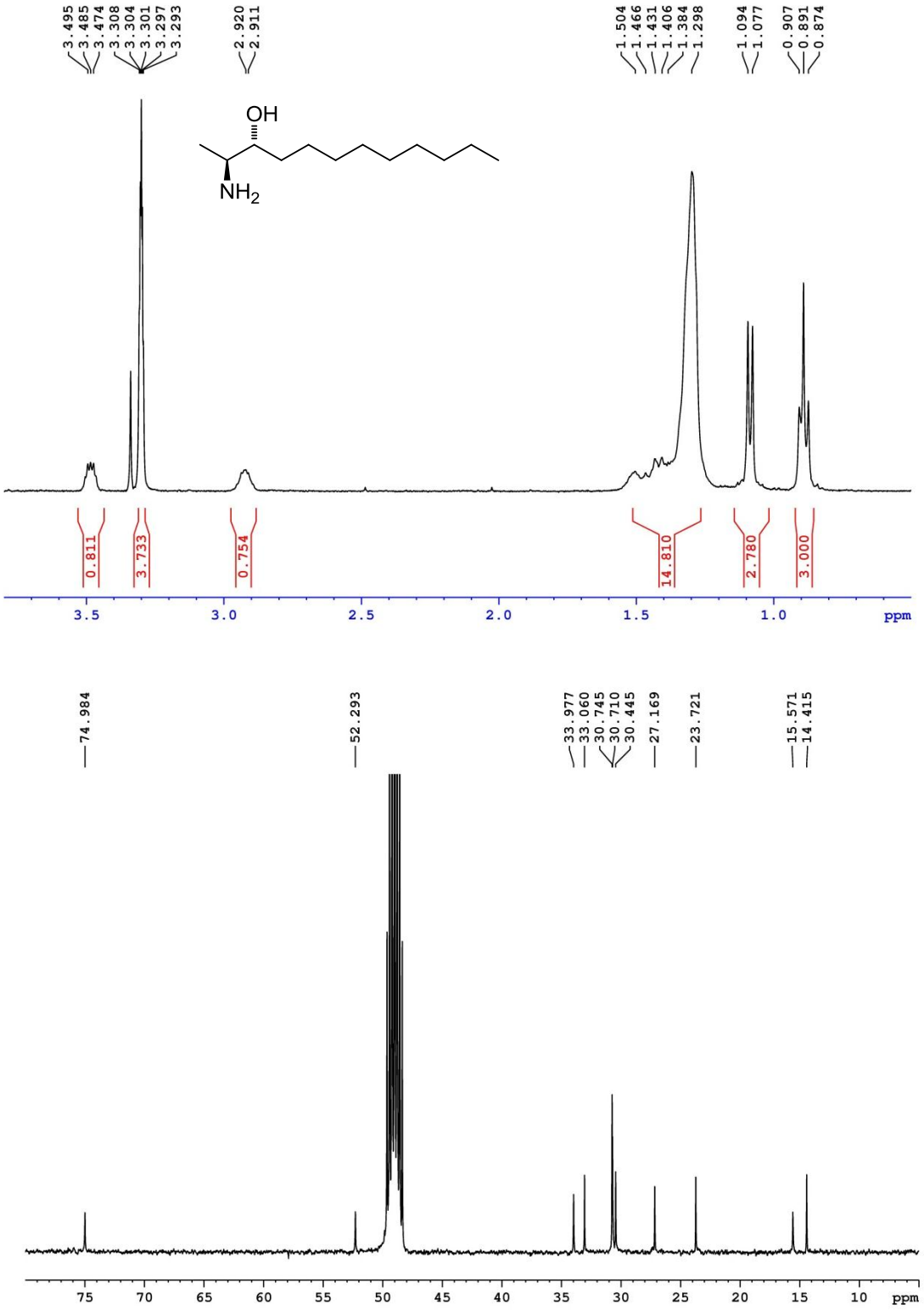

Figure S25. **^{1}H (400 MHz) and ^{13}C (100 MHz) NMR spectra of 4c in CD_3OD.**

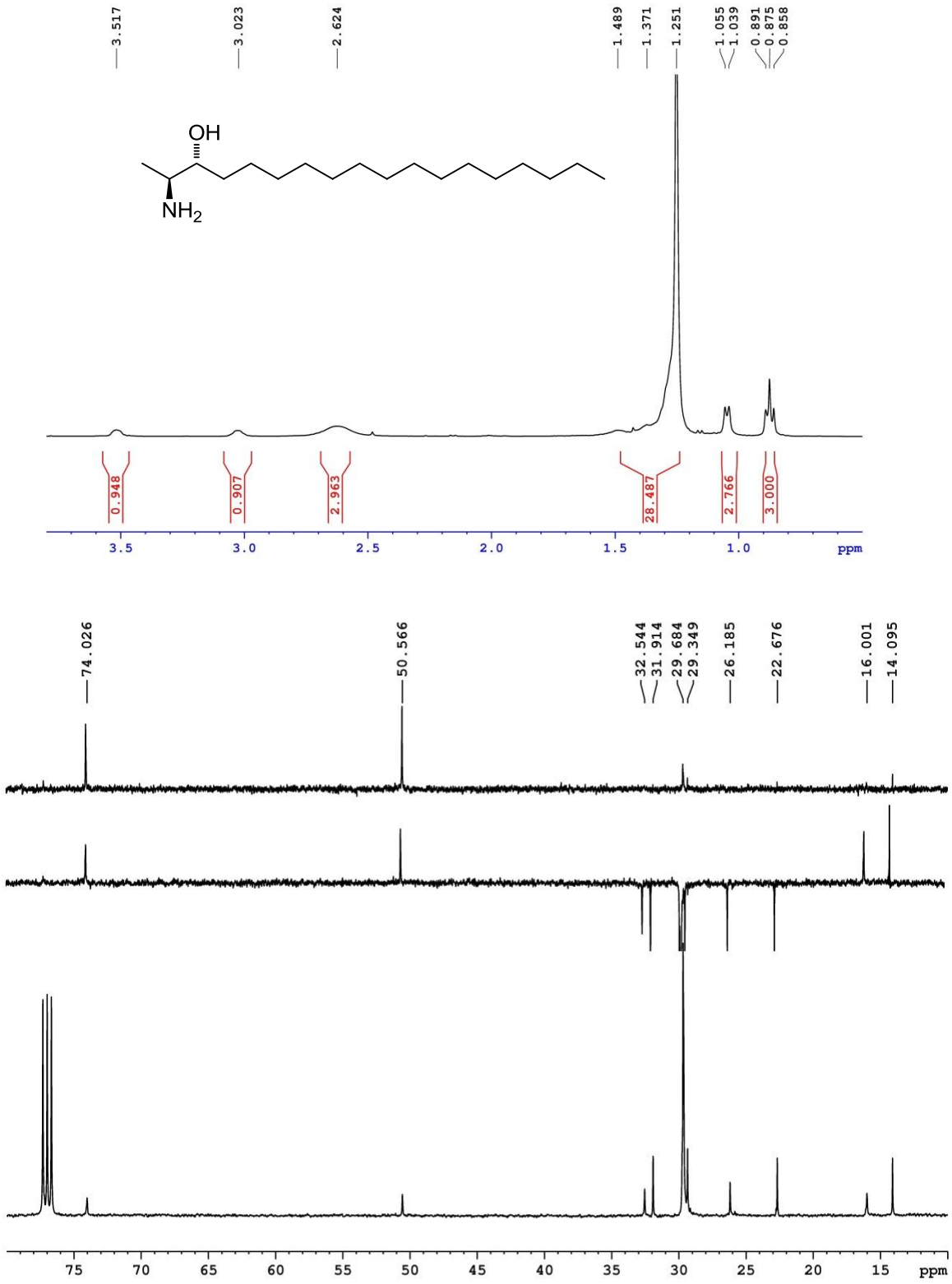

Figure S26. ^{1}**H (400 MHz) and** ^{13}**C (100 MHz) NMR spectra of 1 in** $CDCl_3$.

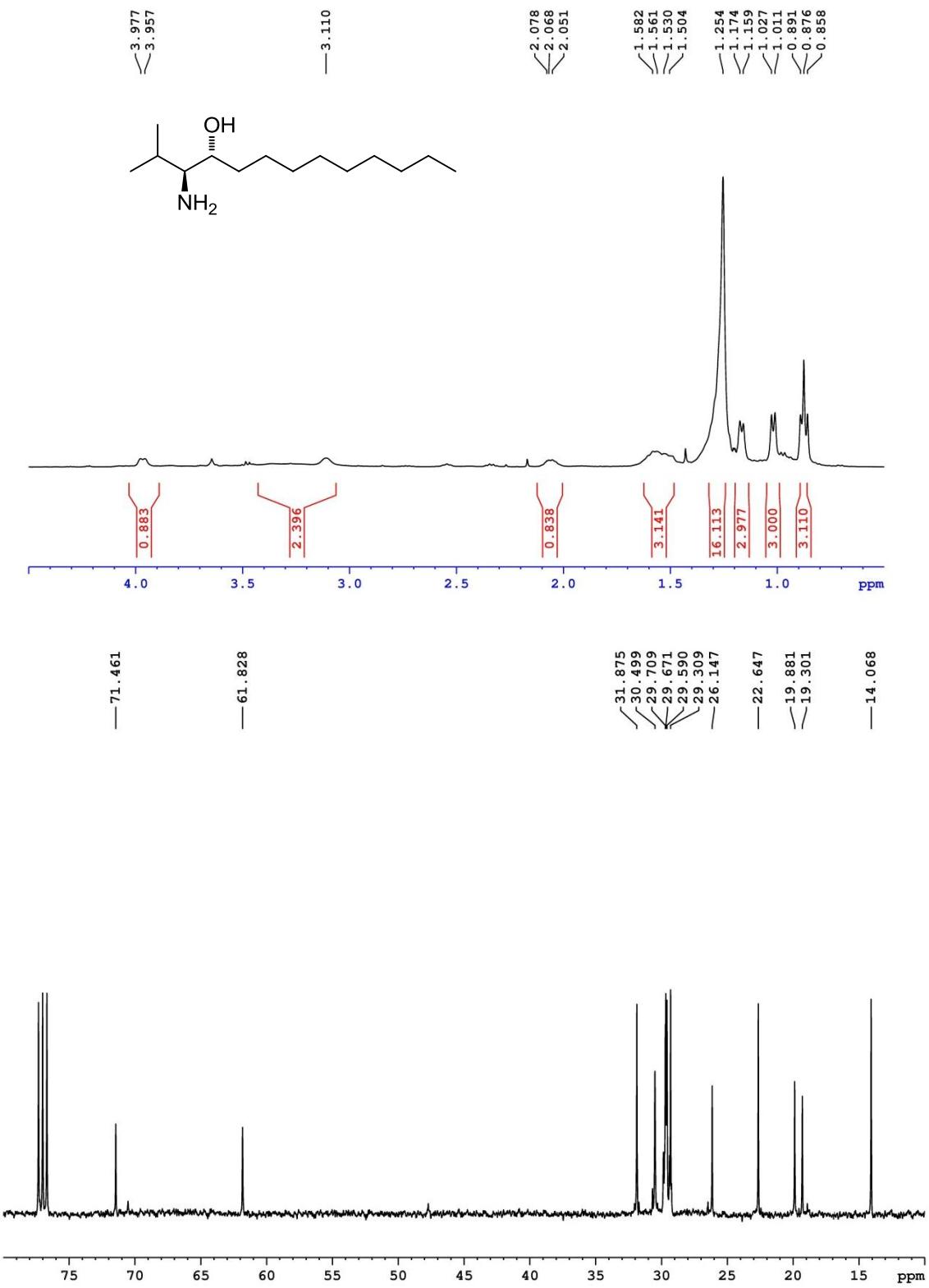

Figure S27. ^{1}H (400 MHz) and ^{13}C (100 MHz) NMR spectra of 5c in $CDCl_3$.

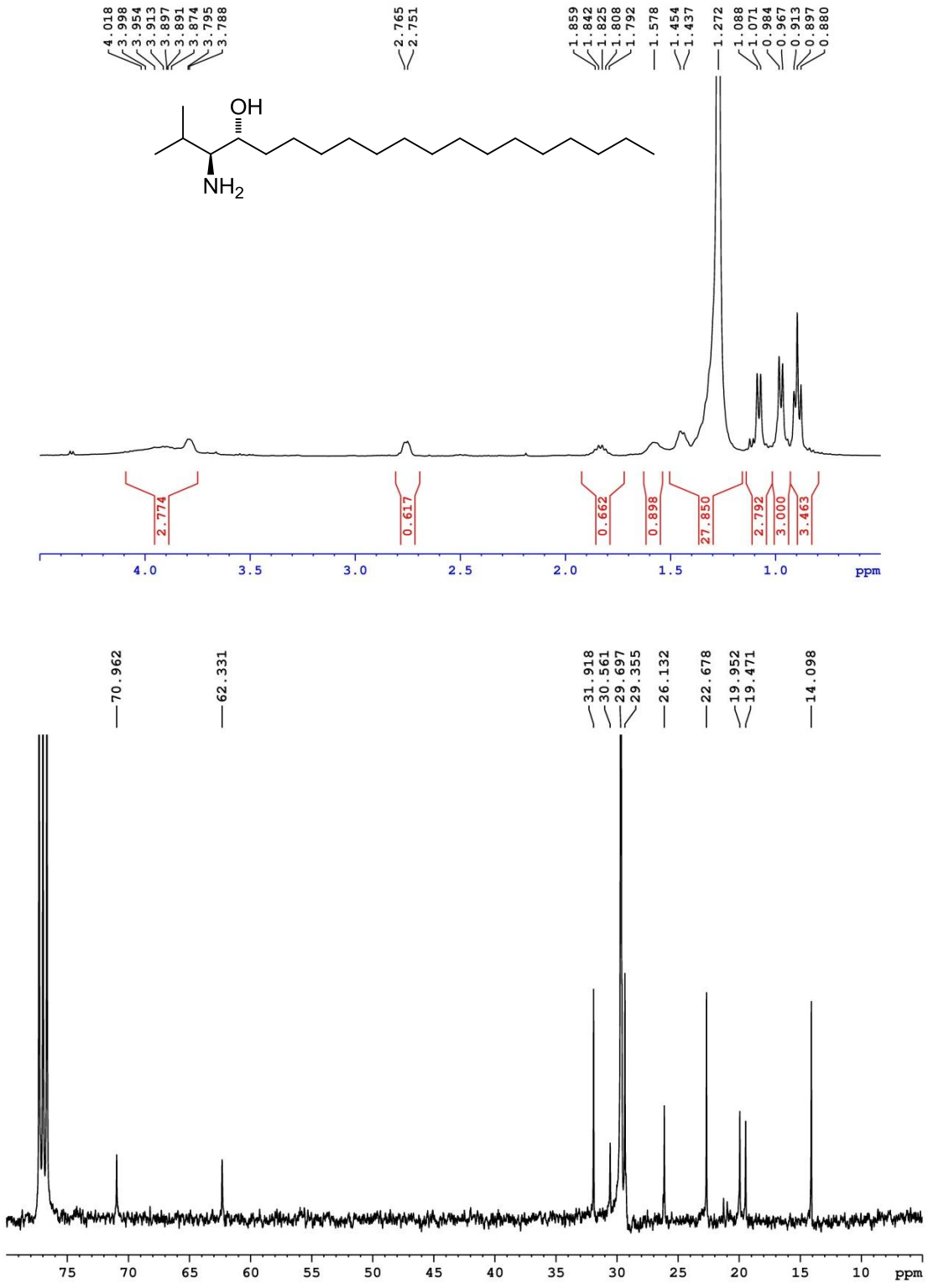

Figure S28. ^{1}**H (400 MHz) and** ^{13}**C (100 MHz) NMR spectra of 5d in** $CDCl_3$**.**

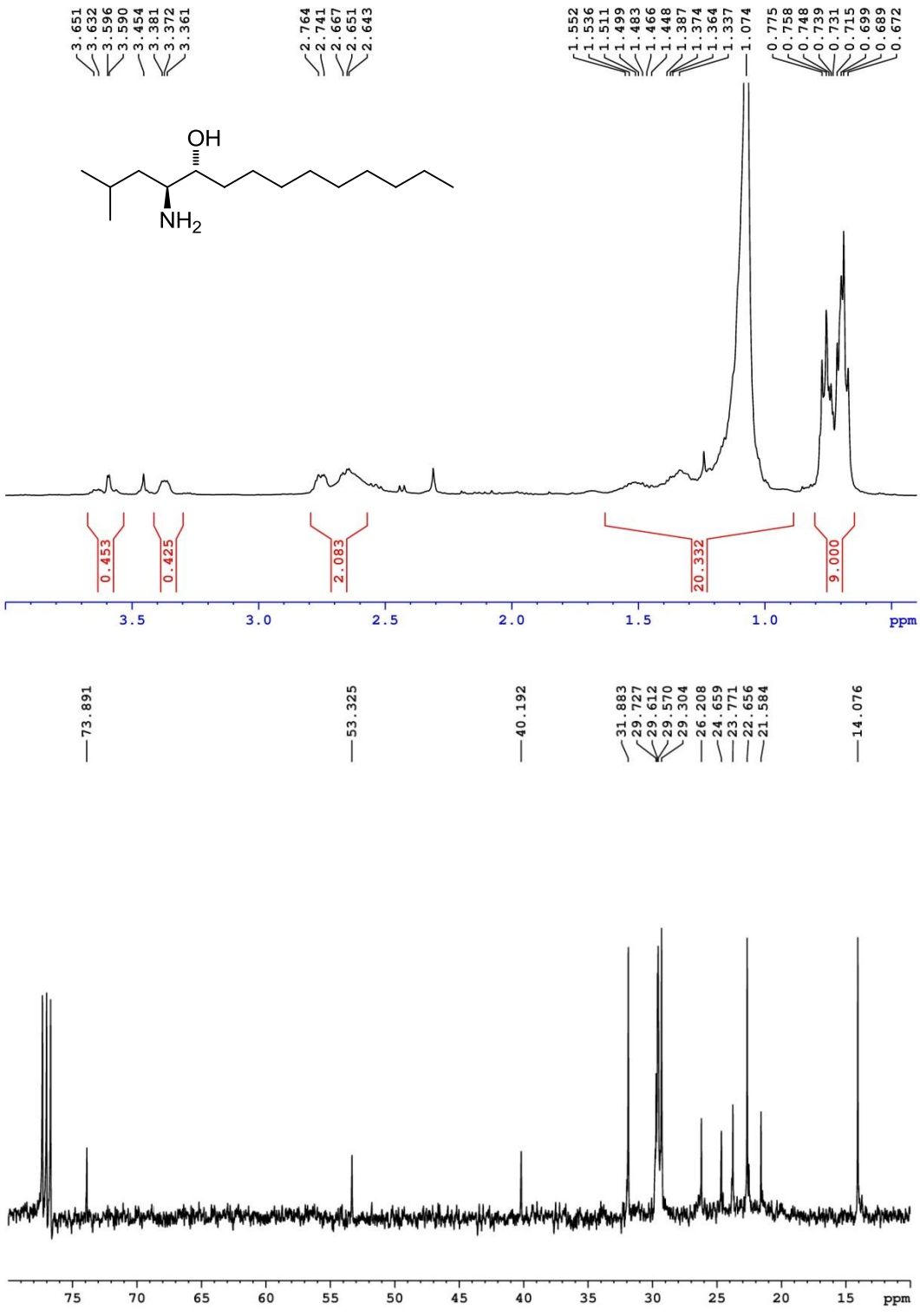

Figure S29. ^{1}H (400 MHz) and ^{13}C (100 MHz) NMR spectra of 6c in $CDCl_3$.

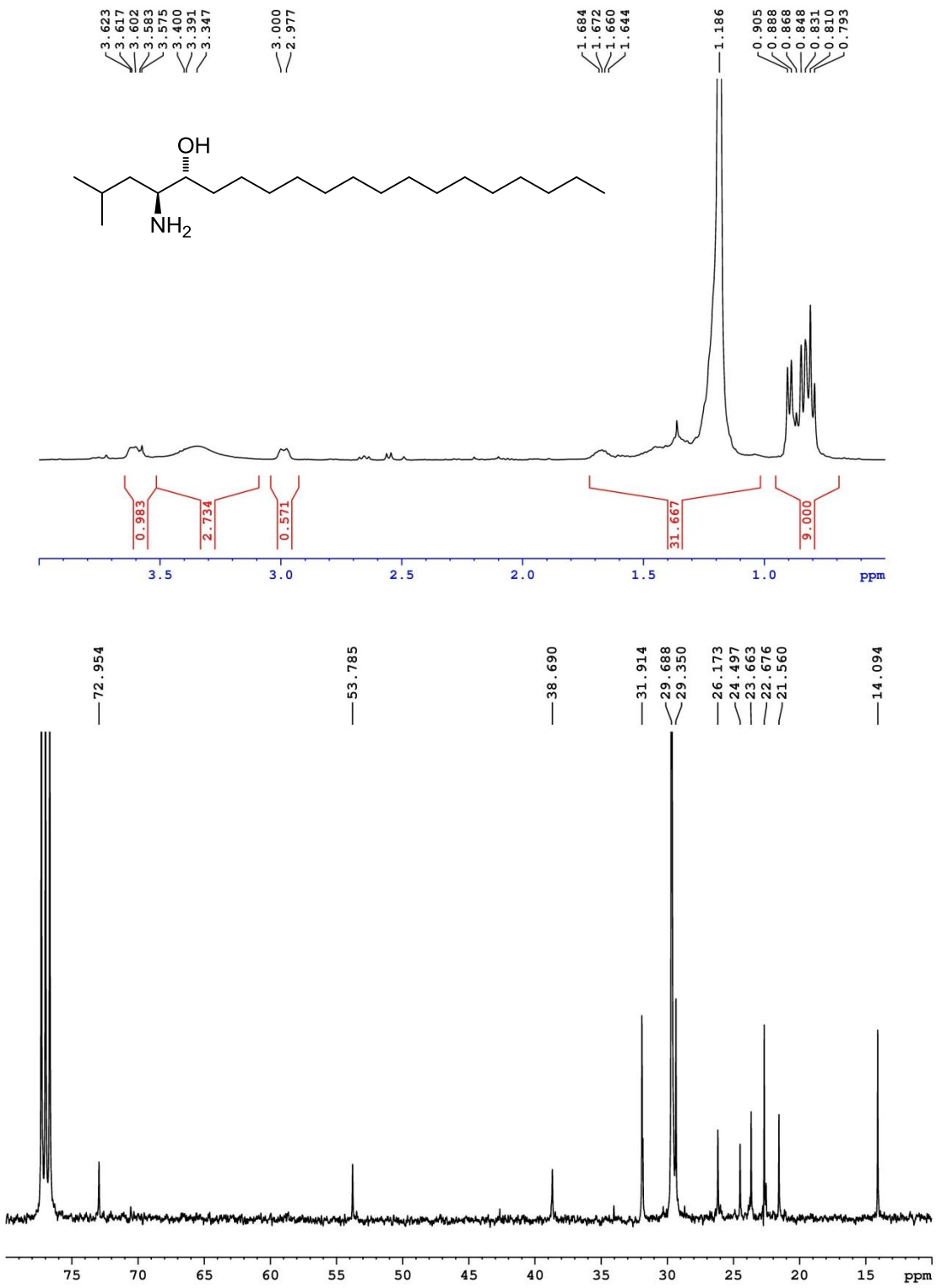

Figure S30. ^{1}**H (400 MHz) and** ^{13}**C (100 MHz) NMR spectra of 6d in** $CDCl_3$**.**

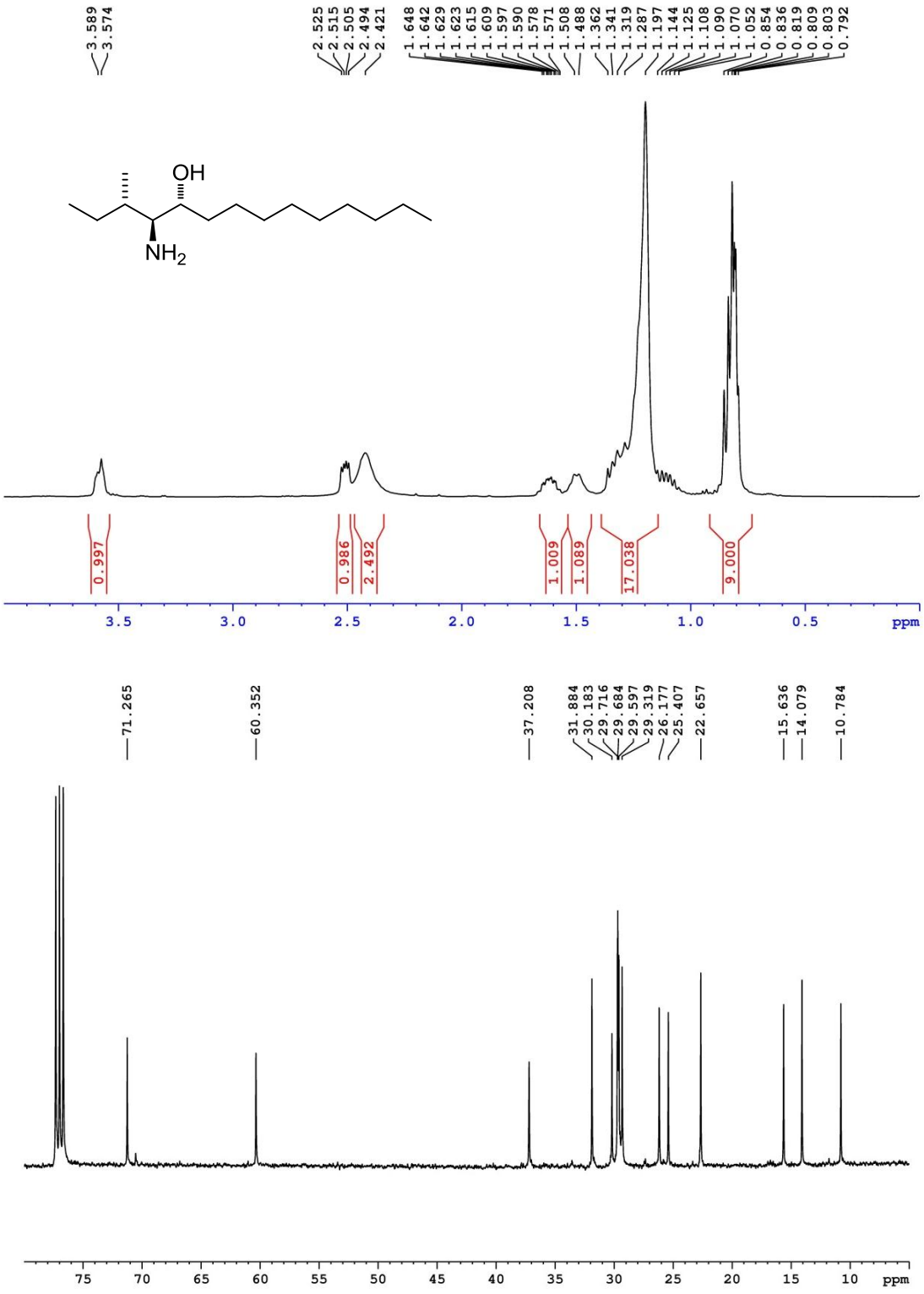

Figure S31. ^{1}H (400 MHz) and ^{13}C (100 MHz) NMR spectra of 7c in $CDCl_3$.

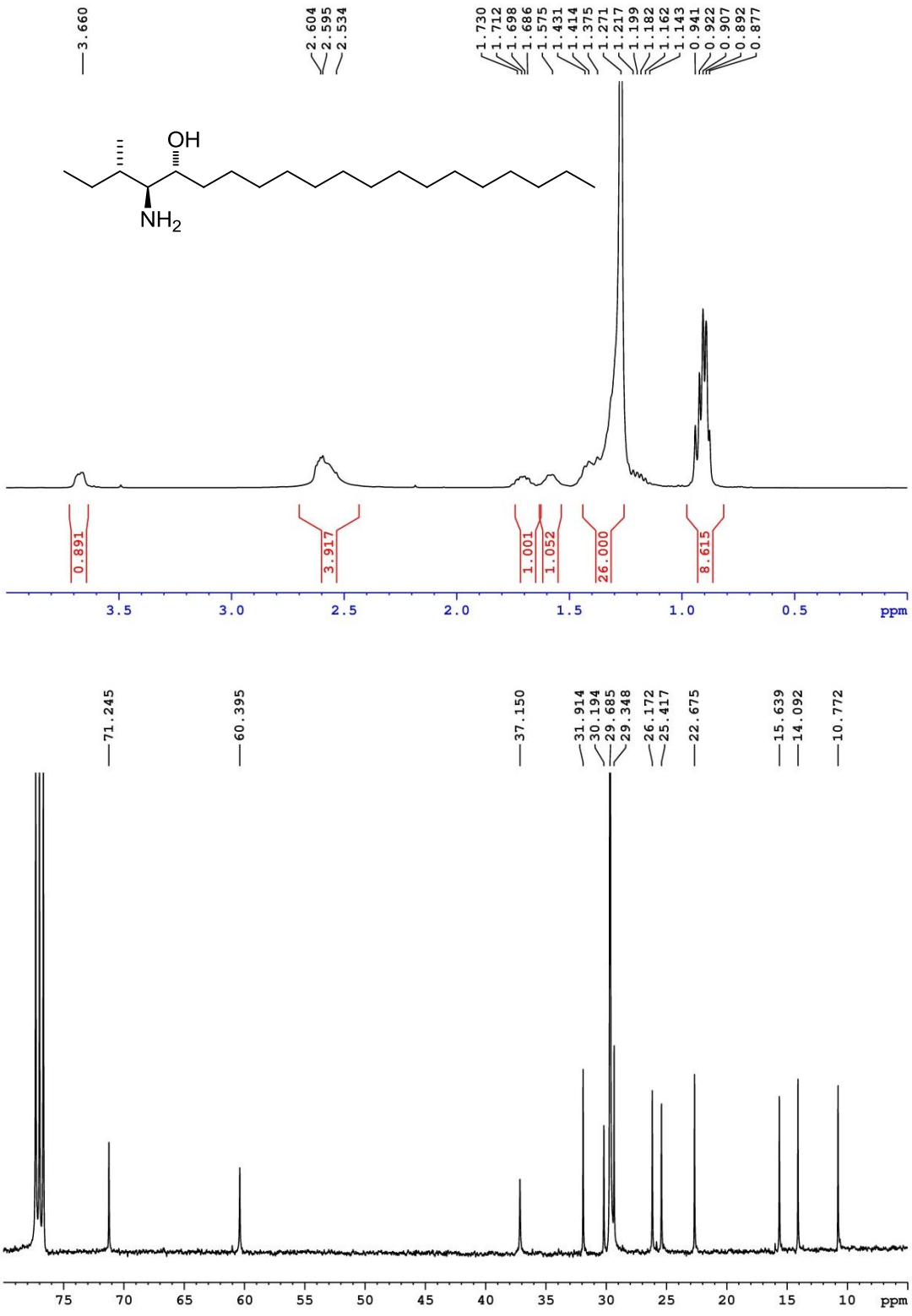

Figure S32. **^{1}H (400 MHz) and ^{13}C (100 MHz) NMR spectra of 7d in $CDCl_3$.**

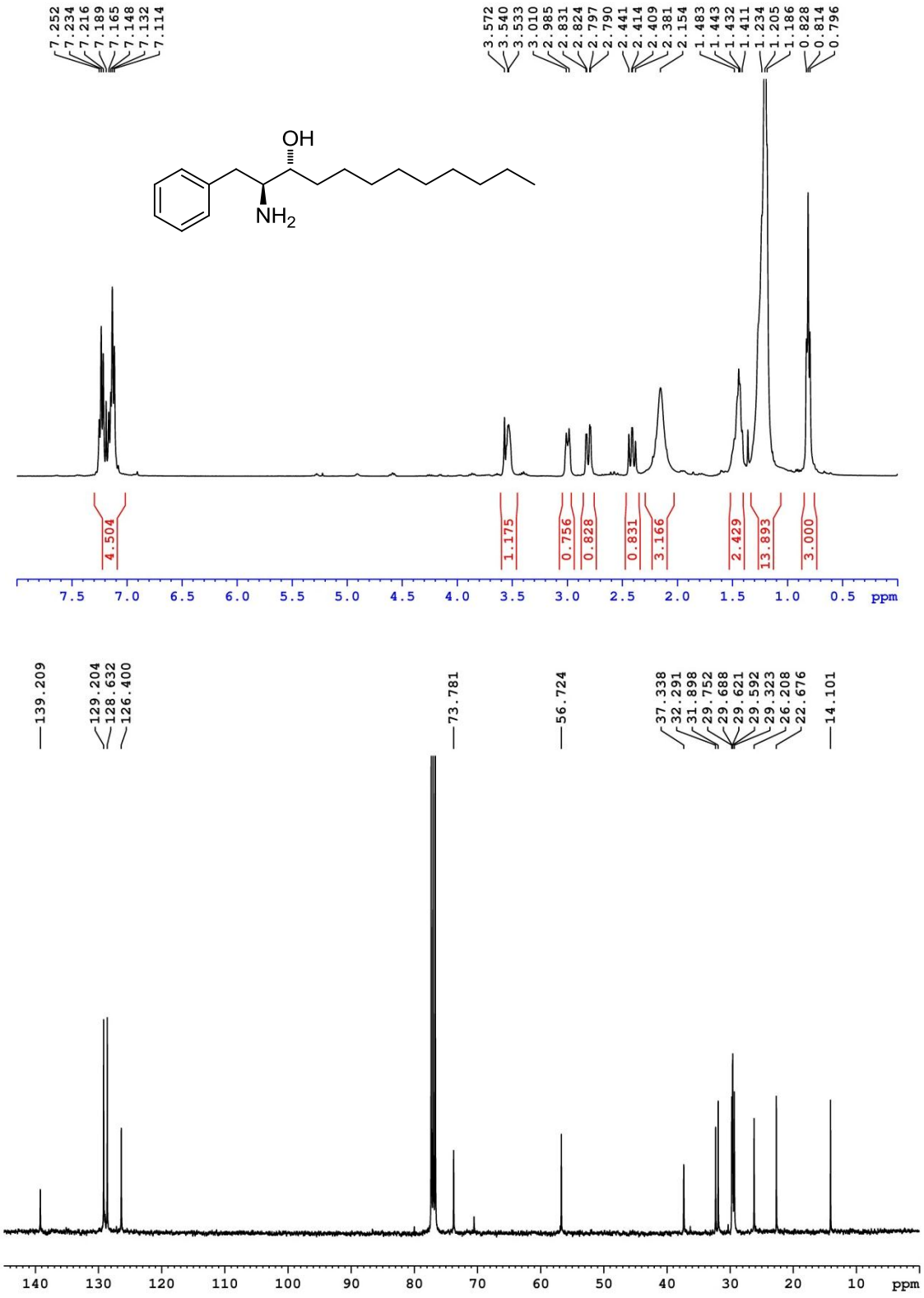

Figure S33. ^{1}H (400 MHz) and ^{13}C (100 MHz) NMR spectra of 8c in $CDCl_3$.

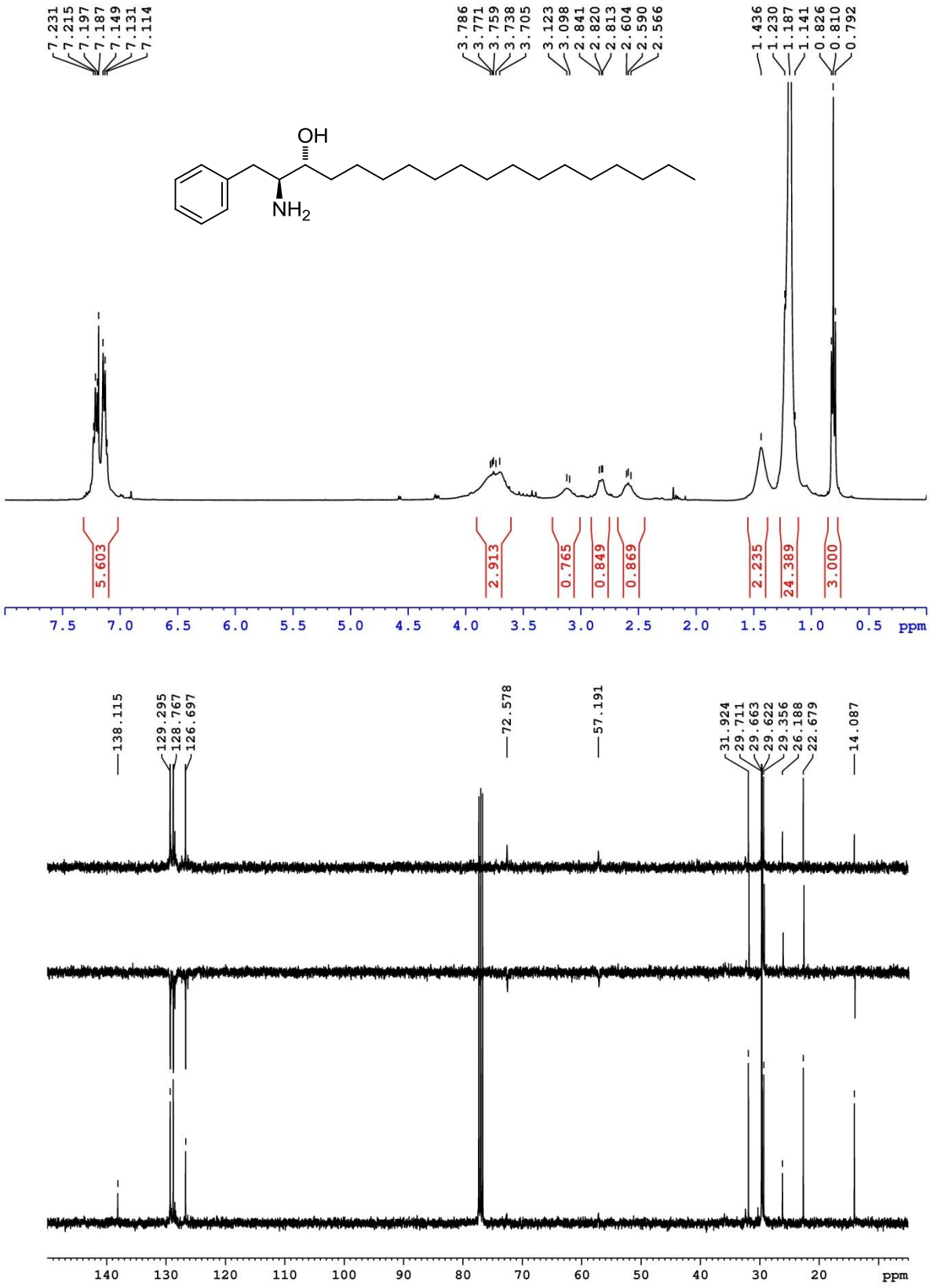

Figure S34. **^{1}H (400 MHz) and ^{13}C (100 MHz) NMR spectra of 8d in $CDCl_3$.**

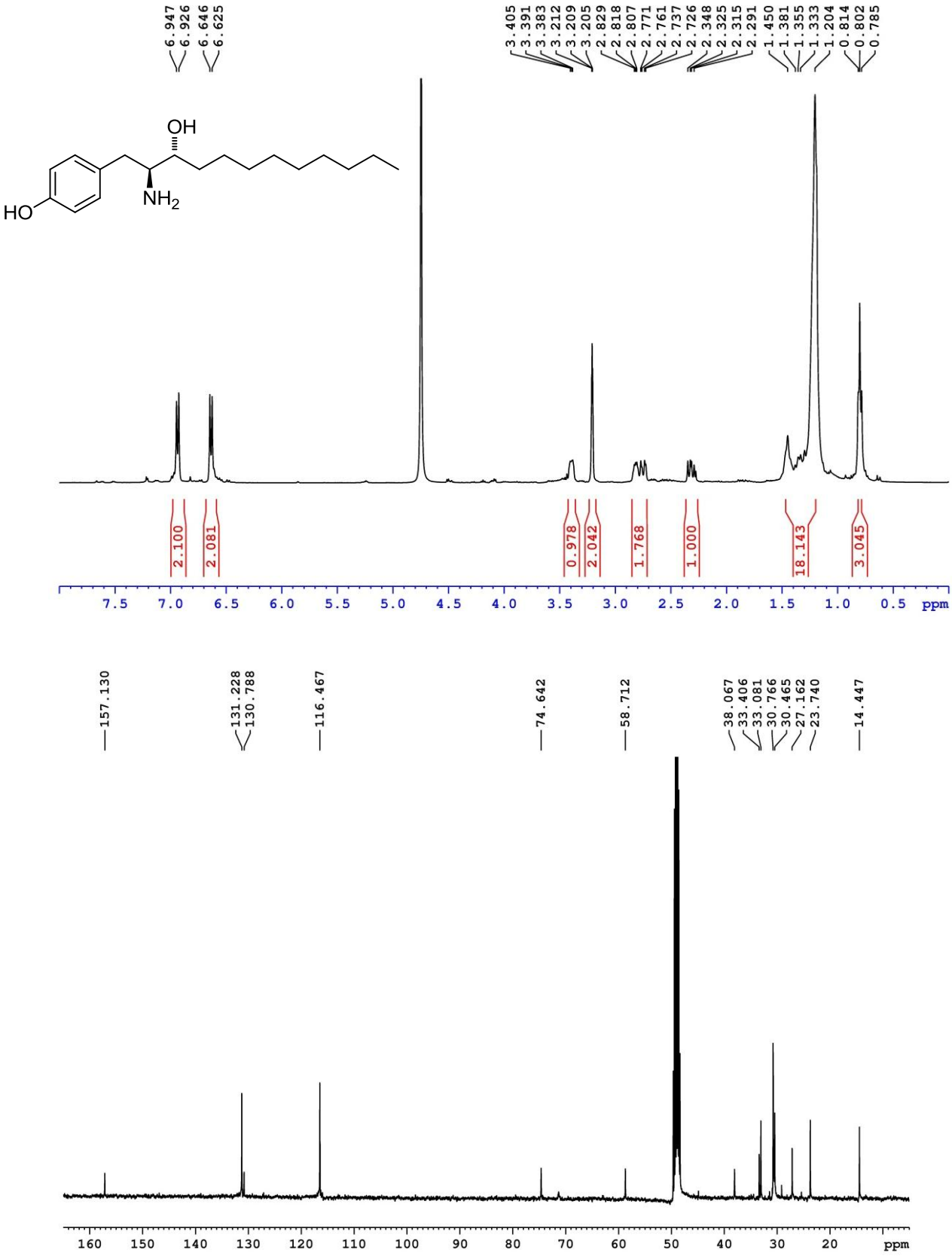

Figure S35. ^{1}**H (400 MHz) and** ^{13}**C (100 MHz) NMR spectra of 9c in** CD_3OD.

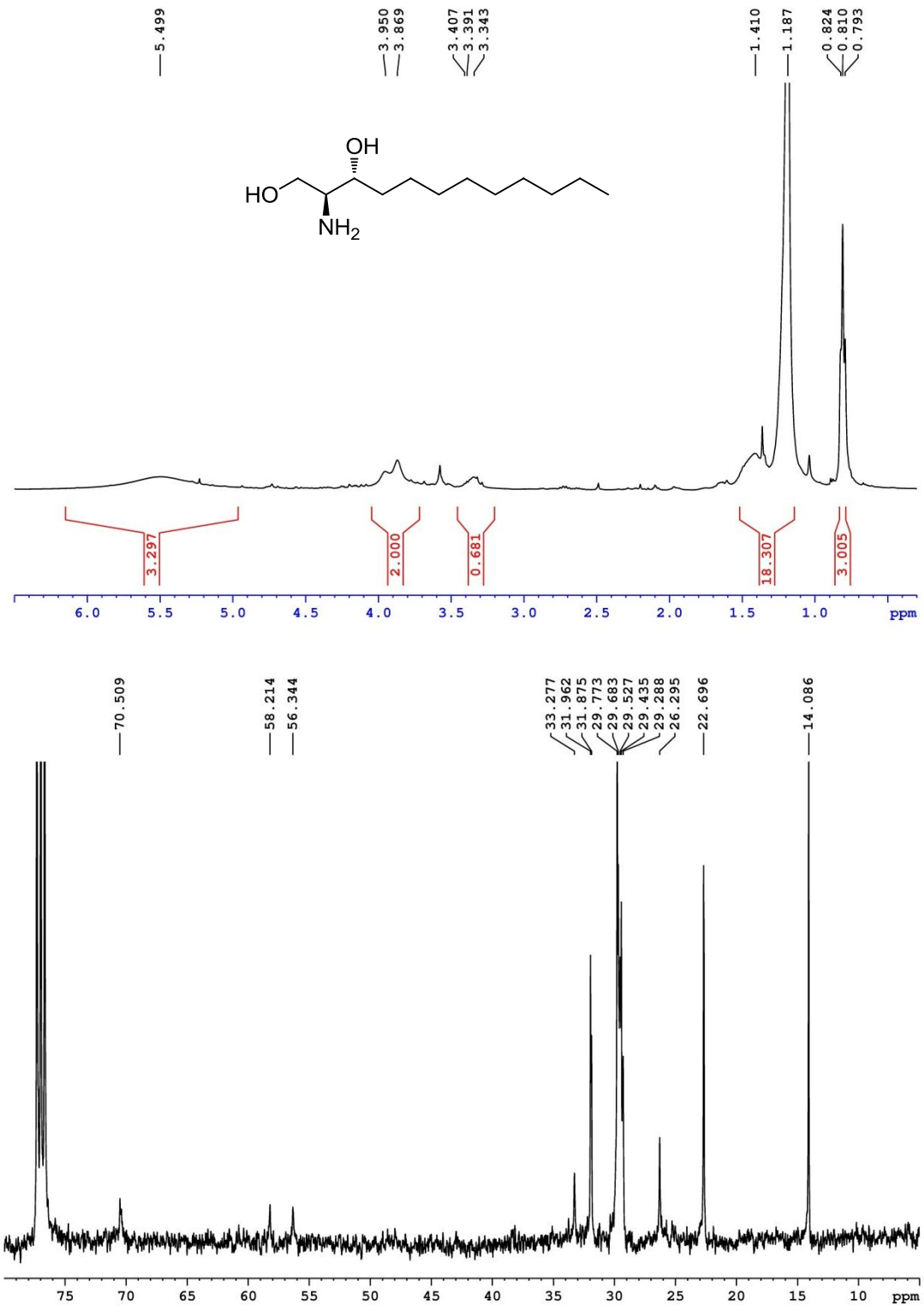

Figure S36. ^{1}H (400 MHz) and ^{13}C (100 MHz) NMR spectra of **10c** in $CDCl_3$.

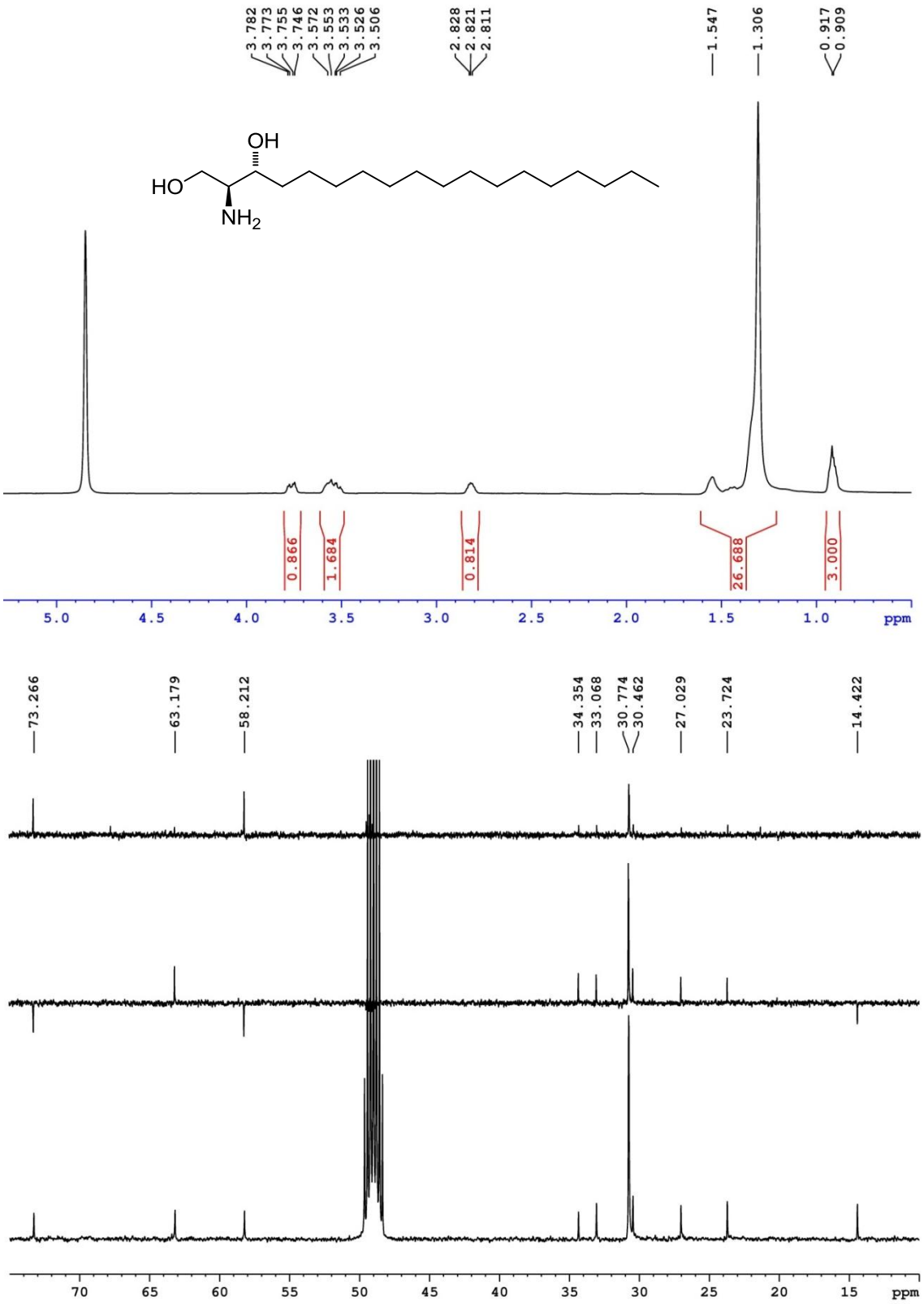

Figure S37. ^{1}**H (400 MHz) and** ^{13}**C (100 MHz) NMR spectra of 10d in** CD_3OD**.**

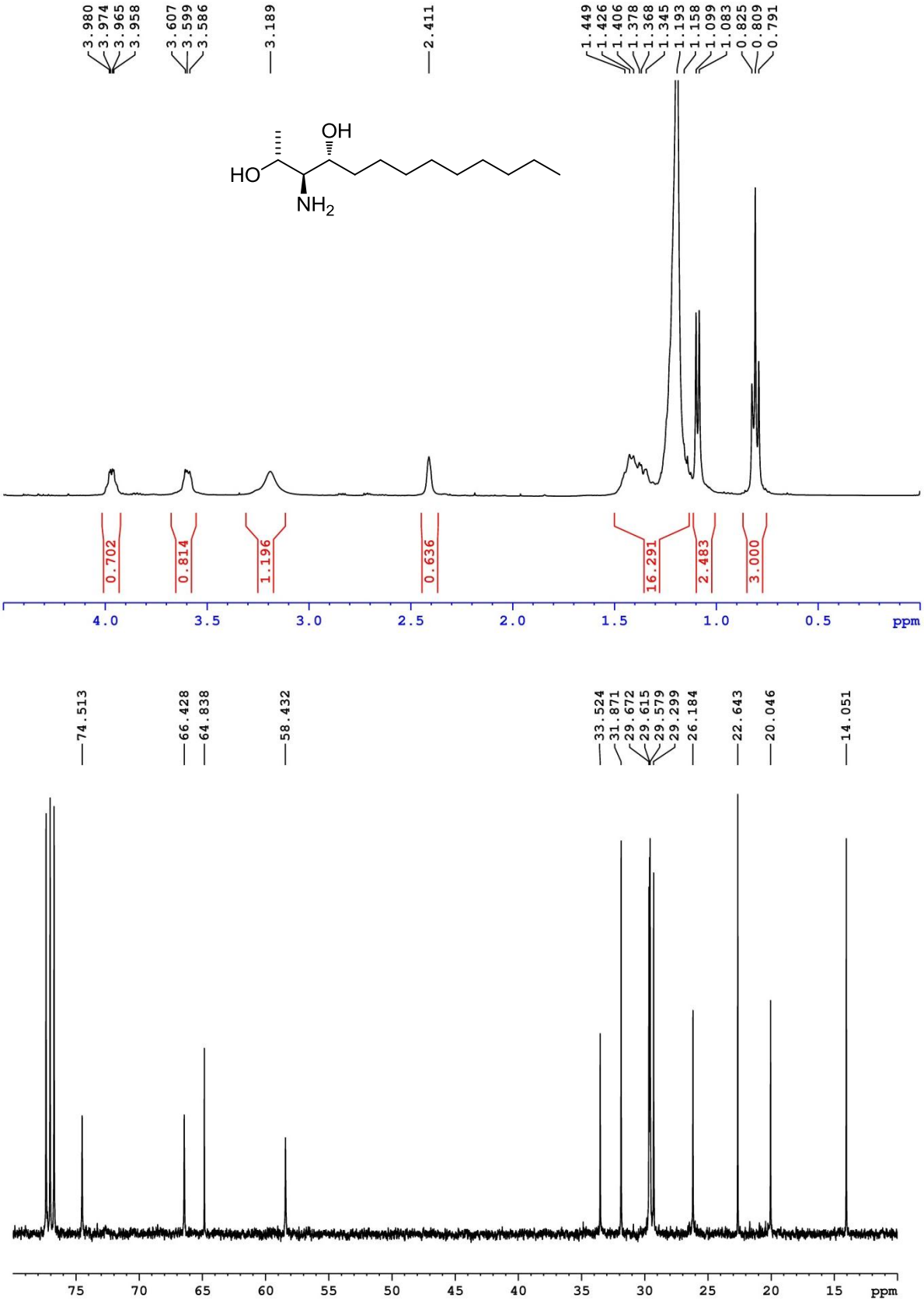

Figure S38. ^{1}**H (400 MHz) and** ^{13}**C (100 MHz) NMR spectra of 11c in** $CDCl_3$**.**

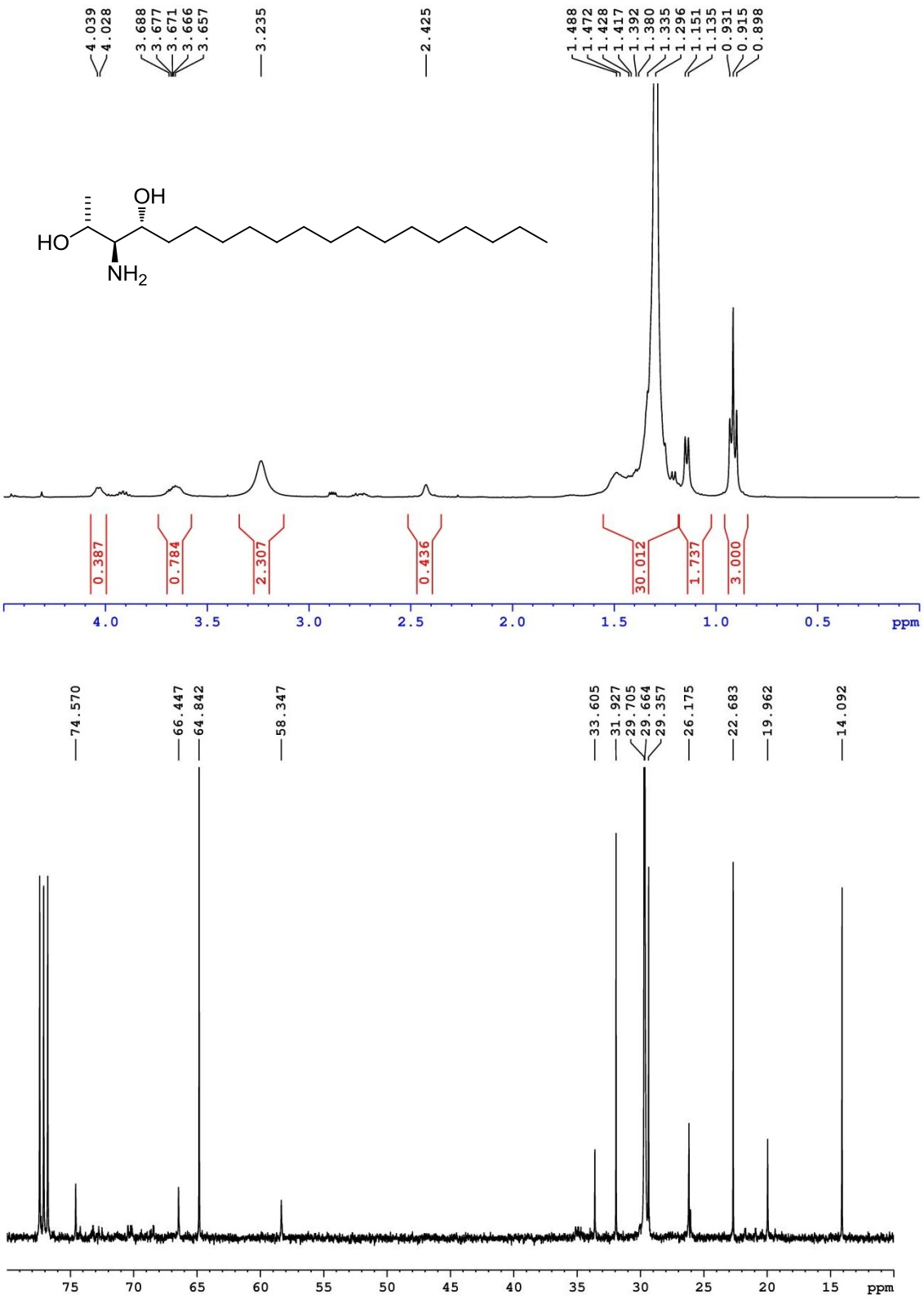

Figure S39. **^{1}H (400 MHz) and ^{13}C (100 MHz) NMR spectra of 11d in $CDCl_3$.**

CHAPTER 5

DIRECT SYNTHESIS OF POLY-BENZYLATED GLUTAMIC ACID MONOESTERS. DISAMBIGUATION OF *N*,*N*-DI-BENZYLGLUTAMIC ACID α- AND γ-BENZYL ESTERS

5. Direct synthesis of polybenzylated glutamic acid monoesters. Disambiguation of *N*,*N*-dibenzyl-glutamic acid α- and γ-benzyl esters

5.1 Introduction

Amino acids represent a natural source of enantiomerically pure building blocks useful in organic synthesis. In this particular context, L-aspartic and L-glutamic acids are potentially valuable provided that the two carboxyl groups could be differentiated. Within our program directed at the discovery of biologically active sphingosine analogues,[1] we have developed general methodologies for the synthesis of saturated[2] and unsaturated[3] lipidic α-amino acids. The latter method is based on the regioselective ω-reduction of *N*,*N*-di-Boc-aspartic or glutamic dialkyl esters. The resulting semialdehydes have proven to be versatile intermediates in the synthesis of biologically relevant substances.[4]

In addition to Boc, other suitable amino protecting groups have been explored extensively, from which the benzyl group remains as highly useful in synthetic organic chemistry.[5] In the particular case of L-glutamic acid (**1**), methods have been reported to prepare diverse *N*,*N*-dibenzylamino acid derivatives (Scheme 5.1). Thus, the perbenzylation of L-glutamic acid (**1**) with excess of BnBr under basic conditions is a commonly used process to obtain derivative **2** in 61-96% yield.[6] The regioselective reduction of perbenzylated L-glutamic acid **2** affords the corresponding γ-aldehyde of *N*,*N*-dibenzylglutamic acid α-benzyl ester (**3**).[3b] Although in less extent, the latter has been used as intermediate for the preparation of biologically significant compounds.[7] Additionally, perbenzylated L-glutamic acid (**2**) served also as the precursor of γ-alcohol **4**[6] and diol **5**[8] (Scheme 5.1). Similarly, the γ-benzyl ester of L-glutamic acid (**6**) is prepared typically under acidic conditions in 84% yield.[9]

Recently, the use of *N*,*N*-dibenzylglutamic acid γ-benzyl ester (**7**) in the synthesis of schulzeines was reported.[10] However, a complete experimental procedure for its preparation and full characterization with relevant spectroscopic data were never reported in the literature. After a thorough search, we found that the preparation of compound 7 in 18% yield was described in a PhD thesis.[11] The low yield of the reaction together with the synthetic versatility of intermediate **7** encouraged us to study the process in more detail.

In this chapter, we investigated the benzylation reaction of L-glutamic acid and the unexpected results obtained when we tried to repeat the procedure reported for the synthesis of **7**.

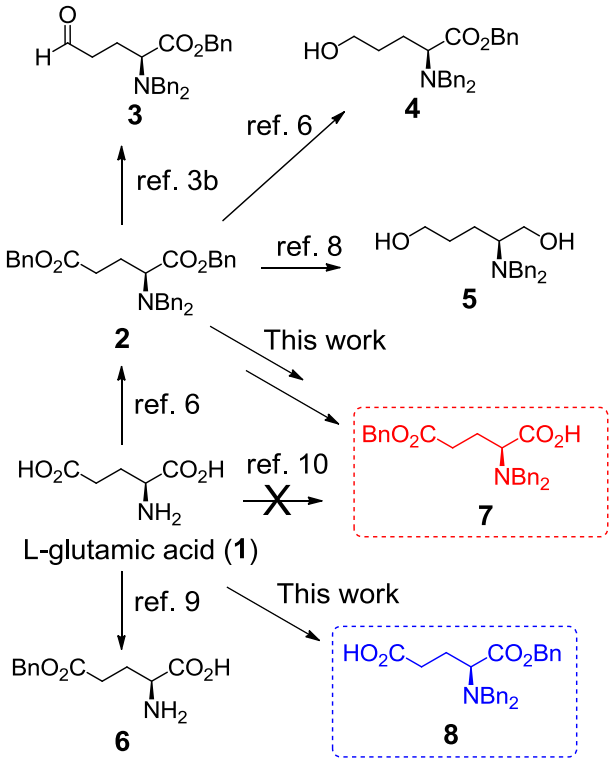

Equation 5.1. Reported methods for the synthesis of (poly)-benzylated L-glutamic acid derivatives.

5.2 Results and discussion

A direct comparison of the ^{1}H NMR spectra of compounds **2** and **3** reported earlier by us[3b] and the ^{1}H NMR spectrum for compound **7** was described by Akkarasamiyo,[11] that showed marked differences in the signals of the benzyl ester protons Ph-C*H*$_2$-O (Figure 5.1). Indeed, the ^{1}H NMR spectrum reported for **7** showed the appearance of the α-ester derivative and not the γ-ester analogue. The same typical ^{1}H NMR signal was found for the reported intermediate in the synthesis of schulzeines.[10]

At this point, we suspected that the compound resulting from the experimental conditions described by Akkarasamiyo was *N*,*N*-dibenzylglutamic acid α-benzyl ester (**8**). This subtle difference was unnoticed for the authors since the *N*,*N*-dibenzylglutamic acid monobenzyl ester was transformed into a 3-amino-2,6-piperidinedione intermediate. The reaction conditions are leading to the synthesis and the undoubtedly identification of compounds **7** and **8** will be discussed below.

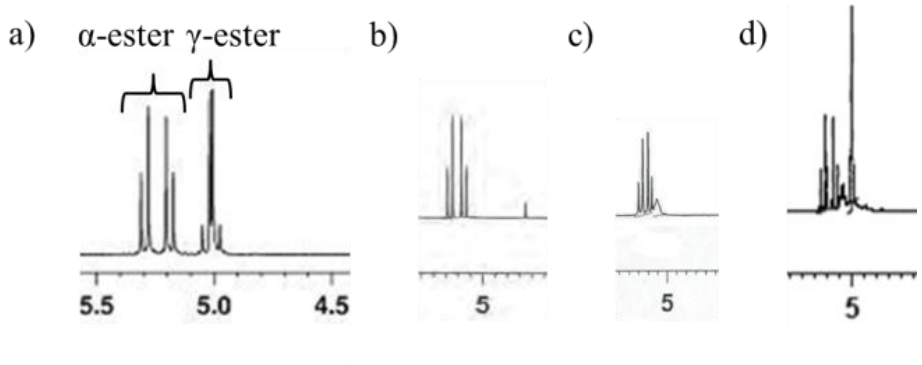

Figure 5.1. **^{1}H NMR signals of benzylic protons (Ph-C*H*$_2$-O) in $_L$-glutamic acid benzyl esters. (a) 2; (b) compound 43 in ref. 11; (c) compound 11 in ref. 10a; (d) compound 13 in ref. 10b.**

As shown in Scheme 5.2, when we repeated the benzylation of $_L$-glutamic acid (**1**) under the experimental conditions described by Akkarasamiyo,[10] *N*,*N*-dibenzylglutamic acid α-benzyl ester (**8**) was obtained in 20% yield (Table 5.1, entry 1). As a byproduct of the reaction, the perbenzylated derivative **2** was isolated in 1% yield. More important, compound **7** was not obtained. Subsequent selective reduction of the carboxylic acid group of **8** using standard methods allowed us to obtain compound **4**. The spectroscopic data was in full agreement with that reported in the literature. Consequently, the compound synthesized using the reported protocol is the α-benzyl ester **8** and not the γ-benzyl ester **7**.

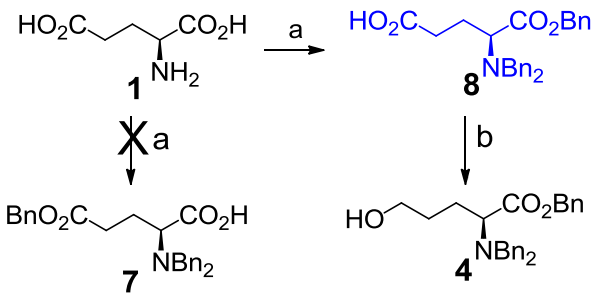

Scheme 5.2. ***Reagents and conditions*: (a) ref. 10, i.e., [BnCl (3.5 eq), K_2CO_3, KOH, MeOH-H_2O (1:1), Δ, overnight]., 20%; (b) BH_3-Me_2S, THF, 0 °C, 4 h, 86%.**

In order to synthesize compound **7**, we envisioned a strategy based on the widely known process to prepare derivative **6** (Scheme 5.2). Our first attempt to prepare **7** was the benzylation of **6** under basic conditions. However, the desired compound could not be obtained. Alternatively, compound **2** was treated under saponification conditions to give diacid **9** in high yield. Selective benzylation of **9** under acidic conditions led to the expected compound **7** in 70% yield. This time the ^{1}H NMR spectrum was consistent, as shown in Figure 5.2.

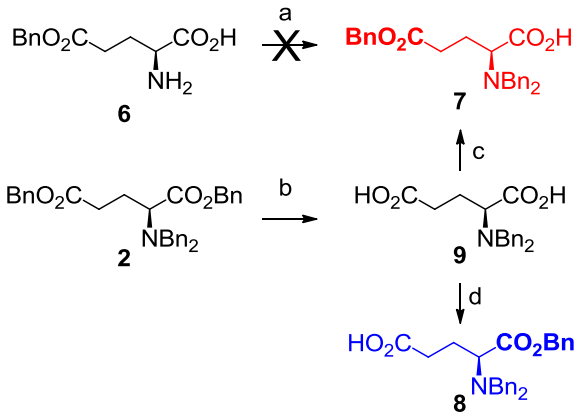

Scheme 5.3. ***Reagents and conditions*: (a) BnCl (2.5 eq), K_2CO_3, KOH, MeOH-H_2O (1:1), Δ, overnight; (b) NaOH, MeOH, Δ, 20 h, 90%; (c) CH_3SO_3H, BnOH, toluene, Δ, 5 h, 70%; (d) BnBr (1.1 eq), K_2CO_3, KOH, MeOH-H_2O (1:1), 70 ºC, 5 h, 25%.**

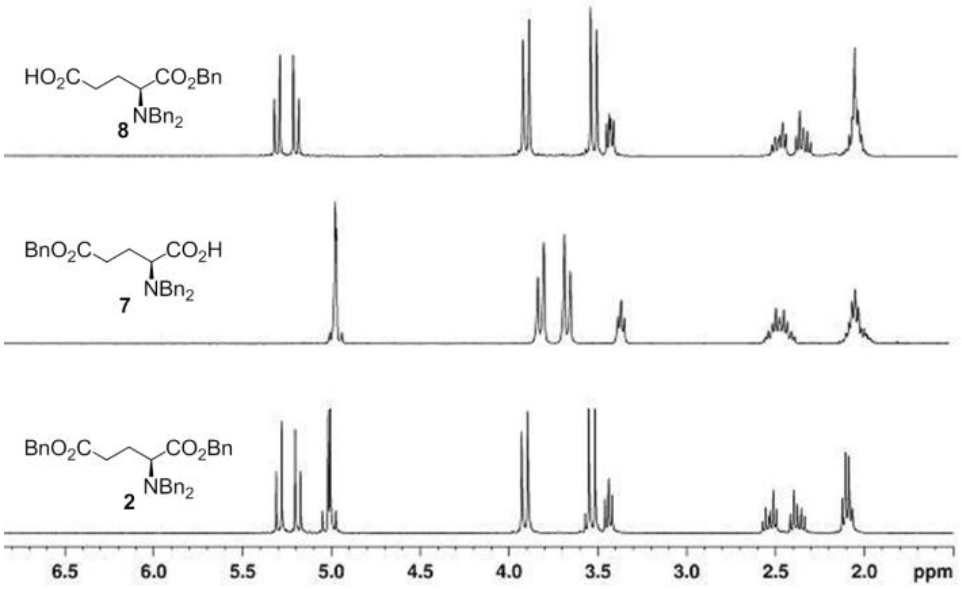

Figure 5.2. Partial ^{1}H NMR spectra of compounds 2, 7 and 8.

Interestingly, we found that upon treatment of **9** under the conditions reported by Akkarasamiyo, but using instead 1.1 equiv of benzyl bromide, the α-benzyl ester **8** was obtained in 25% yield (Scheme 5.3). This intriguing result, due to the similarity with that obtained by the direct benzylation of L-glutamic acid (**1**) with 3.5 equivalents of benzyl bromide, together with the low yield obtained led us to explore the influence of the reaction conditions.

The reaction conditions for the perbenzylation of **1** described in the literature uses indistinctly benzyl chloride or benzyl bromide as alkylating agents and NaOH or KOH as base (together with K_2CO_3). In addition, some methods described the use of MeOH as co-solvent. As additional factors in our study, we selected time and temperature. With these premises we ran a set of reactions and the results are given in Table 5.1.

Table 5.1. Effect of the reaction conditions in the polybenzylation of L-glutamic acid(1).

Reaction conditions[a]							Yield (%)		
Entry	MeOH (%)	Time (h)	Temp (°C)	BnX		Base (2.3 equiv)	8	2	7
				(equiv)	X				
1	50	overnight	reflux	3.5	Cl	NaOH	20	1	n.d[b].
2	50	5	70	3,5	Cl	KOH	25	7	1
3	50	5	70	3.5	Br	KOH	30	20	4
4	50	5	70	3	Cl	NaOH	12	2	n.d.
5	25	2	50	3	Br	KOH	n.d.	n.d.	n.d.
6	25	2	reflux	4	Br	KOH	19	26	1
7	25	12	80	3.25	Br	NaOH	12	19	n.d
8	25	12	80	3.25	Cl	NaOH	12	14	n.d
9	25	12	80	3.25	Cl	KOH	17	16	n.d
10	25	12	80	3.25	Br	KOH	13	19	n.d
11	0	overnight	70	3	Cl	KOH	9	13	n.d
12	75	2	reflux	3	Br	KOH	14	10	n.d
13	75	2	50	4	Br	KOH	23	10	7
14[c]	75	8	reflux	4	Br	KOH	73	n.d.	1

[a] **1** (1 equiv), K_2CO_3 (2.3 equiv), solvent (H_2O-MeOH for 0.23 M). [b] reaction conditions of Ref 11. [c] n.d. = not detected. [d] the α-methyl ester was obtained in 10% yield as a subproduct.

We speculated that under the aforementioned perbenzylation conditions the partial hydrolysis of **2** might occur. This might be an explanation for the low yields obtained by Akkarasamiyo. Thus, initially, we studied the benzylation process at shorter reaction times (5 h) and lower temperature (70 ºC). The results (Table 5.1, entries 2 and 3) showed that lower reaction times and temperature benefit the process since compounds **8** and **2** are obtained in slightly higher yields, while compound **7** is obtained as minor compound. Under these conditions, the base KOH seems to increase the overall yield while the halide BnBr favors the formation of **2**. However, at longer reaction times the effect on the outcome of the reaction was independent of the base or halide used (Table 5.1, entries 7-10). The reduction of the amount of alkylating agent (Table 5.1, entry 4) is concomitant with a decrease in yield. Another point of attention is the solvent. When reducing the percentage of MeOH in the mixture (Table 5.1, entries 5-11) no improvement in yield is obtained, regardless of the other reaction conditions. Similarly, a MeOH-H_2O (3:1) mixture (Table 5.1, entries 12-13) produced 8 in low yields at low reaction times. To our surprise, when we increased the reaction time (Table 5.1, entry 14), the benzylation of 1 to give 8 proceeded in 73% yield giving *N*,*N*-dibenzylglutamic acid α-methyl ester as side product of the process (10% yield). For processes where the α ester should be transformed and thus transesterification is not an inconvenient, the yield adds up to 83%.

5.3 Conclusions

In summary, we have described a methodology to obtain both *N*,*N*-dibenzylglutamic acid monobenzyl esters **7** and **8**, from commercially available $_{L}$-glutamic acid (**1**). Both compounds can be differentiated in terms of their ^{1}H NMR spectra. The unprecedented compound **7** is reported and characterized for the first time. The preferred method to obtaining **7** from $_{L}$-glutamic acid is the three-step process reported herein. We explored the reaction conditions leading to the formation of **8**. A not optimized 73% yield was achieved plus 10% yield of the *N*,*N*-dibenzylglutamic acid α-methyl ester.

5.4. References

1. (a) Padrón, J. M. *Curr. Med. Chem.* **2006**, *13*, 755. (b) Padrón, J. M.; Peters, G. J. *Invest. New Drugs* **2006**, *24*, 195. (c) Markidis, T.; Padrón, J. M.; Martín, V. S.; Peters, G. J.; Kokotos, G. *Anticancer Res***. 2001**, *21*, 2835. (d) Padrón, J. M.; Martín, V. S.; Hadjipavlou-Litina, D.; Noula, C.; Constantinou-Kokotou, V.; Peters, G. J.; Kokotos, G. *Bioorg. Med. Chem. Lett.* **1999**, *9*, 821.
2. Kokotos, G.; Padrón, J. M.; Noula, C.; Gibbons, W. A.; Martín, V. S. *Tetrahedron: Asymmetry* **1996**, *7*, 857.
3. (a) Kokotos, G.; Padrón, J. M.; Martín, T.; Gibbons, W. A.; Martín, V. S. *J. Org. Chem.* **1998**, *63*, 3741. (b) Padrón, J. M.; Kokotos, G.; Martín, T.; Markidis, T.; Gibbons, W. A.; Martín, V. S. *Tetrahedron: Asymmetry* **1998**, *9*, 3381.
4. (a) Sutherland, A.; Caplan, J. F.; Vederas, J. C. *Chem. Commun.* **1999**, 555. (b) Sutherland, A.; Vederas, J. C. *Chem. Commun.* **1999**, 1739. (c) Roche, D.; Prasad, K.; Repic, O.; Blacklock, T. J. *Tetrahedron Lett.* **2001**, *42*, 1459. (d) Adamczyk, M.; Reddy, R.E.; Rege, S. D. *J. Labelled Cpd. Radiopharm.* **2001**, *44*, 185. (e) Hernández, N.; Martín, V. S. *J. Org. Chem.* **2001**, *66*, 4934. (f) Constantinou-Kokotou, V.; Magrioti, V.; Markidis, T.; Kokotos, G. *J. Peptide Res.* **2001**, *58*, 325. (g) Magrioti, V.; Constantinou-Kokotou, V. *Lipids* **2002**, *37*, 223. (h) Wasserman, H. H.; Long, Y.O.; Zhang, R.; Parr, J. *Heterocycles* **2002**, *58*, 393. (i) Constantinou-Kokotou V. *Lett. Peptide Sci.* **2002**, *9*, 143. (j) Wasserman, H. H.; Long, Y. O.; Zhang, R.; Parr, J. *Tetrahedron Lett.* **2002**, *43*, 3351. (k) Hanessian, S.; Angiolini, M. *Chem. Eur. J.* **2002**, *8*, 111. (l) Schleusner, M.; Gais, H.-J.; Koep, S.; Raabe, G. *J. Am. Chem. Soc.* **2002**, *124*, 7789. (m) Cox, R. J.; Gibson, J. S.; Martín, M. B. M. *ChemBioChem* **2002**, *3*, 874. (n) Gerwick, W. H.; Leslie, P.; Long, G. C.; Marquez, B. L.; Willis, C. L. *Tetrahedron Lett.* **2003**, *44*, 285. (o) Bycroft, B. W.; Chhabra, S. R.; Kellam, B.; Smith, P. *Tetrahedron Lett.* **2003**, *44*, 973. (p) Abraham, A.; Howarth, N. M. *Nucleosides Nucleotides Nucleic Acids* **2003**, *22*, 675. (q) Gorohovsky, S.; Meir, S.; Shkoulev, V.; Byk, G.; Gellerman, G. *Synlett* **2003**, 1411. (r) Hallinan, E. A.; Hagen, T. J.; Bergmanis, A.; Moore, W. M.; Jerome, G. M.; Spangler, D. P.; Stevens, A. M.; Shieh, H. S.; Manning, P. T.; Pitzele, B. S. *J. Med. Chem.* **2004**, *47*, 900. (s) Hamilton, D. J.; Sutherland, A. *Tetrahedron Lett.* **2004**, *45*, 5739 (t) Shin, H.; Cama, E.; Christianson, D. W. *J. Am. Chem. Soc.* **2004**, *126*, 10278; (u) Haug, B. E.; Rich, D. H. *Org. Lett.* **2004**, *6*, 4783. (v) Gallos, J. K.; Sarli, V. C.; Massen, Z. S.; Varvogli, A. C.; Papadoyanni, C. Z.; Papaspyrou, S. D.; Argyropoulos, N. G. *Tetrahedron* **2005**, *61*, 565.

5. Silveira-Dorta, G.; Donadel, O. J.; Martín, V. S.; Padrón, J. M. *J. Org. Chem.* **2014**, *79*, 6775.
6. Rodriquez, M.; Taddei, M. *Synthesis* **2005**, *3*, 493.
7. (a) Minassian, F. *C. R. Chimie* **2005**, *8*, 859. (b) Rodriquez, M.; Bruno, I.; Cini, E.; Marchetti, M.; Taddei, M.; Gomez-Paloma, L. *J. Org. Chem.* **2006**, *71*, 103. (c) Rodriquez, M.; Terracciano, S.; Cini, E.; Settembrini, G.; Bruno, I.; Bifulco, G.; Taddei, M.; Gomez-Paloma, L. *Angew. Chem. Int. Ed.* **2006**, *45*, 423. (d) Le Quement, S. T.; Nielsen, T. E.; Meldal, M. *J. Comb. Chem.* **2007**, *9*, 1060. (e) Dzhekieva, L.; Rocaboy, M.; Kerff, F.; Charlier, P.; Sauvage, E.; Pratt, R. F. *Biochemistry* **2010**, *49*, 6411. (f) Culhane, J. C.; Wang, D.; Yen, P. M.; Cole, P. A. *J. Am. Chem. Soc.* **2010**, *132*, 3164. (g) Botta, C. B.; Cabri, W.; Cini, E.; De Cesare, L.; Fattorusso, C.; Giannini, G.; Persico, M.; Petrella, A.; Rondinelli, F.; Rodriquez, M.; Russo, A.; Taddei, M. *J. Med. Chem.* **2011**, *54*, 2165.
8. (a) Oestreich, M.; Fröhlich R.; Hoppe, D. *Tetrahedron Lett.* **1988**, *39*, 1745. (b) Kikuchi, H.; Yamamoto, K.; Horoiwa, S.; Hirai, S.; Kasahara, R.; Hariguchi, N.; Matsumoto, M.; Oshima, Y. *J. Med. Chem.* **2006**, *49*, 4698.
9. Albert, R.; Danklmaier, J.; Hönig, H.; Kandolf, H. *Synthesis* **1987**, 635.
10. (a) Kuntiyong, P.; Akkarasamiyo, S.; Eksinitkun, E. *Chem. Lett.* **2006**, *35*, 1008. (b) Kuntiyong, P.; Akkarasamiyo, S.; Piboonsrinakara, N.; Hemmara, C.; Songthammawat, P. *Tetrahedron* **2011**, *67*, 8034.
11. S. Akkarasamiyo, PhD. Thesis 2008, pp. 28-29 accesible at http://www.thapra.lib.su.ac.th/objects/thesis/fulltext/snamcn/Sunisa_Akkarasamiyo/Fulltext.pdf (last accesed May 15, 2014).

5.5. Experimental section

5.5.1 General Remarks

Reactions were performed using oven-dried glassware under an atmosphere of argon. ^{1}H NMR spectra were recorded at 400 at 298K, ^{13}C NMR spectra were recorded at 100. Chemical shifts were reported in units (ppm) by assigning TMS resonance in the ^{1}H NMR spectrum as 0.00 ppm ($CDCl_3$, 7.26 ppm). Data were reported as follows: chemical shift, multiplicity (s = singlet, d = doublet, t = triplet, q = quartet, quin = quintuplet, sex = sextet, dd = double doublet, ddd = double double doublet, m =multiplet and br = broad), coupling constant (*J* values) in Hz and integration. Chemical shifts for ^{13}C NMR spectra were recorded in ppm from tetramethylsilane as the internal standard. Using the central peak of $CDCl_3$ (77.0 ppm). Reagent-grade chemicals were obtained from diverse commercial suppliers and were used as received. Optical rotations were measured with a polarimeter at the sodium line at different temperatures in $CHCl_3$. Accurate mass (HRMS) were determined by electrospray ionization (ESI-TOF) and electronic impact (EI-TOF). Reactions were monitored using thin-layer chromatography (TLC) on aluminum packed percolated Silica Gel 60 F_{254} plates. Flash column chromatography was carried out with silica gel 60 (particle size less than 0.020 mm) by using appropriate mixtures of ethyl acetate and hexanes as eluent. Compounds were visualized by use of UV light and 2.5% phosphomolybdic acid in ethanol. All reactions involving air- or moisture-sensitive materials were carried out under Argon atmosphere. Anhydrous magnesium sulfate was used for drying solutions. Melting points were measured with micro melting point apparatus. Chemical nomenclature was generated using Chem Bio Draw Ultra 13.0.

5.5.2 Synthetic procedures and characterization for the glutamic acid derivatives

(2*S*)-5-(benzyloxy)-2-(dibenzylamino)-5-oxopentanoic acid (7). Methane sulfonic acid (3.6 mmol, 0.2 mL) was added dropwise to a suspension of **9** (1.0 g, 3 mmol) and benzyl alcohol (4.8 mmol, 0.5 mL) in dry toluene (30 mL). The resulting mixture was heated at reflux in a Dean Stark system for 5 h, after which time it was allowed to cool to room temperature. Then, the solvent was evaporated under reduced pressure. The residue was diluted with water (30 mL), and extracted with Et_2O (2 x 20 mL). The combined organic extracts were washed with brine (30 mL) and dried over $MgSO_4$, filtered and the solvent was removed under reduced pressure. The residue was purified by flash column chromatography (hexanes-EtOAc 20:50) to give 1.3 g of **7** (70% yield) as pale-yellow oil. $[\alpha]^{25}_{D}$ -31.3º (*c* = 0.98, $CHCl_3$). ^{1}H NMR (400 MHz, $CDCl_3$): δ = 2.11-2.21 (m, 2 H), 2.53-2.66 (m, 2 H), 3.47 (t, *J* = 7.0 Hz, 1 H), 3.78 (d, *J* = 13.4 Hz, 2 H), 3.91 (d, *J* = 13.4 Hz, 2 H), 5.08 (AB system, 2 H) 7.29-7.42 (m, 15 H) ppm. ^{13}C NMR (100 MHz, $CDCl_3$): δ = 22.9, 31.1, 54.5, 60.2, 66.3, 127.6, 128.3, 128.6, 129.2, 135.9, 138.2,

172.9, 176.5 ppm. IR: ν_{max} = 3362.1-2328.4, 1729.2, 1257.4, 1162.4 cm^{-1}. HRMS (ESI): calcd. for $C_{26}H_{27}NO_4$ $[M + H]^+$ 418.2018; found 418.2002.

(4*S*)-5-(benzyloxy)-4-(dibenzylamino)-5-oxopentanoic acid (8). To a solution of L-glutamic acid (1.0 g, 6.8 mmol), K_2CO_3 (2.2 g, 15.6 mmol) and KOH (0.87 g, 15.6 mmol) in MeOH:H_2O (75:25, 30 mL) was slowly added benzyl bromide (4.08 g, 27.2 mmol) at room temperature. The mixture was stirred at reflux for 8 h. After being cooled to 0 ºC, it was neutralized (pH = 7) with 5% solution of HCl. Then, the mixture was extracted with CH_2Cl_2 (2 x 50 mL) and the organic layer was dried over $MgSO_4$, filtered and the solvent was removed under reduced pressure. The residue was purified by flash column chromatography (hexanes-EtOAc 90:10-70:30) to give 2.84 g of **8** (73% yield) as a colorless oil. $[\alpha]^{25}_D$ -72.7º (*c* = 1.11, $CHCl_3$). ^{1}H NMR (400 MHz, $CDCl_3$): δ = 2.00-2.14(m, 2 H), 2.33-2.40 (m, 1 H), 2.46-2.54 (m, 1 H), 3.45 (dd, *J* = 6.7, 9.5 Hz, 1 H), 3.54 (d, *J* = 14.3 Hz, 2 H), 3.94 (d, *J* = 14.3 Hz, 2 H), 5.26 (AB system, 2 H), 7.22-7.48 (m, 15 H) ppm. ^{13}C NMR (100 MHz, $CDCl_3$): δ = 23.9, 30.4, 54.5, 59.6, 66.2, 127.2, 128.3, 128.4, 128.6, 128.6, 128.4, 135.9, 138.9, 172.0, 178.79.ppm. IR: ν_{max} = 3450.3-2500.2, 1729.7, 1711.1, 1247.8, 1160.7 cm^{-1}. HRMS (ESI): calcd. for $C_{26}H_{27}NO_4$ $[M + Na]^+$ 440.1838; found 440.1846.

(2*S*)-2-(dibenzylamino)pentanedioic acid (9). Perbenzylated L-glutamic acid (**2**) (10 g, 19.7 mmol) was dissolved in MeOH (70 mL). A freshly prepared, ice-cold aqueous solution of 2.4 M NaOH (22 mL, 50 mmol) was added to the solution and the resulting mixture heated at reflux for 20 h. The reaction mixture was then allowed to cool to room temperature and the solvent was evaporated under reduced pressure. The residue was diluted with water, and extracted with CH_2Cl_2 to remove the benzyl alcohol formed in the hydrolysis. The basic aqueous layer was acidified (pH = 3-4) with concentrated HCl and a precipitate was formed. The water layer was extracted with EtOAc (3 x 50 mL). The organic extracts were combined and the solvent was removed under reduced pressure. The solid residue was recrystallized from MeOH to give **9** as a white solid (5.8 g, 90% yield). M.p. 228–229 °C. $[\alpha]^{25}_D$ -71.3º (*c* = 1.03, DMSO). ^{1}H NMR (400 MHz, DMSO-d_6): δ = 1.84-1.90 (m, 2 H), 2.13-2.21 (m, 1 H), 2.29-2.36 (m, 1 H), 3.12-3.16 (m, 1 H) , 3.59 (d, *J* = 14.2, 2 H), 3.80 (d, *J* = 14.2, 2 H), 7.20-7.32 (m, 10 H) ppm. ^{13}C NMR (100 MHz, DMSO-d_6): δ = 24.2, 30.6, 50.0, 59.86, 126.3, 128.2, 128,4, 139.6, 173.6, 174.05 ppm. IR: ν_{max} = 3340.3-2750.4, 2672.3- 2172.5, 1729.3, 1612.6, 1452.6, 1245.5 cm^{-1}. HRMS (ESI): calcd. for $C_{19}H_{20}NO_4$ $[M + 2Na]^+$ 372.1188; found 372.1180.

5.6. ^{1}H and ^{13}C NMR spectra

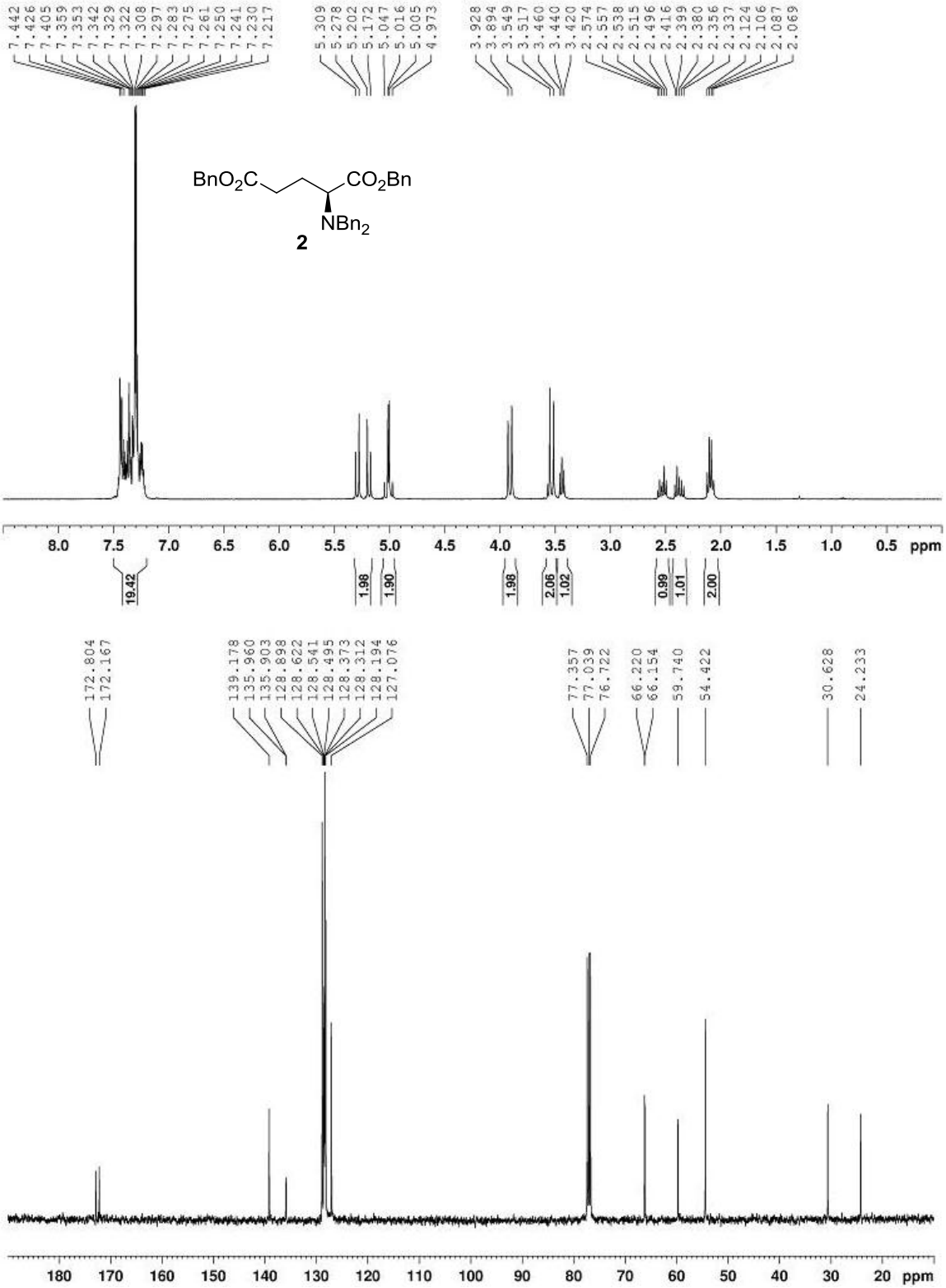

Figure S1. ^{1}H **(400 MHz) and** ^{13}C **(100 MHz) NMR spectra in** $CDCl_3$ **of 2.**

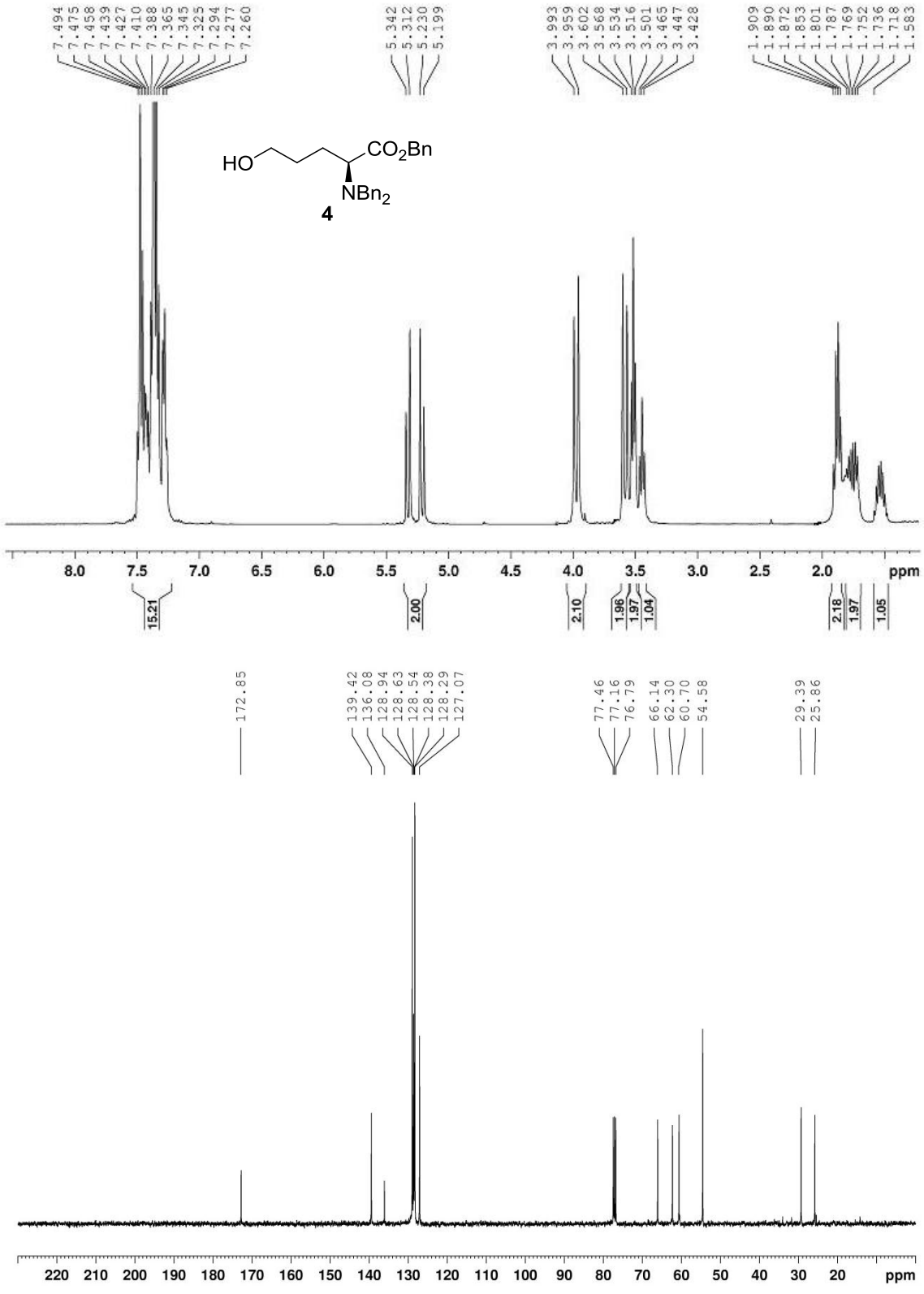

Figure S2. **^{1}H (400 MHz) and ^{13}C (100 MHz) NMR spectra in $CDCl_3$ of 4.**

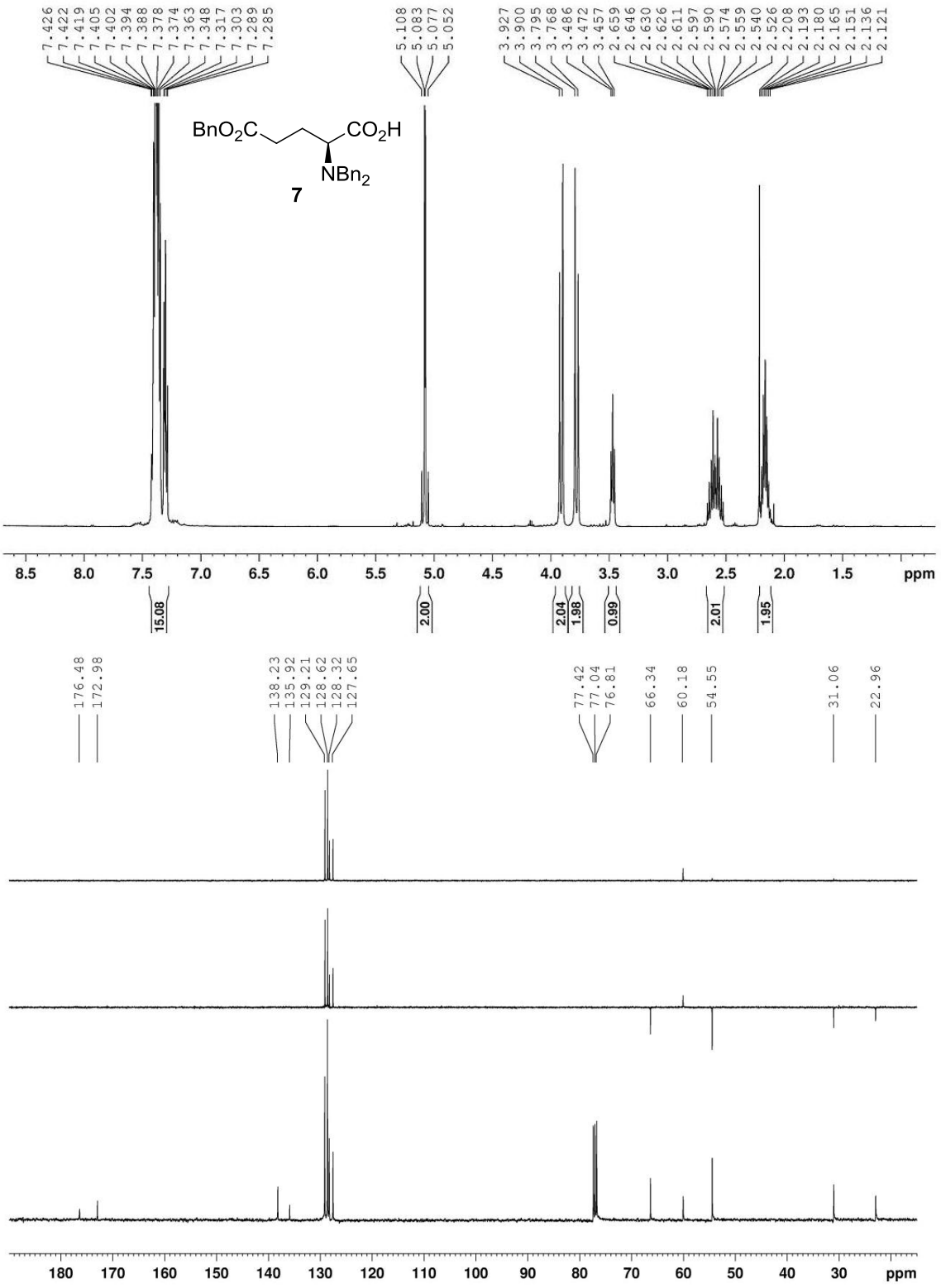

Figure S3. **^{1}H (400 MHz) and ^{13}C (100 MHz) NMR spectra in $CDCl_3$ of 7.**

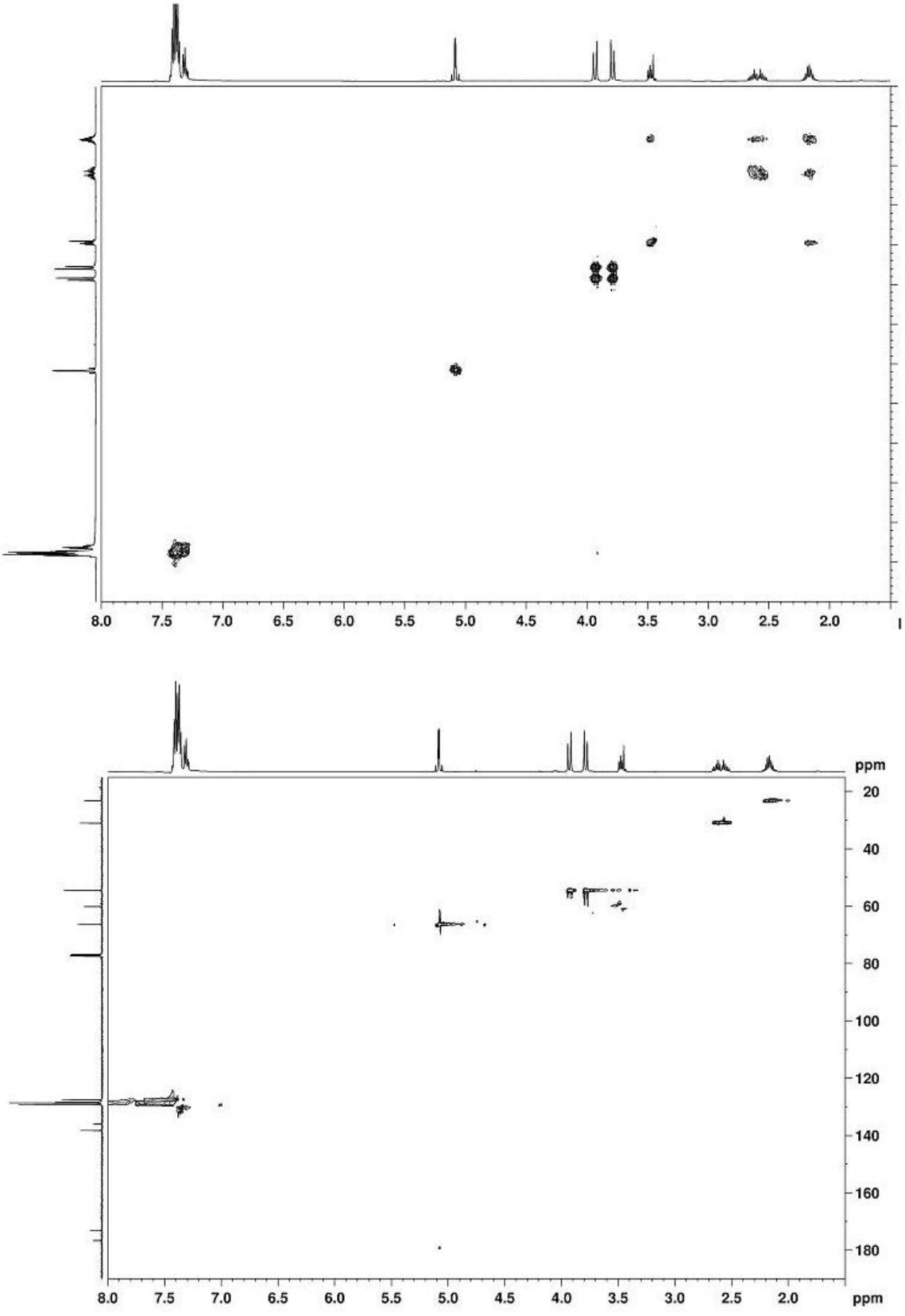

Figure S4. COSY and HSQCspectra in $CDCl_3$ of 7.

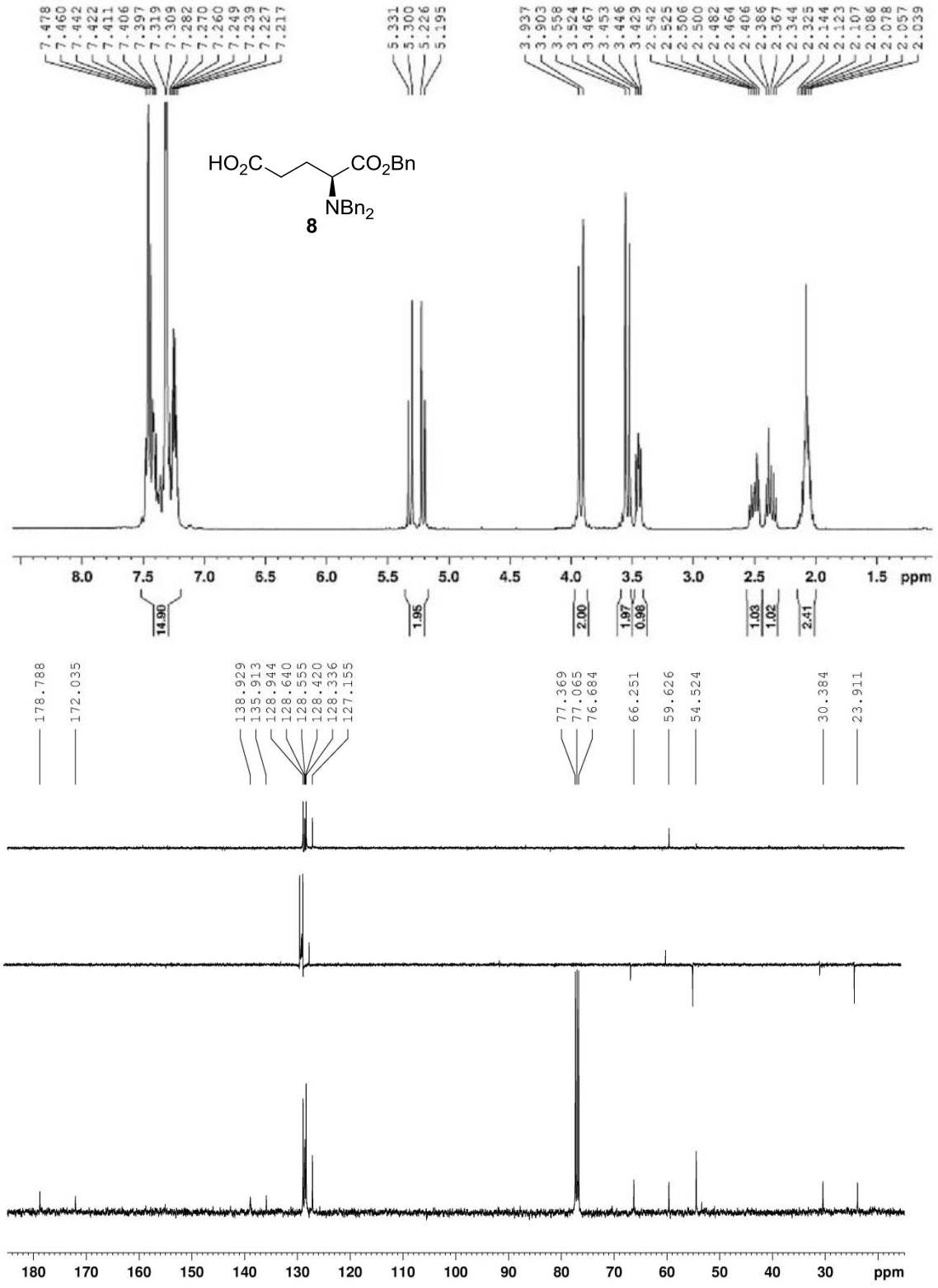

Figure S5. **^{1}H (400 MHz) and ^{13}C (100 MHz) NMR spectra in $CDCl_3$ of 8.**

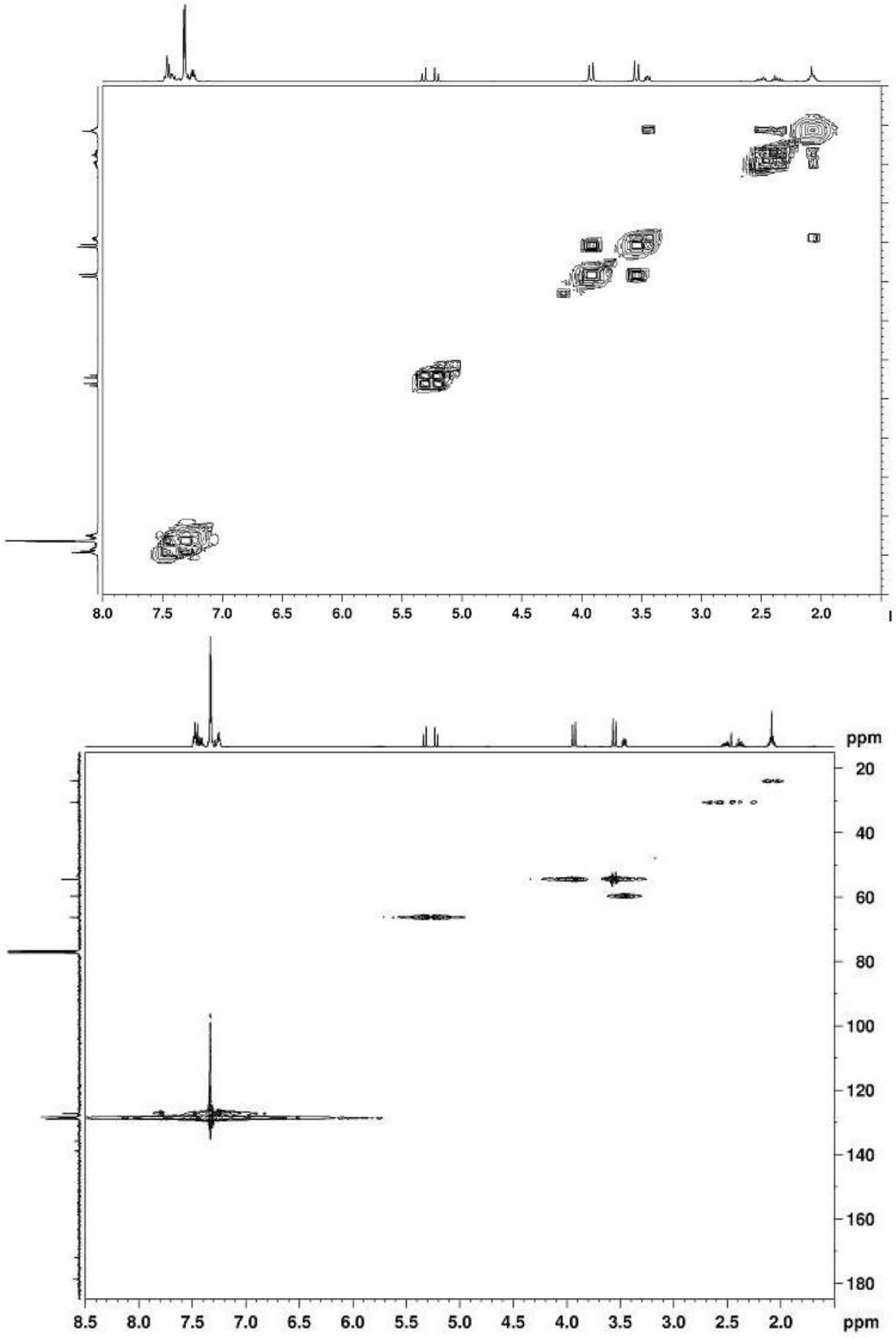

Figure S4. COSY and HSQCspectra in $CDCl_3$ of 8.

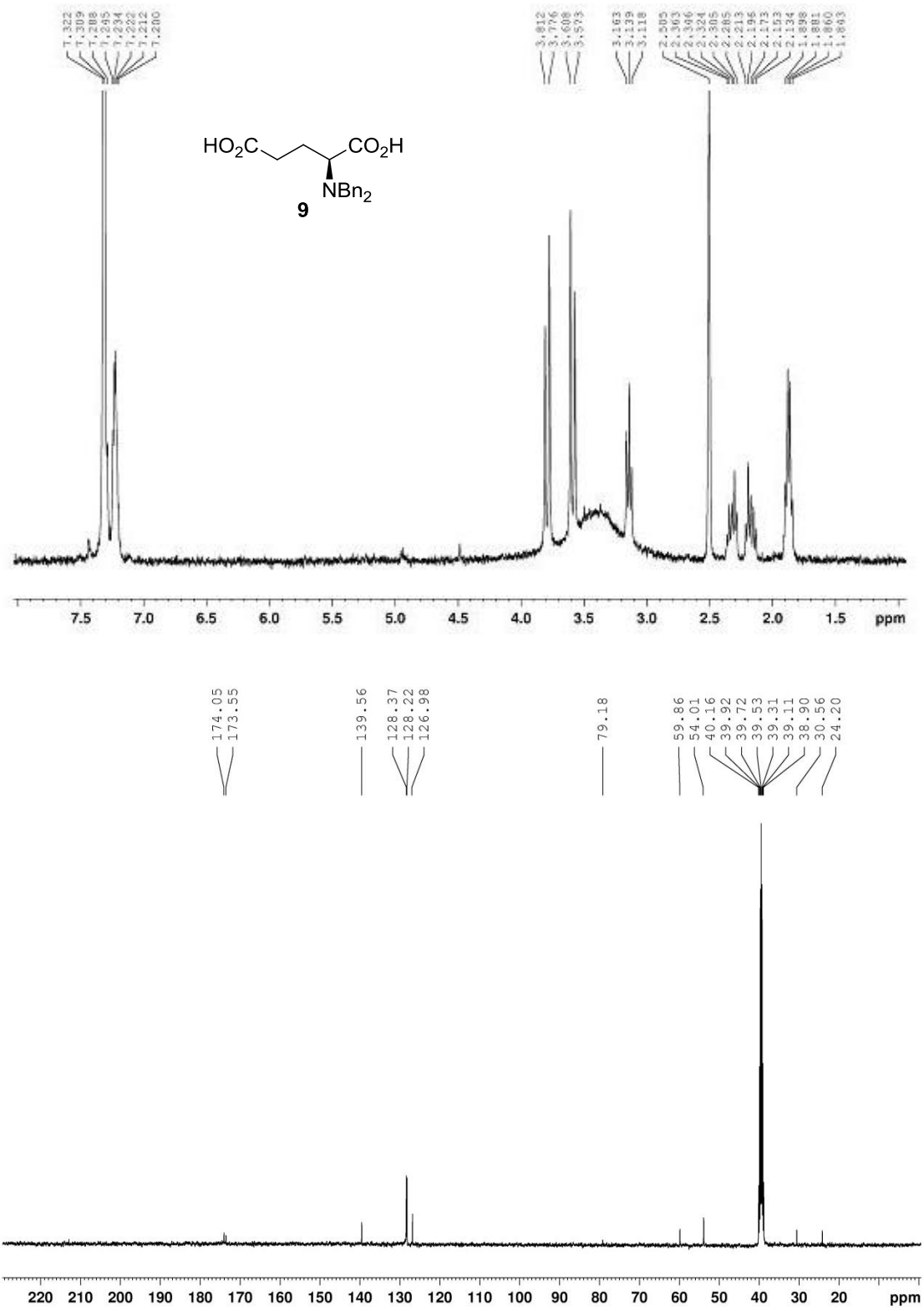

Figure S5. **^{1}H (400 MHz) and ^{13}C (100 MHz) NMR spectra in DMSO-d_6 of 9.**

CHAPTER 6

SYNTHESIS AND ANTIPRO-LIFERATIVE ACTIVITY OF GLUTAMIC ACID-BASED DIPEPTIDES

6. Synthesis and antipro-liferative activity of glutamic acid-based dipeptides

6.1 Introduction

Naturally occurring amino acids represent a powerful source of relatively inexpensive, widely available and enantiomerically pure building blocks, even on a bulk scale. They have been largely used in organic chemistry as intermediates in peptide synthesis or in the synthesis of more complex structures with diverse applications. Of particular interest to us is the use of amino acids as source for antitumor compounds. In this context, L-glutamic acid is present in the antitumor drug aminopterin (**1a**)[1] and its well-known *N*-methylated derivative methotrexate (**1b**).[2] Other anticancer drug´s derivatives of L-glutamic acid are thalidomide (**2a**) and its analogs pomalidomide (CC-4047, **2b**) and lenalidomide (CC-5013, **2c**).[3] In these compounds, L-glutamic acid binds through its amino group to the rest of the molecule forming amide or imide bonds (Figure 6.1a). Another use of L-glutamic acid is as poly-glutamic acid conjugates, which act as drug carrier because they increase the efficacy of anticancer drugs and decrease their toxicity toward normal cells.[4] In this strategy, the drug is mostly linked to the γ-carboxyl group through ester or amide bonds.

The natural amino acid L-glutamine (**3a**) is the γ-amide of L-glutamic acid and it is essential for cell growth and proliferation. In healthy cells, L-glutamine is synthesized from L-glutamic acid by L-glutamine synthetase. However, in neoplastic cells L-glutamine cannot be produced due to the lower reactivity of L-glutamine synthetase. In addition to glucose, cancer cells utilize L-glutamine as a carbon source for ATP production and biosynthesis. L-Glutamine can be internalized through cell surface transporters such as ASCT2.[5] These considerations have increased the interest of targeting glutamine internalization[6] and metabolism[7] in cancer therapy. L-Glutamine derivatives (Figure 6.1b) investigated along these lines include the natural product theanine (**3b**),[8] the glutamine-utilizing enzyme inhibitors **3c**-**3e**, or the ASCT2 inhibitor **4**.[9]

In addition to enzyme inhibitors or drug carriers, amino acids constitute peptides that are being used for the therapy of a significant number of diseases.[10, 11] In particular, anticancer peptides (ACPs) have shown relevant since they exhibit cancer-selective toxicity while avoiding the shortcomings of the conventional chemotherapy.[12] ACPs are small peptides with less than 50 amino acids. The CancerPPD (http://crdd.osdd.net/raghava/cancerppd/) database contains over 3400 experimentally verified ACPs. The statistical analysis in terms of amino acid residues show that small peptides (<5 amino acids) have not being explored exhaustively as potential anticancer agents (Figure 6.1c). When it comes to the study of anticancer dipeptides, literature is

scarce in examples. Although tyrosine- and cystine-based dipeptides have been reported to exhibit antiproliferative activity in human solid tumor cell lines.[13,14] to the best of our knowledge there are no reports on the antiproliferative activity of glutamic acid-based dipetides.

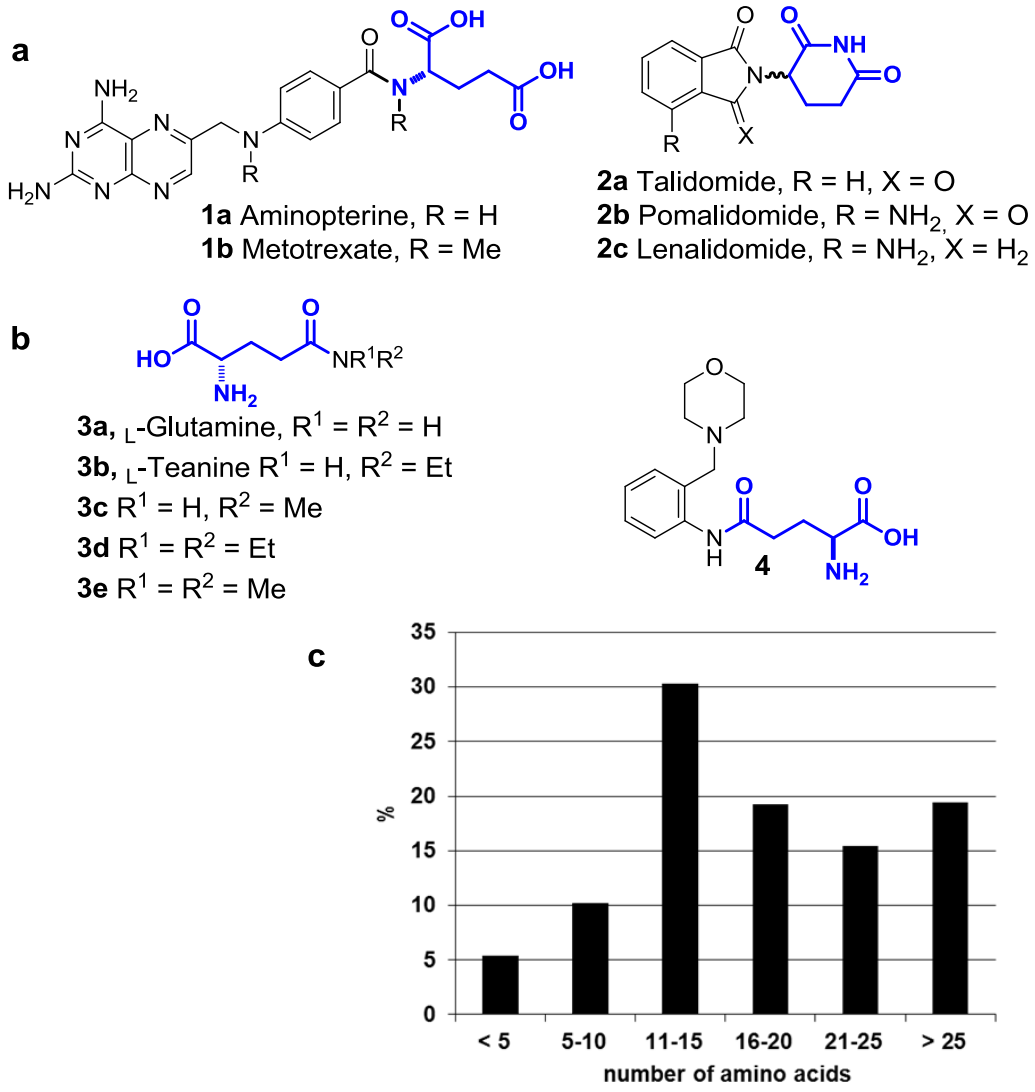

Figure 6.1. **a. L-Glutamic acid derivatives with anticancer activity. Bond thickness emphasizes the L-glutamic acid fragment. b. L-Glutamine and *N*$^{\gamma}$-alkylated derivatives. c. Statistical analysis of amino acid residues of the ACPs listed in the CancerPPD database.**

$_{L}$-Glutamic and $_{L}$-aspartic acid are potentially valuable molecules providing that the two carboxylic groups could be synthetically differentiated. Recently, we have explored the regioselective esterification of $_{L}$-glutamic acid.[15] Our methodology allows to obtain unambiguously both *N*,*N*-dibenzylglutamic acid α- (**5**) and γ-benzyl esters (**6**) from commercially available $_{L}$-glutamic acid (Figure 6.2). As a part of our screening program directed at the discovery of new biologically active molecules with antiproliferative activity, we found that both **5** and **6**, were active against human solid tumor cells. These results together with the lack of antiproliferative activity studies on glutamic acid-based dipeptides encouraged us to explore further this type of molecules as scaffolds for new anticancer drugs. Herein, we report on the synthesis of glutamic acid-based dipeptides and their antiproliferative activity against human solid tumor cells.

6.2 Results and discussion

During the course of our investigation on the regioselective benzylation of $_{L}$-glutamic acid, we analyzed the antiproliferative activity of compounds **5**-**8**. As a model to study the antiproliferative activity, we selected the panel of representative human solid tumor cell lines HBL-100 (breast), HeLa (cervix), SW1573 (non-small cell lung), T-47D (breast), and WiDr (colon). The in vitro antiproliferative activity was evaluated using the National Cancer Institute (NCI) protocol.[16] The standard anticancer drugs cisplatin[17] and etoposide[18] were used as reference agents. The results expressed as GI_{50} are shown in Table 6.1. We found that monobenzyl esters **5**-**6** were able to induce cell growth inhibition in all cell lines with GI_{50} values in the range 22-46 μM, whereas the perbenzylated analog **7** and the diacid **8** were inactive. In addition, compound **5** showed slightly more active than compound **6**. This result encouraged us to synthesize a small library of α- and γ-glutamyl dipeptides and test their antiproliferative activity.

6.2.1 Synthesis of glutamic acid-based dipeptides

The general synthetic pathway for the preparation of the glutamic acid-based dipeptides is outlined in Figure 6.2. The direct regioselective benzylation of commercially available $_{L}$-glutamic acid afforded *N*,*N*-dibenzylglutamic acid α-benzyl ester (**5**) in 73% yield. We have reported recently that the reaction conditions play a critical role in the outcome of the products.[15] However, *N*,*N*-dibenzylglutamic acid γ-benzyl ester (**6**) cannot be obtained directly

from L-glutamic acid. Instead, a three-step sequence is needed. Briefly, conventional perbenzylation of L-glutamic acid afforded compound **7** in high yields as reported earlier.[19]

Table 6.1. Antiproliferative activity (GI_{50}) against human solid tumor cells of compounds 5-8.[a]

Compound	Cell line				
	HBL-100	**HeLa**	**SW1573**	**T-47D**	**WiDr**
5	39 (±2.6)	22 (±6.6)	38 (±4.1)	29 (±5.6)	29 (±7.8)
6	46 (±9.0)	30 (±6.8)	40 (±4.4)	34 (±7.2)	44 (±9.4)
7	>100	>100	>100	>100	>100
8	>100	>100	>100	>100	>100
Cisplatin	1.9 (±0.2)	2.0 (±0.3)	3.0 (±0.4)	15 (±2.3)	26 (±5.3)
Etoposide	2.3 (±0.9)	3.0 (±0.9)	15 (±1.5)	22 (±5.5)	23 (±3.1)

[a]Values are given in μM and are means of two to five experiments; standard deviation is given in parentheses.

Then, hydrolysis of the benzyl ester groups of **7** under standard basic conditions led to diacid **8** in almost quantitative yield. Finally, esterification under acid conditions[20] allowed us to obtain exclusively the γ-benzyl ester **6** in 70% yield. Intermediates **5** and **6** were coupled successfully with the commercially available methyl ester hydrochlorides of the amino acids alanine (**a**), valine (**b**), leucine (**c**), isoleucine (**d**), phenylalanine (**e**), tyrosine (**f**), tryptophan (**g**), threonine (**h**), serine (**i**), proline (**j**) and methionine (**k**) to provide dipeptides **9a-k** and **10a-k**, respectively. In this process, 2-(1H-benzotriazole-1yl)-1,1,3,3-tetramethyluronium tetrafluoroborate (TBTU) was selected as coupling agent. The reactions were carried out in DMF and *N*,*N*-diisopropylethyl amine was used as based. Yields were in the range 50-70%. With this methodology we obtained a small library of dipeptides comprising two sets of regioisomers, the γ- (**9a-k**) and the α-glutamyl series (**10a-k**).

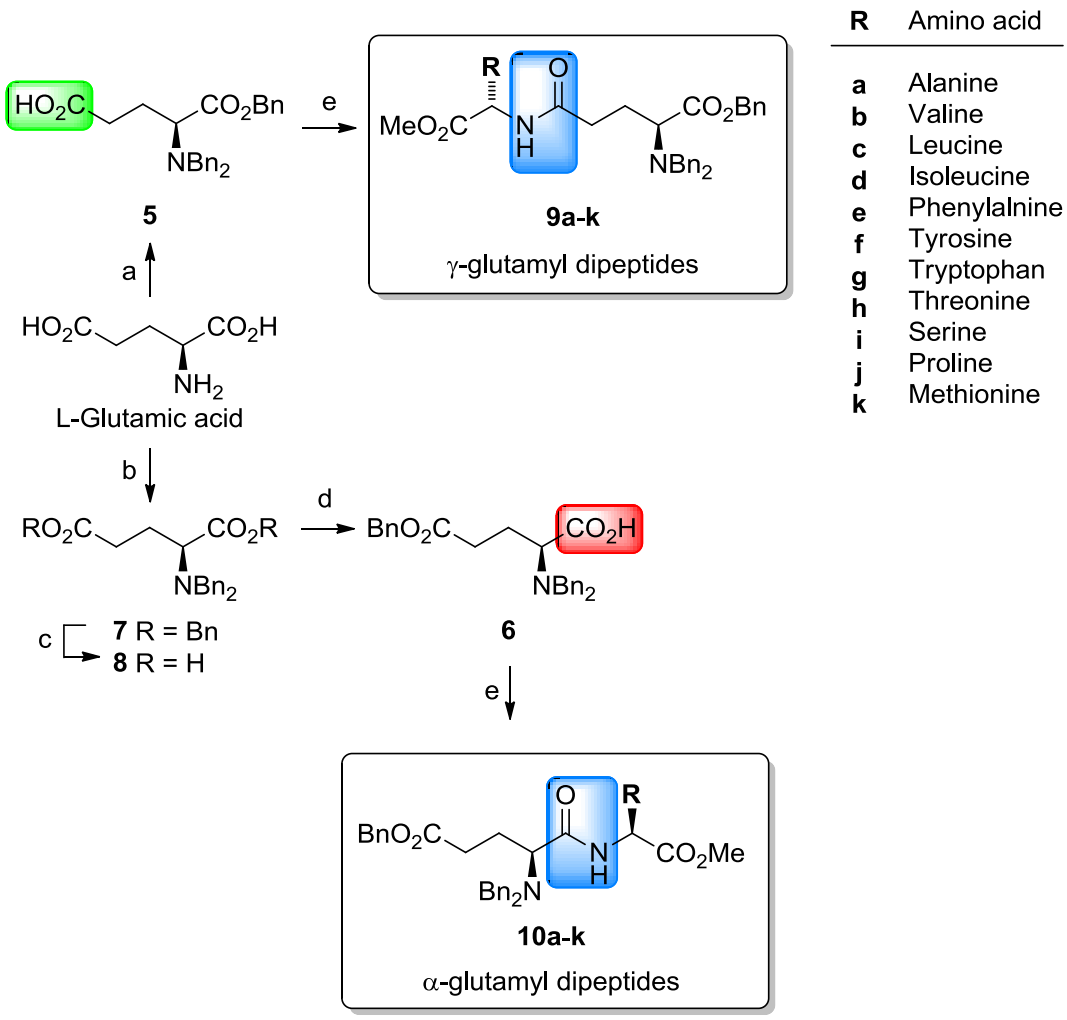

Figure 6.2. Synthesis of glutamic acid-based dipeptides 9-10. Reagents and conditions: (a) BnBr, K_2CO_3-KOH, MeOH-H_2O (75:25), Δ, 8h, 73%; (b) BnBr, K_2CO_3, MeOH-H_2O (1:1), Δ, 20 h, 90%; (c) NaOH, MeOH (1:1), Δ, 20 h, 98%; (d) CH_3SO_3H, BnOH, toluene, Δ, 5 h, 70%; (e) TBTU, DIPEA, DMF, rt, overnight, 50-70%.

6.2.2 Biological evaluation of glutamic acid-based dipeptides

The antiproliferative activity of γ-glutamyl (**9a-k**) and α-glutamyl dipeptides (**10a-k**) was evaluated and the results are shown in Table 6.2 and Figure 6.3. Although the set of compounds is not large, some structure-activity relationships could be inferred from the antiproliferative data. The data showed a clear difference in potency between both set of compounds. Based on average GI_{50} values, α-glutamyl dipeptides (**10a-k**) were more active than the γ-glutamyl derivatives (**9a-k**) in HBL-100, HeLa and SW1573 cells. In the more resistant cell lines T-47D and WiDr, the overall effect favored the γ-glutamyl derivatives. The most

potent compound of both series was the α-glutamyl dipeptide **10j** and exhibited GI_{50} values in the range 7.5-18 μM. In the γ-glutamyl set, the lead in terms of GI_{50} values was **9k** with GI_{50} values in the range 6.0-41 μM. However, in SW1573 cells, none of the designated lead was the most potent compound. Instead, the phenylalanine dipeptide (**e**) was the most active. It is noteworthy that when compared to the standard anticancer drugs etoposide and cisplatin, dipeptides **9i**, **9j**, **10i** and **10j** were more active in the resistant cell line WiDr.

Table 6.2. Antiproliferative activity (GI_{50}) against human solid tumor cells of compounds 9-10.

Compound	Cell line				
	HBL-100	**HeLa**	**SW1573**	**T-47D**	**WiDr**
9a	24 (±2.2)	22 (±4.4)	36 (±2.6)	22 (±2.9)	24 (±1.2)
9b	22 (±8.5)	19 (±2.7)	65 (±26)	38 (±10)	40 (±4.8)
9c	35 (±2.8)	25 (±8.2)	30 (±9.8)	33 (±2.6)	40 (±3.1)
9d	22 (±0.8)	23 (±5.5)	26 (±4.5)	21 (±1.9)	26 (±2.8)
9e	36 (±6.2)	27 (±7.0)	14 (±4.1)	21 (±0.1)	36 (±9.0)
9f	20 (±7.2)	14 (±1.6)	18 (±6.1)	22 (±7.7)	20 (±4.9)
9g	>100	18 (±4.0)	20 (±7.1)	33 (±2.5)	40 (±11)
9h	37 (±7.1)	31 (±2.0)	44 (±7.2)	39 (±8.4)	33 (±8.2)
9i	17 (±2.2)	15 (±2.2)	17 (±4.4)	18 (±2.5)	18 (±5.6)
9j	20 (±4.6)	17 (±1.3)	24 (±4.2)	19 (±1.1)	21 (±1.1)
9k	6.0 (±1.1)	7.9 (±1.2)	41 (±9.6)	11 (±2.3)	13 (±5.3)
10a	17 (±1.2)	10 (±6.5)	31 (±0.1)	27 (±0.4)	32 (±0.3)
10b	9.1 (±1.2)	9.0 (±6.5)	23 (±7.8)	23 (±3.3)	17 (±2.4)
10c	16 (±6.0)	12 (±5.1)	25 (±4.1)	24 (±6.5)	33 (±2.1)
10d	16 (±0.1)	19 (±2.8)	41 (±21)	33 (±4.9)	36 (±5.2)
10e	24 (±9.6)	35 (±14)	7.4 (±0.9)	48 (±3.5)	37 (±15)
10f	18 (±2.9)	19 (±2.4)	26 (±2.0)	30 (±1.4)	37 (±5.6)
10g	>100	21 (±6.3)	31 (±6.8)	36 (±7.8)	57 (±2.8)
10h	19 (±4.0)	18 (±2.1)	30 (±4.6)	31 (±5.9)	24 (±2.7)
10i	16 (±1.3)	16 (±0.3)	18 (±2.1)	19 (±2.3)	18 (±1.7)
10j	7.5 (±0.6)	9.3 (±2.9)	13 (±4.9)	18 (±4.4)	10 (±4.0)
10k	14 (±5.9)	17 (±1.8)	25 (±0.5)	31 (±2.7)	39 (±8.6)

Values are given in μM and are means of two to five experiments; standard deviation is given in parentheses.

All compounds were able to inhibit cell growth in all cell lines with GI_{50} values in the range 6-65 μM with the exception of compounds **9g** and **10g** (tryptophan dipeptides) against HBL-100 cells. We speculate that the difference in activity observed against the mammary epithelial cancer cell lines HBL-100 and T-47D might relate to the $ATB^{0,+}$ (SLC6A14, solute carrier family 6 member 14) transporter. $ATB^{0,+}$ accepts tryptophan as a substrate with high affinity and is up-regulated markedly in some types of cancer.[21,22] Diverse tryptophan derivatives inhibit $ATB^{0,+}$ causing antiproliferative effects in cell lines overexpressing the transporter such as MCF-7, ZR-75.1 and T-47D.[23] However, in HBL-100, HMEC and MCF10A cells the expression of $ATB^{0,+}$ is undetectable and the tryptophan derivatives do not affect cell growth. Our findings for **9g** and **10g** are consistent with these results.

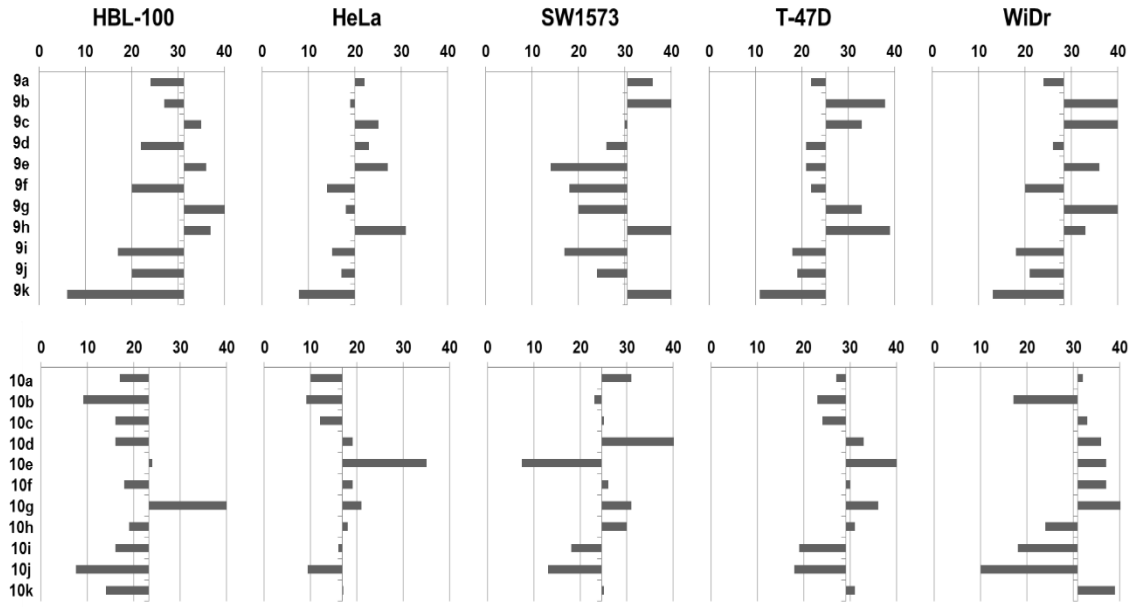

Figure 6.3. Mean graph plots for the antiproliferative activity of glutamic acid-based dipeptides 9a-k (top) and 10a-k (bottom). The middle line represents the median GI_{50} (μM) value of each set of compounds against each individual cell line.

When considering the aliphatic side chain in the α-glutamyl series **10a-d**, valine dipeptide **10b** stands out against all cell lines. However, in the γ-glutamyl set **9a-d** this trend was not observed. The antiproliferative activity of the compounds with an aromatic side chain (**9e-g** and **10e-g**) did not show clear tendency. In peptides containing a hydroxyl group, serine dipeptides (**i**) resulted more active than the corresponding threonine derivative (**h**) in all cell lines tested. Finally, proline dipeptide (**j**) in terms of activity was significant in the γ-glutamyl set, while methionine dipetide (**k**) was relevant in the γ-glutamyl series.

6.3. Conclusion

In summary, we have reported the synthesis of a novel class of *N*,*N*-dibenzylglutamic acid-based dipeptides. Commercially available amino acids were coupled to the appropriate carboxylic acid of glutamic acid to generate the α- and the γ-glutamyl series of dipeptides. The dipeptides were tested for their antiproliferative activity against five human solid tumor cell lines. Overall, the compounds show active against all cancer cell lines tested. Remarkably, some dipeptides were more active in the resistant cancer cell line WiDr than conventional anticancer drugs. From the data on growth inhibition, γ-glutamyl methionine **9k** and α-glutamyl proline **10j** were identified as lead compounds. More experiments are needed to establish the scope and limitations of *N*,*N*-dibenzylglutamic acid derivatives as novel anti-cancer agents, as well as to identify their mechanism of antiproliferative activity. Further research involving novel derivatives of *N*,*N*-dibenzylglutamic acid is in progress and will be reported elsewhere. Finally, the results obtained for the tryptophan dipeptides **9g** and **10g** in breast cancer cells merit further investigation, which remain beyond the scope of our study. In particular, their ability to inhibit the $ATB^{0,+}$ transporter.

6.4. References

1. Farber, S.; Diamond, L. K.; Mercer, R. D.; Sylvester, R. F.; Wolff, J. A.; *N. Engl. J. Med*. **1948**, *238*,787.
2. Skeel, R. T. Handbook of Cancer Chemotherapy, 7th Ed. Lippincott, Williams & Wilkins, New York. **2008**.
3. Bartlett, J. B.; Dredge, K.; Dalgleish, A. G. *Nat. Rev. Cancer* **2004**, *4*, 314.
4. Melancon, M. P.; Li, C. *Mol. Imaging*, **2011**, *10*, 28.
5. Pochini, L.; Scalise, M.; Galluccio, M.; Indiveri, C. *Front Chem*., **2014**, *2*, 61.
6. Wang, Q.; Beaumont, K. A.; Otte, N. J.; Font, J.; Bailey, C. G.; van Geldermalsen, M.; Sharp, D. M.; Tiffen, J. C.; Ryan, R. M.; Jormakka, M.; Haass, N. K.; Rasko, J. E.; Holst, J. *Int. J. Cancer **2014**, 135*, 1060.
7. Lukey, M. J.; Wilson, K. F.; Cerione, R. A. *Future. Med. Chem.* **2013**, *5*, 1685.
8. Liu, Q.; Duan, H.; Luan, J.; Yagasaki, K.; Zhang, G. *Cytotechnology* **2009,** *59*, 211.
9. Schulte, M. L.; Dawson, E. S.; Saleh, S. A.; Cuthbertson, M. L.; Manning, H. C. *Bioorg. Med. Chem. Lett.* **2015**, *25*, 113.
10. Sato, A. K.; Viswanathan, M.; Kent, R. B.; Wood, R. B. *Curr. Opin. Biotechnol*. **2006**, 17, 638.
11. Mustata, G.; Dinh, S. M. *Cri.t Rev. Ther. Drug Carrier Syst*. **2006**, *23*, 111.
12. Thundimadathil, J. *J. Amino Acids* **2012**, 967347. doi: 10.1155/2012/967347
13. Horvat, S.; Mlinarić-Majerski, K.; Glavas-Obrovac, L.; Jakas, A.; Veljković, J.; Marczi, S.; Kragol, G.; Roscić, M.; Matković, M.; Milostić-Srb. *J. Med. Chem*. **2006**, *49*, 3136.
14. Banerji, B.; Pramanik, S. K.; Pal, U.; Maiti, N. C. *Chem. Cent. J*. **2013**, *7*, 91.
15. Silveira-Dorta, G.; Martín, V. S.; Padrón, J. M. *Synlett* **2014**, *25*, 2166.
16. Monks, A.; Scudiero, D.; Skehan, P.; Shoemaker, R.; Paull, K.; Vistica, D.; Hose, C.; Langley, J.; Cronise, P.; Vaigro-Wolff, A.; Gray-Goodrich, M.; Campbell, H.; Mayo, J.; Boyd, M. *J. Natl. Cancer Inst.* **1991**, *83*, 757.
17. Dasari, S.; Tchounwou, P. B. *Eur. J. Pharmacol*. **2014**, *740*, 364.
18. Najar, I. A.; Johri, R. K. *J. Biosci*., **2014**, *39*, 139.
19. Rodriquez, M.; Taddei, M. *Synthesis* **2005**, 493.
20. Albert, R.; Danklmaier, J.; Honig, H.; Kandolf, H. *Synthesis* **1987**, 635.
21. Gupta, N.; Miyauchi, S.; Martindale, R. G.; Herdman, A. V.; Podolsky, R.; Miyake, K.; Mager, S.; Prasad, P. D.; Ganapathy, M. E.; Ganapathy, V. *Biochim. Biophys. Acta* **2005**, *1741*, 215.

22. Gupta, N.; Prasad, P. D.; Ghamande, S.; Martin, P. M.; Herdman, A. V.; Martindale, R. G.; Podolsky, R.; Mager, S.; Ganapathy, M. E.; Ganapathy, V. *Gynecol. Oncol.* **2006**, *100*, 8.
23. Karunakaran, S.; Umapathy, N. S.; Thangaraju, M.; Hatanaka, T.; Itagaki, S.; Munn, D. H.; Prasad, P. D.; Ganapathy, V. *Biochem. J.* **2008**, *414*, 343.

6.5. Experimental section

Chemistry

6.5.1 General Remarks

Reactions were performed using oven-dried glassware under an atmosphere of argon. ^{1}H NMR spectra were recorded at 400 at 298K, ^{13}C NMR spectra were recorded at 100. Chemical shifts were reported in units (ppm) by assigning TMS resonance in the ^{1}H NMR spectrum as 0.00 ppm ($CDCl_3$, 7.26 ppm). Data were reported as follows: chemical shift, multiplicity (s = singlet, d = doublet, t = triplet, q = quartet, quin = quintuplet, sex = sextet, dd = double doublet, ddd = double double doublet, m =multiplet and br = broad), coupling constant (*J* values) in Hz and integration. Chemical shifts for ^{13}C NMR spectra were recorded in ppm from tetramethylsilane as the internal standard. Using the central peak of $CDCl_3$ (77.0 ppm). Reagent-grade chemicals were obtained from diverse commercial suppliers and were used as received. Optical rotations were measured with a polarimeter at the sodium line at different temperatures in $CHCl_3$. Accurate mass (HRMS) were determined by electrospray ionization (ESI-TOF) and electronic impact (EI-TOF). Reactions were monitored using thin-layer chromatography (TLC) on aluminum packed percolated Silica Gel 60 F_{254} plates. Flash column chromatography was carried out with silica gel 60 (particle size less than 0.020 mm) by using appropriate mixtures of ethyl acetate and hexanes as eluent. Compounds were visualized by use of UV light and 2.5% phosphomolybdic acid in ethanol. All reactions involving air- or moisture-sensitive materials were carried out under Argon atmosphere. Anhydrous magnesium sulfate was used for drying solutions. Melting points were measured with micro melting point apparatus. Chemical nomenclature was generated using Chem Bio Draw Ultra 13.0.

6.5.2 General procedures and characterization of the glutamic acid‑based dipeptides

Monobenzyl ester **5** or **6** (150 mg, 0.4 mmol), *N-N*-diisopropyl ethyl amine (94.2 mg, 0.12 mL, 0.8 mmol), and TBTU (176.6 mg, 1.5 mmol) were dissolved in DMF (5 mL). The reaction mixture was stirred at room temperature for 30 min. Amino acid methyl ester (71.6 mg, 0.4 mmol) was added and stirring was continued overnight. The reaction mixture was diluted with water (25 mL) and extracted with Et2O (3 × 25 mL). The combined organic phases were dried over magnesium sulfate, filtered, and the solvent was evaporated. The crude product was purified by column chromatography (silica gel, Hexane:AcOEt 8:2 or 7:3). The title compound **9** or **10** was obtained in 70–80 % yield.

***(S)*-benzyl 2-(dibenzylamino)-5-(((*S*)-1-methoxy-1-oxopropan-2-yl)amino)-5-oxopentanoate (9a).** $[\alpha]^{D}_{25}$ = -65.6 (*c*, 1.15, $CHCl_3$). ^{1}H NMR (400 MHz, $CDCl_3$, 298 K): δ ppm: 1.31 (d,

J = 6.5 Hz), 2.07-2.13 (m, 3H), 2.30-2.37 (m, 1H), 3.37 (t, *J* = 6.4 Hz, 1H), 3.54 (ABsystem, *J* = 13.9 Hz, 2H), 3.74 (s, 3H), 3.90 (ABsystem, *J* = 13.9 Hz, 2H), 4.50 (quint, *J* = 7.0Hz, 1H), 5.24 (ABsystem, 2H), 5.79 (d, *J* = 6.4 Hz, 1H), 7.24-7.46 (m, 15H). ^{13}C NMR (100 MHz, $CDCl_3$, 298 K): δ ppm: 173.5, 172.2, 171.7, 139.3, 136.0, 128.9, 128.6, 128.5, 128.3, 127.1, 66.2, 60.4, 54.6, 52.4, 47.9, 32.8, 25.0, 18.4. HRMS (EI): m/z: calcd for $C_{30}H_{34}N_2O_5$ [M+Na$^+$]: 525.2365, found: 525.2370.

(S)*-benzyl 2-(dibenzylamino)-5-(((*S*)-1-methoxy-3-methyl-1-oxobutan-2-yl)amino)-5-oxopentanoate (9b*). $[\alpha]^D_{25}$ = -49.0 (*c*, 1.08, $CHCl_3$). ^{1}H NMR (400 MHz, $CDCl_3$, 298 K): δ ppm: 0.78 (q, *J* = 6.8 Hz, 6H), 1.96-2.02 (m, 3H), 2.23-2.31 (m, 1H), 3.29 (t, *J* = 7.5 Hz, 1H), 3.45 (ABsystem, *J* = 14.0 Hz, 2H), 3.63 (s, 3H), 3.82 (ABsystem, *J* = 14.0 Hz, 2H), 4.41 (dd, *J* = 8.3; 5.1 Hz, 1H), 5.14 (ABsystem, 2H), 5.68 (d, *J* = 8.78 Hz, 1H), 7.13-7.35 (m, 15 H). **^{13}C** NMR (100 MHz, $CDCl_3$, 298 K): δ ppm**:** 172.6, 172.2, 172.1, 139.3, 136.0, 128.9, 128.6, 128.5, 128.3, 127.1, 66.2, 60.7, 56.9, 54.6, 52.1, 33.1, 31.3, 25.2, 18.9, 17.9. HRMS (EI): m/z: calcd for $C_{32}H_{38}N_2O_5$ [M+Na$^+$]: 553.2678, found: 553.2658.

***(S)*-benzyl 2-(dibenzylamino)-5-(((*S*)-1-methoxy-4-methyl-1-oxopentan-2-yl)amino)-5-oxopentanoate (9c).** $[\alpha]^D_{25}$ = -49.5 (*c*, 1.10, $CHCl_3$). ^{1}H NMR (400 MHz, $CDCl_3$, 298 K): δ ppm: 0.82 (d, *J* = 5.7 Hz, 7H), 1.30-1.58 (m, 4H), 1.99-2.01 (m, 2H), 2.20-2.29 (m, 1H), 3.28 (m, 1H), 3.45 (ABsystem, *J* = 14.0 Hz, 2H), 3.62 (s +m, 3H + 1H), 3.82 (ABsystem, *J* = 14.0 Hz, 2H), 4.43-4.49 (m, 1H), 5.14 (ABsystem, 2H), 5.47 (d, *J* = 5.8 Hz, 1H), 7.13-7.35 (m, 13H). ^{13}C NMR (100 MHz, $CDCl_3$, 298 K): δ ppm: 173.5, 172.2, 172.0, 139.3, 136.0, 129.0, 128.6, 128.5, 128.4, 128.3, 127.1, 66.2, 60.1, 54.6, 52.2, 50.5, 41.7, 33.0, 25.2, 24.8, 22.7, 22.0. HRMS (EI): m/z: calcd for $C_{33}H_{40}N_2O_5$ [M+Na$^+$]: 567.2835, found: 567.2830.

(*S*)-benzyl 2-(dibenzylamino)-5-(((2*S*,3*R*)-1-methoxy-3-methyl-1-oxopentan-2-yl)amino)-5-oxopentanoate (9d). $[\alpha]^D_{25}$ = -39.5 (*c*, 0.93, $CHCl_3$). ^{1}H NMR (400 MHz, $CDCl_3$, 298 K): δ ppm: 1.74-1.83 (m, 1H), 1.97-2.01 (m, 7H), 2.27-2.37 (m, 3H), 3.28 (t, *J* = 7.3Hz, 1H), 3.45 (ABsystem, *J* = 13.9 Hz, 2H), 3.60 (s, 3H), 3.81 (ABsystem, *J* = 13.9 Hz, 2H), 4.51 (dd, 1H, *J* = 13.0, 7.3 Hz, 1H), 5.15 (ABsystem, 2H), 5.78 (d, *J* = 7.6Hz, 1H), 7.15-7.34 (m, 15H). ^{13}C NMR (100 MHz, $CDCl_3$, 298 K): δ ppm: 172.4, 172.2, 172.1, 139.3, 135.9, 128.9, 128.6, 128.5, 128.4, 128.3, 127.1, 66.2, 60.5, 54.6, 52.4, 51.4, 32.9, 31.7, 30.0, 25.1, 15.5. HRMS (EI): m/z: calcd for $C_{33}H_{40}N_2O_5$ [M+Na$^+$]: 567.2835, found: 567.2836.

(*S*)-benzyl 2-(dibenzylamino)-5-(((*S*)-1-methoxy-1-oxo-3-phenylpropan-2-yl)amino)-5-oxopentanoate (9e). $[\alpha]^D_{25}$ = -23.4 (*c*, 1.11, $CHCl_3$). ^{1}H NMR (400 MHz, $CDCl_3$, 298 K): δ ppm: 1.91-2.04 (m, 2H), 2.31-2.39 (m, 1H), 2.55-2.63 (m, 1H), 2.95-3.02 (m ,2H), 3.14 (dd, 1H, *J* = 5.7, 14.1 Hz), 3.46 (s, 4H), 4.73 (q, 1H, J = 6.4 Hz), 4.98 (s, 2H), 6.98-7.28 (m, 20H). ^{13}C

NMR (100 MHz, $CDCl_3$, 298 K): δ ppm: 173.2, 172.6, 172.0, 138.8, 135.9, 129.1, 128.6, 128.5, 128.5, 128.2, 127.2, 127.1, 66.2, 61.1, 54.3, 53.2, 52.3, 38.0, 32.2, 21.0. HRMS (EI): m/z: calcd for $C_{36}H_{38}N_2O_5$ [M+Na^+]: 601.2678, found: 601.2696.

(*S*)-benzyl 2-(dibenzylamino)-5-(((*S*)-3-(4-hydroxyphenyl)-1-methoxy-1-oxopropan-2-yl)amino)-5-oxopentanoate (9f). $[\alpha]^D_{25}$ = -18.9 (*c*, 1.07, $CHCl_3$). ^{1}H NMR (400 MHz, $CDCl_3$, 298 K): δ ppm: 0.86 (d, *J* = 6.8 Hz, 3H), 0.92 (t, *J* = 7.41 Hz, 3H), 1.09-1.17 (m, 1H), 1.37-1.46 (m, 1H), 1.80-1.83 (m, 1H), 2.10-2.11 (m, 3H), 2.40-2.32 (m, 1H), 3.37-3.41 (m, 1H), 3.55 (ABsystem, *J* = 13.9 Hz, 2H), 3.72 (s, 3H), 3.91 (ABsystem, *J* = 13.9 Hz, 2H), 4.55 (dd, *J* = 8.3, 5.1 Hz, 1H), 5.24 (ABsystem, 2H), 5.81 (d, *J* = 8.4 Hz, 1H), 7.23-7.46 (m, 15H). ^{13}C NMR (100 MHz, $CDCl_3$, 298 K): δ ppm: 172.5, 172.2, 171.9, 139.3, 136.0, 128.9, 128.6, 128.5, 128.4, 128.3, 127.1, 66.1, 60.7, 56.2, 54.5, 52.0, 37.9, 33.1, 25.3, 25.2, 15.4, 11.5. HRMS (EI): m/z: calcd for $C_{36}H_{38}N_2O_6$ [M^+]: 595.2808, found: 595.2802.

(*S*)-benzyl 5-(((*S*)-3-(1H-indol-2-yl)-1-methoxy-1-oxopropan-2-yl)amino)-4-(dibenzylamino)-5-oxopentanoate (9g). $[\alpha]^D_{25}$ = -32.9 (*c*, 0.93, $CHCl_3$). ^{1}H NMR (400 MHz, $CDCl_3$, 298 K): δ ppm: 2.11-2.13 (m, 2H), 2.45-2.53 (m, 1H), 2.69-2.77 (m, 1H), 3.12-3.15 (m, 1H), 3.33 (dd, *J* = 9.4, 5.6 Hz, 1H), 3.43-3.55 (m, 5H), 4.90 (q, *J* = 6.0Hz, 1H), 5.10 (d, *J* = 2.4 Hz, 2H), 6.90 (s, 1H), 7.11-7.44 (m, 18H), 7.58 (d, *J* = 8.0 Hz, 1H), 8.00 (br, 1H). ^{13}C NMR (100 MHz, $CDCl_3$, 298 K): δ ppm: 173.3, 172.7, 172.5, 138.8, 136.1, 128.6, 128.4, 128.2, 127.6, 127.1, 122.6, 122.2, 119.6, 118.6, 111.3, 109.9, 66.2, 61.1, 54.2, 52.4, 32.3, 27.7, 20.9. HRMS (EI): m/z: calcd for $C_{38}H_{39}N_3O5$ [M+Na^+]: 640.2787, found: 640.2825.

(*S*)-benzyl 2-(dibenzylamino)-5-(((2*S*,3*S*)-3-hydroxy-1-methoxy-1-oxobutan-2-yl)amino)-5-oxopentanoate (9h). $[\alpha]^D_{25}$ = -56.6 (*c*, 1.07, $CHCl_3$). ^{1}H NMR (400 MHz, $CDCl_3$, 298 K): δ ppm: 1.15 (d, *J* = 6.1, 3H), 2.11-2.18 (m, 3H), 2.40-2.45 (m, 1H), 3.39-3.42 (m, 1H), 3.54 (ABsystem, *J* = 13.9 Hz, 2H), 3.74 (s, 3H), 3.92 (s, 3H), 4.28-4.30 (m, 1H), 4.52 (dd, *J* = 8.7, 2.2 Hz), 5.24 (ABsystem, 2H), 6.13 (d, *J* = 8.4 Hz, 1H), 7.23-7.34 (m, 15H). ^{13}C NMR (100 MHz, $CDCl_3$, 298 K): δ ppm: 172.9, 172.2, 171.5, 139.3, 135.9, 128.9, 128.6, 128.5, 128.4, 128.3, 127.1, 68.0, 66.2, 60.6, 57.2, 54.5, 52.5, 33.0. HRMS (EI): m/z: calcd for $C_{31}H_{36}N_2O_6$ [M+Na^+]: 555.2471, found: 555.2460.

(*S*)-benzyl 2-(dibenzylamino)-5-(((*S*)-3-hydroxy-1-methoxy-1-oxopropan-2-yl)amino)-5-oxopentanoate (9i). $[\alpha]^D_{25}$ = -50.6 (*c*, 1.22, $CHCl_3$). ^{1}H NMR (400 MHz, $CDCl_3$, 298 K): δ ppm: 2.10-2.18 (m, 3H), 2.37-2.42 (m, 1H), 3.38 (t, *J* = 6.5Hz, 1H), 3.53 (ABsystem, *J* = 13.4 Hz, 2H), 3.76 (s, 3H), 3.83-3.92 (ABsystem + m, *J* = 13.4 Hz, 2H + 1H), 4.53-4.55 (m, 1H), 5.24 (ABsystem, 2H), 6.34 (t, *J* = 7.5 Hz, 1H), 7.22-7.46 (m, 15H). ^{13}C NMR (100 MHz, $CDCl_3$, 298 K): δ ppm: 172.7, 172.3, 170.9, 139.3, 135.9, 128.9, 128.6, 128.5, 128.3, 127.1,

66.2, 63.2, 60.4, 54.8, 54.5, 52.6, 38.6, 32.8, 24.9. HRMS (EI): m/z: calcd for $C_{30}H_{34}N_2O_6$ [M+Na^+]: 541.2319, found: 541.2319.

(*S*)-methyl 1-((*S*)-5-(benzyloxy)-4-(dibenzylamino)-5-oxopentanoyl)pyrrolidine-2-carboxylate (9j). $[\alpha]^D_{25}$ = -100.3 (*c*, 1.04, $CHCl_3$). ^{1}H NMR (400 MHz, $CDCl_3$, 298 K): δ ppm: 1.89-2.41 (m, 8H), 3.29-3.34 (m, 1H), 3.40-3.60m, 4H), 3.71+3.73 (s + s, 3H + 1H), 3.88 (ABsystem, *J* = 13.7 Hz, 2H), 4.31-4.34 (m, 1H), 5.24 (ABsystem, 2H), 7.24-7.46 (m, 15H). ^{13}C NMR (100 MHz, $CDCl_3$, 298 K): δ ppm: 172.9, 172.44, 170.8, 139.5, 136.1, 129.0, 128.6, 128.5, 128.3, 128.2, 127.0, 66.1, 60.2, 58.5, 54.5, 52.1, 46.7, 30.7, 29.1, 24.7, 23.9. HRMS (EI): m/z: calcd for $C_{32}H_{36}N_2O_5$ [M+Na^+]: 551.2522, found: 551.2525.

(*S*)-benzyl 2-(dibenzylamino)-5-(((*S*)-1-methoxy-4-(methylthio)-1-oxobutan-2-yl)amino)-5-oxopentanoate (9k). $[\alpha]^D_{25}$ = -37.4 (*c*, 1.09, $CHCl_3$). ^{1}H NMR (400 MHz, $CDCl_3$, 298 K): δ ppm: 0.86 (d, *J* = 6.8 Hz, 3H), 0.92 (t, *J* = 7.4 Hz, 3H), 109-1.17 (m, 1H), 1.37-1.46 (m, 1H), 1.80-1.83 (m, 1H), 2.10-2.11 (m, 3H), 2.32-2.40 (m, 1H), 3.37-3.41 (m, 1H), 3.55 (ABsystem, *J* = 13.9 Hz, 2H), 3.72 (s, 3H), 3.91 (ABsystem, *J* = 13.9 Hz, 2H), 4.55 (dd, *J* = 5.1, 8.3 Hz, 1H), 5.24 (ABsystem, 2H), 5.81 (d, *J* = 8.4 Hz, 1H), 7.23-7.46 (m, 15H). ^{13}C NMR (100 MHz, $CDCl_3$, 298 K): δ ppm: 172.5, 172.2, 171.9, 139.3, 136.0, 128.9, 128.6, 128.5, 128.4, 128.3, 127.1, 66.1, 60.7, 56.2, 54.5, 52.0, 37.9, 33.1, 25.3, 25.2, 15.4, 11.5. HRMS (EI): m/z: calcd for $C_{32}H_{38}N_2O_5S$ [M+Na^+]: 585.2399, found: 585.2397.

(*S*)-benzyl 4-(dibenzylamino)-5-(((*S*)-1-methoxy-1-oxopropan-2-yl)amino)-5-oxopentanoate (10a). $[\alpha]^D_{25}$ = -8.4 (*c*, 1.26, $CHCl_3$). ^{1}H NMR (400 MHz, $CDCl_3$, 298 K): δ ppm: 1.44 (d, *J* = 6.8 Hz, 3H), 2.14-2.16 (m, 2H), 2.43-2.51 (m, 1H), 2.71-2.79 (m, 1H), 3.17-3.19 (m, 1H), 3.64-3.78 (m, 8H), 4.56 (quint, *J* = 7.3 Hz, 1H), 5.11 (s, 3H), 7.26-7.40 (m, 16H). ^{13}C NMR (100 MHz, $CDCl_3$, 298 K): δ ppm: 173.2, 172.6, 138.9, 136.0, 128.9, 128.6, 128.5, 128.2, 127.3, 66.2, 61.0, 54.4, 54.2, 50.5, 42.1, 32.2, 24.9, 22.6, 21.9, 20.7. HRMS (EI): m/z: calcd for $C_{30}H_{34}N_2O_5$ [M+Na^+]: 525.2365, found: 525.2354.

(*S*)-benzyl 4-(dibenzylamino)-5-(((*S*)-1-methoxy-3-methyl-1-oxobutan-2-yl)amino)-5-oxopentanoate (10b). $[\alpha]^D_{25}$ = -11.7 (*c*, 1.07, $CHCl_3$). ^{1}H NMR (400 MHz, $CDCl_3$, 298 K): δ ppm: 0.80 (d, *J* = 6.8 Hz, 3H), 0.85 (d, *J* = 6.8 Hz, 3H), 2.01-2.12 (m, 3H), 2.35-2.43 (m, 1H), 2.62-2.70 (m, 1H), 3.10 (dd, *J* = 8.5, 4.6 Hz, 1H), 3.59-3.71(m, 8H), 4.42 (dd, *J* = 8.7, 4.7, 1H), 5.00 (ABsystem, *J* = 2H), 7.18-7.33 (m 16H). ^{13}C NMR (100 MHz, $CDCl_3$, 298 K): δ ppm: 173.2, 172.7, 172.2, 139.0, 138.8, 136.8, 136.0, 129.0, 128.6, 128.5, 128.4, 128.2, 127.3, 66.2, 61.2, 57.1, 54.4, 54.0, 52.1, 32.3, 31.4, 21.0, 19.1, 18.0. HRMS (EI): m/z: calcd for $C_{32}H_{38}N_2O_5$ [M+Na^+]: 553.2678, found: 553.2678.

(*S*)-benzyl 4-(dibenzylamino)-5-(((*S*)-1-methoxy-4-methyl-1-oxopentan-2-yl)amino)-5-oxopentanoate (10c). $[\alpha]^{D}_{25}$ = 17.3 (*c*, 0.91, $CHCl_3$). ^{1}H NMR (400 MHz, $CDCl_3$, 298 K): δ ppm: 0.9-0.96 (d + d, *J* = 5.9 + 5.9 Hz, 6H), 1.52-1.69 (m , 3H), 2.09-2.15 (m, 2H), 2.43-2.51 (m, 1H), 2.72-2.79 (m, 1H), 3.19 (dd, *J* = 8.0, 5.1 Hz, 1H), 3.77-3.65 (m, 8H), 4.56-4.64 (m, 1H), 5.10 (ABsystem, 2H), 7.15 (d, *J* = 8.8 Hz, 1H), 7.26-7.39 (m, 15 H). ^{13}C NMR (100 MHz, $CDCl_3$, 298 K): δ ppm: 173.2, 172.6, 138.9, 136.0, 128.9, 128.6, 128.5, 128.2, 127.3, 66.2, 61.0, 54.4, 52.2, 50.5, 42.1, 32.2, 24.9, 22.6, 21.9, 20.7. HRMS (EI): m/z: calcd for $C_{33}H_{40}N_2O_5$ [M+Na^+]: 567.2835, found: 567.2836.

(*S*)-benzyl 4-(dibenzylamino)-5-(((2*S*,3*R*)-1-methoxy-3-methyl-1-oxopentan-2-yl)amino)-5-oxopentanoate (10d). $[\alpha]^{D}_{25}$ = -6.4 (*c*, 1.02, $CHCl_3$). ^{1}H NMR (400 MHz, $CDCl_3$, 298 K): δ ppm: 0.78-0.85 (m, 6H), 1.01-1.09 (m, 1H), 1.32-1.36 (m, 1H), 1.78-1.83 (m, 1H), 2.01-2.09 (m, 1H), 2.35-2.43 (m, 1H), 2.62-2.70 (m, 1H), 3.10 (dd, *J* = 8.3, 4.5 Hz, 1H), 3.58-3.70 (m, 8H), 4.46 (dd, *J* = 8.5, 4.8 Hz, 1H), 5.00 (ABsystem, 2H), 7.17-7.32 (m, 15H). ^{13}C NMR (100 MHz, $CDCl_3$, 298 K): δ ppm: 173.2, 172.6, 172.1, 139.0, 138.8, 136.0, 128.9, 128.6, 128.5, 128.4, 128.2, 127.3, 66.2, 61.1, 56.4, 54.3, 52.0, 38.2, 32.4, 25.4, 20.9, 15.6, 11.6. HRMS (EI): m/z: calcd for $C_{33}H_{40}N_2O_5$ [M+Na^+]: 94.0419, found: 94.0415.

(*S*)-benzyl 4-(dibenzylamino)-5-(((*S*)-1-methoxy-1-oxo-3-phenylpropan-2-yl)amino)-5-oxopentanoate (10e). $[\alpha]^{D}_{25}$ = +3.3 (*c*, 1.05, $CHCl_3$). ^{1}H NMR (400 MHz, $CDCl_3$, 298 K): δ ppm: 2.01-2.11 (m, 3H), 2.28-2.36 (m, 1H), 3.07 (ABXsystem, *J* = 14.0, 6.0 Hz, 2H), 3.35-3.38 (m, 1H), 3.55 (ABsystem, *J* = 13.9Hz, 2H), 3.72 (s, 3H), 3.90 (ABsystem, *J* = 13.9Hz, 2H), 4.81 (q, *J* = 5.9 Hz, 1H), 5.26 (ABsystem, 2H), 5.74 (d, *J* = 7.1 Hz, 1H), 7.07 (d, *J = 7.2 Hz, 2H), 7.23-7.44 (m, 18H).* ^{13}C NMR (100 MHz, $CDCl_3$, 298 K): δ ppm: 172.1, 172.0, 171.8, 139.3, 135.9, 129.2, 128.9, 128.6, 128.5, 128.4, 127.1, 66.2, 60.5, 54.5, 53.0, 52.2, 37.9, 33.0, 25.1. HRMS (EI): m/z: calcd for $C_{36}H_{38}N_2O_5$ [M+Na^+]: 601.2678, found: 601.2684.

(*S*)-benzyl 4-(dibenzylamino)-5-(((*S*)-3-(4-hydroxyphenyl)-1-methoxy-1-oxopropan-2-yl)-amino)-5-oxopentanoate (10f). $[\alpha]^{D}_{25}$ = -1.8 (*c*, 0.91, $CHCl_3$). ^{1}H NMR (400 MHz, $CDCl_3$, 298 K): δ ppm: 1.94-2.03 (m, 3H), 2.30-2.38 (m, 1H), 2.55-2.63 (m, 1H), 2.86-2.92 (m, 1H), 3.02-3.08 (m, 2H), 3.48-3.65 (m, 7H), 4.68 (q, *J* = 6.7 Hz, 1H), 4.99 (ABsystem, 2H), 5.67 (br, 1H), 6.53 (d, *J* = 8.1 Hz, 2H), 6.83 (d, *J* = 8.1 Hz, 2H), 7.13-7.26 (m, 17H). ^{13}C NMR (100 MHz, $CDCl_3$, 298 K): δ ppm: 173.3, 172.8, 172.1, 155.1, 138.7, 135.9, 130.2, 128.9, 128.6, 128.5, 128.4, 128.2, 127.2, 115.5, 66.3, 61.2, 54.3, 53.4, 52.3, 37.3, 32.2, 20.9. HRMS (EI): m/z: calcd for $C_{36}H_{38}N_2O_6$ [M+Na^+]: 617.2628, found: 617.2631.

(*S*)-benzyl 5-(((*S*)-3-(1H-indol-2-yl)-1-methoxy-1-oxopropan-2-yl)amino)-4-(dibenzyl-amino)-5-oxopentanoate (10g). $[\alpha]^{D}_{25}$ = +11.3 (*c*, 0.93, $CHCl_3$). ^{1}H NMR (400 MHz, $CDCl_3$,

298 K): δ ppm: 2.11-2.13 (m, 2H), 2.45-2.53 (m, 1H), 2.69-2.77 (m, 1H), 3.12-3.15 (m, 1H), 3.33 (dd, *J* = 9.4, 5.6 Hz, 1H), 3.43-3.55 (m, 5H), 4.90 (q, *J* = 6.0Hz, 1H), 5.10 (d, *J* = 2.4 Hz, 2H), 6.90 (s, 1H), 7.11-7.44 (m, 18H), 7.58 (d, *J* = 8.0 Hz, 1H), 8.00 (br, 1H). ^{13}C NMR (100 MHz, $CDCl_3$, 298 K): δ ppm: 173.3, 172.7, 172.5, 138.8, 136.1, 128.6, 128.4, 128.2, 127.6, 127.1, 122.6, 122.2, 119.6, 118.6, 111.3, 109.9, 66.2, 61.1, 54.2, 52.4, 32.3, 27.7, 20.9. HRMS (EI): m/z: calcd for $C_{38}H_{39}N_3O5$ [M+Na^+]: 640.2787, found: 640.2825.

(*S*)-benzyl 4-(dibenzylamino)-5-(((2*S*,3*S*)-3-hydroxy-1-methoxy-1-oxobutan-2-yl)amino)-5-oxopentanoate (10h). $[\alpha]^D_{25}$ = -11.2 (*c*, 1.38, $CHCl_3$). ^{1}H NMR (400 MHz, $CDCl_3$, 298 K): δ ppm: 1.21 (d, *J* = 6.2 Hz, 3H), 2.14-2.21 (m, 3H), 2.46-2.54 (m, 1H), 2.72-2.80 (m, 1H), 2.64 (dd, *J* = 8.2, 4.8 Hz, 1H), 3.69-3.81 (m, 7H), 4.38 (bt, 1H), 4.57 (dd, *J* = 8.9, 2.0 Hz, 1H), 5.11 (ABsystem, 2H), 7.25-7.45 (m, 15H), 7.62 (d, *J* = 8.9 Hz, 1H). ^{13}C NMR (100 MHz, $CDCl_3$, 298 K): δ ppm: 173.5, 173.2, 171.2, 138.8, 136.0, 129.0, 128.7, 128.6, 128.5, 128.2, 127.4, 68.2, 66.2, 61.2, 57.2, 54.4, 52.5, 32.3, 20.9, 20.3. HRMS (EI): m/z: calcd for $C_{31}H_{36}N_2O6$ [M+Na^+]: 555.2471, found: 555.2504.

(*S*)-benzyl 4-(dibenzylamino)-5-(((*S*)-3-hydroxy-1-methoxy-1-oxopropan-2-yl)amino)-5-oxopentanoate (10i). $[\alpha]^D_{25}$ = +1.0 (*c*, 1.35, $CHCl_3$). ^{1}H NMR (400 MHz, $CDCl_3$, 298 K): δ ppm: 2.13-2.19 (m, 2H), 2.44-2.52 (m, 1H), 2.70-2.78 (m, 2H), 3.22 (dd, *J* = 7.8, 4.7 Hz, 1H), 3.64-3.80 (m, 8H), 3.93-4.02 (m, 2H), 4.60-4.63 (m, 1H), 5.11 (ABsystem, 2H), 7.27-7.42 (m, 15H), 7.79 (d, *J* = 7.2 Hz, 1H). ^{13}C NMR (100 MHz, $CDCl_3$, 298 K): δ ppm: 173.4, 173.2, 170.6, 138.9, 138.8, 135.9, 128.9, 128.8, 128.6, 128.5, 128.2, 127.4, 66.3, 63.8, 61.1, 54.8, 54.4, 52.7, 32.2, 20.5. HRMS (EI): m/z: calcd for $C_{30}H_{34}N_2O_6$ [M+Na^+]: 541.2315, found: 541.2313.

(*S*)-methyl 1-((*S*)-5-(benzyloxy)-2-(dibenzylamino)-5-oxopentanoyl)pyrrolidine-2-carboxylate (10j). $[\alpha]^D_{25}$ = -28.4 (*c*, 0.97, $CHCl_3$). ^{1}H NMR (400 MHz, $CDCl_3$, 298 K): δ ppm: 1.71-1.90 (m, 3H), 2.07-2.21 (m, 3H), 2.38-2.25 (m, 1H), 2.65-2.72 (m, 1H), 2.92-3.06 (m, 2H), 3.58 (t, *J* = 6.7 Hz, 1H), 3.71 (s, 3H), 3.77 (ABsystem, *J* = 14.1 Hz, 2H), 3.91 (ABsystem, *J* = 14.1 Hz, 2H), 4.50 (q, *J* = 4.1 Hz, 1H), 5.09 (ABsystem, *J* = 12.2, 5.0 Hz), 7.25-7.37 (m, 15H). ^{13}C NMR (100 MHz, $CDCl_3$, 298 K): δ ppm: 173.0, 172.7, 171.7, 139.9, 135.9, 129.2, 128.9, 128.6, 128.5, 128.2, 127.1, 66.2, 60.5, 54.5, 53.0, 52.2, 37.9, 33.0, 25.1. HRMS (EI): m/z: calcd for $C_{32}H_{36}N_2O_5$ [M+Na^+]: 551.2522, found: 551.2525.

***(S)*-benzyl 4-(dibenzylamino)-5-(((*S*)-1-methoxy-4-(methylthio)-1-oxobutan-2-yl)amino)-5-oxopentanoate (10k).** $[\alpha]^D_{25}$ = -1.6 (*c*, 1.09, $CHCl_3$). ^{1}H NMR (400 MHz, $CDCl_3$, 298 K): δ ppm: 1.65-1.68 (m, 1H), 2.05-2.18 (m, 7H), 2.37-2.51 (m, 3H), 2.72-2.80 (m, 1H), 3.18-.22 (m, 1H), 3.67 (ABsystem, *J* = 14.3 Hz, 2H), 3.75-3.78 (m, 5H), 4.65 (q, *J* = 6.8 Hz, 1H), 5.11 (ABsystem, 2H), 7.26-7.41 (m, 15H), 7.50 (d, *J* = 7.7 Hz, 1H). ^{13}C NMR (100 MHz, $CDCl_3$,

298 K): δ ppm: 173.2, 172.8, 172.2, 138.7, 136.0, 128.6, 128.5, 128.2, 127.4, 66.2, 61.0, 54.4, 52.5, 51.4, 32.3, 32.0, 30.0, 20.6, 15.4. **HRMS (EI): m/z: calcd for** $C_{32}H_{38}N_2O_5S$ [M+Na^+]: 585.2399, found: 585.2391.

Biology

6.5.3 General Remarks

Cells were maintained in 25 cm^2 culture flasks in RPMI 1640 supplemented with 5% heat inactivated fetal calf serum and 2 mM L-glutamine in a 37 ºC, 5% CO_2, 95% humidified air incubator. Exponentially growing cells were trypsinized and re-suspended in antibiotic containing medium (100 units penicillin G and 0.1 mg of streptomycin per mL). Single cell suspensions displaying >97% viability by trypan blue dye exclusion were subsequently counted. After counting, dilutions were made to give the appropriate cell densities for inoculation onto 96-well microtiter plates. Cells were inoculated in a volume of 100 µL per well at densities of 10 000 (HBL-100, HeLa and SW1573), 15 000 (T-47D), and 20 000 (WiDr) cells per well, based on their doubling times.

6.5.4 Chemosensitivity testing

Cells were inoculated onto 96-well microtiter plates in a volume of 100 µL per well at densities of 10,000 (HBL-100, HeLa and SW1573), 15,000 (T-47D), and 20,000 (WiDr) cells per well, based on their doubling times. Compounds **9**–**10** were initially dissolved in DMSO at 400 times the desired final maximum test concentration. Control cells were exposed to an equivalent concentration of DMSO (0.25 % v/v, negative control). Each agent was tested in triplicate at different dilutions in the range of 1–100 µM. The drug treatment started on day 1 after plating. Drug incubation times were 48 h, after which cells were precipitated with 25 µL ice-cold TCA (50 % w/v) and fixed for 60 min at 4 °C. Then, the SRB assay was performed. The optical density (OD) of each well was measured at 492 nm, using BioTek's PowerWave XS Absorbance Microplate Reader. Values were corrected for background OD from wells only containing medium. The antiproliferative activity for each compound, expressed as GI50 values, was calculated according to NCI formulas.[16]

6.6 ^{1}H and ^{13}C NMR spectra

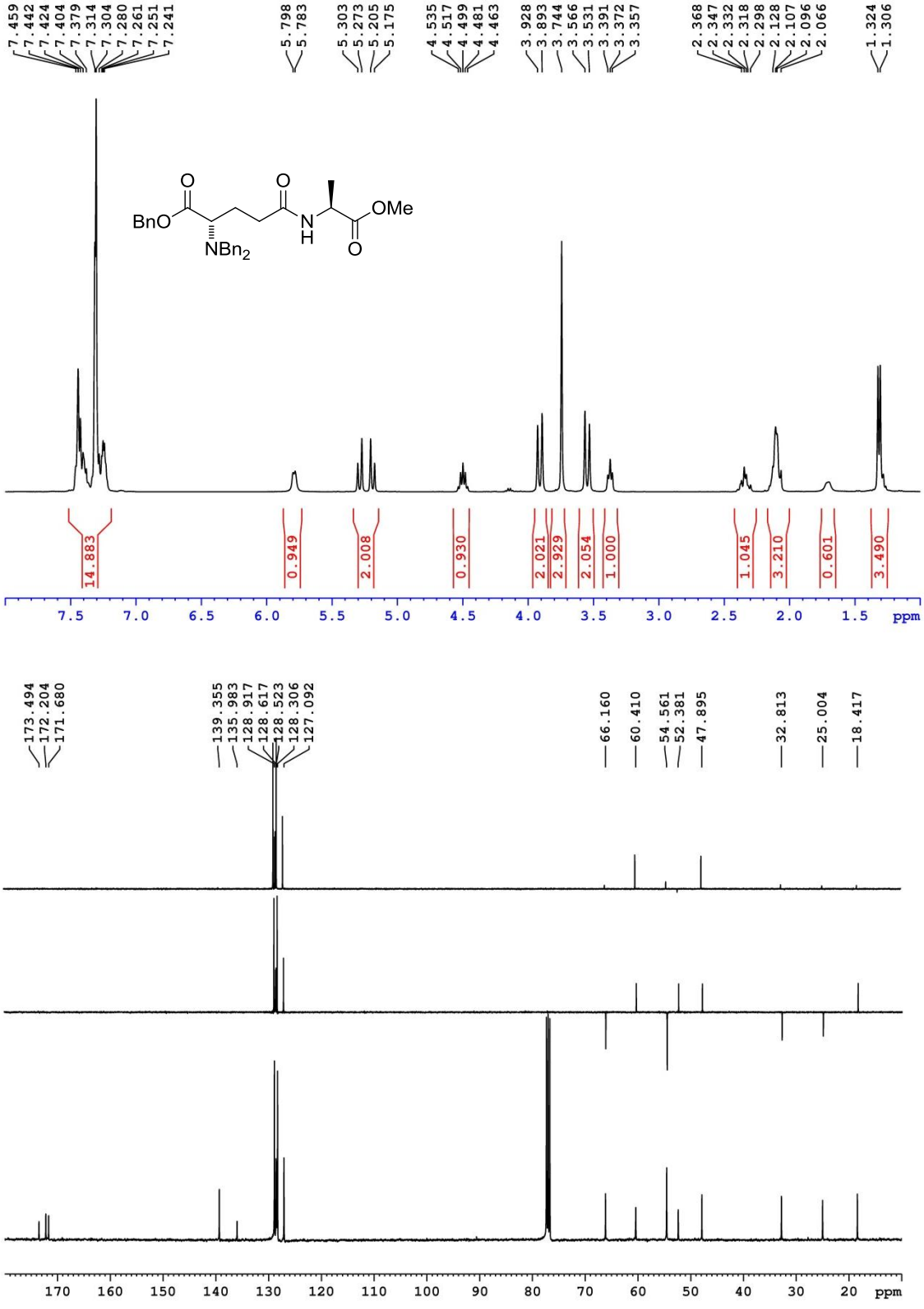

Figure S1. ^{1}H (400 MHz) and ^{13}C (100 MHz) NMR spectra in $CDCl_3$ of 9a.

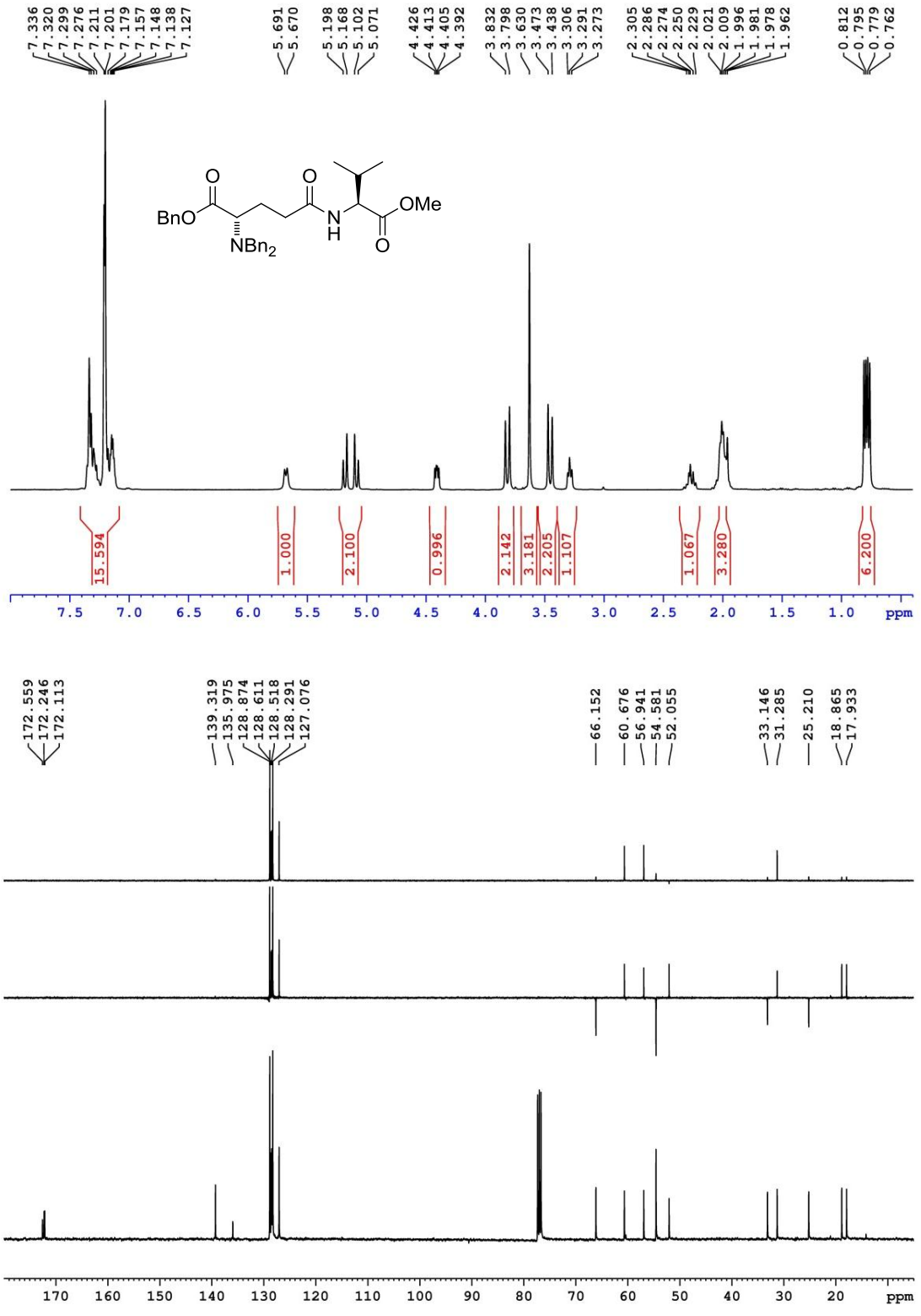

Figure S2. **^{1}H (400 MHz) and ^{13}C (100 MHz) NMR spectra in $CDCl_3$ of 9b.**

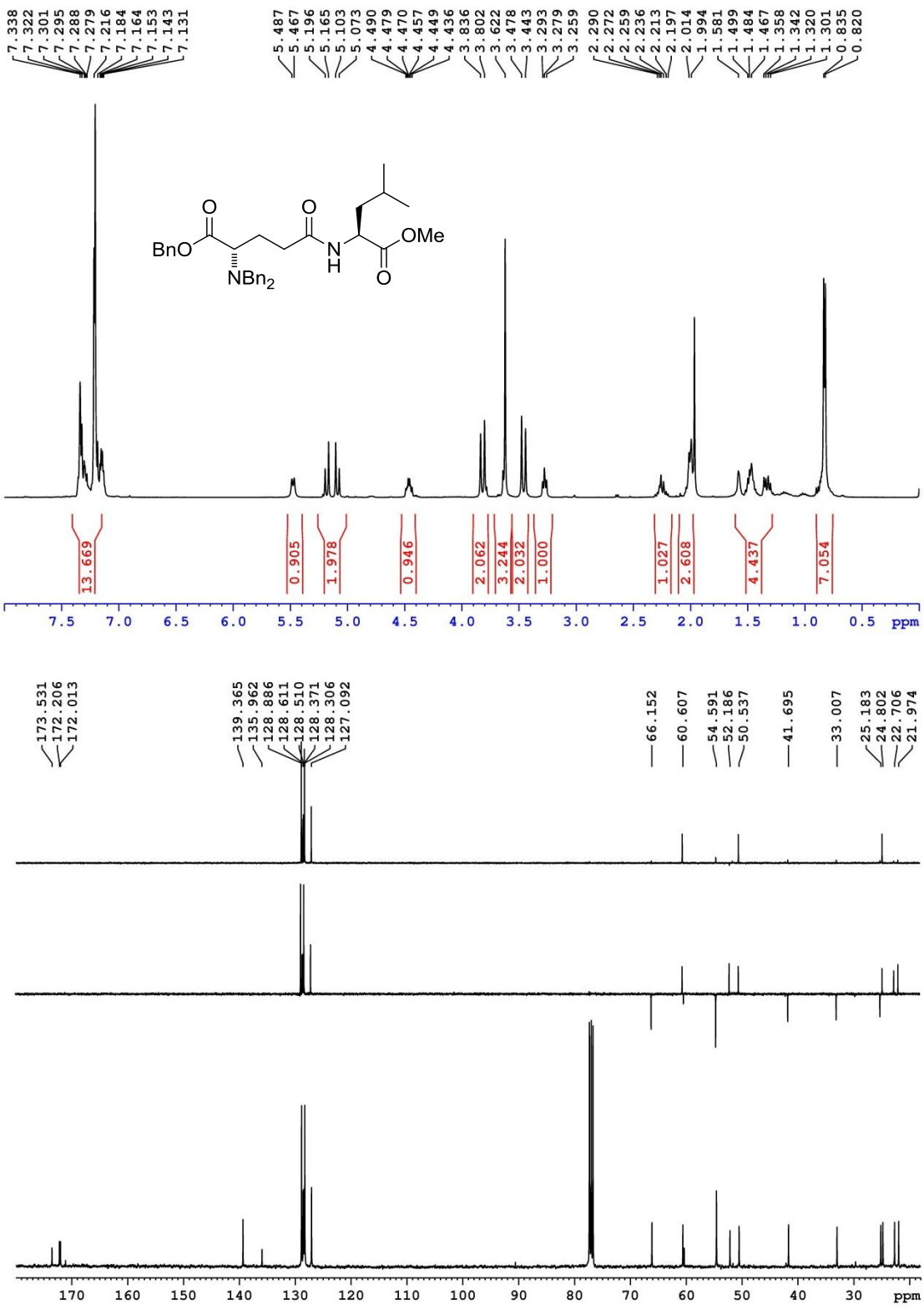

Figure S3. **^{1}H (400 MHz) and ^{13}C (100 MHz) NMR spectra in $CDCl_3$ of 9c.**

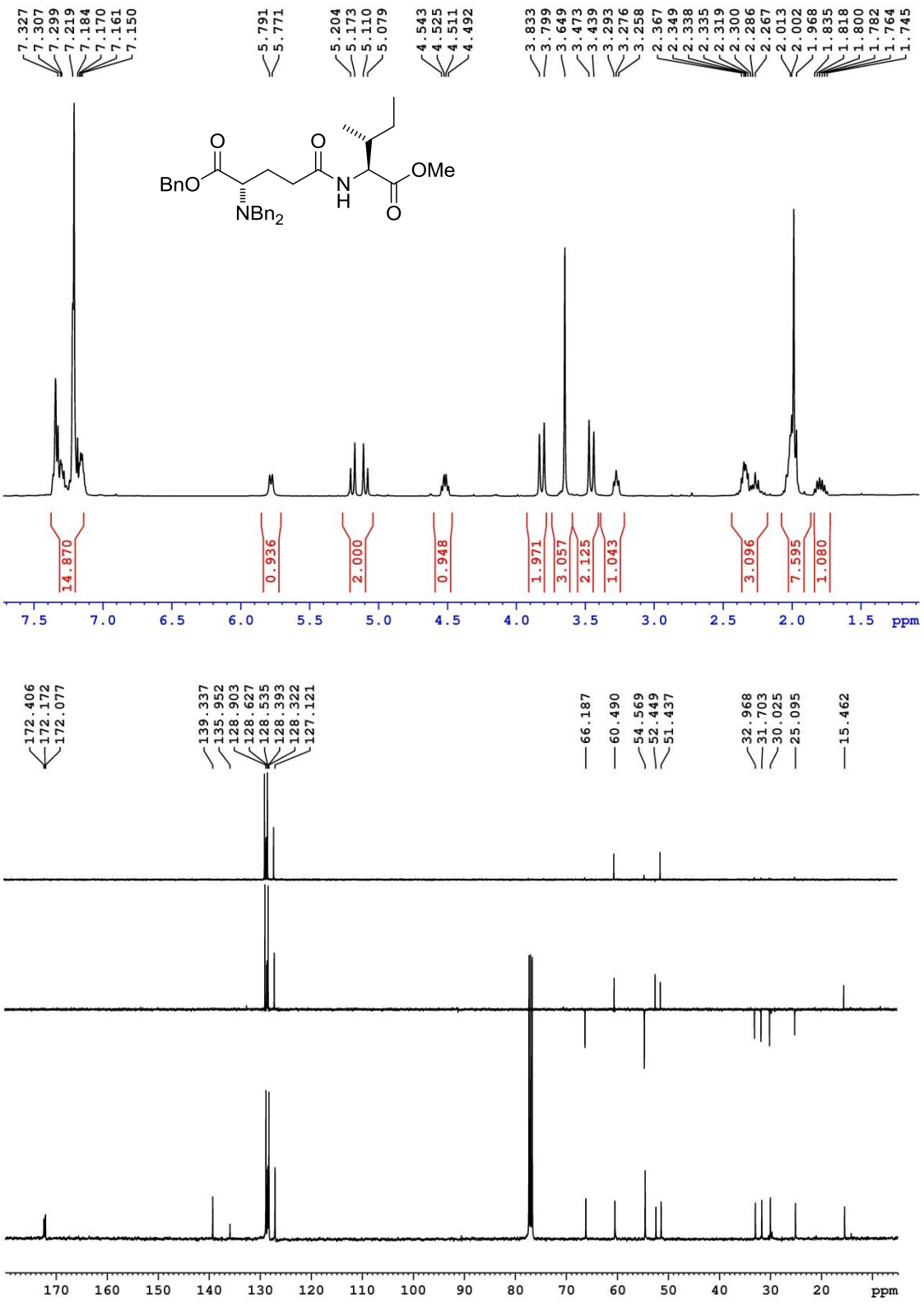

Figure S4. **^{1}H (400 MHz) and ^{13}C (100 MHz) NMR spectra in $CDCl_3$ of 9d.**

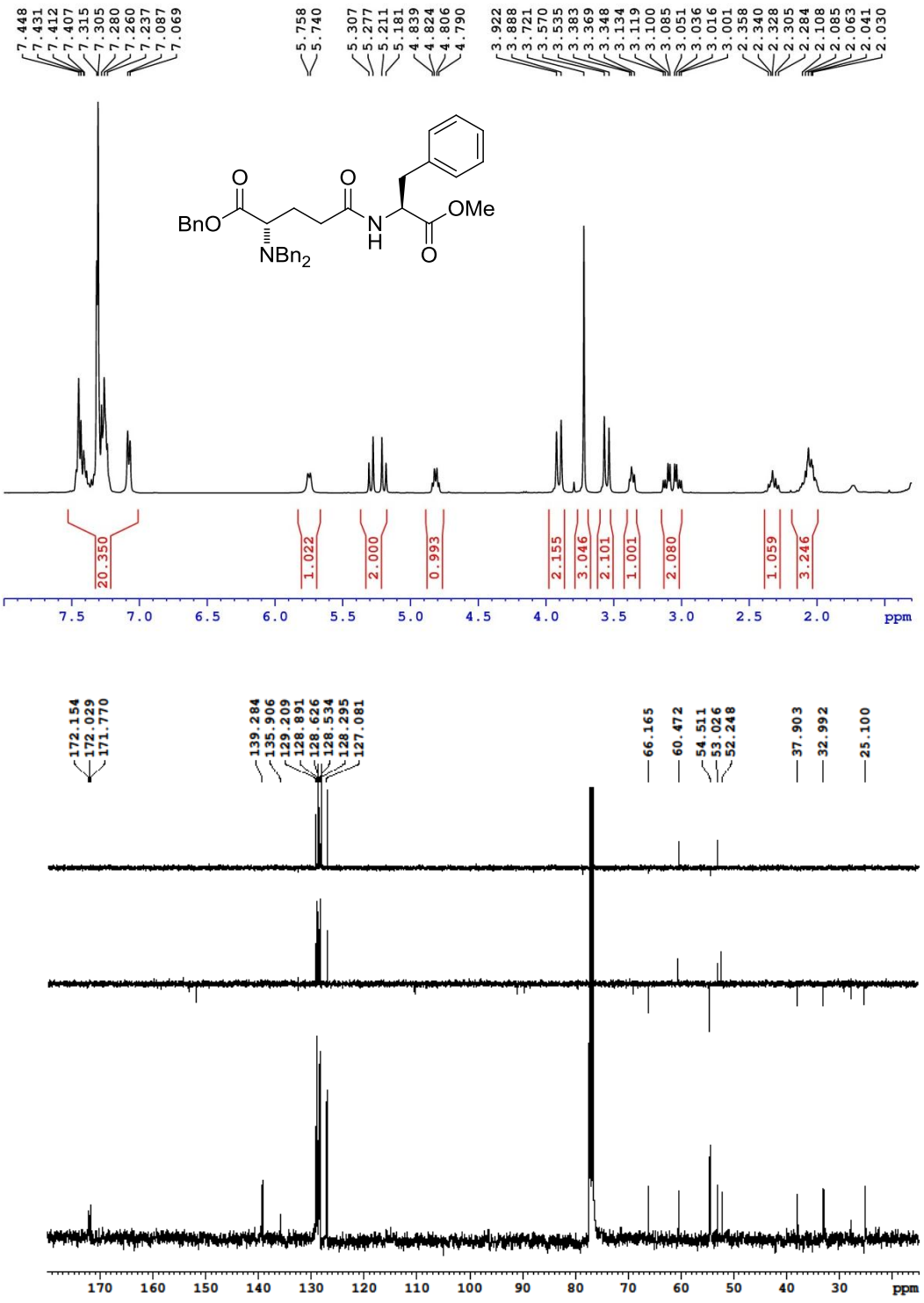

Figure S5. **^{1}H (400 MHz) and ^{13}C (100 MHz) NMR spectra in $CDCl_3$ of 9e.**

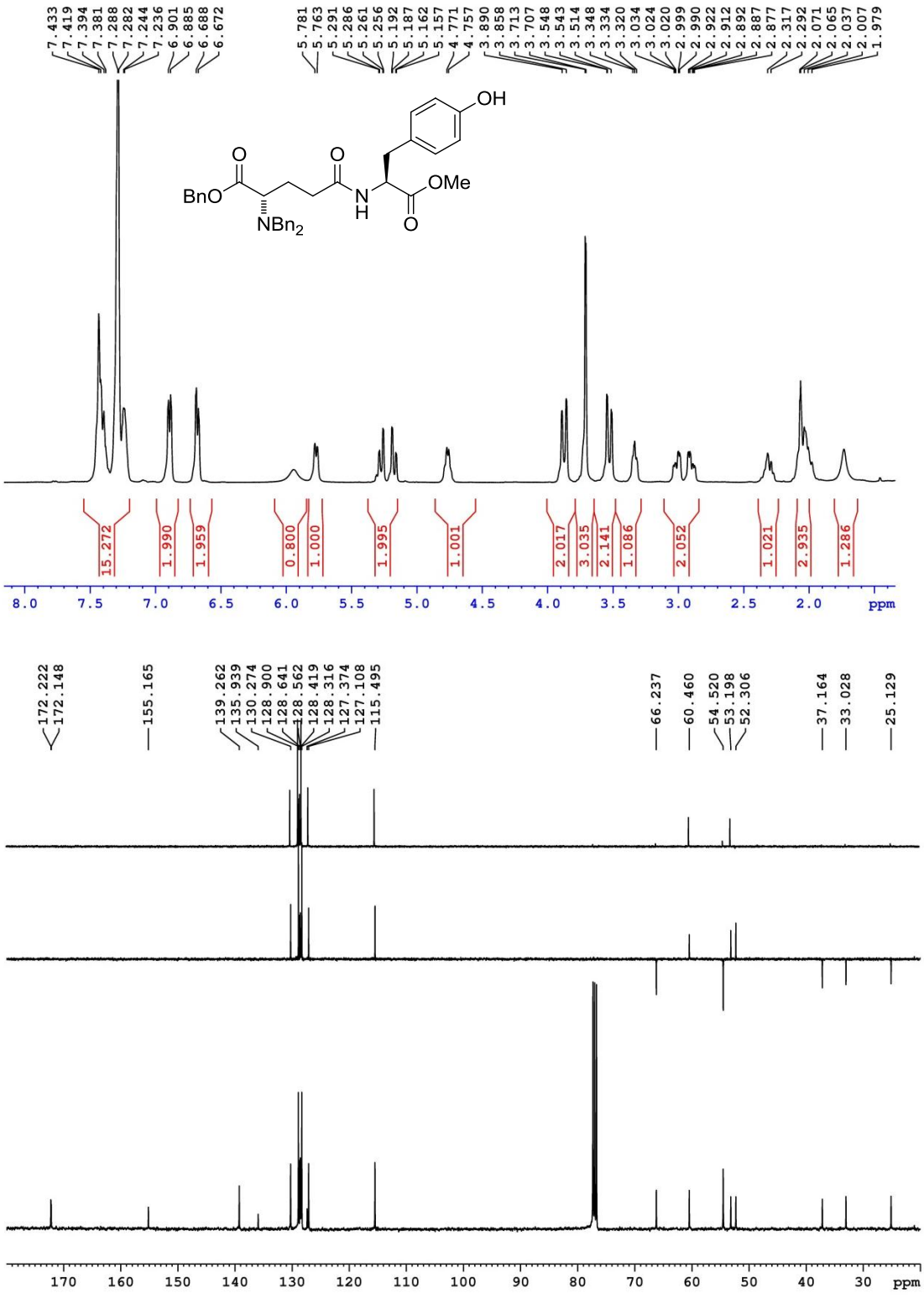

Figure S6. **^{1}H (400 MHz) and ^{13}C (100 MHz) NMR spectra in $CDCl_3$ of 9f.**

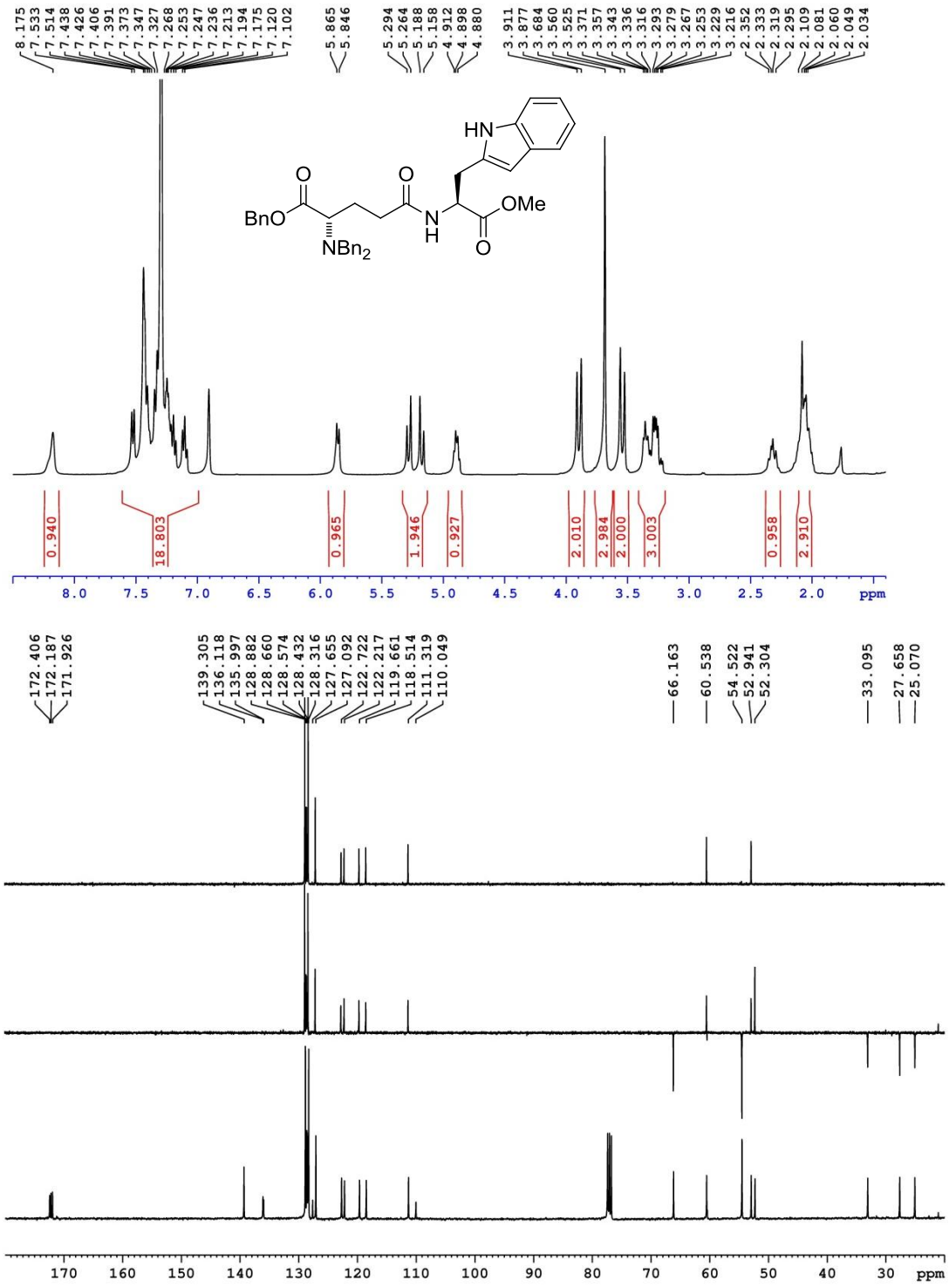

Figure S7. ^{1}H **(400 MHz) and** ^{13}C **(100 MHz) NMR spectra in** $CDCl_3$ **of 9g.**

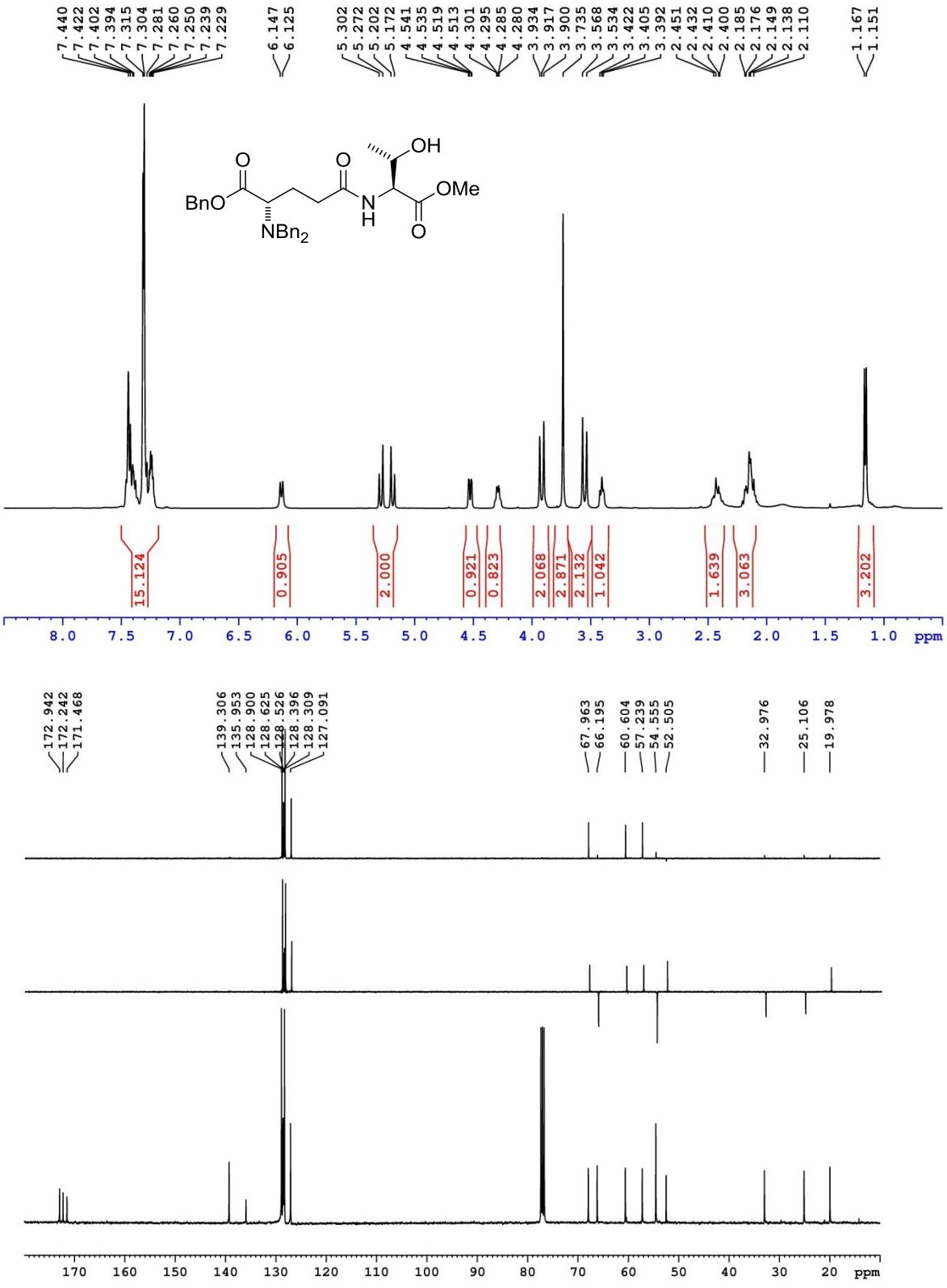

Figure S8. **^{1}H (400 MHz) and ^{13}C (100 MHz) NMR spectra in $CDCl_3$ of 9h.**

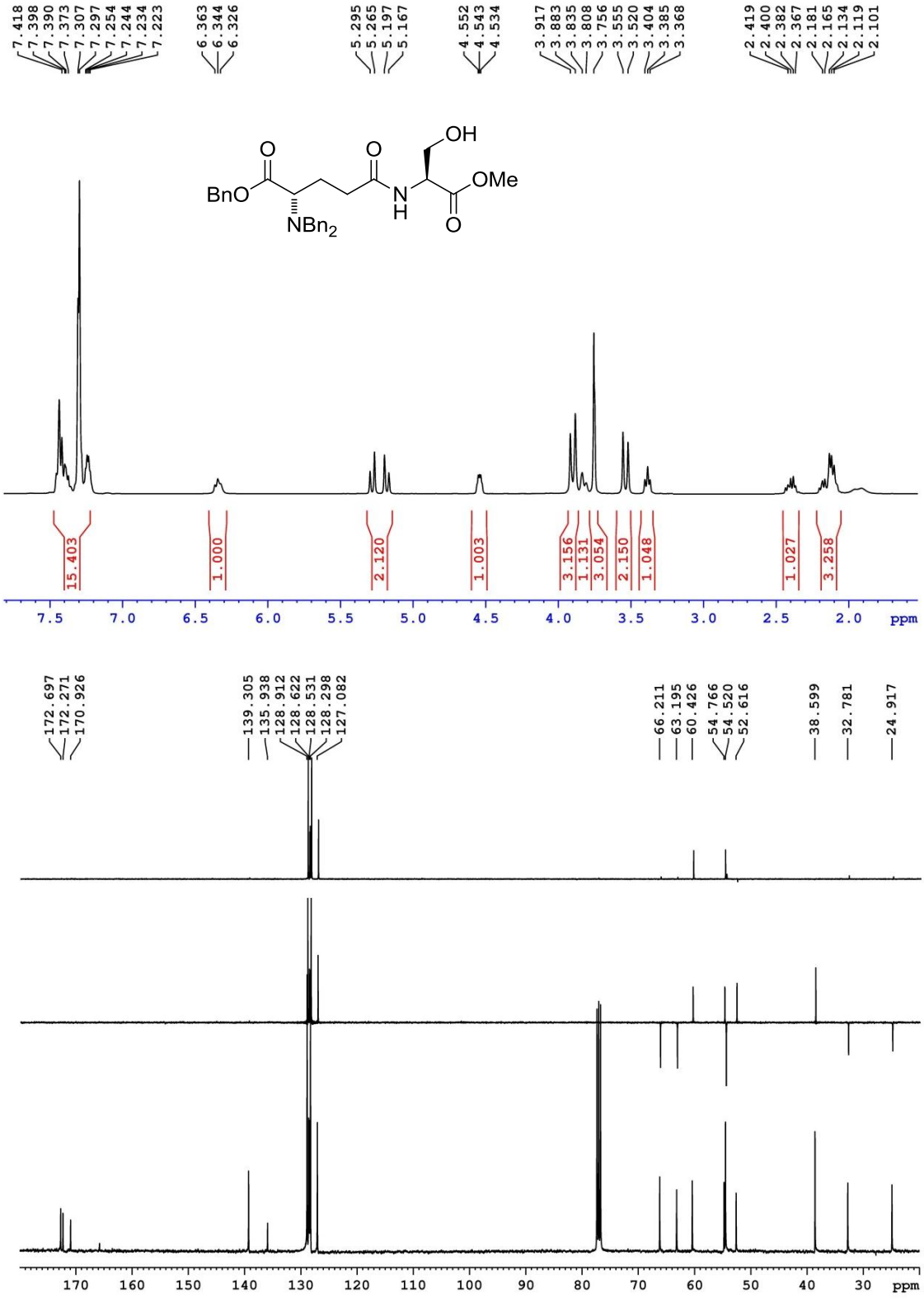

Figure S9. **^{1}H (400 MHz) and ^{13}C (100 MHz) NMR spectra in $CDCl_3$ of 9i.**

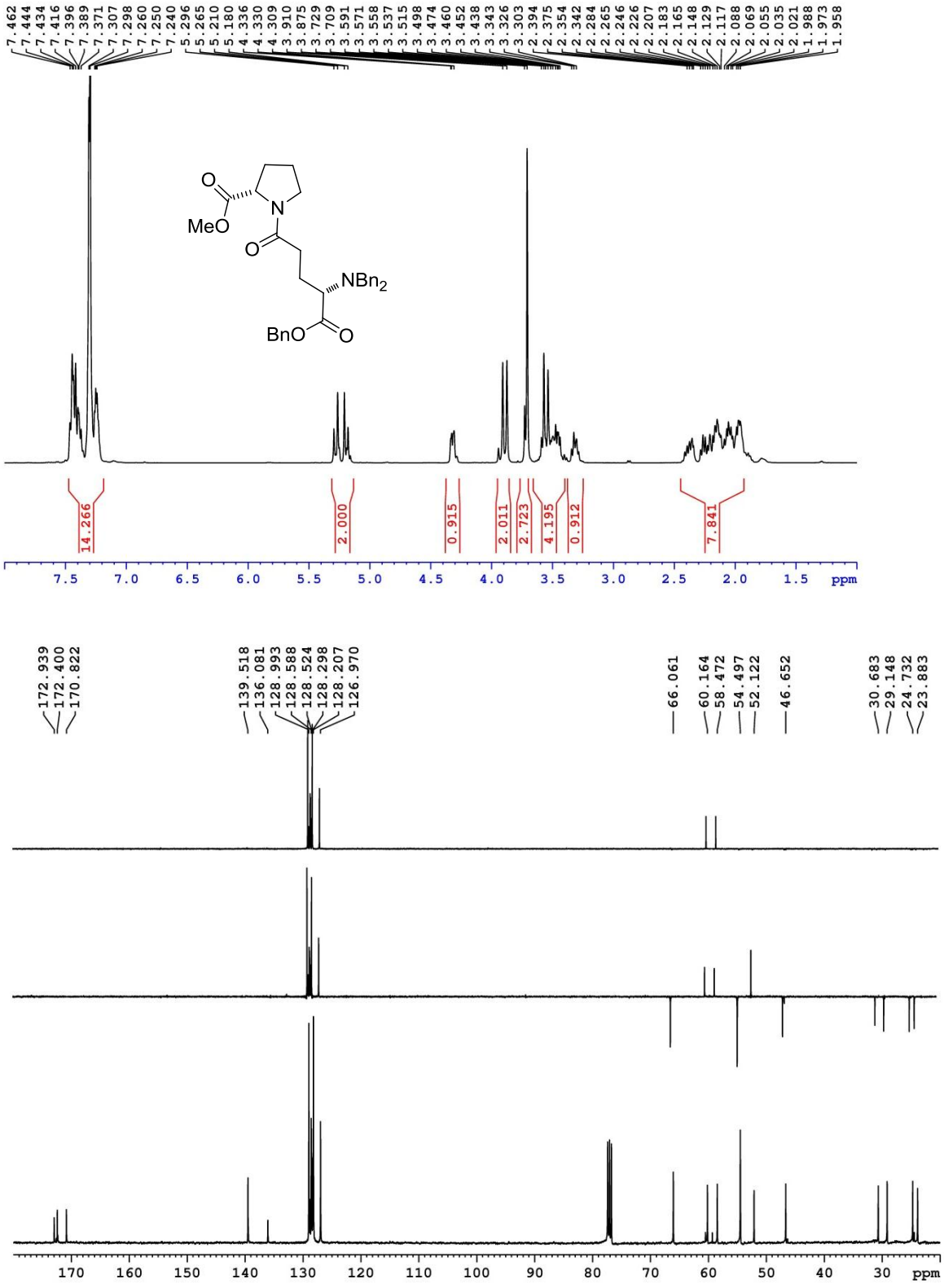

Figure S10. **^{1}H (400 MHz) and ^{13}C (100 MHz) NMR spectra in $CDCl_3$ of 9j.**

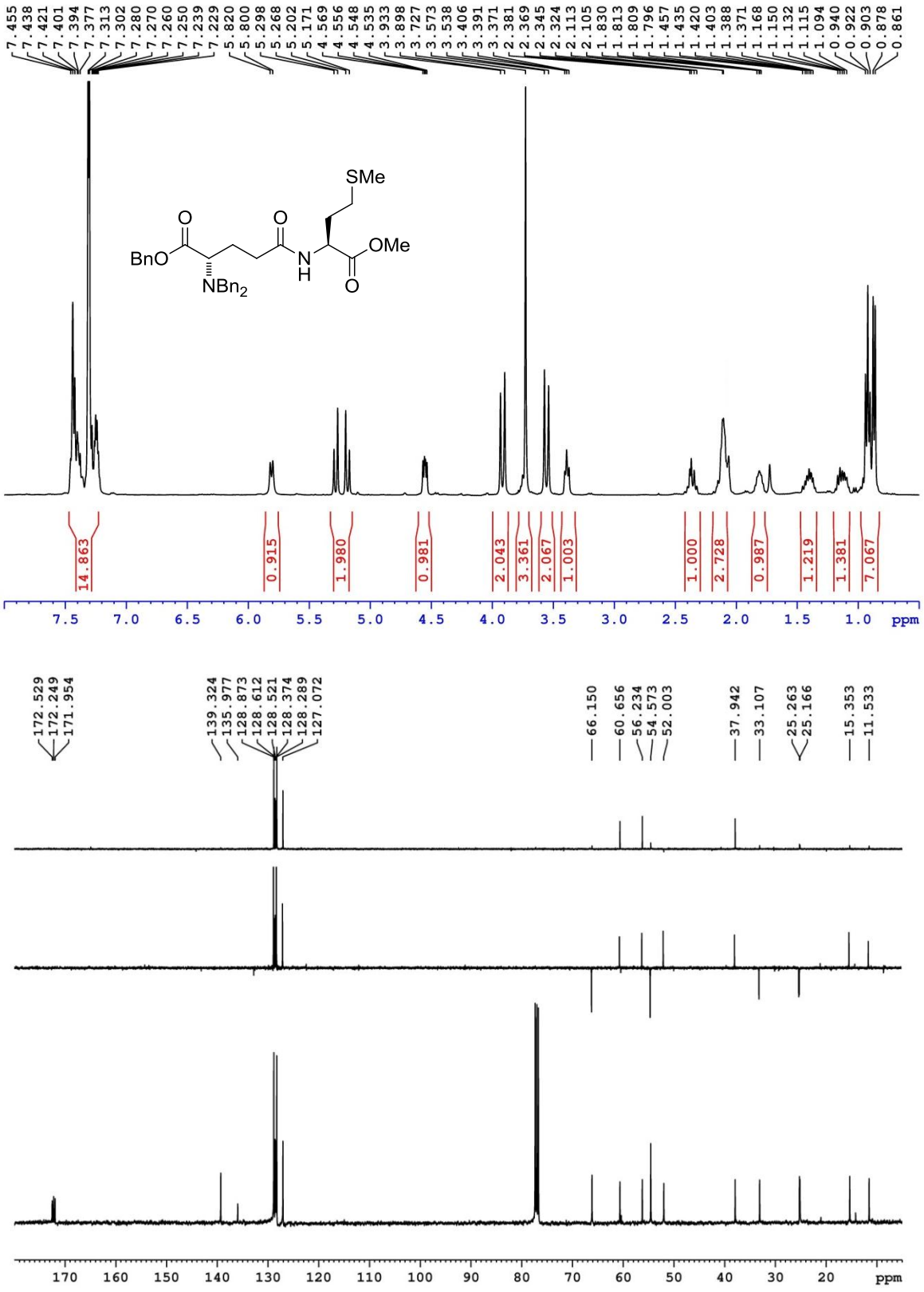

Figure S11. ^{1}H (400 MHz) and ^{13}C (100 MHz) NMR spectra in $CDCl_3$ of 9k.

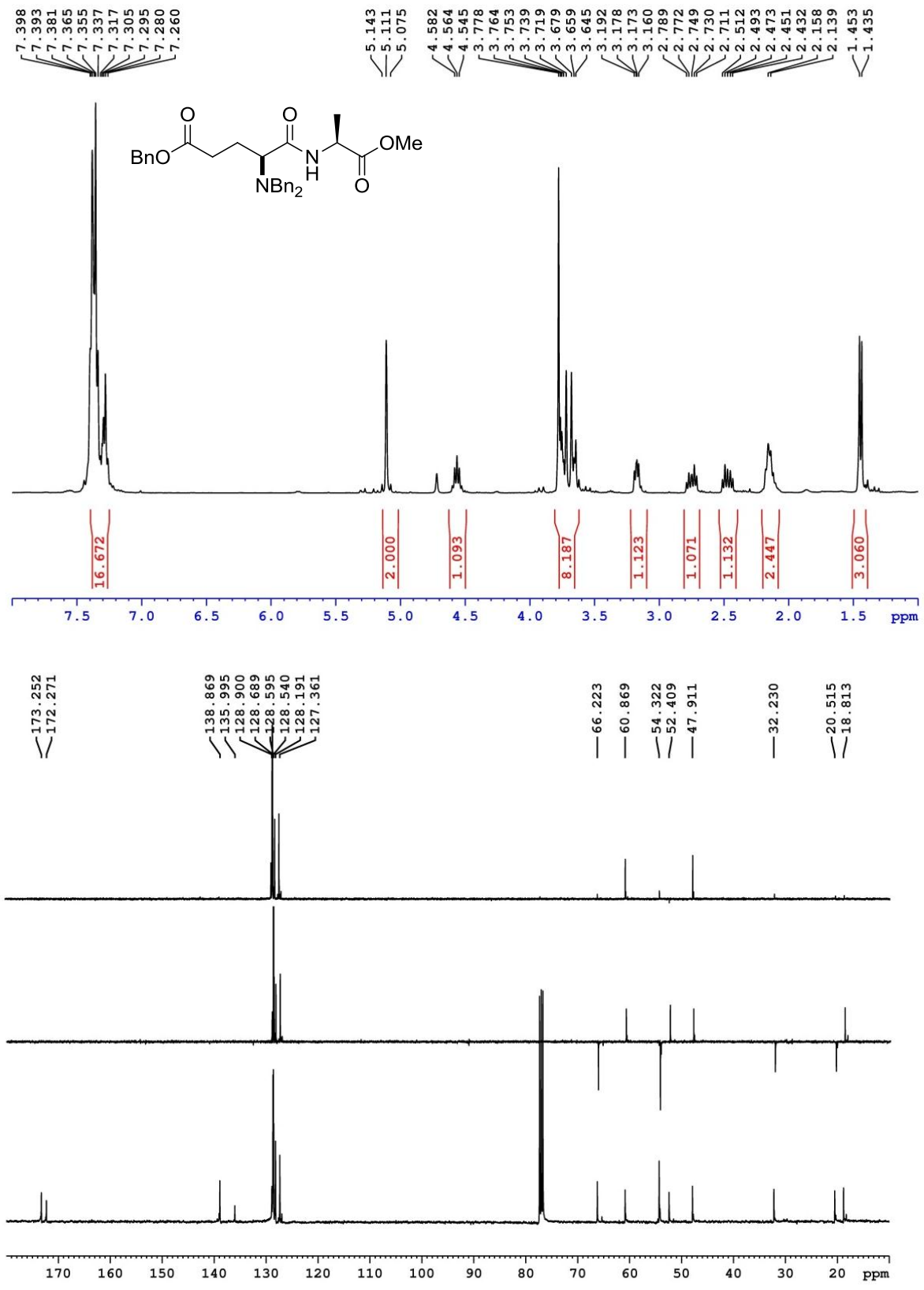

Figure S12. **^{1}H (400 MHz) and ^{13}C (100 MHz) NMR spectra in $CDCl_3$ of 10a.**

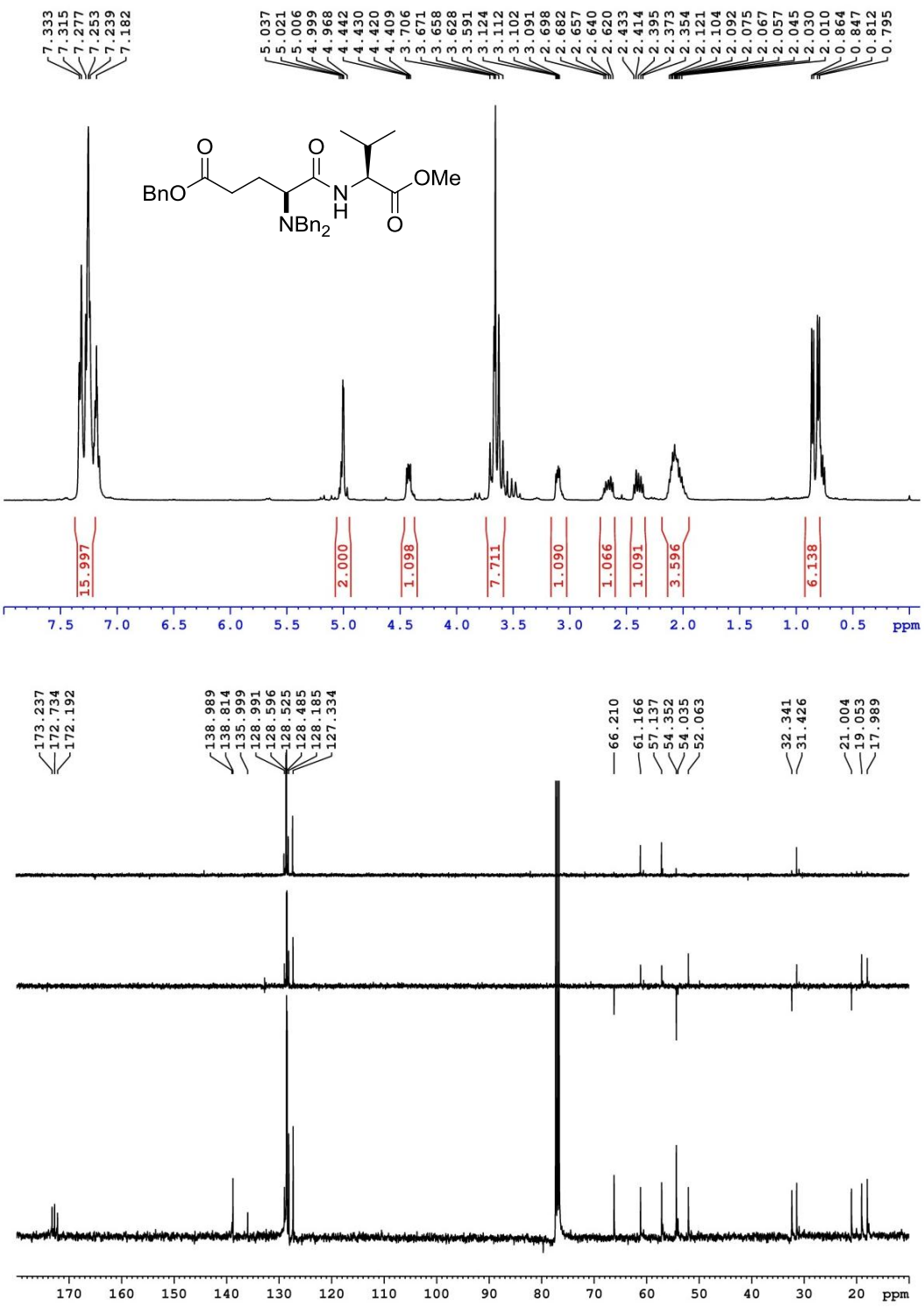

Figure S13. **^{1}H (400 MHz) and ^{13}C (100 MHz) NMR spectra in $CDCl_3$ of 10b.**

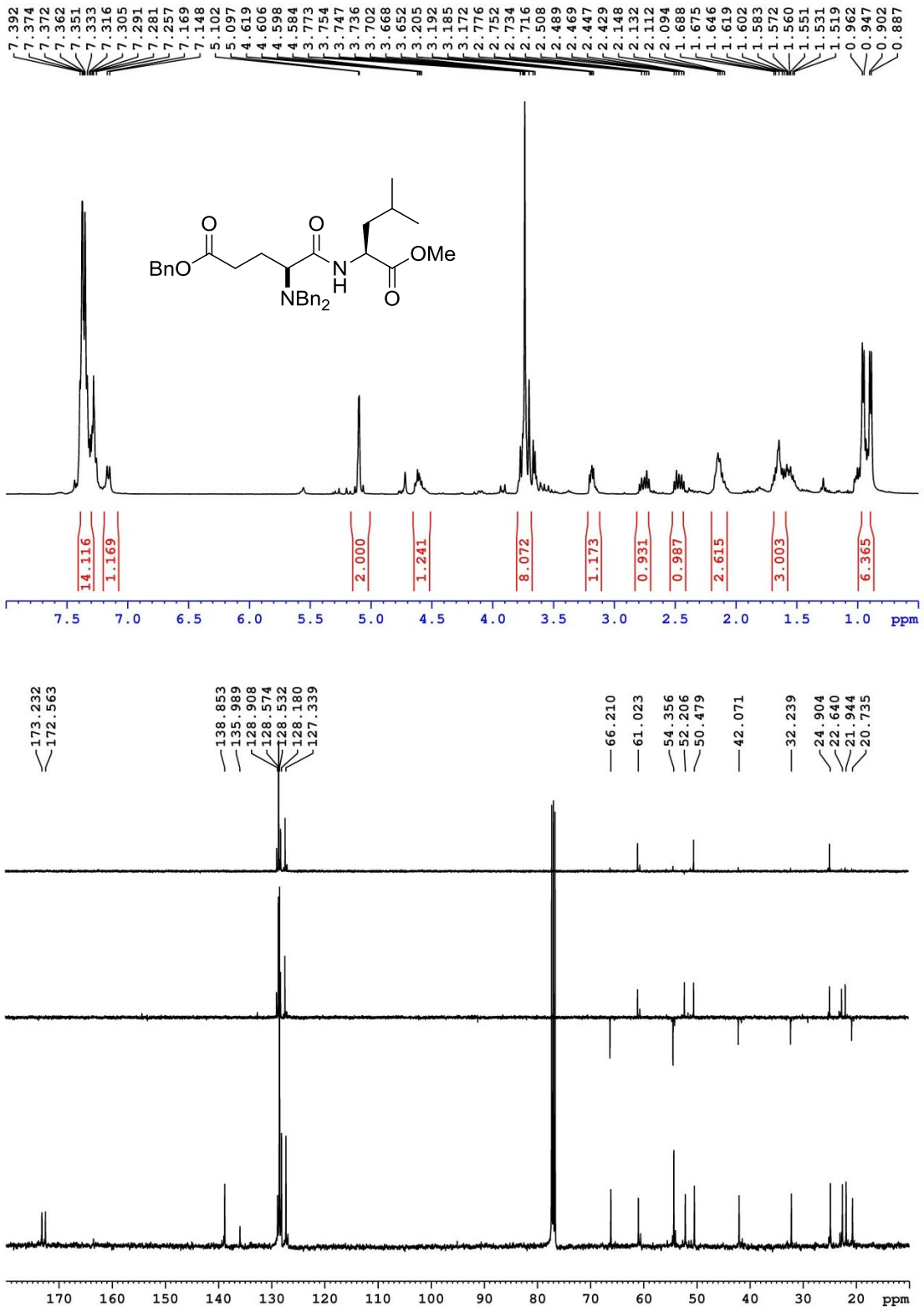

Figure S14. **^{1}H (400 MHz) and ^{13}C (100 MHz) NMR spectra in $CDCl_3$ of 10c.**

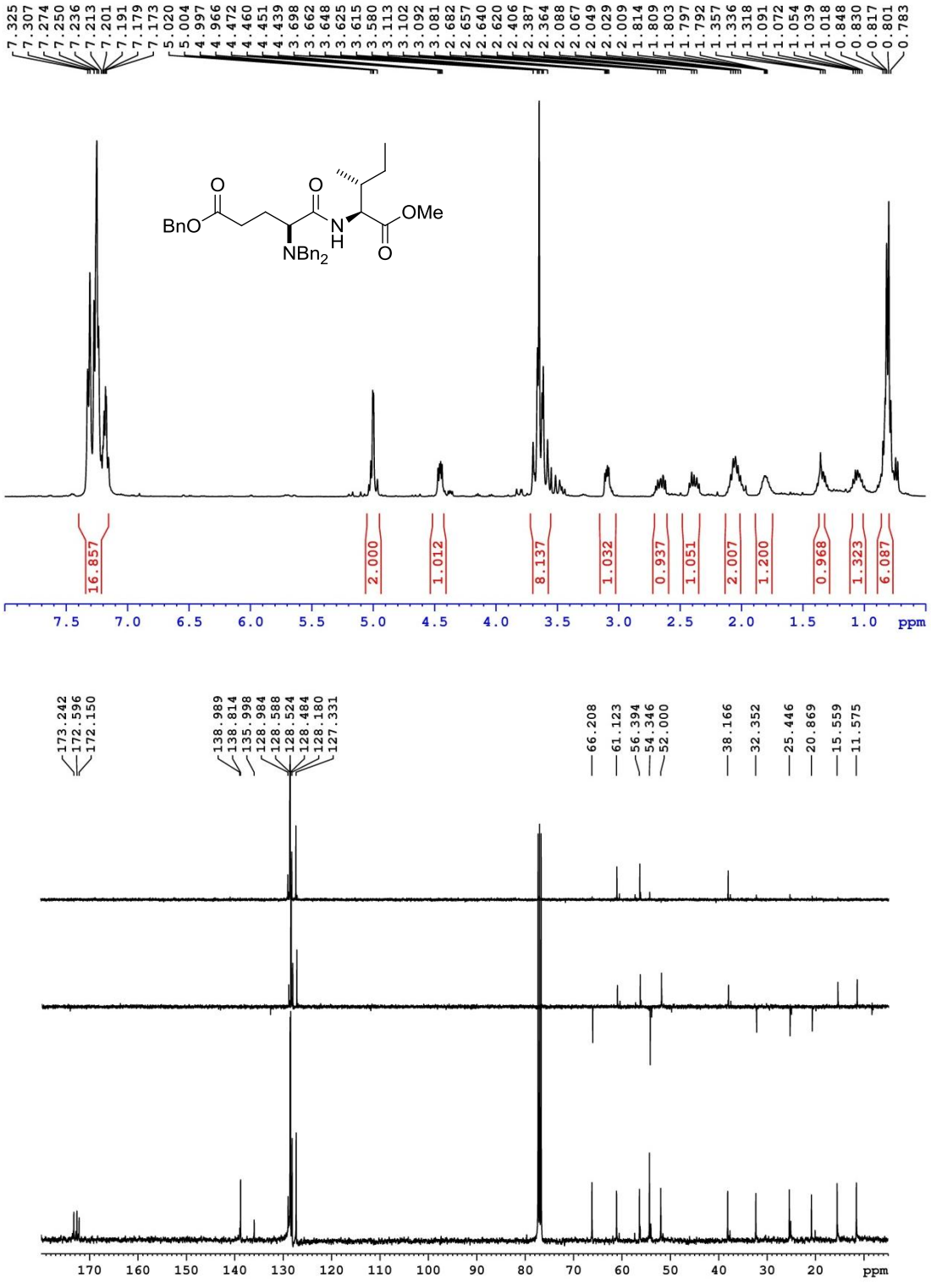

Figure S15. **^{1}H (400 MHz) and ^{13}C (100 MHz) NMR spectra in $CDCl_3$ of 10d.**

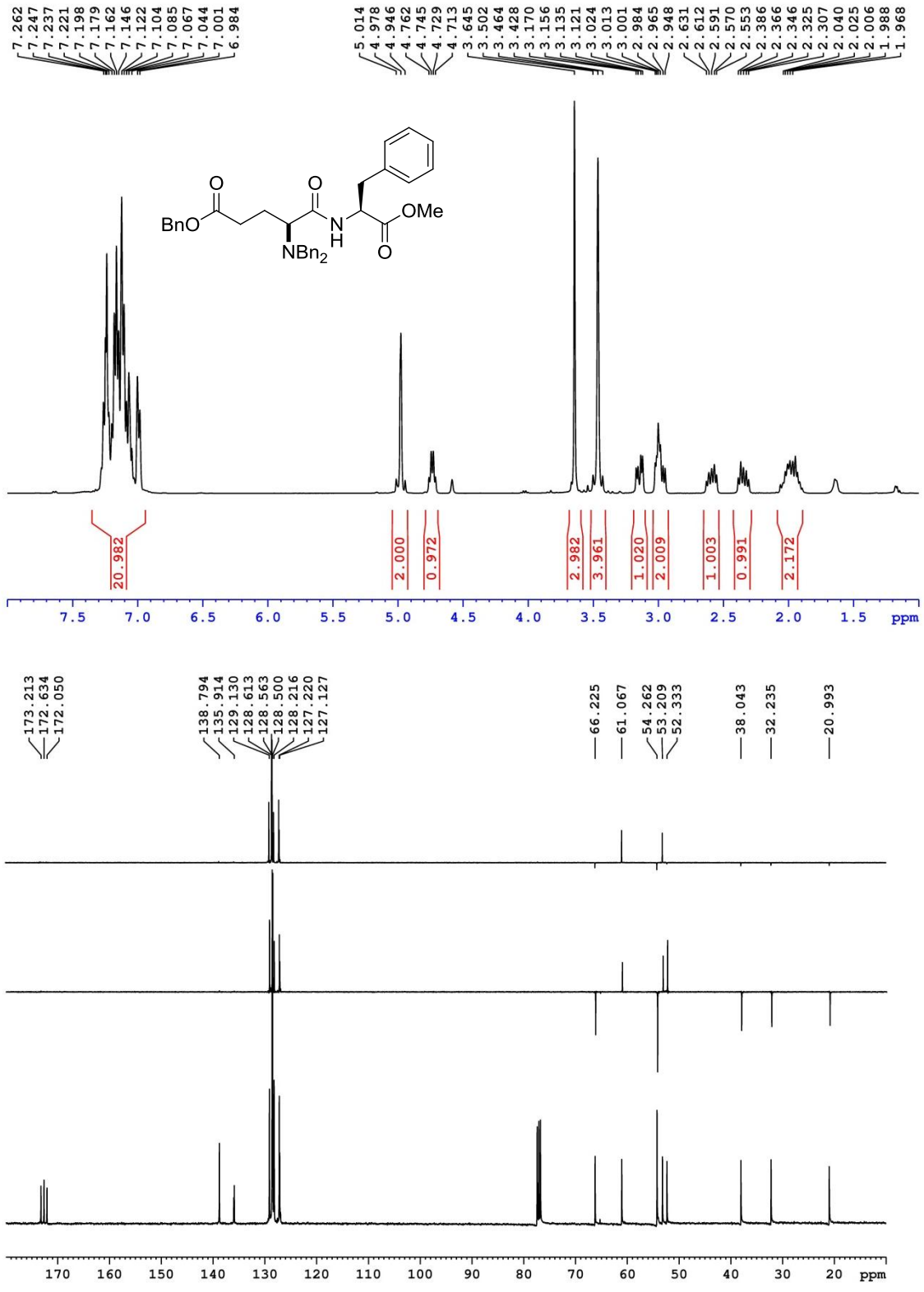

Figure S16. **^{1}H (400 MHz) and ^{13}C (100 MHz) NMR spectra in $CDCl_3$ of 10e.**

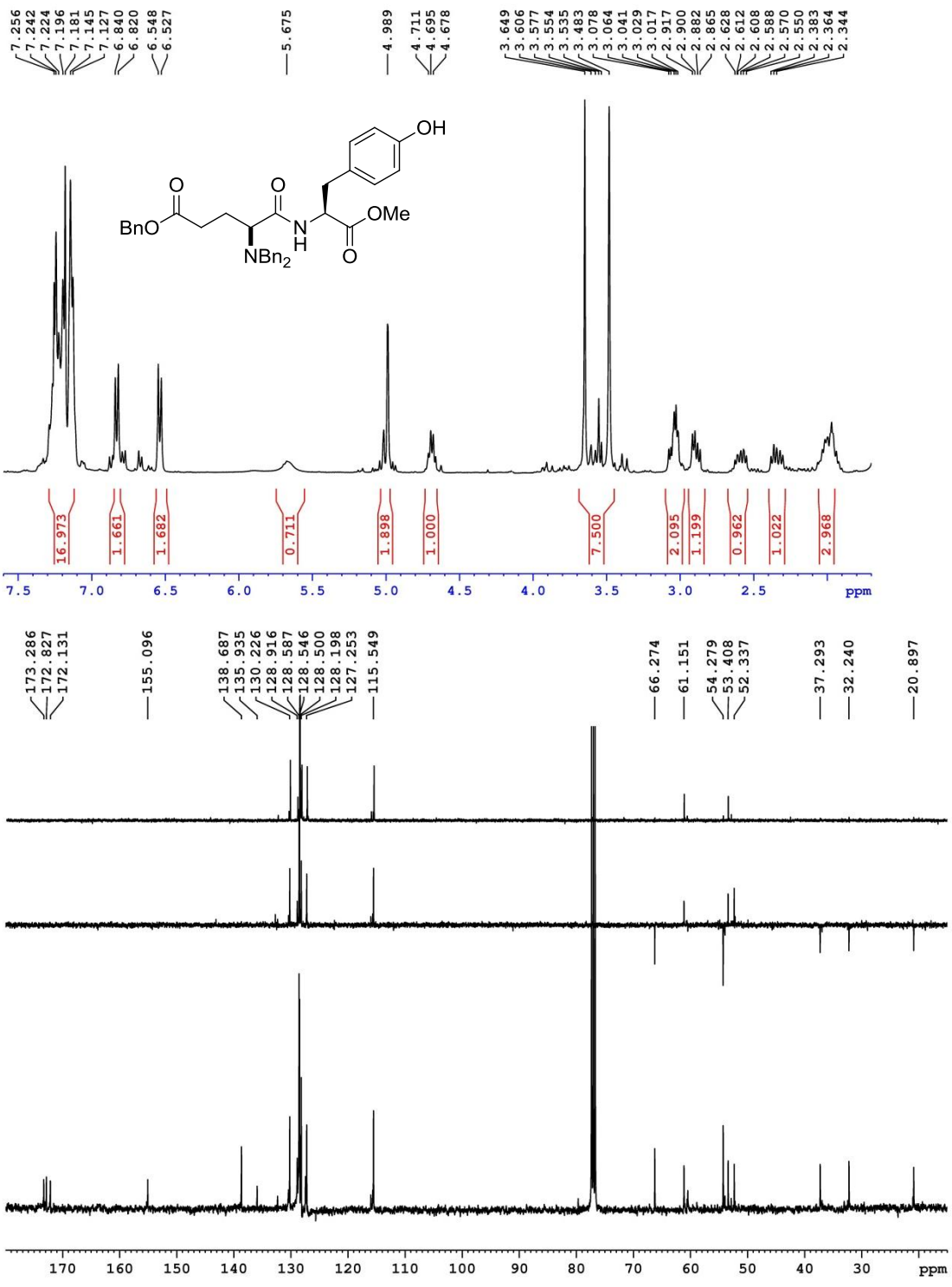

Figure S17. ^{1}H (400 MHz) and ^{13}C (100 MHz) NMR spectra in $CDCl_3$ of 10f.

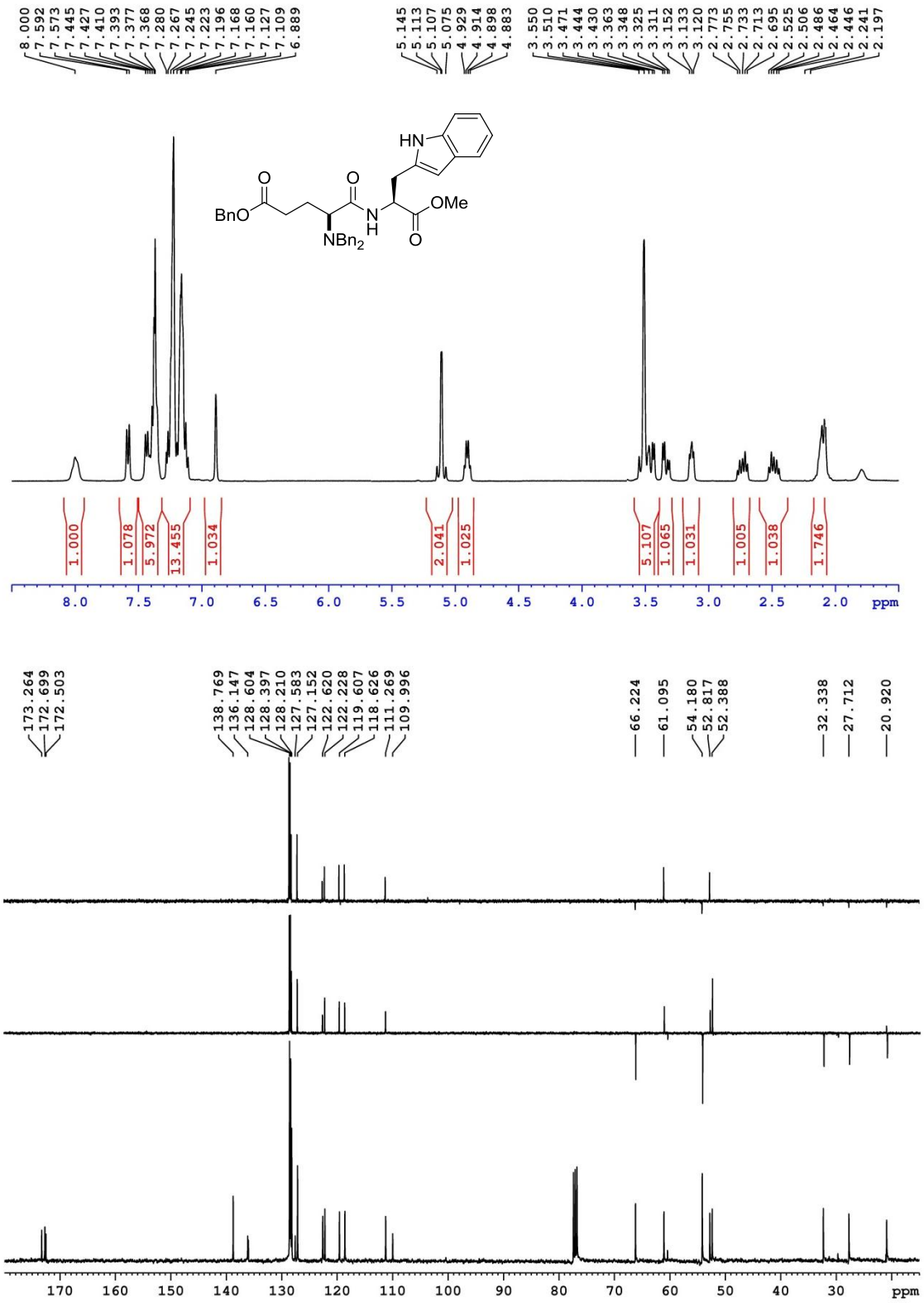

Figure S18. ^{1}**H (400 MHz) and** ^{13}**C (100 MHz) NMR spectra in** $CDCl_3$ **of 10g.**

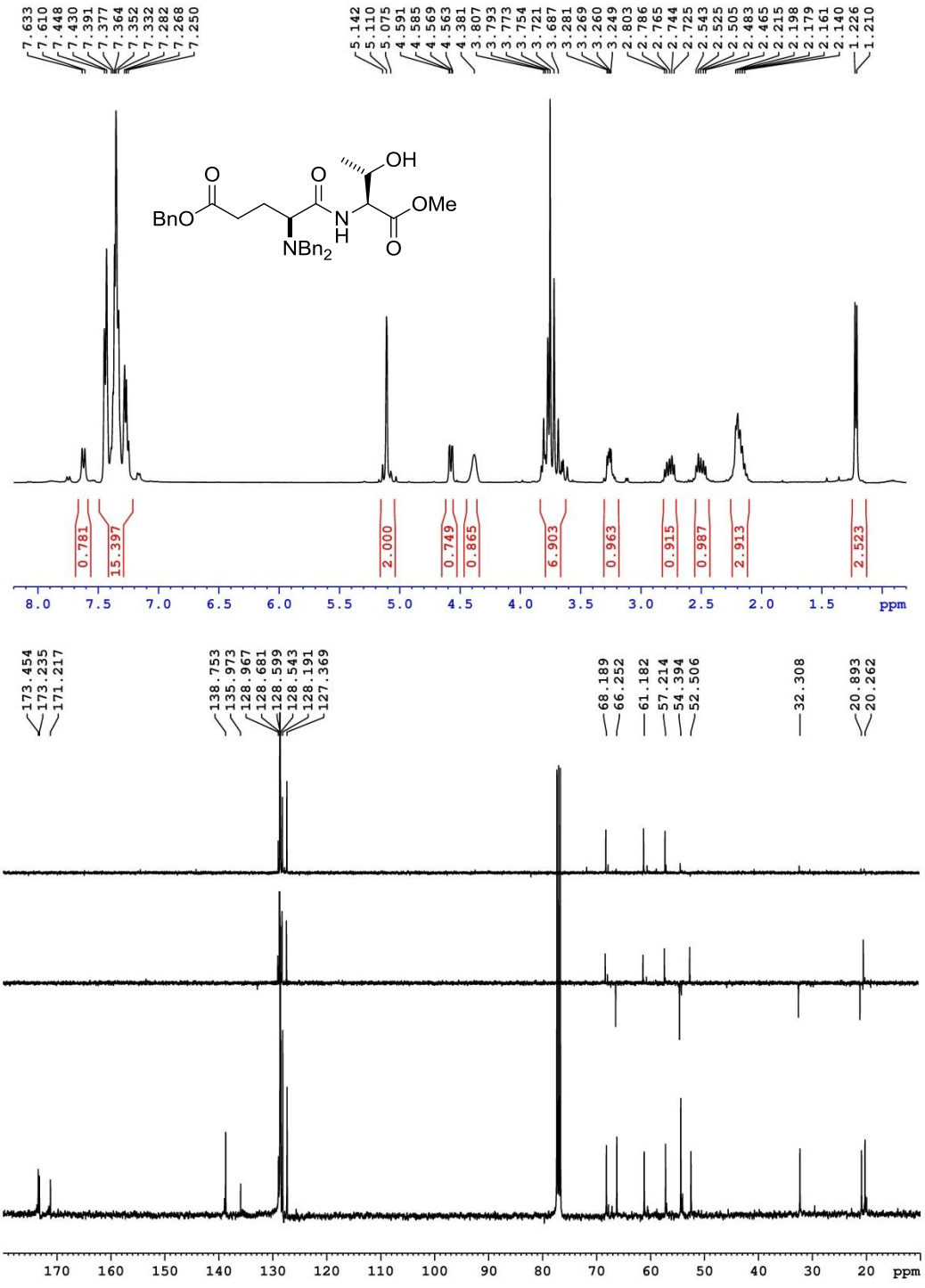

Figure S19. ^{1}H **(400 MHz) and** ^{13}C **(100 MHz) NMR spectra in** $CDCl_3$ **of 10h.**

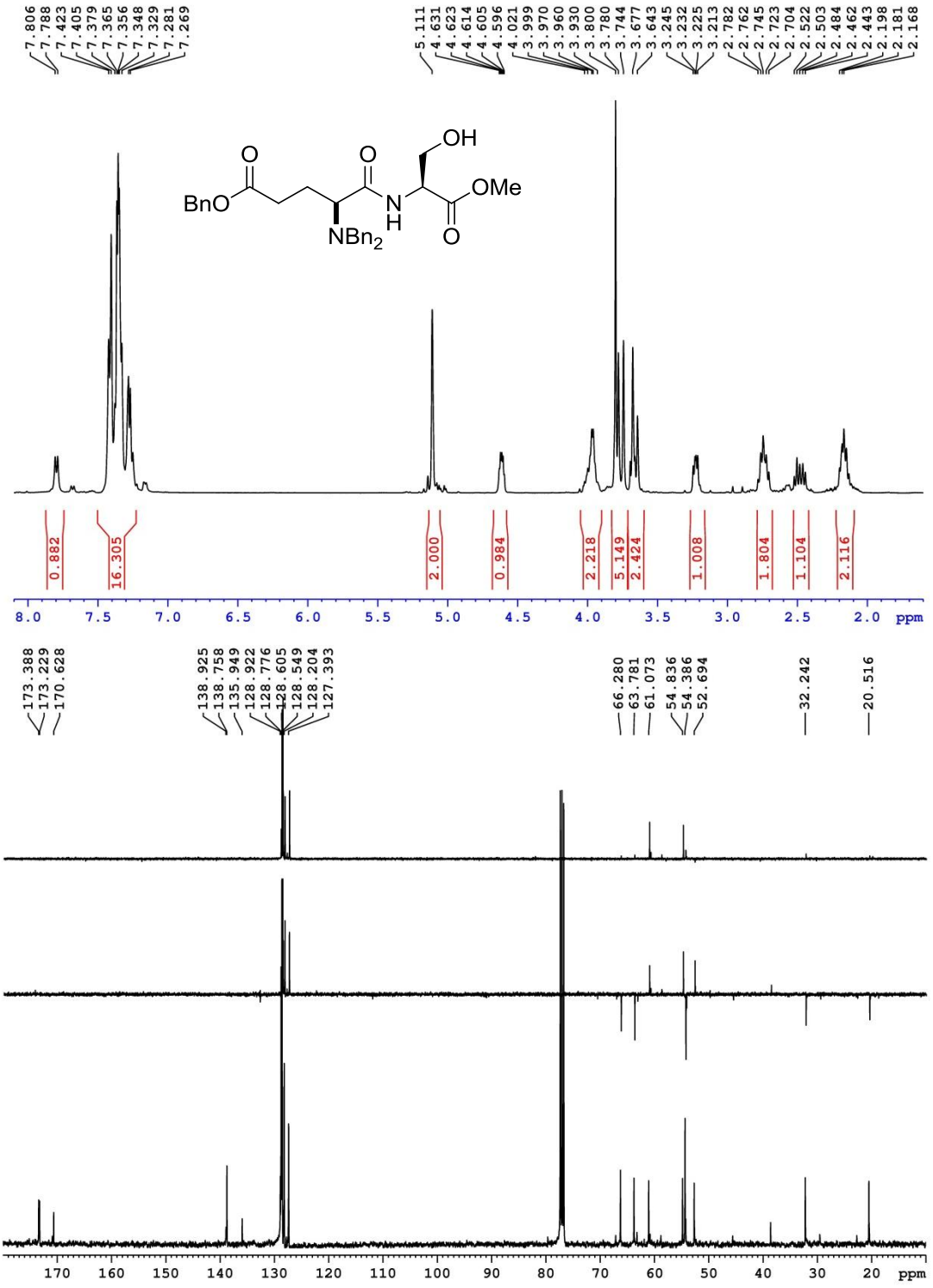

Figure S20. **^{1}H (400 MHz) and ^{13}C (100 MHz) NMR spectra in $CDCl_3$ of 10i.**

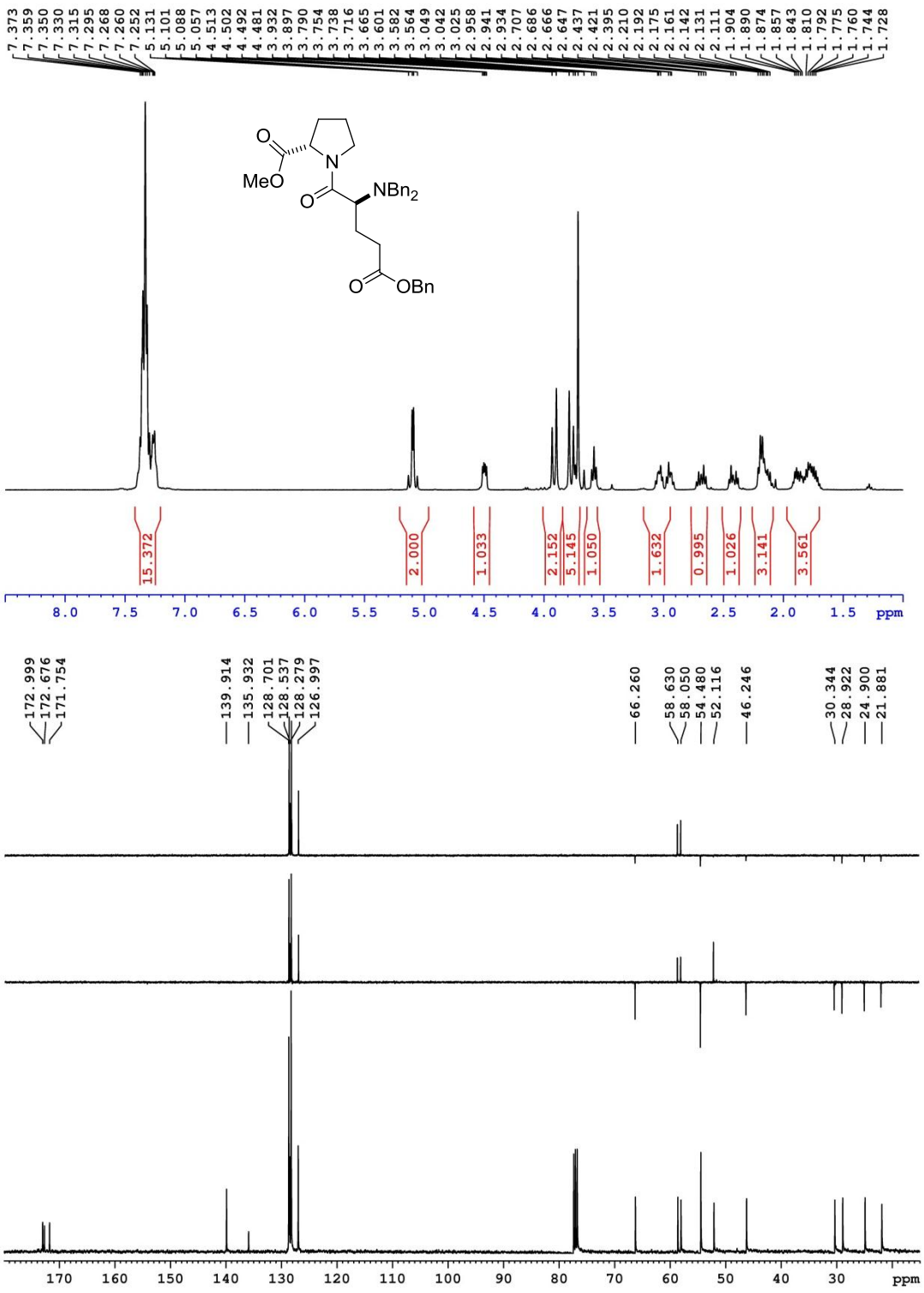

Figure S21. **^{1}H (400 MHz) and ^{13}C (100 MHz) NMR spectra in $CDCl_3$ of 10j.**

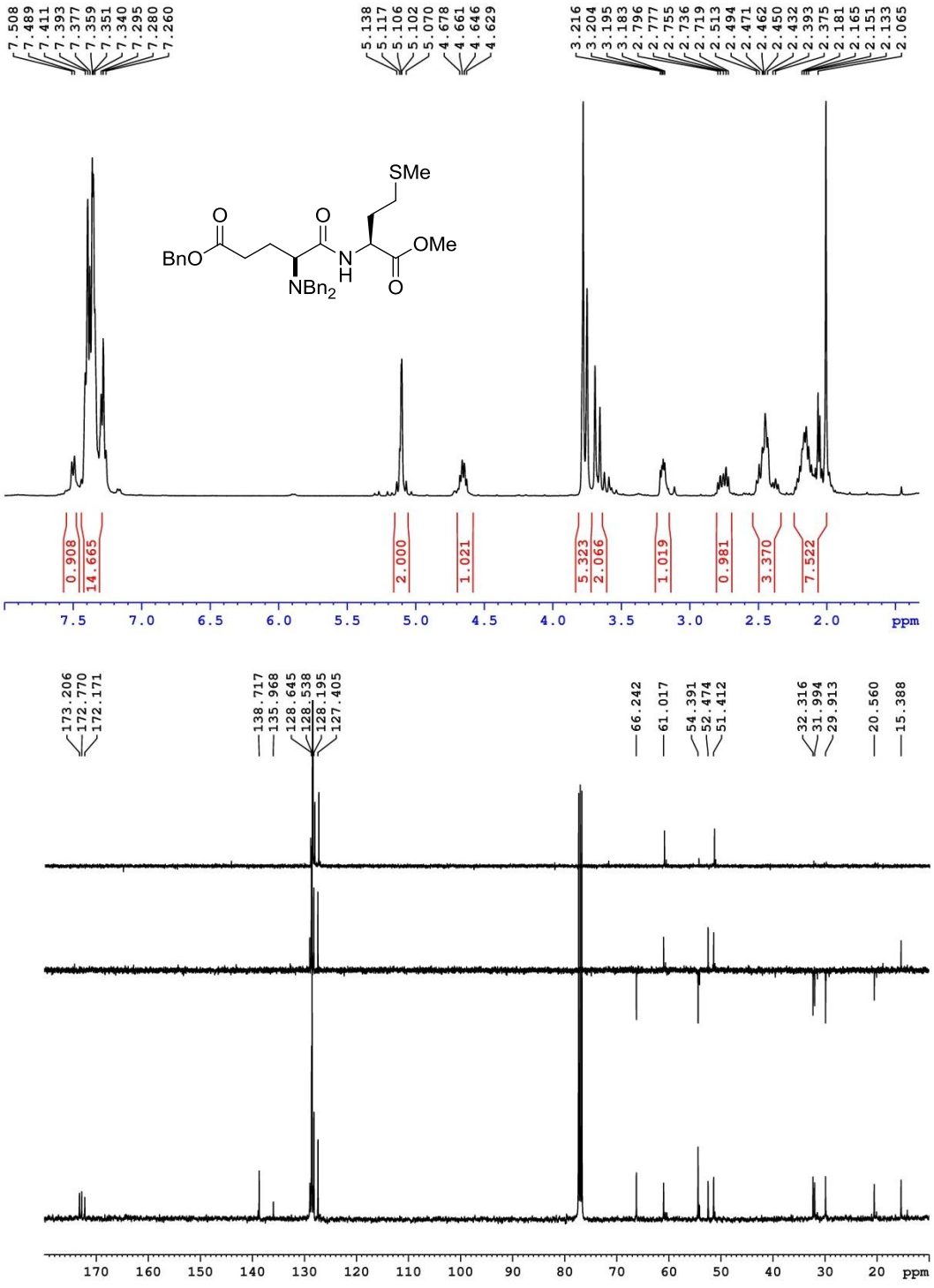

Figure S22. ^{1}**H (400 MHz) and** ^{13}**C (100 MHz) NMR spectra in** $CDCl_3$ **of 10k.**

CHAPTER 7

CONCLUSIONS

7. Conclusions

Our investigations have afforded the following conclusions:

7.1 A new general one-pot methodology has been developed for the synthesis of enantiopure *anti*-β-amino alcohols from α-dibenzylamino esters having their origin in α-amino acids, in good yields and excellent diastereoselectivity. This strategy has avoided the problem of instability of the aldehydes. We have also demonstrated that this methodology is compatible with free hydroxyl groups present in the substrate. The potential of this methodology was applied to the synthesis of a small and biased library of enantiopure *anti*-β-amino alcohols.

7.2 The small and biased library of enantiopure *anti*-β-amino alcohols were tested against human solid tumor cell lines showing all of them the ability to inhibit cell growth, with GI_{50} values in the range 1-20 μM. This study allowed us to define a structural activity-relationship (SAR), where we observed that the side chain of the amino acid, did not affect the activity, however the large of the alkyl chain affect the activity, mainly observed in SW1573 cells. We also observed that hydroxyl groups presented in the side chain did not improve the activity.

7.3 A computational approach was designed to anticipate the molecular target(s) on the basis of the chemical structure and the antiproliferative activity. The methods pointed to kinases as plausible candidates. Experimental determination of the interaction with 456 kinases indicated that the *anti*-β-amino alcohols behave as selective CK1ε inhibitors. Docking studies agreed with these findings, being the compound **8d** (**Chapter 4**) the lead compound.

7.4 We have described a methodology to obtain both *N*,*N*-dibenzylglutamic acid monobenzyl esters **7** and **8**, from commercially available $_{L}$-glutamic acid (**1**). Both compounds could be differentiated in terms of their ^{1}H NMR spectra, The unprecedented compound **7** is reported and characterized for the first time.

7.5 We have reported the synthesis of a novel class of *N*,*N*-dibenzylglutamic α- and γ-glutamyl acid-based dipeptides series.

7.6 The dipeptides were tested for their antiproliferative activity against five human solid tumor cell lines. Remarkably, some dipeptides were more active in the resistant cancer cell line WiDr than conventional anticancer drugs. From the data on growth inhibition, γ-glutamyl methionine **9k** and α-glutamyl proline **10j** were identified as lead compounds.

PUBLICATIONS LIST

Publication List

1. **Enantioselective Synthesis of Cis-Decalins using Organocatalysis and Sulfonyl Nazarov Reagents** Authors: Javier Peña, Gastón Silveira-Dorta, Rosalina Moro, Narciso Garrido, Isidro S. Marcos, Francisca Sanz, David Díez. *Molecules*, 2015, ***20***, 6409-6418. DOI: 10.3390/molecules20046409.

2. **Oxidations with air by ascorbate-driven quinone redox cycling**. Authors: Gastón Silveira-Dorta, Diego M. Monzón, Fernando P. Crisóstomo, Tomás Martín, Víctor S. Martín, Romen Carrillo. *Chemical Communication*, 2015, ***51***, 7027-7030. DOI: 10.1039/C5CC01519G.

3. **Synthesis and identification of unprecedented selective inhibitors of CK1*ε***. Authors: Gastón Silveira-Dorta, Inês J. Sousa, Víctor S. Martín, Miguel X. Fernandes, José M. Padrón. *European Journal of Medicinal Chemistry*, 2015, ***96***, 308-317. DOI: 10.1039/C5CC01519G.

4. **Synthesis and antiproliferative activity of glutamic acid-based dipeptides Amino Acids.** Authors: Gastón Silveira-Dorta, Víctor S. Martín, José M. Padrón. *Amino Acids.* DOI: 10.1007/s00726-015-1987-0.

5. **Direct Stereoselective Synthesis of Enantiomerically Pure anti-β-Amino Alcohols.** Authors: Gastón Silveira-Dorta, Osvaldo J. Donadel, Victor S. Martín, José M. Padrón. *The Journal of Organic Chemistry*, 2014, ***79***, 6775-6782. ***Featured Articule***. *Selected as Cover of the Journal*. DOI: 10.1021/jo500481j.

6. **Direct Synthesis of Polybenzylated Glutamic Acid Monoesters: Disambiguation of *N,N*-Dibenzylglutamic Acid α- and γ-Benzyl Esters.** Authors: Gastón Silveira-Dorta, Victor S. Martín, José M. Padrón. *Synlett.* 2014, ***25***, 2166–2170. DOI: 10.1055/s-0034-1378532.

7. **Molecular docking studies of the interaction between propargylic enol ethers and human DNA topoisomerase IIα**. Authors: Gastón Silveira-Dorta, Inês J. Sousa, Carla Ríos-Luci, Víctor S. Martín, Miguel X. Fernandes, José M. Padrón. *Bioorganic & Medicinal Chemistry Letters*, 2013, ***23***, 5382-5384. DOI: 10.1016/j.bmcl.2013.07.055.